The Conceptual Design and Development of a Micro Gas Turbine Generator

Matthys M Steyn
M.Eng. (Mechanical)

Dissertation submitted as partial fulfilment of the requirements for the degree Magister Engineering

School of Mechanical and Materials Engineering
at the North-West University

Supervisor: **Dr B Botha**
Assistant Supervisor: **Prof GP Greyvenstein**

2006
Potchefstroom Campus

Abstract

All over the world interest in small scale stand alone power generators is growing. This interest is motivated by lower electrical costs and/or the capability to be unaffected by power failures and blackouts that could damage electronic networks and machinery. The potential of small scale power supplying units is being recognized, as generating capacity is quickly becoming too small. Furthermore, the need for off-grid power supply to remote areas, additional power supply to reduce grid power usage during peak demand periods when power is expensive, as well as the advantages of distributed generation, also increases the demand for this type of power. Technology that holds great potential for small scale power generation is the use of gas turbine machinery to drive these generators.

Gas turbine machinery is mainly based on the Brayton cycle and variants hereof. These variants are compared and evaluated under different parameter changes (Chapters 2 and 3) while different configurations of gas turbine systems were evaluated as well. The selection of turbine machinery is done with the help of the software package (Flownex®) where the same potential turbine machinery is compared in Chapter 4.

A gas turbine system mostly consists out of the following components: Compressor, Turbine, Heater / Combustion chamber and Heat exchangers. The compressor and turbine configuration are discussed as part of the turbine machinery selection process in Chapter 4. The following Chapters (5, 6 and 7) are dedicated to design of the rest of the components. All of these components are simulated as a system both under steady state conditions as well as under transient conditions in Chapter 7. Different operating conditions like start-up and load-following are simulated as well in this part if the study. The simulations are done for a small scale (60 – 80kW) micro gas turbine generator

It is recommended that now that the concept of a micro gas turbine generator was proven, that firstly prototypes of the components like the combustor chamber and heat exchangers are built, followed by a complete system, based on the outputs of this study.

Uittreksel

'n Groei in belangstelling aan klein onafhanklike elektrise krag opwekkers is besig om werleld wyd toe te neem. Die vermoë om onafhanklik van die eletrisiteits voorsienings stelsel self aan jou behoeftes te voorsien, saam met die finansiële voorsprong wat dit bied, maak hierdie krag opwekkers nog meer aantreklik. Verdere voordele wat ook in ag geneem moet word, is die feit dat bestaande netwerke nie kan voorbly om aan die groeiende behoefte van elektrisiteit te voorsien nie, as ook die voorsiening aan verafgeleë gebiede. Tegnologie wat groot potensiaal inhou wat hierdie klein onafhanklike krag opwekkers aanbetref is die gebruik van mikro gas turbine stelsels in stede van gewone binnebrand enjins.

Meeste gas turbine stelsels is gebaseer op variante van die Brayton-siklus, en daarom word die ideale as ook die ware Brayton kringlope ondersoek deur die effek van verskillende veranderlikes te ondersoek. Dit word in Hoofstukke 2 en 3 van hierdie studie gedoen. Verskillende kringloop konfigurasies word ondersoek om die mees geskikte een bloot te stel. Die seleksie van turbo masjienerie word met behulp van 'n rekenaar pakket (Flownex®) gedoen en dit word beskryf in Hoofstuk 4.

Gas turbine stelsels bestaan gewoonlik uit minstens die volgende onderdele: Kompressor en Turbine ennheid, Verhitter of Verbrander, en Hitte ruilers. Die ontwerp van die komponente wat gebruik work in hierdie studie word in Hoofstukke 4 to 7 bespreek. Die onderdele work individeel ondersoek, maar ook as 'n stesel. Die stelsel word onder gestadigde toestande as ook nie-gestadigde toestande ondersoek (in Hoofstuk 7), en operasionele omstandighede word gesimuleer. Hier toestande sluit "aan-skakeling" en "las-volging" omstandighede in, en word gedoen vir elekstrisiteits generasie band van 60 – 80kW.

Dit ward aanbeveel dat eerstens elk van die onderdele individeel geproduseer mot word volgens die uitsette van hierdie studie. Tweedens: dat 'n voledige mikro gas turbine stelsel gebou en getoets moet word.

Table of contents

List of figures

List of tables

Nomenclature

		m^2
A	Area	
BC	Basic Cycle without recuperation	
BRC	Basic Cycle with Recuperation	
CC	Combustion Chamber	
Cp	Specific heat transfer value	
eta	Efficiency	
D	Diameter	m
h	Enthalpy	
HP	High Pressure	
HPC	High Pressure Compressor	
HPT	High Pressure Turbine	
IB	Ideal Basic cycle without recuperation	
IBR	Ideal Basic cycle with Recuperation	
IC	Inter-cooler	
ITCIR	Ideal Two-stage Compression cycle with Inter-cooling and Recuperation	
LP	Low Pressure	
LPC	Low Pressure Compressor	
LPT	Low Pressure Turbine	
n	Number of stages, tubes, etc.	
N	Rotational speed	rpm
NDM	Non-Dimension Mass flow rate	
NDS	Non-Dimension Speed	
$\dot{m}$	Mass flow rate	kg/s
Mf_s	Non-dimensional Mass Flow on the Surge line	
Mf_w	Non-dimensional Mass Flow on the Working line	
p	Pressure	kPa
Pr	Pressure ratio	

Q	Heat	kW
R	Gas constant, Thermal resistance	kJ/kg,
RX	Recuperator	
T	Temperature	$^{\circ}C$
TCIR	Two-stage Compression cycle with Inter-cooling and Recuperation	
TIT	Turbo Inlet Temperature	$^{\circ}C$
V	Velocity	m/s
Vol	Volume	m^3
UA	Heat transfer coefficient	
W	Work	kW
$\dot{W}$	Specific Work	kWs/kg

Suffixes

0	stagnation value
1,2 etc.	reference planes
η	efficiency
Δ	Delta (difference)
γ	gamma
∞	polytropic
a	ambient, air
act	actual
c	compressor, coolant
e	exit
f	fuel
g	gas
i	intake
m	mechanical
o	outlet
s	stage
t	turbine
w	water

1 Micro Gas Turbine

Western companies have recently shown increasing interest in small-scale power generating units recently, enabling them to generate power in-house. This interest is motivated by lower electrical costs and/or the capability to be unaffected by power failures and blackouts that could damage electronic networks and machinery. The potential of small scale power supplying units is being recognised, as generating capacity is quickly becoming too small. Interest is further fuelled by power failures across the USA in 2003 and more recently in 2006 Cape Town in South Africa, which created a sizeable market for back-up power units. Furthermore, the need for off-grid power supply to remote areas, additional power supply to reduce grid power usage during peak demand periods when power is expensive, as well as the advantages of distributed generation, also increases the demand for this type of power.

1.1 INTRODUCTION TO MICRO GAS TURBINE MACHINES

The drive by governing bodies to supply rural areas in Southern Africa with electrical power has done a great deal to improve the reliability of these power plants in the South African market. Apart from reducing the load on local electricity providers' networks (such as Eskom) and limiting the impact of power failures, the technology presents companies with an opportunity of earning revenue from supplying power to utilities, addressing the developing need for electrical power. It would therefore be of great value if knowledge could be gained in the development and manufacture of such small scale power generator units.

Technology that holds great potential for small scale power generation is gas turbines. This, in its simplest form, consists of a compressor, turbine, combustion chamber and generator. The advantages of small or micro gas turbines are:

- Superior reliability.
- Low maintenance cost.
- Potential high thermal efficiency (when using a recuperator).

The ability of these systems to simultaneously produce usable heat and power (co-generation) thereby further increasing the efficiency and utilisation of the system.

Realising these benefits, international companies, like Elliot and Capstone, have developed micro gas turbine machines for overseas markets, [DER 2003]. These distributors have regional offices that supply generator systems to the South African market. However, there is little or no technical support and a few custom designs are available to the local client. Systems designed for the international market do not always take into account factors such as the local fuel types, required frequencies and skill levels of maintenance staff. Research on current products to better understand existing technology should be conducted in South Africa. This will create the possibility of developing a system that will meet the demands of this growing and developing continent. The research into micro gas turbines will also contribute to the establishment of local knowledge necessary to optimally operate and maintain these units.

1.2 BACKGROUND TO MICRO GAS TURBINES

Gas turbines are usually associated with the aero industry, because it is the most common power source in both civil and military aircraft. Other industries where gas turbines are used extensively include the power generation industry, the process industry, mobile applications and pump houses for gas and oil pipelines. A variety of micro gas turbine systems exist, including stand alone units and units which are combined with steam turbine cycles or with fuel cells. These include systems with single or multi-shaft configurations and/or single or multi compression stages as well as recuperated or un-recuperated system configurations. Together with layout variances, micro gas turbines have high grade waste heat, low capital cost, compact size, high flexibility and reliability, fast starting times, lower maintenance costs, and low emission pollution, giving them the advantages over other power generation technologies. Taking advantage of these benefits, the development of a micro gas turbine system involves all of the subsystem components and the balancing of the performance of all the components to maximise the system's performance. In this study an effort will be made to use standard components that are commercially available, while an investigation will also be conducted into the advantages of custom designed components.

Challenges facing the designer can be separated into two areas: technical and non-technical. Technical challenges include the development of a compact, low-cost micro gas turbine with

efficiencies comparable or higher than that of reciprocating engines. The non-technical challenges include the development of a micro gas turbine with uncomplicated technology, so maintenance can be carried out by low-skilled people.

1.3 DESCRIPTION OF A SIMPLE MICRO GAS TURBINE SYSTEM

Most modern gas turbine cycles are based on the closed Brayton cycle, which ideally consists of the following four processes:

- Isentropic compression.
- Isobaric heating.
- Isentropic expansion.
- Isobaric cooling.

Note: Traditionally seemingly open cycles can also be analyzed as a closed system, if the atmosphere is taken as a large heat exchanger at constant (atmospheric) pressure, without any loss in efficiency. Figure 1.1 shows a schematic of the system.

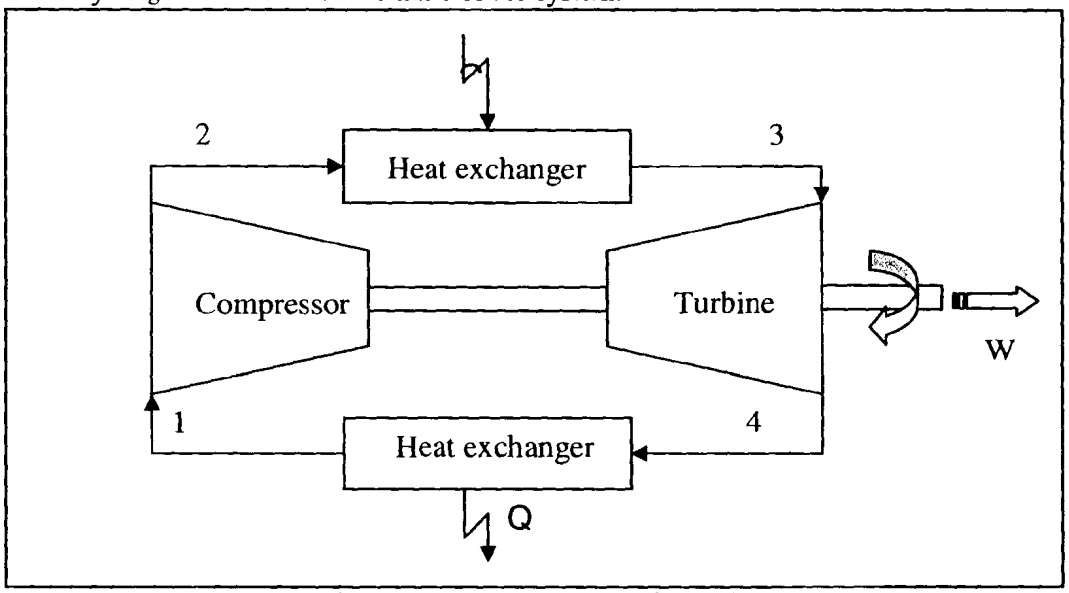

Figure 1.1: Brayton Cycle (Closed system).

Gas (usually air) is compressed isentropically in the compressor (1-2) before being heated in the heat exchanger (2-3). The hot gas leaves the heat exchanger and expands isentropically through the turbine (3-4) that drives both the compressor and load. Thereafter the gas is cooled (4-1) back to the original condition (temperature and pressure).

Turbo–machinery consists of two main components: compressors and turbines. Two types of turbines exist, namely axial and radial flow turbines. As is the case with compressors, axial flow turbines are generally more suited to higher flow rate applications while radial flow turbines are more suited to lower flow rate applications. Radial flow turbines can also deal with higher pressure ratios which implies fewer stages per given pressure ratio.

The two most common compressor types used in gas turbine machines are axial and centrifugal flow compressors. Axial compressors are more suited for higher flow applications and consist of a number of stages each consisting of a stator and rotor blade combination. The compression ratio per stage is usually small and large numbers of stages are required in order to produce high pressure ratios, making axial flow compressors relatively expensive. Centrifugal compressors are

more suited to lower flow applications. The pressure ratio of a single centrifugal stage is usually much higher than that of an axial compressor stage, which often makes it possible to use only one stage. Therefore centrifugal compressors are more compact and cheaper than axial compressors for lower flow applications.

As the name implies, micro gas turbines are small, compact, electrical power generating units best suited to applications where space is limited. Centrifugal turbine units are therefore more desirable for micro gas turbine application, as they are more compact than axial configurations, plus the cost advantage of radial flow compressors and turbines make them the machine of choice for micro turbine applications.

The compact gas turbine system shown in Figure 1.1 is known as a closed cycle where a heat exchanger is used to cool the gas leaving the turbine in its initial condition. In open air cycles, the air at the outlet of the turbine is discharged to the atmosphere. Open air cycles therefore eliminate the need for a cooler (heat exchanger). A typical open air cycle is illustrated in Figure 1.2.

The presence of oxygen in the intake air makes it possible to heat the air in a combustor where internal energy of fuel is converted into heat by burning it in the presence of oxygen. The design of combustion chambers is an advanced discipline where principles of fluid dynamics, heat transfer and chemistry come into play. The design is critically dependent on operational conditions which highlight the need for accurate system analyses as the operating conditions of the combustion chamber are determined by cycle performances.

A variant of the ideal Brayton cycle, which found primary application in high performance power generation systems, is the recuperated Brayton cycle illustrated in Figure 1.2. Here the gas at the outlet of the turbine is used to pre-heat (5-6) the compressed air before entering the combustion chamber (2-3), lowering the energy needed for combustion (3-4).

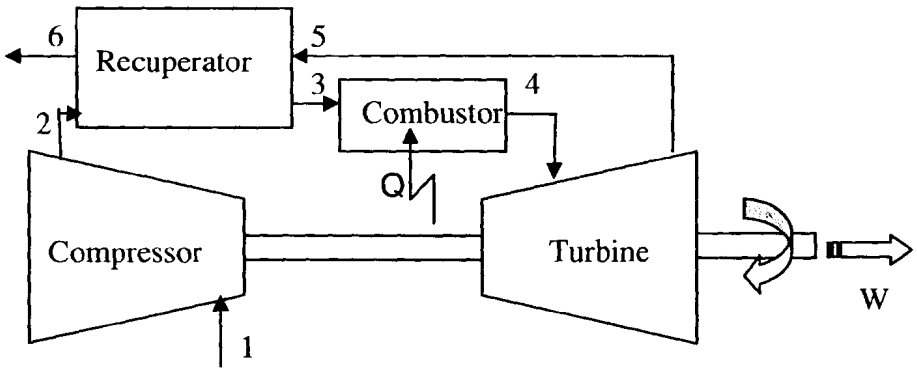

Figure 1.2: The recuperated Brayton (open) cycle.

1.4 PROBLEM STATEMENT

Designers of micro gas turbine systems need to determine the system configuration and operating conditions followed by the detail design of the individual components. System configuration refers to the actual layout of the system. This includes a choice between single or multi-stage compression, recuperated or un-recuperated cycle and the number of independent shafts. The configuration of the system and layout is different for each of the above options. Different configurations and their characteristics will be discussed in Chapter 3. Characteristics of systems are determined by the operational conditions. These operating conditions refer to mass flow,

temperature and pressure at each point in the cycle. The operational conditions determine the thermal efficiency and specific work output of the system and also impact the system design and size of individual components. This relationship between operational conditions and performance (efficiency and specific work output) is different for each configuration and the challenge is to find a combination that will minimize life cycle cost. Tools used to address this issue are cycle analysis combined with techno-economic analysis.

Even with these tools, the design of gas turbine machinery is a specialised field in its own right and the challenge is to design machines to a reasonable cost that will operate close to their optimal efficiency. A choice should be made whether to use specially designed machines that will operate at high efficiencies (an expensive exercise), or to use off-the-shelf machines, which might not operate at equally high efficiencies while being cheaper. Simulations will be done to compare the different approaches, in order to provide the best performance solution.

The drive to improve the performance for a system by selecting the best suitable turbo machinery calls for, amongst others, the use of high performance heat exchangers. Though heat exchanger design is an established field, the challenge is to find an optimum design balancing the pressure drop, heat exchange efficiency and cost.
Aspects such as the start-up and control of the system needs to be proved by system simulation and will play an important role in illustrating performance during transient conditions.

1.5 OBJECTIVE OF STUDY

The object of this study is to perform a conceptual thermo-fluid design of a low cost micro-turbine power generator that generates 60 – 80 kW of electrical poewer. As the design, development and manufacturing of gas turbine machines is rather costly, it has been decided to investigate the feasibility of using commercially available components rather than designing purpose built components. This study will focus on identifying the most appropriate machine from a list of available machines.

During the study, attention will be given to aspects such as the cycle layout, the concept design of heat exchangers and combustors and the sizing of the interconnecting pipe work. Once the system layout has been finalized, a simulation model will be generated to simulate the system during start-up and load following. This will be done using the thermal fluid network solver Flownex®.

1.6 METHODOLOGY OF THE STUDY

In Chapter 2 a literature survey will be done to review previous work on micro turbine power generators together with a discussion of the ideal Brayton cycle and its variants.

The difference between the ideal Brayton cycle and the real practical cycle will be discussed in Chapter 3, together with a comparison between the different cycles to determine the cycle best suited for the micro gas turbine application. An investigation into the sensitivity of this gas turbine system will be done, analysed and the limitations noted. Also, the outputs of an optimistic cycle will be shown to illustrate the chosen cycle's characteristics with all the components operating under ideal conditions (best possible efficiency of the cycle).

With the operational parameters of the real gas turbine system known, an investigation into the system components can be done. The first components to be analysed will be the turbo machines. Chapter 4 will concentrate on turbo machine characteristics and its selection process. Due to the

complexity of turbo machinery, the emphasis will be on the process of selection and not the detail design. This part of the study will be addressed in detail to gain a thorough understanding of all the aspects that influence the system characteristics. Finally an investigation into the feasibility of the use of a custom designed and built turbo – machine instead of a commercially available product will be done.

Chapter 5 is dedicated to the design of the heat exchangers to be used in the system. The characteristics and sensitivity of these machines are reflected in this chapter.

Heat needed by the micro gas turbine is supplied by combusting of fuel, which is discussed in Chapter 6. This discussion will include information on the combustion process, chemical reaction during combustion and the combustion chamber performances due to aerodynamics and geometrical limitations

Secondary components not discussed previously include inter-connecting pipes and auxiliaries and are covered in Chapter 7. Here the system will be simulated for the first time as a whole, with all the components defined as the pre-discussed units in previous chapters. Up to this point in the study, certain assumptions were made regarding components such as heat exchangers and the combustor. Here, all known boundary conditions and limitations will be entered into the system. With all of this information available, a steady state model will be simulated for evaluation. The system will run with all components interacting with each other, influencing, while being influenced by others, to reach steady state where all degrees of freedom are in balance with the system boundaries and limitations.

Different transient conditions will then be simulated to verify the operation of the micro gas system at different conditions. These conditions will include start-up, steady load following and sudden load following like load rejection. Investigation into the micro gas turbine system's reaction to these operational inputs will be done in Chapter 7, where the designed micro gas turbine system's output under different conditions will be illustrated.

2 Theoretic al background

In order to achieve the objective of this study, as stated in Chapter 1, it is necessary to obtain more theoretical information about micro gas turbine machinery and the thermal dynamics. The purpose of this chapter is to provide background on the underlying technology of small gas turbine generators and their evolution, which led to the current state of micro gas turbine systems. This is followed by information on the ideal Brayton cycle and its variants. The design process and the role of systems simulation in modern thermal-fluid systems are discussed, followed by a review of recent developments in micro turbine technology.

2.1 INTRODUCTION INTO THE LI TRATURE SURVEY

Since the first gas turbine was patented in 1791, the gas turbine has evolved alongside technology aimed mostly for the aircraft industry. Technology dedicated solely to gas turbine power generation is a recent trend resulting in a new, but highly competitive technology (with a long track record in the aircraft industry), [Islas 1999]. "Micro gas turbine" is a term used in various fields, i.e. model jet fighters, small spy drones and the production of electricity to name a few. In this study, the term 'micro gas turbine' will be used when referring to small turbine systems, approximately the size of a refrigerator, with internal combustion and generating 20 – 200kW of shaft power.

2.2 MARKET FOR MICRO GAS TURBINES GENERATORS

Micro gas turbines can be used for power generation in the industrial, commercial and residential sectors. They could be used for continuous power generation, premium power, peak skimming, emergency standby, remote power, combined heat and power, mechanical drive, and wastes and bio-fuels burning. Industries that have the best potential for micro gas turbines include chemical, food and drink, pulp, paper and textile industries, while remote power application include off-grid locations such as oil, mining and the tourism operations. The market for wastes and bio-mass burning micro gas turbines are found in industries that produce fuel as a waste or by-product such as pulp, paper and food processing and mining operations.

Combined heat and power (CHP) systems may be the biggest use for micro gas turbines yet. The exhaust temperature of the micro gas turbine is at elevated temperatures and can be used to produce heat for industrial processes or space heating. In order to achieve high efficiencies, micro gas turbines use a recuperator to increase the electrical efficiency, but result in a lower exhaust temperature. In CHP applications, micro gas turbine plants could achieve overall thermal efficiencies of 80% [Pilavachi 2002].

Power failures in the United States, Europe, Asia and Africa proved that existing power suppliers are not capable of providing electricity to all of their customers. During August 2003, London (England) experienced a blackout that left hundreds and thousands of commuters stranded. The blackout was due to a failure in the national grid [CNN 2003/08/29]. Earlier the same month, North America and Canada were hit by a massive blackout, disabling cities from New York to Detroit and Toronto to Ottawa. More than 50 million people were affected by these incidents. The American Stock Exchange, New York Stock Exchange, NASDAQ and hospitals were not affected by this blackout as all of them had back-up power generators. A spokesman for the group that supplies power in seven states in the District of Columbia stated the blackout was caused by a major power drain outside their district and that the grid was not capable of transferring that much power [Terrett & Carter 2003].

Across the United States there have been numerous reports of electrical systems pushed to the limit due to the lengthy and acute power shortage during the previous three summers. Rolling blackouts have struck San Francisco, San Diego and other California cities, costing millions of dollars in losses to business productivity [Find 2003].
With the increased use of technology requiring electricity together with the increased number of people requiring access, there are growing concerns worldwide that the electrical power generated will not satisfy the power needs. The South African electricity suppliers not only have to provide for the power need of South Africa, but also that of its neighbouring countries.

Namibia, Zimbabwe, Lesotho and Swaziland also depend on South Africa to provide them with electricity.

Zimbabwe has not been able to increase its electrical generation capacity since 1985 even though demand has been growing steadily. The country imports about 40% of its electrical power from its neighbouring countries [Kayo 2002]. Because of the remoteness of villages in Africa, no real effort is made to link all of them to the existing grid. These remote villages and businesses will benefit by using distributed power generation. The onsite generation of electricity is known as disrupted generation, which offers several advantages over grid provided power. Distributed generation replaces back-up generator by offering a reliable, high quality source of power, [Klett & Wilson 2001]. By providing for their own needs and that of their immediate neighbours, the village will be self sufficient and thus promoting the villagers.

Recently South Africa also encountered major power failures in the Western Cape Province during February 2006. The Koeberg nuclear power facility experienced a failure, and shut down, leaving a big part of the Western Cape without electrical power. Serious consideration in order to install a second nuclear power plant, (in addition to the planned pebble bed modular reactor) is underway. [NAN, 2006]. ESCOM, the South African electricity supplier lost all its credibility as a power supplier [O'Conner, 2006]. Businesses in Cape Town are considering installing back-up stand alone, mobile power plants to ensure that they always have electrical power, thus not relying on ESCOM for providing them with power.

As stated earlier in this study, micro gas turbine generators are able to reduce the load on electrical power provision installations, while providing the owner reliable, high quality and economical feasible alternatives than to be dependent on the already overloaded distribution systems.

2.3 COMMERCIALLY AVAILABLE SYSTEMS

A number of micro gas turbine generator systems available are commercially. Companies like Capstone Turbine Corporation, Elliot Energy Systems and Ingersoll-Rand to mention a few [DER 2003]. More that 20 companies worldwide are involved in the development and commercialization of micro turbines. According to Preston [2003] Capstone enjoys approximately 85% of the market, Elliot Energy Systems represent 4%, and Ingersoll-Rand has a 3% share. The remainder [8%] is made up by a number of smaller companies.

Capstone provides a system with a configuration that is developed in such a way that the induction air is drawn past cooling fins that surround the generator before entering the one stage, centrifugal flow compressor. The generator is cooled, but the intake temperature increases. The air is then forced into the metallic, counter flow, prime surface recuperator where it is pre-heated to around 600 °C before it enters the combustion chamber. Capstone uses an annular, reverse flow combustor, and uses a dry, lean premixed combustion system where fuel is added and the mixture combusts and expands through the single stage, radial inflow turbine driving the compressor and generator at speeds of up to 96 000 min^{-1} [Capstone 2006]. Air bearings also feature in this system and models are produced that run on natural gas or propane [Autospeed 2002].

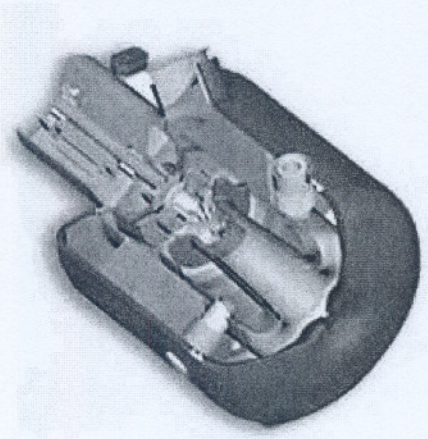

Figure 2.1: Illustration of the Capstone micro turbine (Capstone, 2006)

Elliot developed their micro turbines primarily with power generation in mind. A high speed alternator mounted directly to the turbine shaft is used by Elliot. This enables them to increase their electrical efficiency (from their previously reduced gearbox driven generator), and thus reduce maintenance costs. The output voltage is filtered by changing the high frequency AC voltage to DC and back to AC again, by a high frequency inverter / rectifier system in a computer controlled [Ebra 2006].

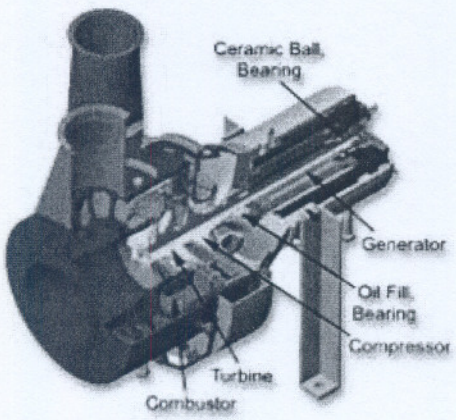

Figure 2.2: Illustration of the Elliot micro turbine (Ebara, 2002)

Capstone and Elliot developed their own technologies, including turbines, compressors, combustion chambers and systems, recuperates, as well as their generation systems. Both also use single shaft configurations.

Micro gas turbines are currently available in the following power capacities.

Capstone:	30 kW and 60 kW
Ingersoll-Rand	70 kW and 250 kW
Elliot	80 kW and 100 kW

This indication reflects that a vacancy exists in the market for micro gas turbines providing electrical power in the 50 to 75 kW range as well as in the range higher than 100 kW, but only up to 200 kW.

A gas turbine power plant p rovides a magnificent amount of energy for its size and weight, therefore has shown increased demand in petrochemical industry and utility applications throughout the world. Its compactness, low weight, and multiple fuel application make it a natural choice for a power plant on remote and off-shore applications [Boyce 1982].

Now that the growing market for micro gas turbine generators have been stated, as well as the shortcomings of commercially available systems, it is logical to investigate the possibility of developing a small micro gas turbine generator system that will be able to provide to al the requirements. These requirements include: a reliable power source, generating high quality electrical power on remote spots, with the minimum maintenance, running of a variety of fuels, with the option of stand alone or integrated installations, generating 50 – 80 kW of electrical power.

Since most of the micro turbine generator systems are based on the Brayton cycle, the next step is to investigate this cycle. The different variants of the Brayton cycle will be evaluated, together with known technologies. These systems and layouts will be evaluated by using various software packages. Simulation of systems with the use of computer software in order to evaluate them have the advantage that the designer can evaluate any number of systems, without actually building all of the systems, therefore saving a large amount of money. More on the advantages of simulation later in this study, but, the software that will be used during the design process are: Engineering Equation Solver [EES], C++, Matlab and Flowex®

2.4 THE BRAYTON CYCLE

The ideal Brayton cycle is the theoretical cycle which forms the basis for the design of most modern gas turbines. An illustration of the ideal open Brayton cycle is shown in Figure 2.3.
Since shaft work is applied to the working fluid during the compression stage, both the temperature and pressure of the fluid will rise from 1 to 2, as shown in Figure 2.4. Heat is added in the combustor at a constant pressure from 2 to 3. This combusted gas then expands through the turbine, transferring heat energy into shaft power, dropping the temperature and pressure of the working fluid over the turbine between 3 and 4. Figure 2.4 shows these changes in a temperature – entropy [Ts] diagram for the ideal cycle

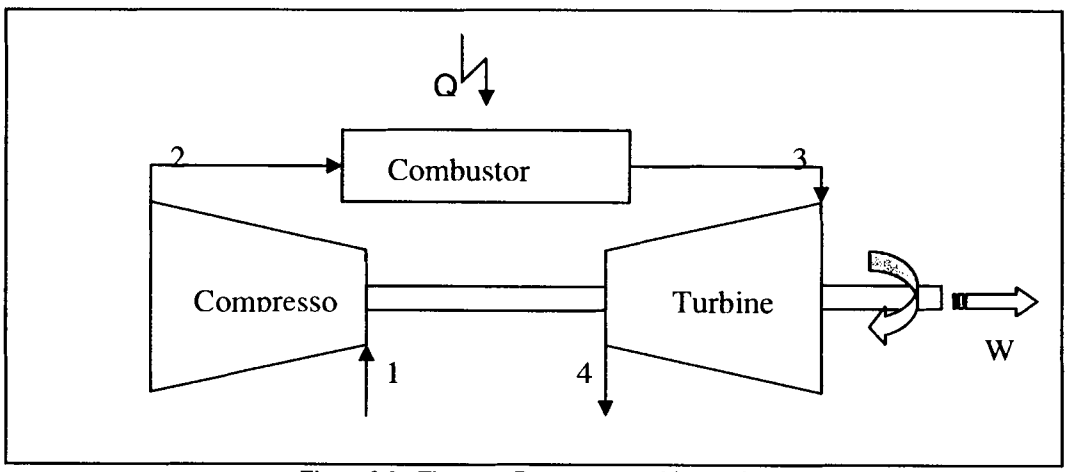

Figure 2.3: The open Brayton gas turbine cycle.

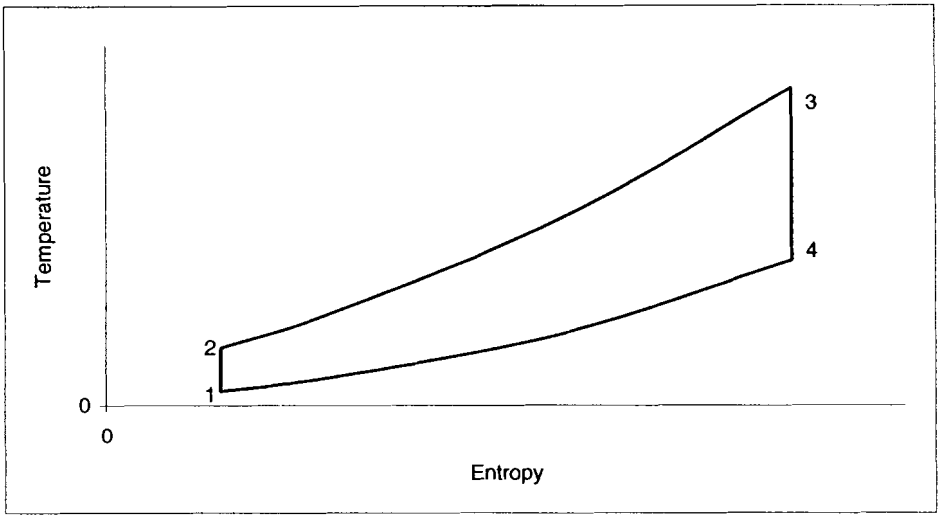

Figure 2.4: Ts diagram of the ideal Brayton cycle.

The real Brayton cycle differs from the ideal cycle because of losses in turbo machinery, heat exchangers, flow passages and combustion chamber. The deviation of actual cycle from the ideal cycle is shown in Figure 2.5. It is shown that the entropy changes during the compression and expansion stages, while isobaric combustion is not achieved, as assumed in the case of the ideal Brayton cycle.

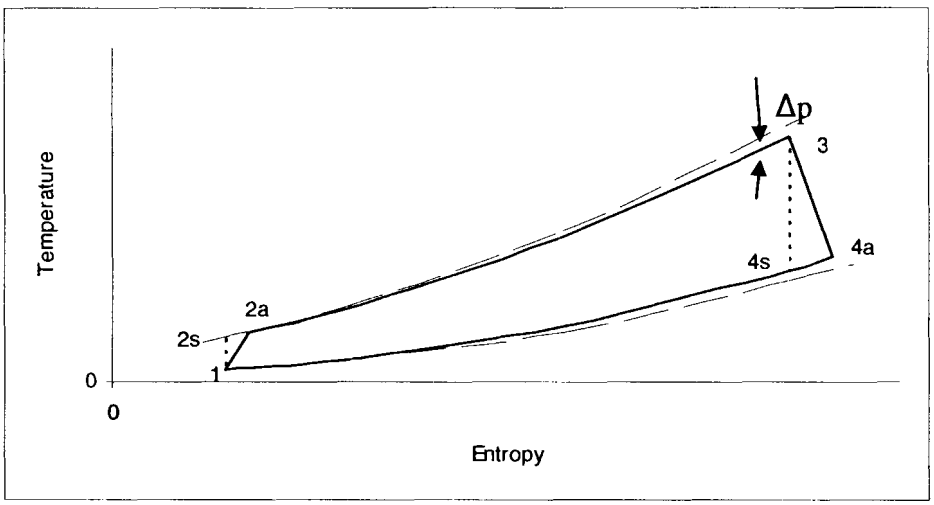

Figure 2.5: Ts diagram of the real Brayton cycle.

It is important to understand the difference between the real and ideal Brayton cycles, and the implications of these differences have on the design and simulations of gas turbine machinery. A thorough discussion on the real and ideal Brayton cycles can be followed in Appendix A. Also included in this discussion are some of the common variances that the Brayton cycle generally has, which include recuperation and multi-shaft configurations.

A characteristic of gas turbines is their high exhaust temperatures and by utilizing this heat, preheating the compressed air before combustion, it is possible to reduce fuel consumption and thus the energy needed by combustion. The cold inlet air never comes in direct contact with the hot exhaust gas, thus only exchanging heat in the recuperator. An illustration of the recuperated

Brayton cycle can be seen i n Figure 2.6, followed by the temperature – entropy [Ts] diagram in Figure 2.7. The temperature difference of the cold gas $(T_2 - T_3)$ is equal to the temperature difference of the hot gas $(T_5 - T_6)$ and the recuperator efficiency is defined as actual heat exchanged over the maximum heat difference of the heat exchanger:

$$\eta_{rec} = \frac{(T_3 - T_2)}{(T_5 - T_2)} \qquad \text{Eq 2.1}$$

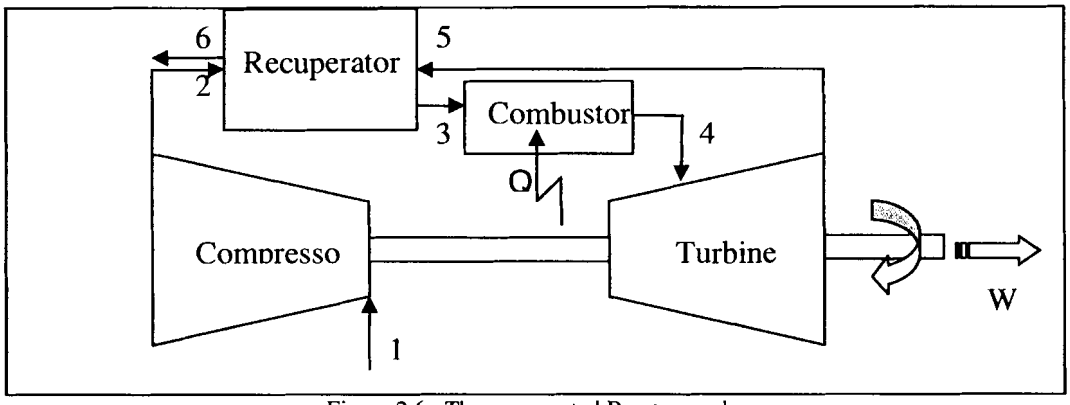

Figure 2.6: The recuperated Brayton cycle.

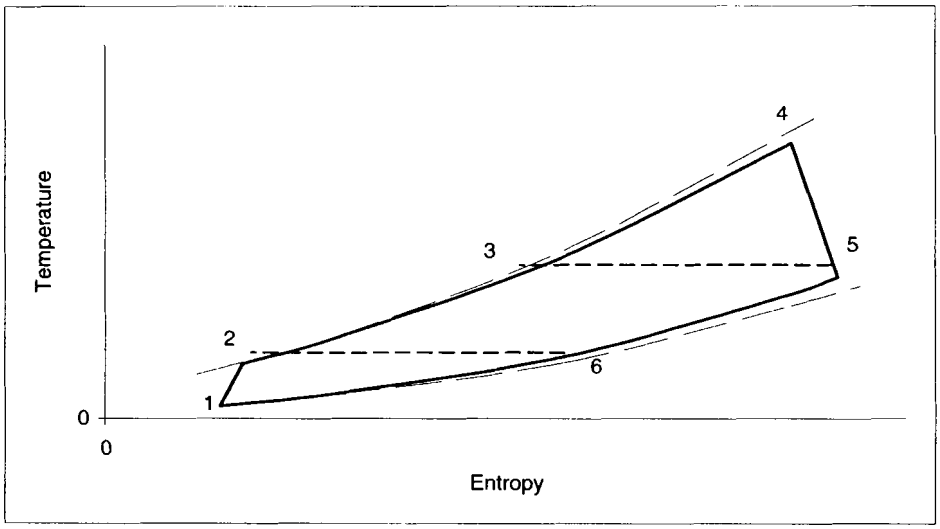

Figure 2.7: Ts diagram of the recuperated Brayton cycle

The specified work output differs only slightly from that experienced with the real Brayton cycle, and will not be evaluated in this part of the study.

The recuperator increases the temperature of the air entering the combustor, which leads to a reduction in the fuel-to-air ratio and an increase in the thermal efficiency. The thermal efficiency is thus a function of the recuperator efficiency $\left[\eta_{th} = f(\eta_{rec})\right]$. The effect of different recuperator efficiencies ranging from 80% to 95% are shown in Figure 2.8. A detail discussion of the recuperator and the design thereof will follow in Chapter 5.

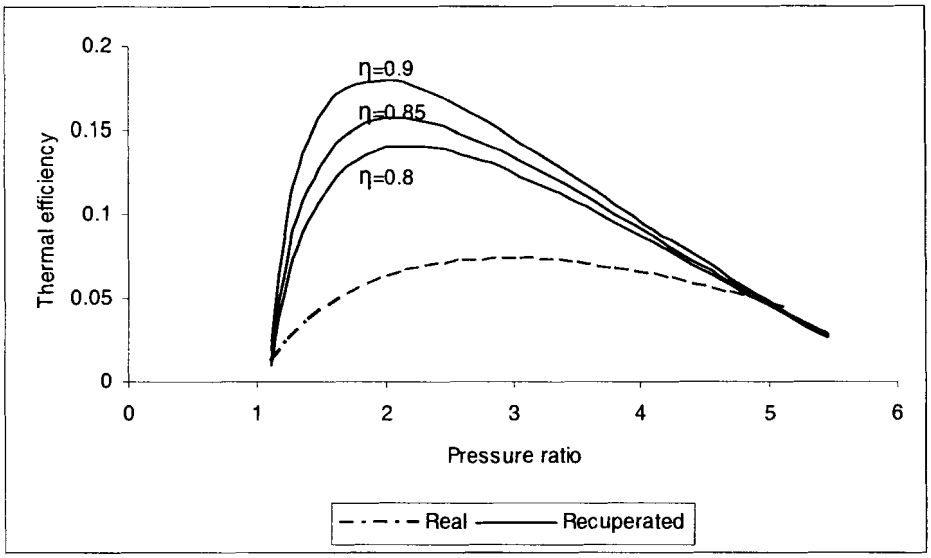

Figure 2.8: Thermal efficiency as a function of pressure ratio of the recuperated Brayton cycle.

The comparison between the recuperated Brayton cycle and the real Brayton cycle is also shown in Figure 2.8. This proves that a system's efficiency can be boosted by utilizing the heat of the exhaust gas [also known as waste heat], but note that this is limited by both too low and high pressure ratio values. An optimum operation pressure ratio value needs to be found, and will be discussed during Chapter 3 and 4 of this study.

The above discussions on the variations of the Brayton cycle should be sufficient to outline the characteristics of some of the variations of these cycles. With this overview of gas turbine cycles one can begin to understand the complexity of these machines. The complexity and influences will become clearer during the discussion of the design process

2.4.1 Performance of gas turbine systems

An investigation into a wide range of different parameters that affect the performance of gas turbines was done, and the conclusions made by Badran [1999] that the location of the plant plays an important role as the compressor inlet temperature depends on ambient conditions. Thermal efficiency improves as the inlet air temperature decreases. Pilavachi [2000] stated that an increase in output power is possible by using the exhaust gases to power a refrigerator system. By decreasing the inlet temperature of the system, it is possible to increase the turbine output work.
The efficiencies of the compressors and turbines affect the characteristics of the gas turbine system.
An optimum pressure ratio value exists where maximum cycle thermal efficiency occurs.
The turbine's inlet temperature (TIT) is directly linked to the cycle efficiency. Higher TIT increases the net work and system efficiency. Pilavachi [2000] reported that the TIT is normally limited by metallurgical restrictions set by the material characteristics of the turbine blades. The increase in TIT is achieved by development of better materials, including ceramics or thermal barrier coatings (TBC) and with the aid of blade cooling techniques. Next generation engines will be expected to operate at TIT's of above 1500°C
TIT is dependent on the combustion chamber efficiency.
Steam and water injection into the combustor is also a practice used to boost power in various applications. By injecting steam into the combustion chamber, the gas mass flow is increased and

expands simultaneously with the gas through the turbine [Wang & Chiou 2002]. Since the specific heat of steam is more than that of air, the enthalpy and exergy (work potential) of steam is higher than that of air per unit flow rate.
Water is injected into the combustion chamber to reduce emissions and to boost power, but it leads to a decrease in thermal efficiency. Water injection also leads to a decrease in un-burnt hydrocarbon emissions [Pilavachi 2000].

2.5 THE DESIGN PROCESS

The design process will consist of different phases building on each other, resulting in a conceptual design of a micro gas turbine machine, complete with simulation models of the performance of the designed model.

First order system analysis will be the first phase where different system configurations are compared, while setting the optimum range for the levels of the performance parameters: [Pr, TIT and η_{rec}].

Phase Two will start with re-evaluating the system analysis with all of the Phase One's conditions, at every point of the cycle known. During this stage of the design process, preliminary boundary conditions are to be fixed for each component. Aspects such as the mass flow rate of the working fluid, temperature and pressure should be known at each point of the cycle in order to make reasonable decisions regarding system operations. These operating conditions determine the thermal efficiency and specific work output of the system, as well as the design and size of the individual components. The designer is challenged to find the best arrangement for both thermal efficiency and specific work output, while maintaining minimum life cycle cost.

Phase Three consists of the detail design of the system's components. Each of the components needs to be designed according to the specifications set by the system's configuration boundary conditions (Phase Two). These components include the heat exchangers, combustion chamber and connecting ducts. An important factor during the component analysis is the thermodynamic design simulations. These are detailed calculations, taking into account all important aspects such as the expected component efficiencies, air-bleeds, variable fluid properties and pressure losses, which are carried out over a wide range of pressure ratios and turbine inlet temperatures.

In this stage, the design of the micro gas turbine is concluded for the specific pre-determined boundary conditions and operating conditions. However, the machine's performance at off-design conditions needs to be evaluated. Phase Four of the design process evaluates the performance of the micro gas turbine by using a simulation model that enables the designer to evaluate the system over a wide range of conditions. The difference between design and simulation is defined as: Design refers to a situation where the characteristics of a system need to be specified so that it will enable the execution of specific functions, at an acceptable level of performance. Simulation refers to a situation where the characteristics of the system are known and models must be set up to predict its functionality and performance level [Rousseau 2002].
System simulation is the calculation of operating variables (mass, momentum and energy transfer) in a thermal system, with the addition of performance characteristics of all components as well as the thermodynamic properties of the fluid used in the system. A set of equations relating to the operational variables is formed by simultaneously using performance characteristics equations of the components and properties with the balances for mass and heat. Therefore, the mathematical description of system simulation is the implicit or explicit solving of

the relevant equations. The definition of a system is a collection of components that are linked together to achieve something that the individual components could not achieve, thus their performance parameters are interrelated. System simulation means observing a system that imitates the performance of a real system. There are two main types of system simulations: first, where the simulation is done by calculation procedures and the other is where a physical system is simulated by observing another physical system. An example of this is the heat-flow system in a solid wall that is represented by an electrical system of resistors and capacitors [Stoecker 1989]. These types of simulations are done as part of Phase Four, but considering steady state conditions only.

The designer is responsible for selecting realistic values for the operating variables and corresponding components. Besides being useful in the optimization of the system at specified design conditions, simulation may also be used to predict the system performance at off-design conditions (as done in Phase Five). This will enable the designer to identify and understand possible operating and control problems. Situations like these are typical during part load and start-up conditions. Simulations are also used extensively in component failure tests. If these failure tests were done on a physical model, they would be destructive and the resulting costs would be very high. All possible tests, faults, failures and conditions can be tested on a simulation model, without the risk of cost and safety. The ability to, and the advantage in simulating the performance of a component or a system, prior to building it, has gone from a "nice-to-have" to an "absolute necessity" reported Stone [2003].
System simulations are used during optimization of components and systems alike to improve the design or they can be applied to existing systems to evaluate potential modifications. In this study various simulation processes will be done. Each of these simulations will be discussed in the study where they are relevant.

The design process is concluded by showing the physical layout configuration of the system, where all the components are placed while ensuring that all the parameters of the layout are within specifications. Phase Five also illustrates the interaction between the system and the auxiliaries needed by the system.

2.6 CONCLUSION

A miniature literature study will be conducted during the discussion of most of the components and subsystems as this study progresses. However, the theoretical background given in this chapter indicates that a recuperated system is to be used if a highly effective micro gas turbine system with good useful output work is needed. Variations of the real Brayton cycle layouts make different configurations possible, each with its own characteristics. These configurations will be analysed and optimized in Chapter 3, where a sensitivity analysis will be done. The development done recently, together with component development will be taken into account when system analysis is done in Chapters 4 to 6.

3 Cycle analysis and optimization

A background study of the micro gas turbine theory was undertaken in the previous chapter where different cycles were evaluated. However, a more detailed investigation into the different layout configurations is needed. Thus, the first phase of the design process, as discussed in Chapter 2, calls for cycle configuration comparison, evaluating certain cycle configurations and identifying the best suitable configurations for this application. A sensitivity analysis will be done in this chapter to establish the effect different parameters have on the cycle as mentioned during the theoretical background.

3.1 INTRODUCTION INTO THE CYCLE ANALYSIS AND OPTIMIZATION

Comparison of the cycle layouts can only be done through cycle configuration analysis, where each of the cycle's performance parameters is evaluated under given conditions. Performance parameters that will be evaluated are the thermal efficiency $[\eta_{th}]$ and specific work output $[W]$ of the given cycle.

The differences between ideal and real cycles will be discussed and analyzed in detail during this chapter. These evaluations will be done with computer aided simulations that enable the designer to evaluate the effect that different operating conditions have on the cycle's performance. Simulations used in this part of the study were programmed in Microsoft Visual C++ and is given in Appendix A, while the mathematical algorithms simulating all the processes are presented in Appendix B.

Performance of micro gas turbines is governed by certain operating parameters, and the effect these parameters have on the turbine's performance will be proven by evaluating the following parameters: the overall pressure ratio [Pr], minimum temperature [T_i], turbine inlet temperature [TIT], recuperator efficiency [η_{recup}] and compressor and turbine efficiencies [η_c and η_t]. The same set of boundary conditions will be used during the evaluation, in order to do a just comparison.

As mentioned previously, most modern micro gas turbine machines consist of two main components (compressor and turbine). Designs of micro gas turbine machines revolve predominantly around the compressor and turbine and their operating boundaries.

This chapter should give the reader an in-depth understanding of the gas turbine cycle and the effect different parameters have on the systems output

3.2 CYCLE ANALYSIS

The following conceptual cycles is investigated in Appendix A:

- Brayton cycle without recuperation. (As discussed in the previous chapter.)
- Brayton cycle with recuperation. (Similar to above, but with a recuperator added.)
- Two-stage compression with inter-cooling and recuperation. (Brayton cycle with a recuperator, two stage compression and inter-cooling.)

These different cycles were evaluated and the best suited configuration was established to be the two-stage compression with inter-cooling and recuperation [TCIR] cycle. The detail analysis and comparison can be followed in Appendix C.

3.3 SENSITIVITY ANALYSIS

The performance of the TCIR cycle is dependent on a number of variables, which are factors of components, gas properties, and configuration between these components. Parameters that influence the output of a system include the overall pressure ratio, inlet temperature, turbine inlet temperature and recuperator efficiency. A sensitivity analysis will be done where the influence of these parameters on the performance of the cycle will be determined by varying individual parameters under controlled conditions.

3.3.1 Pressure ratio

The effect of change in pressure ratio is shown in Appendix B, and will not be repeated in this part of the study. From the work done previously, there is an optimum overall pressure ratio value that will be calculated for specific operating conditions. The effect of variations in overall pressure from the optimum value will be discussed alongside the influence of TIT in the following section.

3.3.2 Maximum turbine inlet temperature

The effect of the maximum TIT on the thermal efficiency and specified work output can be calculated by using thermodynamic equations and properties that are included in Appendix C. The results are illustrated in Figure 3.1. It shows that higher TIT values increase both the cycle's specific work output and thermal efficiency for a constant overall pressure ratio of 3.

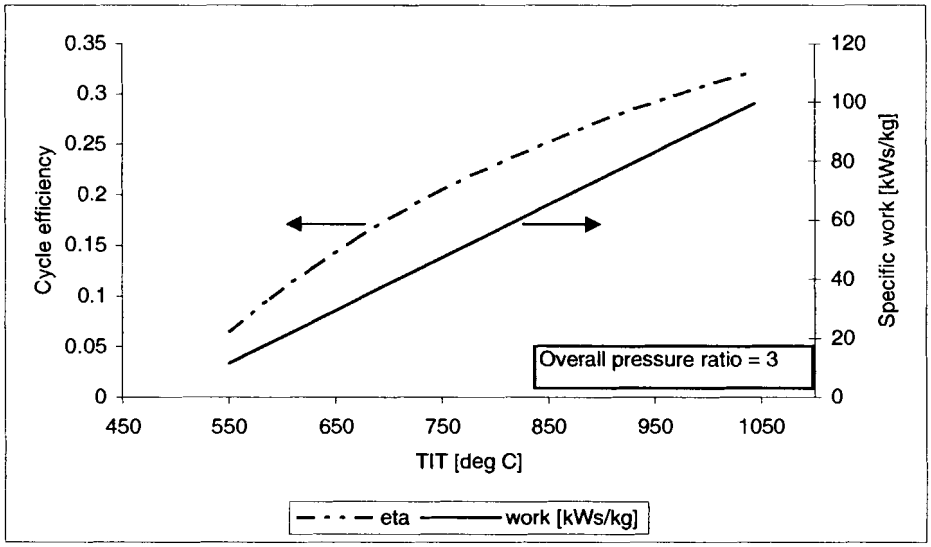

Figure 3.1: Cycle efficiency and specific work as a function of TIT.

As the TIT increases, the value of the optimum pressure ratio increases. The optimum pressure ratio for efficiency differs from the optimum pressure ratio for specific work. Figure 3.2 shows both the cycle efficiency and the specific work as a function of TIT and pressure ratio.

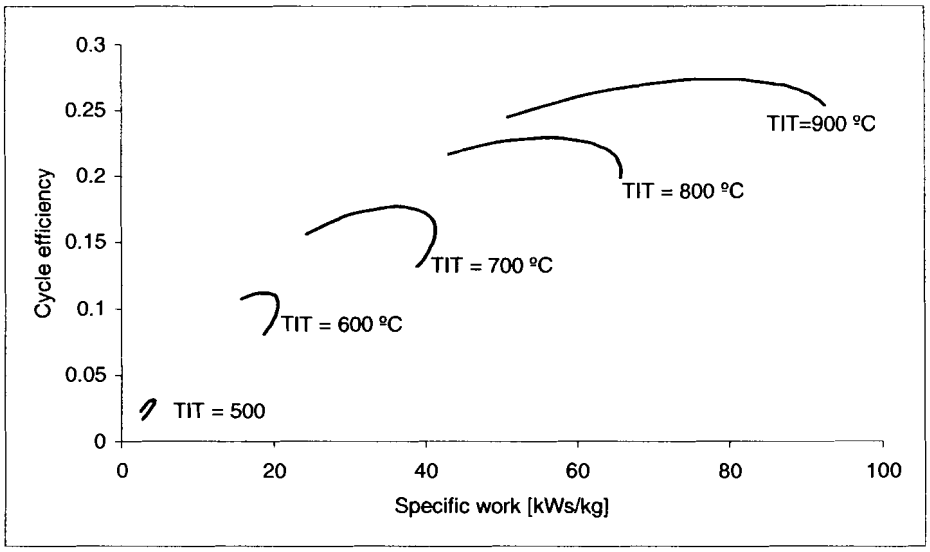

Figure 3.2: TCIR performance map for optimization of TIT and overall pressure ratio.

Maximum cycle temperature is limited by metallurgic considerations. Due to the mechanical stress of turbine blades during operation, it is important that the blade temperature must be kept at a safe working value, limited by the material of the blades. TIT can be raised providing that blade cooling occurs. An investigation into this technology will not be done in this study. Therefore, maximum safe TIT will be limited to 700 °C for this study.

Figure 3.3 is an enlargement of a part of the curve in Figure 3.2 and represents a TIT of 700 °C. At optimum thermal efficiency [Point A] the curve's gradient is shallow; indicating that a small change in thermal efficiency can cause a huge change in specific work. Whereas, with the sharp gradient at point B, a small change in specific work output results in vast changes in the thermal efficiency of the cycle. There has to be a compromise between thermal efficiency and specific work output to select an operating point for the cycle.

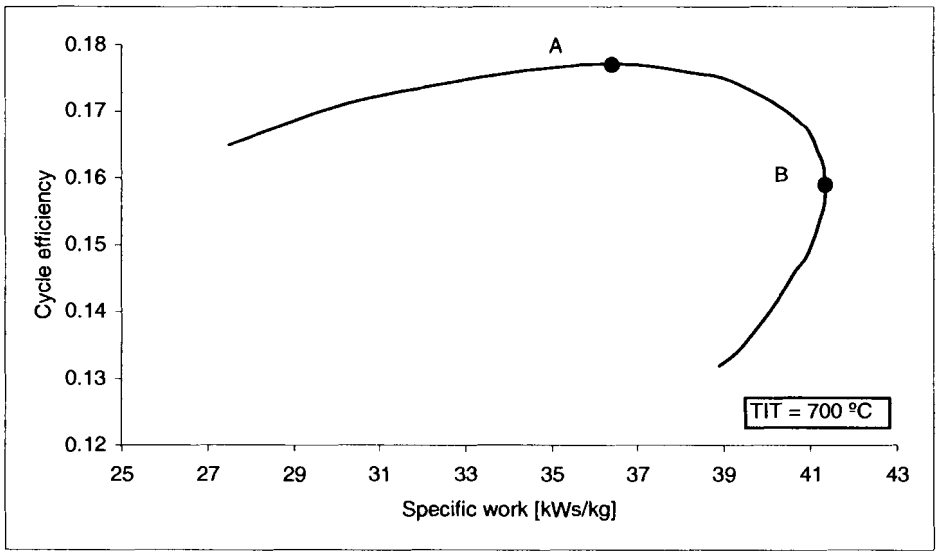

Figure 3.3: Optimum cycle efficiency versus optimum specific work.

3.3.3 Minimum temperature

The performance of the gas turbine unit is particularly sensitive to the minimum temperature of the compressor inlet air. Higher cycle efficiencies are achieved by decreasing the compressor inlet temperature as illustrated in Figure 3.4.

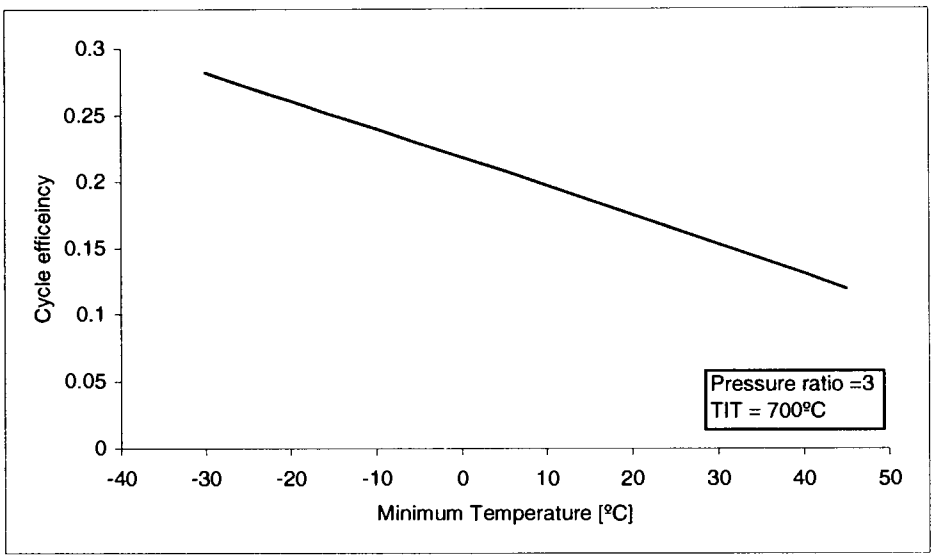

Figure 3.4: The effect of minimum temperature on the cycle efficiency.

It may be necessary to cool the compressor inlet air to produce high cycle efficiency in areas with high ambient temperature.

3.3.4 Recuperator efficiency

The energy that is needed by the compressed air to reach TIT at the exit of the combustor is achieved by the exothermal chemical reaction between fuel and oxygen in the combustion chamber. The temperature difference between that of the TIT and the combustor inlet temperature is directly related to the system's thermal efficiency. The thermal efficiency is a function of the specific work output and the energy needed by the system. $\left[\eta_{th} = \frac{\dot{W}_{nett}}{Q_{in}}\right]$. By reducing the temperature between the TIT and the combustor inlet temperature, the energy needed by the system is reduced, which improves the thermal efficiency. This is done by adding a heat exchanger that utilizes the high temperature exhaust gas to heat the gas entering the combustor. This application is discussed in the previous chapter and the effect of this heating of gas can be seen in Figure 2.11, which is an illustration of a temperature – entropy diagram of recuperation.

The recuperator is a heat exchanger that uses the energy in the exhaust gas [waste heat] to heat the compressed air before combustion, thus lowering the energy requirements of the combustion system. High recuperator efficiencies result in high thermal efficiencies as seen in Figure 3.5, but no significant effect on the specific work output.

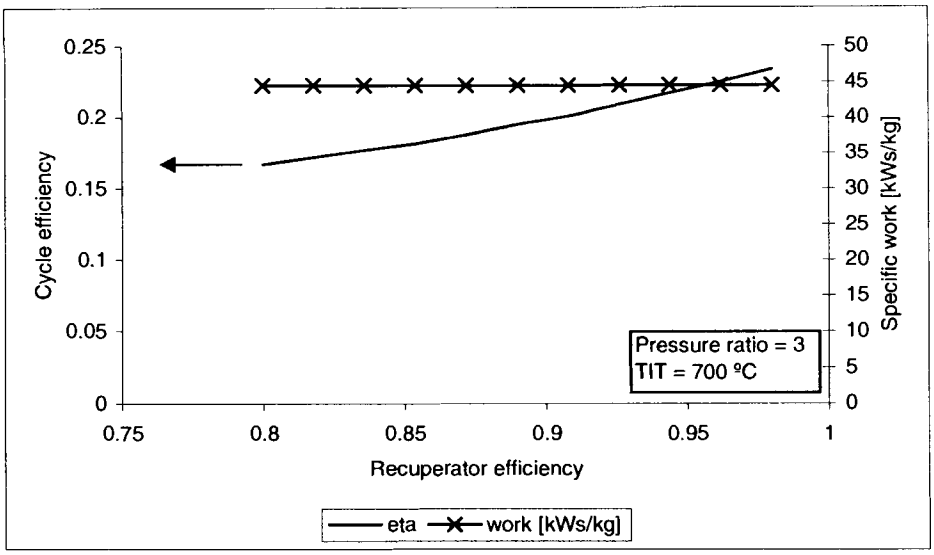

Figure 3.5: Cycle efficiency and specific work as a function of recuperator efficiency.

In order to see the effect that a recuperator has on the system, it is necessary to plot a curve that illustrates the combined effect of the recuperator efficiency and the overall power ratio on the performance of the micro gas turbine system. Investigation of Figure 3.6 proves that the optimum value for the pressure ratio becomes smaller as the recuperation efficiency increases.

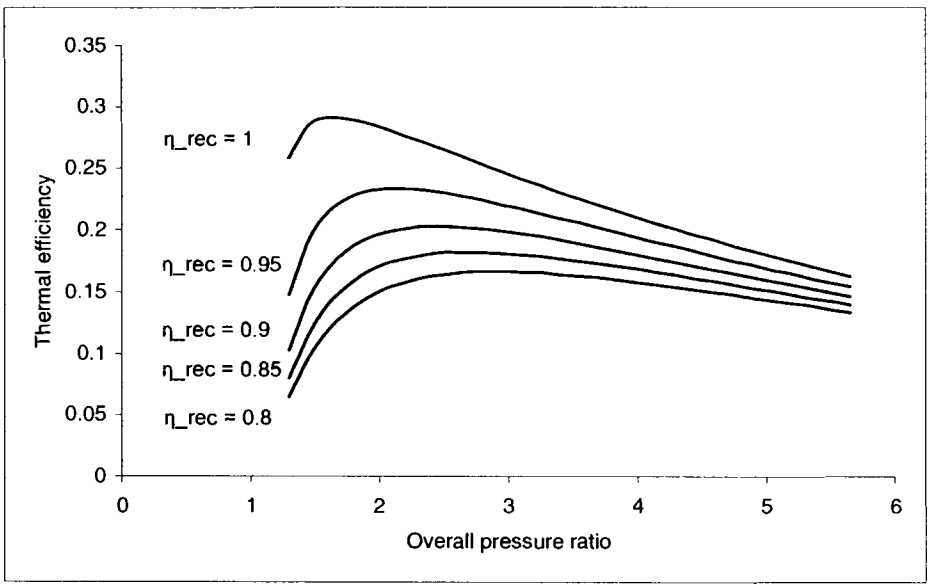

Figure 3.6: Cycle efficiency as a function of recuperator efficiency and overall pressure ratio.

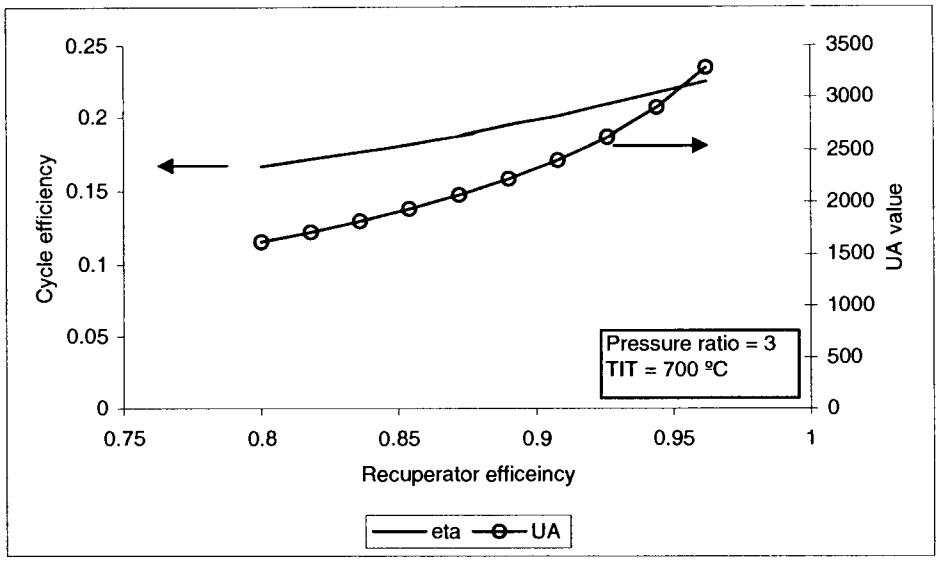

Figure 3.7: The effect of cost (UA) versus recuperator efficiency.

Recuperators with high efficiency levels need large heat exchange areas resulting in high costs. Figure 3.7 illustrates the relation between the recuperator efficiency and the UA value of the recuperator. The UA value represents the heat transfer capacity of the recuperator, therefore the cost of the heat exchanger. System cost increases exponentially at high efficiencies, therefore recuperation efficiency is usually compromised to reduce the cost of the recuperator. Recuperator efficiency of approximately 90 % will therefore be accepted for the rest of this study.

A detailed investigation into recuperator design will be done in Chapter 5 of this study.

3.3.5 Turbo machinery efficiency

The effect of compressor and turbine efficiency can be seen in Figure 3.8 and Figure 3.9. Both result in an increase in thermal efficiency and specific work as the component's efficiency increases.

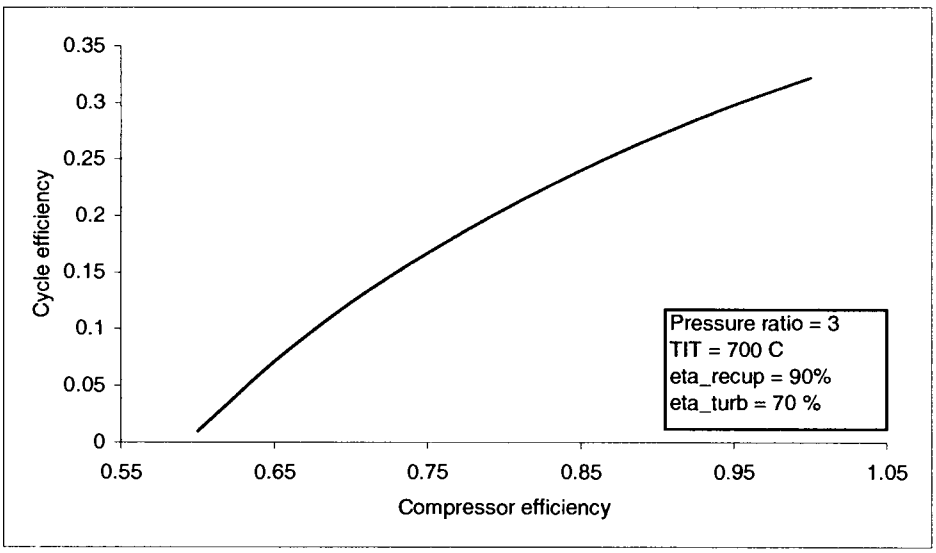

Figure 3.8: The effect of compressor efficiency on the cycle efficiency.

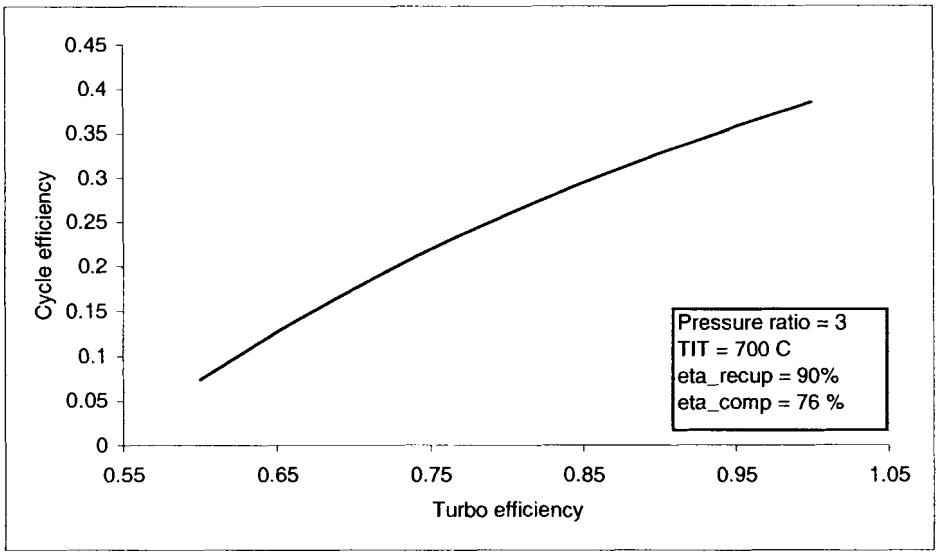

Figure 3.9: The effect of turbine efficiency on the cycle efficiency.

To assume that the components in the system will operate at certain efficiency levels will be wrong. The operating point of the components is the driving force behind efficiency. The same component can have a high efficiency at certain operating conditions, while experiencing low efficiencies at slightly different operating conditions. The detailed selection process of the turbo machines is outlined in Chapter 4.

3.4 POSSIBLE OUTPUTS FOR THIS CYLE

It is possible to generate a system with components that operate at better efficiencies and with fewer losses than the system used in the simulations up to now. Unfortunately, components with high performances are normally very expensive and could therefore not be used in this study. The turbo machinery used in this cycle, usually applied in the commercial sector of the automotive industry, has efficiencies of 80% for the compressor and 85% for the turbine. Recuperator efficiencies as high as 95% are achievable if cost considerations are not a limitation. Therefore, if a system is built for high efficiencies as mentioned above, the performance can be predicted and is illustrated in Figure 3.10.

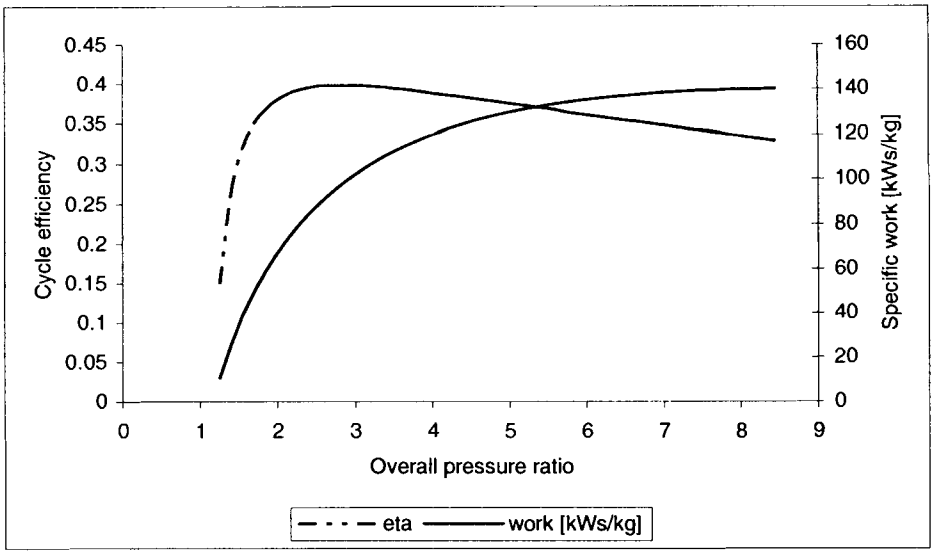

Figure 3.10: Possible efficiency and specific work output for the TCIR cycle.

This cycle will operate under higher pressure ratios and will operate at a higher efficiency, delivering higher specific work output than the TCIR cycle with boundary conditions as set in the cycle analysis section. If technology and components become cheaper in future, the TCIR cycle could achieve similar performances to those shown in Figure 3.10. The current TCIR cycle as described in Section 3.2 will be investigated for the remainder of this study due to lack of financial support to acquire the technology and components needed to build the cycle described in Section 3.4.

3.5 LIMITATIONS DUE TO THE CYCLE ANALYSIS

The sensitivity analysis produced the following results as starting parameters in order to do the cycle analysis. These results will be refined during the next chapters to comply with real components and boundary conditions.
The optimum pressure ratio range for the TCIR cycle is limited to 1.9 – 4.2. The pressure ratio range is limited due to the evaluation done in Section 3.3.1 where output work and cycle efficiency were considered as a function of overall pressure ratio. For this study an investigation will be done to see the effect the pressure ratio has on the cycle.
Minimum temperature is equal to ambient conditions and is set to 26 °C.
Due to turbine blade material characteristic constraints of the automotive turbo machinery, the maximum safe operator TIT is set at 700 °C.
Recuperator efficiency is equal to 90% by compensating on efficiency for cost.
Turbo machine efficiencies will remain equal to the assumed values of 76% for the compressor and 70% for the turbine, but will be refined during the next chapter where an investigation into the choice and matching of turbine machinery will be done. This matching will be done at different pressure ratios.

3.6 CONCLUSION

Evaluation of the real Brayton cycle layouts proved that the two-stage compression with inter-cooling and recuperation cycle layout [TCIR] generates the best performance when considering both work output and cycle efficiency. The limitations for this particular micro gas turbine layout are highlighted through a sensitivity analysis. The best possible outputs for this layout are

calculated and can only be achieved if more time, money, technology and research are to be invested in a study into this.

The next step will be to select turbo machinery (each consisting of a compressor and a turbine) that is capable of operating under the condition specified for the micro gas turbine. A discussion that explains the different types of turbo machinery will be done before different combinations of available machinery are evaluated in order to choose the best suited units for this application. The selection process of the turbo machinery, as well as a comparison between "off-the-shelf's' and custom designed turbo machinery will be done in Chapter 4.

4 Selection of turbine machines

Different cycles were analysed in the previous chapter, along with the effects of drifting values of various parameters. It was proven that the most promising cycle of those analysed was the two-stage compression cycle with inter-cooling and recuperation [the TCIR] cycle. The selection of turbine machinery to be used in a system based on the TCIR cycle can now be done.

4.1 INTRODUCTION TO TURBINE MACHINES

This chapter examines the performance characteristics of compressors and turbines, as well as the effect that the cycle operating point has on the outputs of the TCIR cycle. Different types and configurations of turbine machinery will be evaluated before comparing the benefits and disadvantages of custom designed turbine machinery versus the selection of available turbine machinery. Thereafter the process of selection and matching of turbine machinery will follow.
At the end of this chapter, the reader should be familiar with the behaviour of the turbine machinery used by the TCIR cycle and will have some knowledge of the complexity of the selection options of these machines. The results of this chapter will enable the system designer to start with the designing of the other components of the system.

4.2 CHARACTERISTICS OF TURBINE MACHINES

The overall performance characteristics of turbines and compressors will be evaluated in this part of the study. These machines have a common characteristic: the main element is a rotor with blades or vanes and the passageway of the fluid through the rotor, which can be radial, axial or a combination of both. Differences between these types of turbine machines are discussed in Appendix B.

4.2.1 Compressor performance characteristics

The performance of a compressor may be specified by curves of delivery pressure and temperature plotted against mass flow at various fixed values of rotational speed. *Cohen et al.*(1996) describes the method of using dimensional analysis to derive the non-dimensional variables that describe the performance of a compressor. These non-dimensional variables can be used for any compressor as they are not dependent on the geometrical or dynamic configuration of the compressor and are known as the non-dimensional mass flow rate [*NDM*] and the non-dimensional rotational speed [*NDS*].

$$NDM = \frac{\dot{m}\sqrt{T_{oi}}}{p_{oi}} \qquad \text{Eq. 4.1}$$

$$NDS = \frac{N}{\sqrt{T_{oi}}} \qquad \text{Eq. 4.2}$$

with $\dot{m}$ the mass flow rate in [kg/s], T_{oi} the total temperature at the inlet in [K] and p_{oi} the total inlet pressure in [bar], and N the rotational speed in [Hz].
A typical compressor performance map with *NDS* in terms of compressor pressure ratio and *NDM* is illustrated in Figure 4.1.

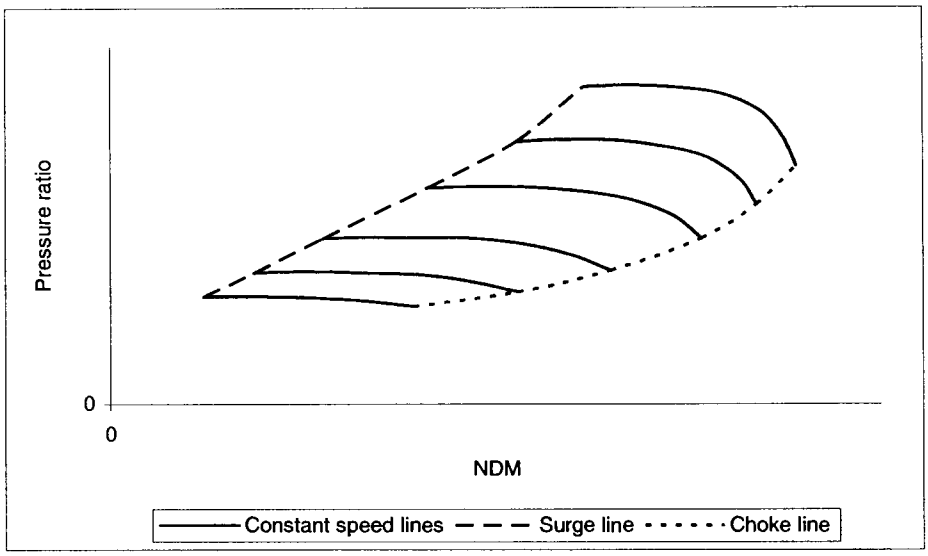

Figure 4.1: Typical compressor performance map.

When regarding compressors, a phenomenon called surging needs to be considered. An explanation of surging and the definition of surge margin can be seen in Appendix B. Another aspect that adds value to an evaluation of compressors is the efficiency of compressors.
The efficiency of the compressor η_c can be written in terms of the total changes in entropy:

$$\eta_c = \frac{\text{ideal input work}}{\text{Actual input work}} = \frac{(h_{2_s} - h_1)}{(h_{2_{ACT}} - h_1)} \qquad \text{Eq. 4.3}$$

with h_1 the enthalpy at inlet, h_2 the actual enthalpy at outlet and h_{2_s} the isentropic enthalpy at outlet. The equation can be rewritten in terms of temperature and pressure:

$$\eta_c = \frac{\left[\left(\frac{p_{02}}{p_{01}}\right)^{\frac{\gamma-1}{\gamma}} - 1\right]}{\left(T_{02}/T_{01}\right) - 1} \qquad \text{Eq. 4.4}$$

with T_{01} and p_{01} respectively the inlet temperature and pressure and T_{02} and p_{02} the exit temperature and pressure respectively. The constant speed lines that represent the compressor efficiency as a function of *NDM* can be seen in Figure 4.2

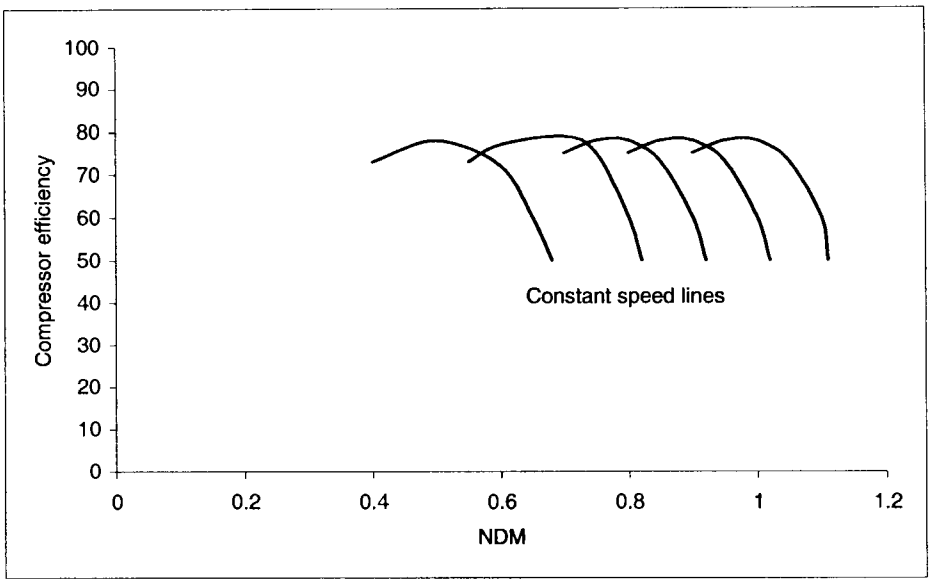

Figure 4.2: Compressor efficiency as a function of NDM.

By plotting the compressor efficiency as a function of both pressure ratio and *NDM*, and combining this with the speed lines of Figure 4.1, it is possible to predict the compressor's characteristic performances at any given mass flow and pressure ratio, as seen in Figure 4.3. The high efficiency island A is illustrated where the maximum efficiency occurs and how the performance deteriorates towards the surge and choke areas (away from A in any direction). The optimum operating point for any compressor is in the high efficiency island A. Any other working point will cause the compressor to be less efficient.

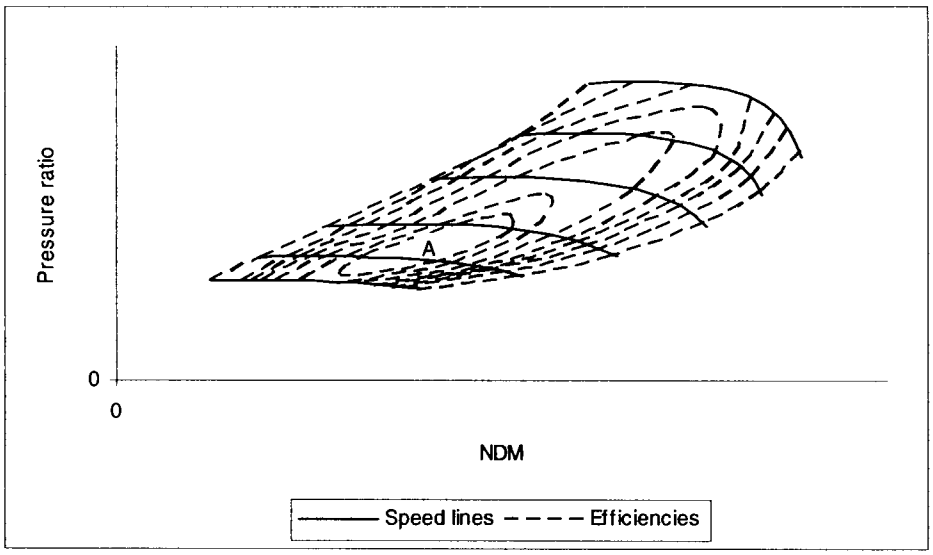

Figure 4.3: Compressor characteristic performance map.

4.2.2 Turbine performance characteristics

The non-dimensional variables that are used to predict turbine performance are the same as that of the compressor i.e: *NDM* and *NDS*. The turbine performance map, however, only provides a single line that is assumed to be sufficient for all rotational speeds. In reality, more lines could have been provided but these are quite close together and it is therefore assumed that one line is

sufficient (Rousseau & Greyvenstein 2002). A typical turbine performance map can be seen in Figure 4.4.

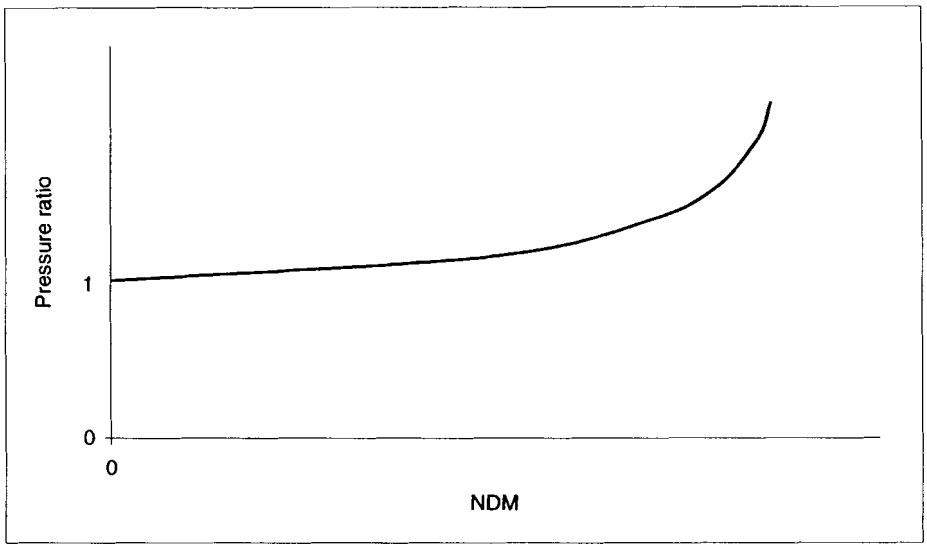

Figure 4.4: Typical turbine performance map.

Inspection of the turbine performance map reveals that when no mass flow occurs, the pressure ratio over the turbine will be equal to 1, indicating that the pressure on both sides of the rotor is equal. As the mass flow rate increases, the pressure ratio increases up to a point where the mass flow rate stagnates. The maximum value for *NDM* is reached at the pressure ratio which produces choking in the turbine.

The turbine efficiency $[\eta_t]$ can be written in terms of the total changes in entropy as

$$\eta_t = \frac{\dot{W}_{T_{ACT}}}{\dot{W}_{T_s}} = \frac{(h_1 - h_{2_{ACT}})}{(h_1 - h_{2_s})} \qquad \text{Eq. 4.5}$$

with $\dot{W}_{T_s}$ the isentropic power output, $\dot{W}_{T_{ACT}}$ the actual power output, h_1 the enthalpy at the inlet, $h_{2_{ACT}}$ the actual enthalpy at the outlet and h_{2_s} the isentropic enthalpy at the outlet.
This equation can be rewritten in terms of temperature and pressure:

$$\eta_t = \frac{\left[1 - \left(T_{02}/T_{01}\right)\right]}{1 - \left(\frac{p_{02}}{p_{01}}\right)^{\frac{\gamma-1}{\gamma}}} \qquad \text{Eq. 4.6}$$

with T_{01} and p_{01} the inlet temperature and pressure and T_{02} and p_{02} the exit temperature and pressure respectively.

4.3 TURBINE MACHINE SELECTION PROCESS

The choice between axial and radial machinery has to be made based on the following requirements:

Pressure ratio: 2 – 4.5
Mass flow rate: less than 2 kg/s.
Need to produce less than 100 kW power.

No limitation in weight and size.
Long life is expected.
Waste heat recovery can be utilized.
Low maintenance costs.
Availability of components.

The cost of these machines is high and due to the limited budget available for this study, only centrifugal turbine machinery will be considered. The availability of centrifugal machines and cost of maintenance thereof are better suited for the budget limitations of this study.

Selection of turbine machines for the TCIR cycle is very important as these components will determine the operating levels for the system. Work output and the cycle efficiency are therefore dependent on the choice of turbine machines.

The selection process consists of stages that follow on each other: During the first order analysis, the designer has to choose the turbine machine to be used as the low pressure unit; this choice, together with the pressure ratio, will affect the choice of the second turbine machine which will be used as the high pressure turbine machine. Therefore, at least two possibilities need to be evaluated to ensure the best choice for the low pressure turbine machine.

During the previous chapter, an investigation into the effect of different cycle parameters was done. It was shown that the overall pressure ratio and TIT have the most influence on the system's work output and cycle efficiency. The TIT is limited by material considerations, thus leaving the overall pressure ratio as one of the only parameters left that enjoys some degree of freedom. The pressure ratio will therefore be varied during the first order analysis to ensure a broad overview of the cycle's characteristics.

First order analysis is done with the assumed values of the previous chapter, also listed in Table 4.1, with the exception of the overall pressure ratio.
Results of the first order analysis will be in the form of potential system layouts, together with some options for each layout. Each layout will represent a choice for the low pressure turbine machine, while the selected low pressure machine will influence the effect of a change of the high pressure unit on the system.

The complexity level of the second order analysis is higher than that of the first order analysis, as the efficiency of each turbine machine is now taken into account. The second order analysis will calculate each component's operating points more accurately by taking drift in efficiency of each component into account. The whole system will be a better comparison to a real physical system under equal conditions.

Up to this point in the turbine machine selection process, the assumption that both the compressor's pressure ratios are equal held true. This is not the case when considering real systems. Each turbine machine will run at its maximum possible efficiency on a certain speed line, as governed by the load restrictions. Turbine machine's shaft speed is governed by the compressor, resulting in a pressure ratio determined by the compressors operating conditions. Pressure ratio is therefore a result of other component's operating parameters and not an input value as assumed previously.

By limiting the low pressure turbine machine shaft speed to pre-set values, the various pressure ratios of both compressors can be determined, and thus the overall pressure as well. During the third order analysis, the best layout configuration of the second order analysis will be investigated

by varying the low pressure turbine machine's speed. This allows evaluation of the effect on the performances of the layout's different options. Factors shush as component and cycle efficiency, work output and surge margins of the compressors will be taken into account. At the end of the third order analysis (and turbine machine selection process), the reader will have a thorough idea of the complexity involved in the choice of turbine machines, and the effect it has on the system.

4.3.1 First order analysis

The first order analysis is used extensively during the turbine machine selection process. Identical boundary conditions, as used during the previous chapter (Table 4.1), are used to determine the turbine machines to be used. The first order analysis calculates all the operation parameters for the given inputs.

Table 4.1: Assumed boundary conditions for the first order analysis.

Component	Assumption
Mass flow	1 kg/s
Inlet Temperature	26°C
Heater outlet Temperature	700°C
Pipe pressure loss (each)	98%
Heat exchanger pressure loss (each)	10%
Recuperator efficiency	90%
Mechanical Efficiency	98%
Compressor Efficiency	76%
Turbine Efficiency	70%
Overall pressure ratio range	2.5 3 3.5 4

The non-dimensional mass flow rate [*NDM*] is a function of mass flow rate, inlet temperature and inlet pressure as mentioned previously. Therefore, the *NDM* of the low pressure turbine machine [LPT] is the largest as it operates at the lowest pressure level. An applicable turbine machine has to be selected that will be able to accommodate these operational parameters to be used as the LPT. Different turbine machines are available and a few possibilities need to be evaluated to ensure the best selection. An illustration of typical turbine performance characteristics is show in Figure 4.5.

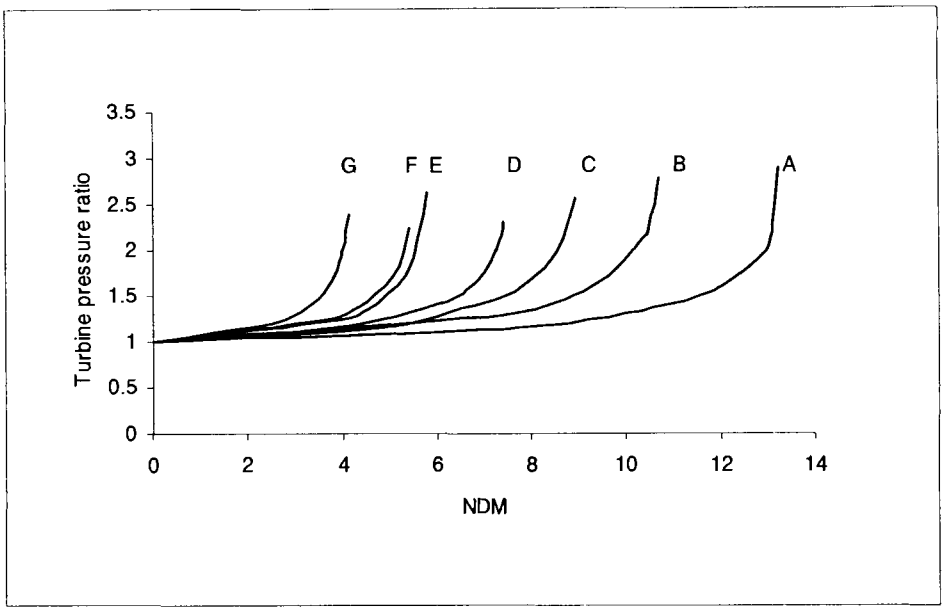

Figure 4.5: Typical turbine performance maps of different turbine machines.

Figure 4.5 shows different turbine machine models and their turbine performances. Note that the mass flow rate through the turbines is an indication of the size of the machine. Therefore, a model A turbine machine is larger than a model B turbine machine and the rest follow the same pattern. Therefore, only the three largest turbine machines will be evaluated as the low pressure system, and the following selections for the low pressure turbine machine will be evaluated:

- Layout A: Model A
- Layout B: Model B
- Layout C: Model C

Each of these layouts will be evaluated at all the pre-selected pressure ratios (2.5, 3, 3.5 and 4).
Note: During the first order analysis the assumption that the low and high pressure compressor ratios are equal, will be held true.

4.3.2 Second order analysis

The second order analysis is done by using the first order analysis repetitively in order to refine the system to better simulate real systems. Each repetition will have an adjustment in operation parameter that was prompted by the results of the previous first order analysis results. By using the values in Table 4.1 as initial boundary conditions, all parameters are calculated, evaluated and adjusted for the next iteration until the difference between flowing iterations are neglected.

The first step in the second order analysis is to recalculate the mass flow rate in order to allow the LPT's operating point to fall on the selected turbine model as in Figure 4.5. By adjusting the system's mass flow rate, other boundary conditions have changed and repetitive first order analysis iterations need to be done with adjusted boundary conditions to 'ripple out' the adjustment in mass flow rate.

Factors that are taken into consideration during the second order analysis include:

- Mass flow rate
- Component efficiency is calculated according to performance maps
- Selection of different turbine machines to be used as the high pressure unit.

Limitations of the second order analysis include that only steady state calculations are possible, and that components experience limited influence from neighbouring components. The copy of the algorithm of the second order analysis can be seen in Appendix D. The pressure ratios of the two compressors are assumed to be equal, which is a further limitation.

Results of the initial first order analysis proved that three possible layouts need to be considered. Each of these layouts has at least one possible configuration. (Any change in turbine machine combinations results in a new configuration.) All the second order layouts are evaluated in Appendix B. They are, however, all listed in the next section and their evaluations results are shown here as well, but the evaluation in proven in Appendix B.

4.3.2.1 Second order analysis on Layout A

By observation of the operating points of Layout A at different overall pressure ratios, the following configurations are possible:

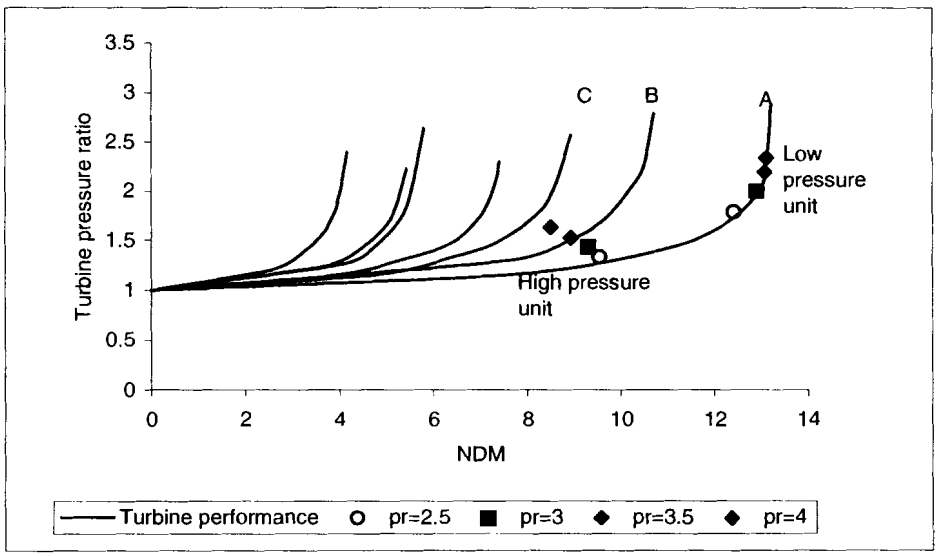

Figure 4.6: Turbine machine selection for Layout A.

Configuration 1: Low pressure unit: Model A
High pressure unit: Model A

Configuration 2: Low pressure unit: Model A
High pressure unit: Model B

4.3.2.2 Second order analysis on Layout B

This configuration is where Model B turbine machine is chosen as the low pressure unit. The turbine performance map will look as follows.

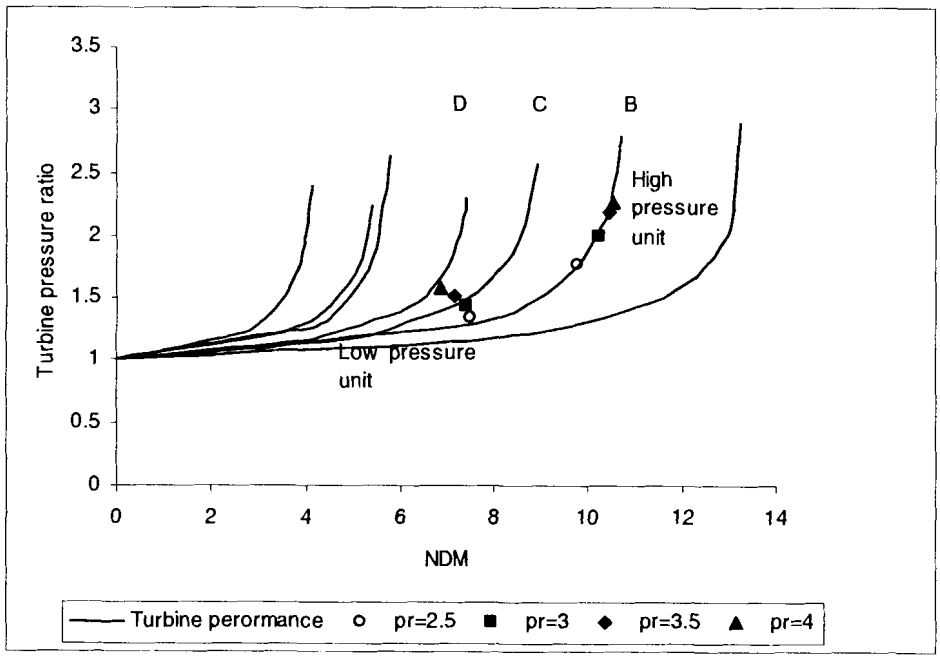

Figure 4.7: Turbine machine selection for Layout B.

Inspection of Figure 4.7 show the possible options that can be derived from the use of the Model B turbine machine as the low pressure unit are:

Configuration 3: Low pressure unit – Model B
High pressure unit – Model B

Configuration 4: Low pressure unit – Model B
High pressure unit – Model C

Configuration 5: Low pressure unit – Model B
High pressure unit – Model D

4.3.2.3 Second order analysis on Layout C

By using Model C turbine machine as the low pressure unit the following option is available:

Configuration 6: Low pressure unit – Model C
High pressure unit – Model D

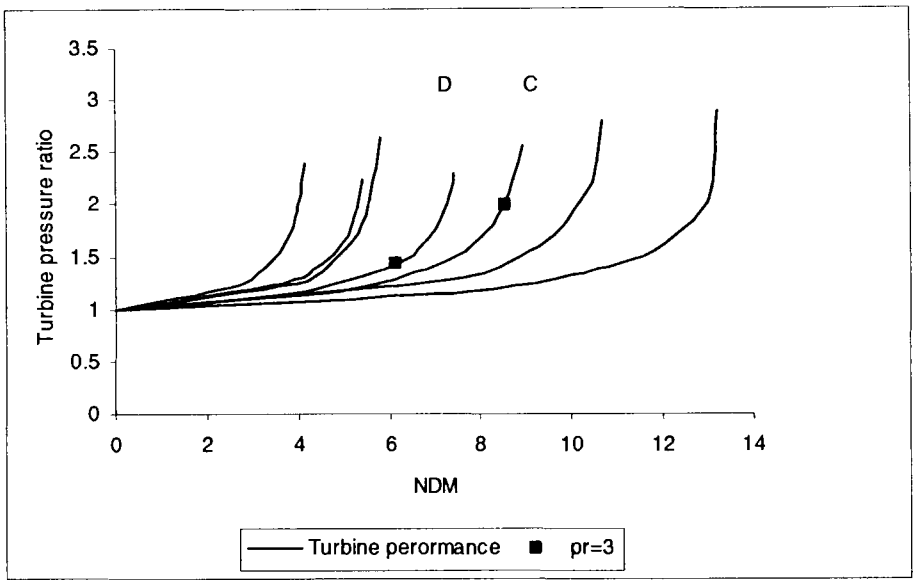

Figure 4.8: Turbine machine selection for Layout C.

4.3.3 Results of first and second order analysis

System performance characteristics of Configuration 1 – 6 were evaluated and compared where different turbine machinery was used in Appendix B. The results are tabulated in Table 4.2 where the individual component efficiency, as well as the mass flow rate and overall pressure ratio is shown.

Note that all these calculations were made under the assumption that the pressure ratios of the low and high pressure compressors are equal. However, this is not true in practise, as the cycle determines each compressor's pressure ratio according to the speed, efficiency and load of each unit.

Table 4.2: The operating points of the different layouts and options.

Configuration	LP unit model	HP unit model	P_r	$\dot{m}$ $[kg/s]$	η_{LPC} [%]	η_{HPC} [%]	η_{HPT} [%]	η_{LPT} [%]
1	A	A	3	0.7213	72	76	70.07	72.13
			3.5	0.9682	70	76	69.9	74.03
2	A	B	3.5	0.9655	70	76	69.48	74.02
			4	1.031	70	74	68.31	74.23
3	B	B	2.5	0.5801	78	70	60	70.44
			3	0.5846	78	68	60	71.18
4	B	C	3	0.5846	77	70	67.47	71.16
			3.5	0.6442	77	70	66.47	73.37
			4	0.7274	78	72	66.12	72.97
5	B	D	3.5	0.6899	78	74	72.03	70.93
			4	0.6207	78	76	68.32	71.34
6	C	D	3	0.4813	70	72	70	72.08

These configurations have to be evaluated by a simulation process where the pressure ratios of the compressors are not inputs but results of the calculation. Therefore, an evaluation will be done where the shaft speed of a low pressure turbine machine will be varied over a range of 400 to 1200 revolutions per second [min^{-1}]. This evaluation is called the third order analysis. For each third order analysis operation, multiple second order analyses need to be done.

4.3.4 Third order analysis

Up to this point, most of the calculations and simulations were done either by hand or using computer aided programs solving numerical equations with fixed boundary values. This was done to select the correct layout for this system. These calculations are ungainly and not accurate regarding component operations. For instance: the TCIR system analysis was done with the assumption that both the low-pressure and the high-pressure unit have the same pressure ratio. In practice, this is not true, as the compressor's operating point is not an input value, but a result of the component itself and its interaction with the other components interacting with it. It is therefore necessary to use a method that is able to predict the gas properties and system's performance characteristics more accurately by consideration of all the limitations and characteristics of the components.

The third order analysis was simulated in a software package called Flownex®. Flownex® is a general-purpose thermal-fluid network analytic code, solving the flow, pressure and temperature distribution in large unstructured thermal-fluid networks, using an intergraded system based CFD analysis code based on a network approach. Results generated by Flownex® gives the designer essential information on the interaction between network components and the behavior of complex systems.

Flownex® offers the capability of simulating systems in which turbine machines operate. The performance of these machines is determined by their measured non-dimensional performance characteristics, as mentioned earlier in this chapter. This feature enables the designer to generate results for systems with various turbine machines, where it is possible to compare systems with different components, configurations, boundary conditions, or at different power or speed levels. Not only steady-state calculations, but results for transients can be generated by using Flownex®.
During this part of the study, the third order analysis will be done with the help of the Flownex® package; by evaluating Configuration 1 to 6 at different operating conditions. The low pressure turbine machine's speed will be varied for this investigation, in order to simulate a change in operating conditions.
By using Flownex®, it is possible to predict the systems efficiency and work output for each state. An illustration of the TCIR network can be seen in Figure 4.9.

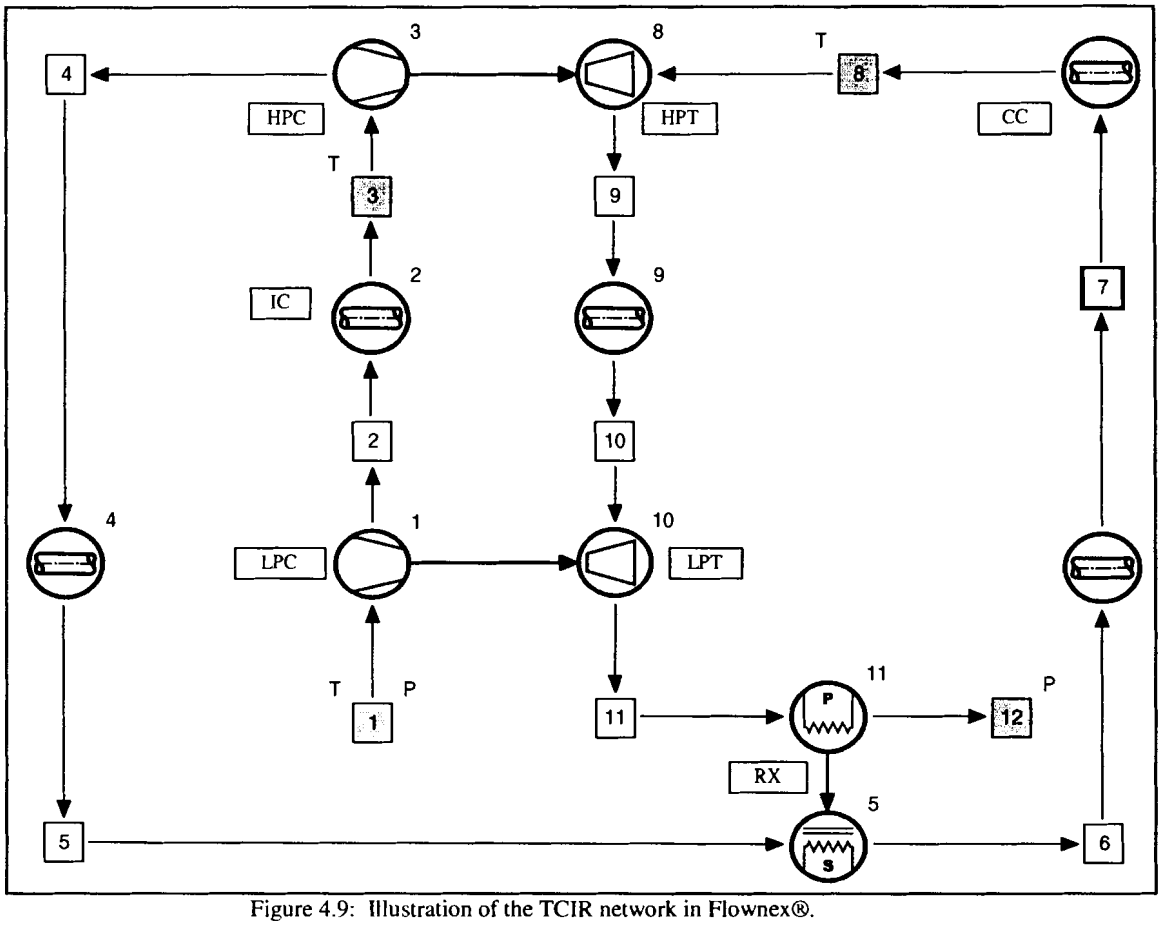

Figure 4.9: Illustration of the TCIR network in Flownex®.

Table 4.3: Acronyms used by Flownex®

Symbol	Component	Acronym	
	Compressor	LPC	Low pressure compressor
		HPC	High pressure compressor
	Turbine	LPT	Low pressure turbine
		HPT	High pressure turbine
	Pipe		Standard pipe
		CC	Combustion chamber

		IC	Heat exchanger [Inter-cooler]
	Recuperator [RX]	P	Primary side
		S	Secondary side
	Node		Operating points

Note: For the third order analysis (this chapter only), both the inter-cooler [IC] and combustion chamber [CC] are represented as pipes with constant exit temperatures and the recuperator [RX] is illustrated as a heat exchanger with an efficiency of 90%. Both the heat exchangers and combustion chamber will be discussed and investigated in Chapters 5 and 6 respectively, while both steady state as well as transient system simulations, with Flownex®, will be discussed in Chapters 7 and 8.

The speed of the LPT was varied from 400 to 1200 min^{-1} during the third order analysis on all the configurations discussed in Appendix B. Cycle efficiency as well as work output are plotted against the low pressure turbine machine's shaft speed can be seen in Figure 4.10 and Figure 4.11 for all the pre-mentioned configurations.

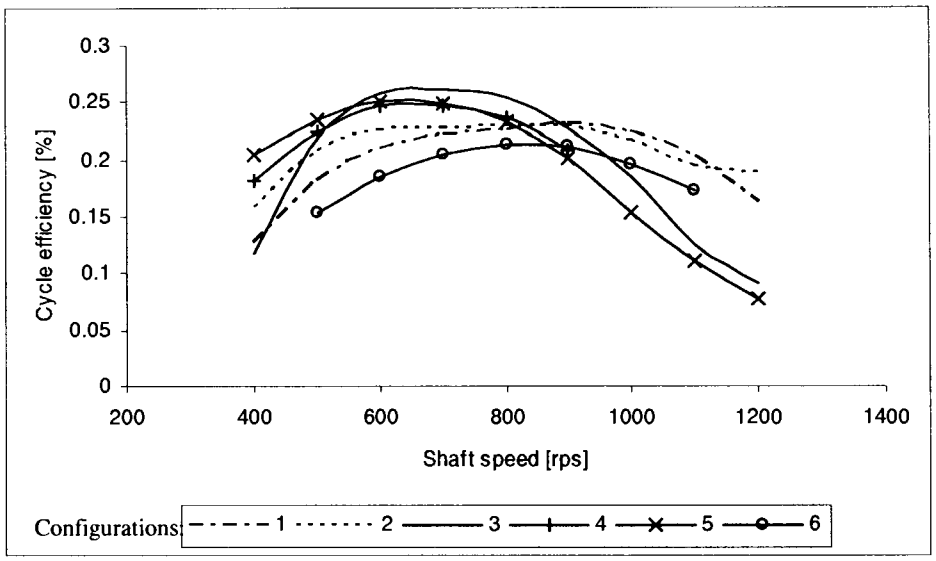

Figure 4.10: Cycle efficiency comparison as function of the low pressure turbine unit's rotational speed for the different configurations.

Comparison of different cycle efficiencies in Figure 4.10 showed that the three configurations in Layout B (Configuration 3, 4 and 5) have the highest cycle efficiencies of all the configurations evaluated. Figure 4.11 show that Layout A (Configuration 1 and 2) provides the maximum work output at high shaft speeds [±1100 min^{-1}]. Layout B however, has higher efficiencies and better work output values than Layout A at lower speeds [400 – 900 min^{-1}].

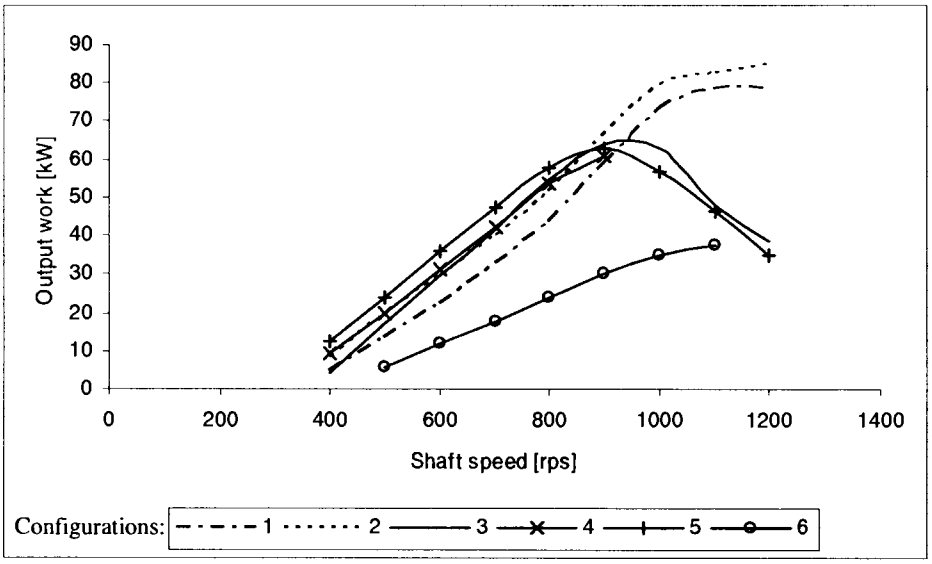

Figure 4.11: Cycle output work comparison as function of the low pressure turbine unit's rotational speed for the different configurations.

Layout A (Configuration 1 and 2) proved to generate the best output work of all of the configurations evaluated at LPT shaft speed higher than 900 min^{-1}. Therefore, Configuration 1 and 2 will be evaluated over a speed range of 800 – 1200 min^{-1}.

Since Layout B performs the best when considering cycle efficiencies as well as work output when considering LPT shaft speeds of 400 to 900 min^{-1}, configurations of Layout B (configuration 3, 4 and 5) will be evaluated over these speeds.
Layout C (Configuration 6) does not compare well at all to the other two layouts in this evaluation for its low efficiency and work output levels, and will not be evaluated any further in this study.

Note: The third order analysis and the evaluation of the different configurations are discussed in detail in Appendix B.

4.3.5 Results of the third order analysis

As illustrated in Figure 4.10 and Figure 4.11, Configuration 1 has a slight advantage over Configuration 2 when comparing Layout A two configuration's performance characteristics. Since Configuration 3 is the best performer in Layout B, both Configuration 4 and 5 are eliminated as well. Configuration 6 from Layout C does not compare well to the other configuration in Layout A and B and is eliminated as a possible configuration for the micro gas turbine system.

Therefore, the only configurations considered further in this study are Configurations 1 and 3, and factors that will to be taken into account when evaluating these remaining configurations are cycle efficiency and cycle work output.

Evaluating the cycle efficiency for Configurations 1 and 3 as a function of the low pressure turbine machine's rotational speed can be seen in Figure 4.12. The best cycle efficiency values are generated by Configuration 3 at LPC shaft speeds up to a shaft speed of 900 min^{-1}, after which Configuration 1 produces better efficiency values. Configuration 1 produces a graph with gentle gradients, ensuring that sudden changes in LPC operation speeds do not affect the system's efficiency as much as the steep gradients of Configuration 3 will.

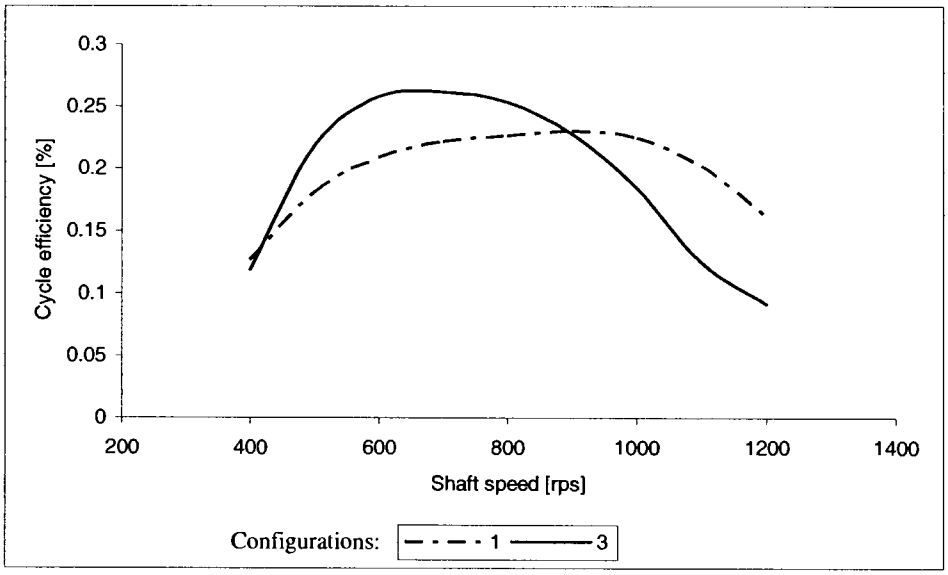

Figure 4.12: Cycle efficiency comparison of Configuration 1 and 3 as function of the low pressure turbine unit's rotational speed.

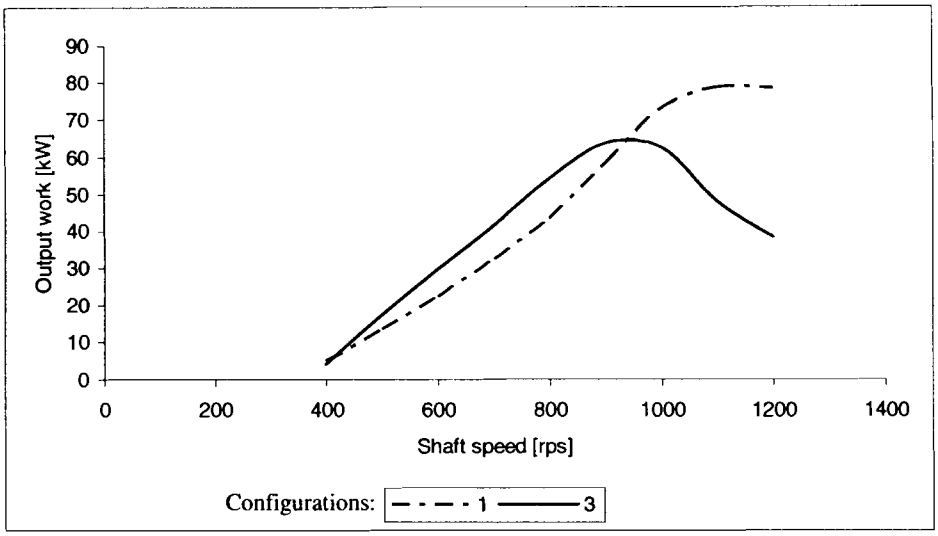

Figure 4.13: Output work comparison of Configuration 1 and 3 as function of the low pressure turbine unit's rotational speed.

Work output as a function of the LPC shaft speed is represented in Figure 4.13 where Configuration 3 has a higher work output value up to a shaft speed of 900 min^{-1}, where the work output drops rapidly, opposed to Configuration 1, whose values still increase to a maximum value at an approximate shaft speed of 1200 rps. The average difference in work output between Configuration 1 and 3 in the shaft speed range of 400 – 900 min^{-1} is calculated at 6.25 kW, whereas the average value in the shaft speed range of 900 – 1200 min^{-1} is calculated at 21.66 kW. The gain in work output at higher shaft speeds exceeds the loss of work output at low shaft speeds if Configuration 1 is considered.

Factors that affect the choice of turbine machinery have been evaluated and the results analyzed, and the configuration that will be used for the TCIR system will be based on Configuration 1 and 3 will consist of identical model A turbine machines for both the low and the high pressure unit.

Excluding the next part of the study (Custom design versus selection of turbine machinery), the term "TCIR system" will indicate a micro gas turbine system that has identical model A turbine machines for the low and high pressure turbine units.

4.4 CUSTOM DESIGN VERSUS SELECTED TURBINE MACHINERY

Bardan (1999:267) proved that the thermal efficiency will increase with increases in compressor efficiency. Increases in compressor efficiency will also decrease the cost of energy and lead to an increase of net work output. The compressor performance map, as seen in Appendix B shows that the LPC operating point occurs to the lower right of the optimum region. It is therefore possible to use this layout more efficiently by applying a bigger compressor for the LPC. By redesigning the compressor impeller to operate within the 'most optimum region' where the highest efficiency values occur, a more sufficient compressor can be created.

4.4.1 Custom design of new LPC

By using a software package called Concepts NREC – COMPAL, it is possible to generate characteristics performance maps for compressors by inserting the geometrical dimensions of the impeller, diffuser and shroud into the compressor intake. The operating point of the LPC is in

terms of pressure ratio and non-dimensional mass flow rate. These values cannot be changed as it will affect the system's output.

The output of the NREC software can be seen in Appendix D. The result is the compressor performance map which can be seen in Figure 4.14, together with the work point of the designed compressor. The efficiency of this machine is 78.5% at a speed of 35 285 min^{-1} or 588 Hz.

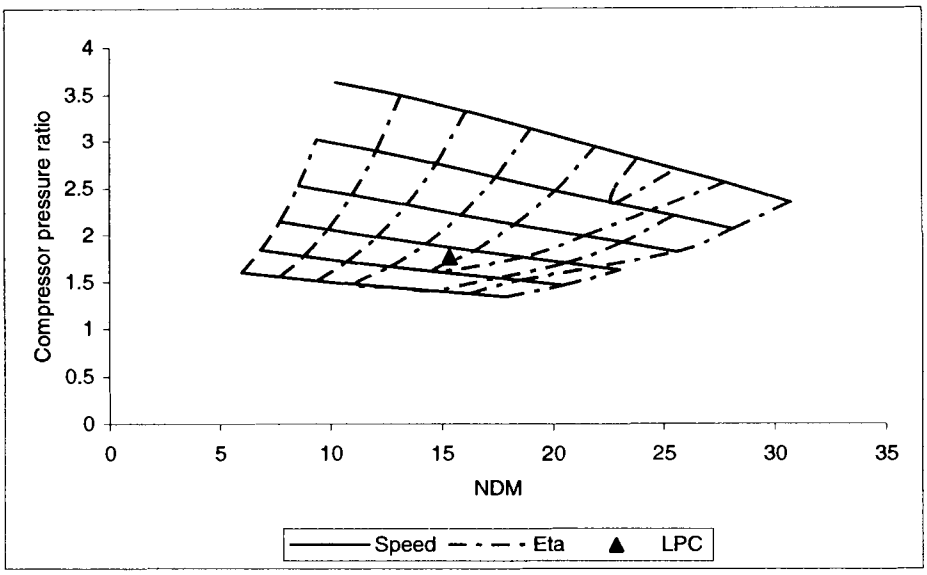

Figure 4.14: Performance map for a special designed LPC.

The resulting effect that the designed compressor has on the system is shown in Table 4.4. The increase in cycle efficiency due to the new compressor is 3.26%, or 7,231 kW in work output.

Table 4.4: Comparison between the standard selected and custom designed LPC.

Parameter	Standard machine	Custom designed machine
Cycle η	0.2349	0.2675
Work [W]	50 434	57 665
LPC η	0.7	0.785
Speed [Hz]	555	588

4.4.2 Conclusion of custom designed versus selected turbine machinery

While it is possible to design a compressor that will enhance the performance of the system for the given conditions, the gain in efficiency and work output does not justify the cost of designing and manufacturing a new compressor. The standard commercially available Model A turbine machine will still be used with its original compressor without any change to the impeller.

4.5 RESULTS OF THE TURBINE MACHINE SELECTION

The option of designing a compressor impeller especially for the turbine machine was evaluated and found not to be feasible where costs are concerned for this study.
The best cycle efficiencies for Configuration 3 are achieved at low pressure turbine shaft speeds of between 550 and 1000 min^{-1}, while the best work output occurs at a shaft speed of 950 min^{-1}. Any low pressure turbine shaft speed higher than 1000 min^{-1} will result in loss of work output, as

well as cycle efficiency, as both curves will be on a negative slope at speeds higher than 1000 min^{-1}. The same effect occurs at speeds lower than 550 min^{-1}, where both the efficiency and work output curves are on a positive slope where both the efficiency and the work output will drop. The best operating shaft speed region for the low pressure turbine unit will therefore be between 550 and 1000 min^{-1}. The low pressure turbine machine's rotation speed will be fixed at 700 min^{-1} for the rest of the study. This will be varied again during the transient cycle simulation that will include start-up and load following in Chapter 8.

4.6 CONCLUSION

The characteristics of turbine machinery and the selection process of turbine machinery were discussed. Different configurations of the TCIR system were compared where the best suitable turbine and compressor units were selected to be used for the rest of this study. A comparison between the use of a standard commercially available machine and a custom design machine was done. Due to economical considerations, a commercially available turbine machine will be used for the rest of this study. The layout of the system will be that of Configuration 3 illustrated in this study.
The results for the selected turbine machines, Configuration 3, are listed in Table 4.5.

Table 4.5: Turbine machine results for the TCIR cycle.

Unit	Δp [kPa]	P_r [kPa]	NDM	ΔT [$°C$]	η [%]	W [kW]
LPC	77.73	1.78	11.762	69.96	76.36	47.794
HPC	94.339	1.53	6.648	51.75	75.62	35.36
HPT	67.292	1.33	7.825	45.8	67.64	35.36
LPT	103.363	2.03	10.164	116.38	76.03	89.126

The rest of this study will be directed towards the other components, including the heat exchangers, pipes and combustion chambers, which will be designed for the TCIR system according to the operating conditions Table 4.6:

Table 4.6: Boundary conditions for the micro gas turbine system.

Component	Assumption
Mass flow	0.68 kg/sec
Total pressure ratio	2.728
Cycle efficiency	26%
Cycle work output	41.332 kW
Steady state LPT shaft speed	700 rps

These boundary conditions will be refined again as soon as the individual component detail designs are completed later in this study.
The turbine machine units that will be used in the TCIR system are now considered fixed. Some crucial components such as the heat exchangers, combustor chamber and pipes that link components still need to be investigated and designed. These investigations into component characteristics will be done in the following chapters, and will be concluded with an illustration of the geometrical layout of the complete micro gas turbine system, based on the TCIR cycle. Once all of these component designs are fixed, a study will be done to evaluate the system's

performance under transient conditions. This simulation will include start-up and load following and will be done with the software package named Flownex®.

5 Design and Optimization of Heat Exchangers

Gas turbine systems are thermal dynamic driven machines and therefore need efficient heat exchangers. The discussion on the Brayton cycle and its variants in previous chapters proved that by utilizing heat exchangers, the micro gas turbine system's performances can be increased. These heat exchangers are designed and optimized during this chapter and the relevant appendix supporting these calculations.

5.1 INTRODUCTION TO HEAT EXCHANGERS

The previous chapters explained the selection of the system and related turbo machine configuration. After analyzing the performance, the operating points were fixed or specified, therefore, determining the size of the heat exchangers required to ensure the predicted performance. This chapter subsequently explains the heat exchanger design process followed.

Heat exchangers are an integral part of gas turbine machines and therefore need to be optimized to operate within the system's requirements. The use of heat exchangers to improve gas turbine cycle efficiency was discussed in Chapters 2 and 3, and is applicable to a wide range of gas turbine applications. In this chapter, factors influencing the design and manufacture of heat exchangers used in the TCIR cycle will be discussed. The operating range of these components and the optimization thereof is also done in this chapter.

5.2 HEAT EXCHANGER REQUIREMENTS

In the TCIR cycle, there are two heat exchangers present i.e. the inter-cooler [IC] and the recuperator [RX]. The location of these units can be seen in an illustration of the cycle in Figure 5.1, and boundary conditions were calculated.

The boundary conditions limiting the design of the heat changers as calculated in the previous chapter are listed in Table 5.1.

Table 5.1: Boundary conditions limiting the heat exchangers

	Inter-cooler		Recuperator	
	Gas side	Coolant side	Cold gas side	Hot gas side
Mass flow rate [kg/s]	0.68	1.5	0.68	0.68
Inlet pressure [kPa]	178	300	273	100
Inlet temperature [°C]	96	20	77	536
Acceptable efficiency [%]	80		90	

Note: An inter-cooler efficiency of 80% is quite possible; where as an inter-cooler efficiency of 90% is only possible with a tremendous amount of technology and cost. Therefore, an inter-cooler efficiency of 80% is accepted for this study, while the minimum recuperator efficiency is limited to 90%.

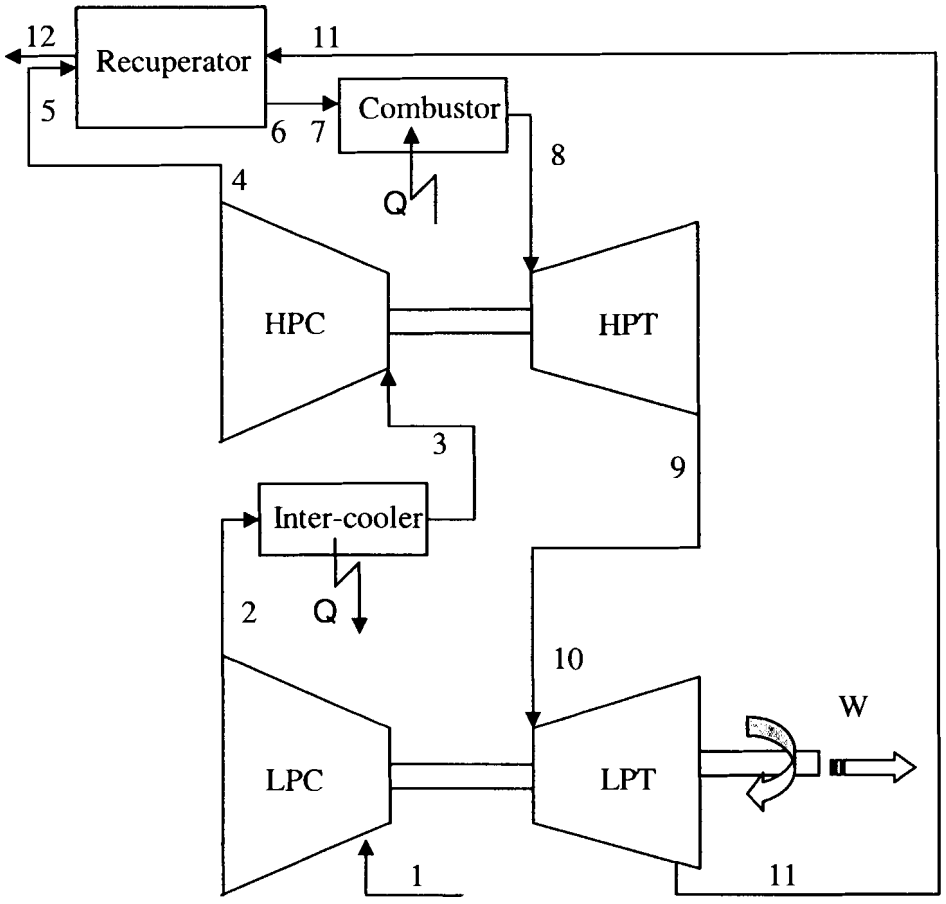

Figure 5.1: Illustration of the TCIR cycle

The process of designing the heat exchangers will follow the same process as used in the turbo machine selection process. Low order analysis will be done first on the various aspects that influence the operation of the heat exchangers. The analysis will determine the sensitivity of the heat exchanger to these factors.

5.3 CHARACTERISTICS OF HEAT EXCHANGERS

Heat exchangers are classified according to flow arrangements and type of construction. Classifications include: concentric tube, cross flow, shell and tube and compact heat exchangers. Compact heat exchangers are used to achieve a very large heat transfer surface per unit volume (around $700 m^2/m^3$). These devices have dense arrays of tubes or plates and are typically used when at least one of the fluids is a gas and is therefore characterized by a small convection coefficient. Flow passages associated with compact heat exchangers are small (± 5mm) and flow is usually laminar (Incropera & De Witt 1996).

The performance of a heat exchanger is evaluated in terms of its efficiency, which is defined by:

$$\eta = \frac{\text{actual heat transfer}}{\text{maximum heat transfer}} \qquad \text{Eq. 5.1}$$

Efficiency is a function of the number of transfer units (*NTU*) defined by:

$$NTU = \frac{UA}{\dot{m} \cdot cp_{\min}} \qquad \text{Eq. 5.2}$$

An essential part of the heat exchanger analysis is the determination of the overall heat transfer coefficient [*UA*]. It is defined in terms of the total thermal resistance [*R*] to heat transfer [*q*] between two fluids. The overall heat transfer coefficient can be defined as:

$$UA = \frac{q}{\Delta T} = \frac{1}{R} \qquad \text{Eq. 5.3}$$

with q the heat transfer rate and ΔT the overall temperature difference.
Fins are often used to increase the heat transfer area and *UA* can be calculated by using the following equation:

$$\frac{1}{UA} = \frac{1}{(\eta_0 hA)_c} + \frac{R_c}{(\eta_0 hA)_c} + R_w + \frac{R_h}{(\eta_0 hA)_h} + \frac{1}{(\eta_0 hA)_h} \qquad \text{Eq. 5.4}$$

with R the resistance and η_o the overall surface efficiency of a finned surface.
For non-finned, tubular heat exchangers, *UA* in equation 5.4 reduces to:

$$\frac{1}{UA} = \frac{1}{hA_i} + \frac{R_i}{A_i} + \frac{\ln\left(D_o / D_i\right)}{2\pi kL} + \frac{R_o}{A_o} + \frac{1}{hA_o} \qquad \text{Eq. 5.5}$$

where subscripts *i* and *o* refer to the inner and outer tube surfaces respectively.
It is important to note that this equation's results rely on clean, un-finned surfaces and that a fouling factor should be introduced to incorporate an additional operating resistance that is experienced in systems.

According to McDonald (2000), heat exchanger design is a compromise between three objectives: maximizing the heat exchanger effectiveness; minimizing the fluid friction in the heat exchanger [pressure loss over the exchanger] and minimizing of manufacturing costs of the exchanger [the volume of the exchanger]. The investigation into heat exchanger sensitivity will evaluate the resulting effects on the efficiency, pressure loss and heat transfer volume.

5.3.1 Inter-cooler characteristics

The TCIR cycle has an inter-cooler between the LPC and HPC that cools the gas leaving the LPC down to ambient temperature. The heat removed by the inter-cooler [Q_{IC}] is a function of the overall temperature difference across the inter-cooler:

$$Q_{IC} = \dot{m} \cdot cp\left(T_{in} - T_{out}\right) \qquad \text{Eq. 5.6}$$

while a pressure drop is expected:

$$p_{out} = p_{in} \cdot p\_loss_{IC} \qquad \text{Eq. 5.7}$$

The efficiency of the inter-cooler is a function of the real heat transfer [Q] and the maximum transfer possible by the inter-cooler

$$[Q_{max}]: \ \eta_{ic} = \frac{Q}{Q_{\max}} \qquad \text{Eq. 5.8}$$

The efficiency could also be calculated by using the *NTU* method:

$$\eta_{ic} = \frac{NTU}{1 + NTU} \qquad \text{Eq. 5.9}$$

or

$$NTU = \frac{1}{C_r - 1} \ln\left(\frac{\eta_{ic} - 1}{\eta_{ic} \cdot Cr - 1}\right) \qquad \text{Eq. 5.10}$$

with

$$C_r = \frac{cp_{\min}}{cp_{\max}} \qquad \text{Eq. 5.11}$$

The inter-cooler that will be used in the TCIR cycle is a shell and tube heat exchanger. It consists of tubes that carry the gas through the cooler. Figure 5.2 shows the path that the coolant follows through the volume of the cooler together with an illustration of the inter-cooler.

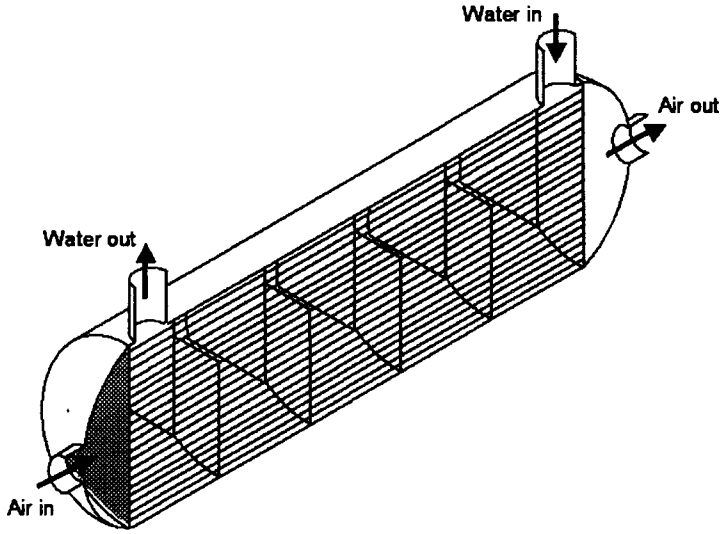

Figure 5.2: Shell and tube inter-cooler

Inter-cooler simulation is done in Engineering Equation Solver [EES] and the algorithm used as well as the results can be seen in Appendix E, while mathematic equations are presented in Appendix C.

5.3.2 Inter-cooler sensitivity

Heat transfer between the tube side and the shell side of the inter-cooler is determined by the geometric factors. For this study an inter-cooler with the following geometric parameters will be considered: shell diameter $[D_{shell}]$, tube inside diameter $\left[D_{i[tube]}\right]$ and tube outside diameter $\left[D_{o[tube]}\right]$, the number of tubes [n] and the length [L] of the inter-cooler. The inter-cooler will experience counter flow, since the flow directions of the gas and the coolant are opposite to one another. Accordingly, the impact of the geometric parameters on the efficiency and the pressure loss over the inter-cooler will be investigated in this study.

Before any parameter can be investigated, it is necessary to acknowledge some relationships between the parameters. The number of tubes $[n_{tube}]$ is dependent on both the shell diameter $[D_{shell}]$ and the tube outside diameter $\left[D_{o[tube]}\right]$. An increase in $[D_{shell}]$ causes $[n_{tube}]$ to increase (Figure 5.3), while an increase in $\left[D_{o[tube]}\right]$ causes $[n_{tube}]$ to decrease (Figure 5.4).

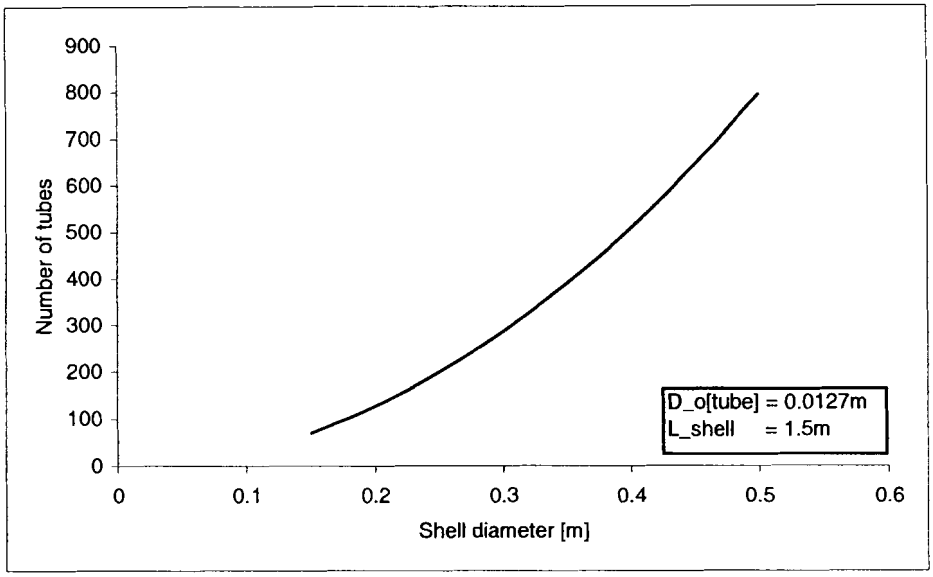

Figure 5.3: Number of tubes as a function of shell diameter.

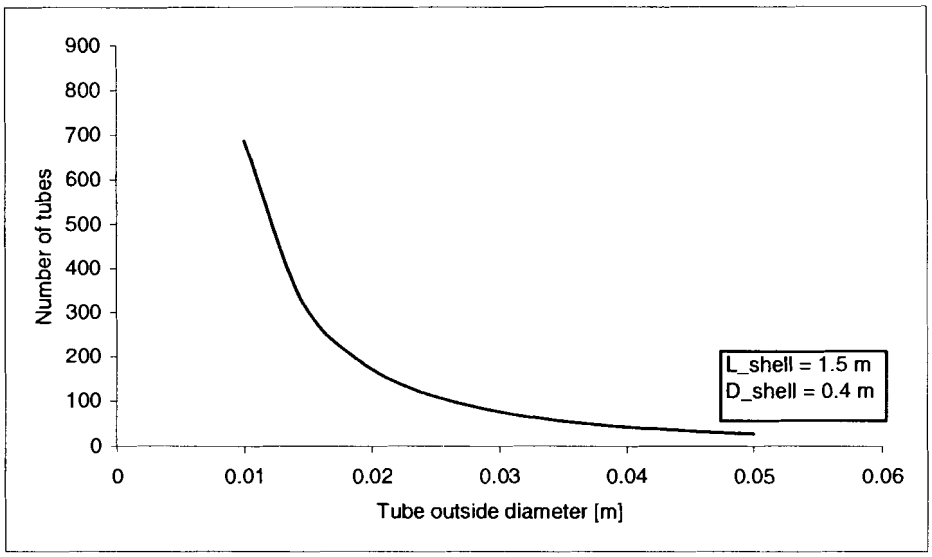

Figure 5.4: Number of tubes as a function of tube outside diameter.

An optimum ratio between the shell- and tube- diameter has to be established, for both of these have an influence on the number of tubes used in the heat exchanger. This optimization will follow in Appendix A.

5.3.3 Inter-cooler results

The inter-cooler performance characteristics were evaluated against each other and against the geometrical dimensions as well in Appendix A. The geometrical limitations were derived and a simulation was done to establish the best configuration for the inter-cooler for these conditions. The resultant geometrical dimensions and the inter-cooler characteristics can be seen in Table 5.2.

Table 5.2: Geometrical and characteristic results of the designed inter-cooler

Geometric dimensions

Inter-cooler length [L]	1.5 m
Inter-cooler shell diameter [D_{shell}]	0.4 m
Inter-cooler tube diameter [$D_{o\,tube}$]	12.7 mm
Number of tubes [n]	508
Inter-cooler characteristics	
Inter-cooler efficiency [η_{ic}]	82%
Real heat transfer [Q]	43 kW
Maximum heat transfer [Q_{max}]	47 kW

All the applicable information was fed in to the simulation program written to calculate the inter-cooler's performances. The results of this simulation are listed in Table 5.3

Table 5.3: Boundary conditions for the inter-cooler

Condition	Gas side	Coolant side
Inlet pressure	180 kPa	300 kPa
Inlet temperature	97°C	20°C
Exit pressure	179.85 kPa	295.66 kPa
Exit temperature	28°C	27°C
Pressure loss	0.15%	1.44%

Figure 5.5 shows the axial temperature distribution through the inter-cooler with the given geometric limitations. Note that the gas enters at increment 0, and exits at increment 10, while the coolant (water) enters at 10 and exits at increment 1, thus cross-flow heat exchanger.

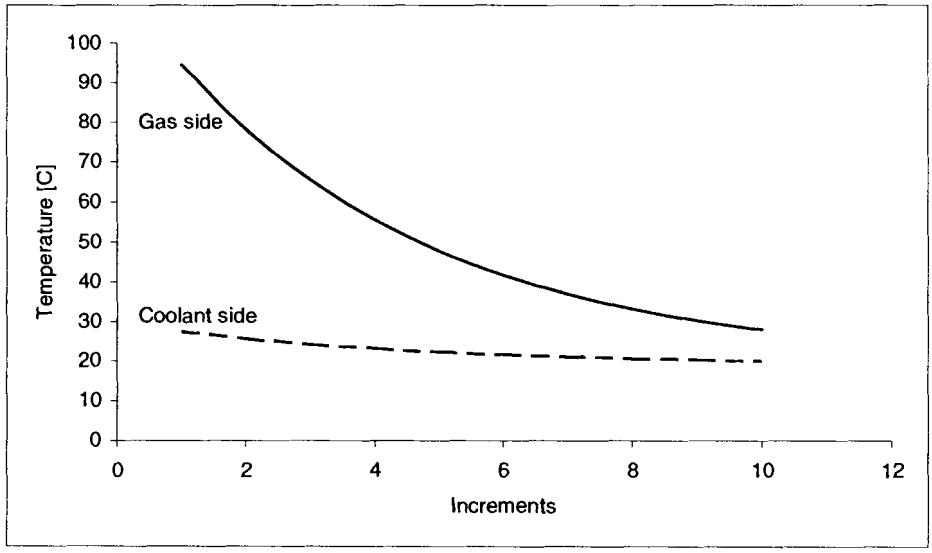

Figure 5.5: The axial temperature distribution of the inter-cooler.

5.3.4 Recuperator characteristics

The TCIR cycle uses a recuperator to pre-heat the air entering the combustor, thus less fuel is needed to raise the temperature of the air to the required level at the turbine inlet. A recuperator is nothing more than a heat exchanger that exchanges heat between two gases, whereas the inter-cooler was a fluid to gas heat exchanger.

The recuperator in the TCIR layout is a micro-channel recuperator and is built up by staggered plates that are sealed by a micro structure growth process as discussed by Wallnöfer et al. (2001) and Doty et al. (1991). The channels used in this application are square with the height equal to the width. Carman et al. (2002) have shown that different channel–channel cross section exists and proved that a triangle design provides better performance than square designs.

The recuperator's efficiency $[\eta_{recup}]$ definition is identical to that of the inter-cooler: A relation between the real heat transfer $[Q]$ and the maximum possible heat transfer

$$[Q_{max}]: \eta_{recup} = \frac{Q}{Q_{max}} \qquad \text{Eq. 5.15}$$

The total heat transfer $[UA]$ can be calculated with:

$$UA/cp_{min} = NTU = (1-\eta_{recup})/\eta_{recup} \qquad \text{Eq. 5.16}$$

The recuperator has a double effect on pressure loss, as both streams are part of the cycle. The air stream enters the recuperator twice and is subjected to pressure losses both times. Calculation of pressure loss, and the simulation of the recuperator, can be seen in Appendices A and E.

5.3.5 Recuperation sensitivity

Thermodynamic models and the optimization of micro channel heat exchangers have proved to be more efficient alternatives than current metallic primary surface heat exchangers of equal volume, Carman et al. (2002). Thus, the heat transfer of a heat exchanger is determined by the geometric parameters. The recuperator's geometric parameters are the dimensions of the channels $[b]$, the number of channels $[m]$ and the length of the channels $[L]$. (Channel height is equal to the width of the channel, and the number of hot channels.)

The recuperator sensitivity analysis will be done by investigating the effect that the geometric parameters have on the efficiency $[\eta_{recup}]$, pressure drop $[\Delta p]$, the Reynolds number [Re] and the volume $[V]$ of the recuperator.

5.3.6 Recuperator results

Optimizing, designing and simulation of the TCIR cycle recuperator was done and is available in Appendix E. These analyses resulted in the following:

Table 5.4: Geometrical and characteristic results of the designed recuperator

Geometric dimensions	
Recuperator length $[L]$	0.5 m
Recuperator height $[H]$	1 m
Recuperator width $[W]$	1 m
Channel dimension $[b]$	2.5 mm
Number of channels $[m]$	60 000
Recuperator characteristics	
Recuperator efficiency $[\eta_{rec}]$	91%
Recuperator real heat transfer $[Q]$	279 kW

Recuperator max heat transfer [Q_{max}]	306 kW

Table 5.5: Boundary conditions for the recuperator

Condition	Cold gas side	Hot gas side
Inlet pressure	274 kPa	100.4 kPa
Inlet temperature	274°C	537°C
Exit pressure	85 kPa	100 kPa
Exit temperature	508°C	115°C
Pressure loss	0.05%	0.38%

Axial temperature distribution through the Recuperator with the given geometric limitations is illustrated in Figure 5.6. Note that the hot gas enters at increment 1, while the cold gas enters at 11 and exits at increment 1, thus making up a cross-flow heat exchanger.

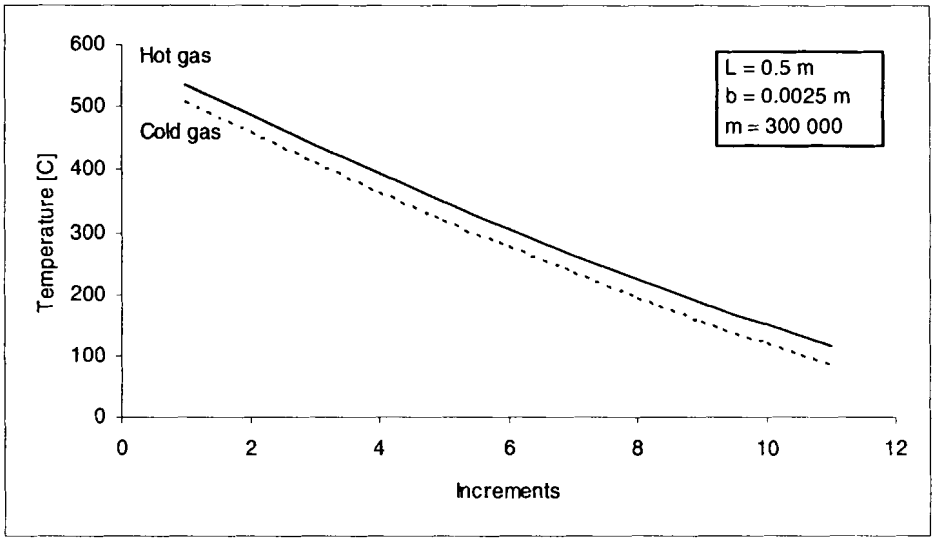

Figure 5.6: Axial temperature distribution through the recuperator.

The hot gas enters the recuperator and cools down towards the exit, while the cold gas heats up from entering the recuperator until exiting at a high temperature. Note that the exit temperature of the hot gas still exceeds 100 °C, thus still possessing energy that can be utilized. This option will not be investigated further during this study.

5.3.7 Future recuperators

Recuperators currently under development are spherical (spiral) heat exchangers that fit around the turbo machine, and take less space than external heat exchangers, Treece et al. (2002). Characteristics shush as: low pressure ratios, exhaust temperatures more suitable to stainless steal material characteristics and limited allowance for leakage that does not impair performances are possible according to Antione & Prieels (2002). The testing of these types of recuperators, manufacturing and evaluating of materials are covered in a paper by Stewart et al. (2002). These types of recuperators will not be evaluated in this study.

5.4 CONCLUSION

The simplified simulation of the TCIR cycle resulted in the desired operating points for each component of the system. These points represent the limits of the components like heat

exchangers. Using these boundary conditions as starting parameters, the heat exchangers are designed and optimized. The designed heat exchangers will therefore meet the requirements of the TCIR cycle, and better them in terms of needed efficiency and pressure losses. These true values will be introduced into the cycle to represent the true micro gas turbine machine more closely than previously. The following chapters will address the design of the remaining components as well as the physical geometric layout of the micro gas turbine system, followed by the transient simulations in Chapter 8, where all the refinements will be introduced into the simulation model.

6 Design of the Combustion Chamber

Most of the micro gas turbine components' boundary conditions were set due to system and component limitations during previous chapters of this study. This chapter will discuss the combustion chamber design, where fuel burns in order to provide heat for the operation of the micro gas turbine system.

6.1 INTRODUCTION TO THE COMBUSTION CHANBER

This chapter discusses the characteristics of an external combustion chamber capable of providing enough heat for the operation of the TCIR cycle. Requirements of combustion chambers, types of chambers, applicable design factors, chemical reactions and aerodynamics of the combustion chamber will also be discussed. Thereafter, the current trends in combustion chamber designs will be shown.

The combustion process can be seen as an exothermal reaction of fuel (gaseous or liquid) and an oxidant (oxygen in air). The combustion process is rapid and lasts about 1 ms to reach 80% completion and is characterized by the presence of a flame that propagates through the un-burnt mixture (Lefebre 1998) at speeds that equal that of the mass flow rate through the combustor. Compared with un-burnt gases, the burnt gases are higher in volume and temperature, but lower in density.

6.2 COMBUSTION PROCESS

A common configuration for a combustion chamber is shown in Figure 6.1. Also illustrated in Figure 6.1 is the injection of fuel into the air stream, before combustion can occur. Ignition and flame stability is difficult due to the high gas velocity if the flame is carried downstream faster than flame propagation (when gas speed is higher than flame propagation). Flame stability is difficult to sustain continuously when the flame is blown away faster than it can develop against the gas stream. Therefore, a combustion chamber with stable flame propagation throughout the micro gas turbine system's operating range is needed to achieve high combustion efficiencies.

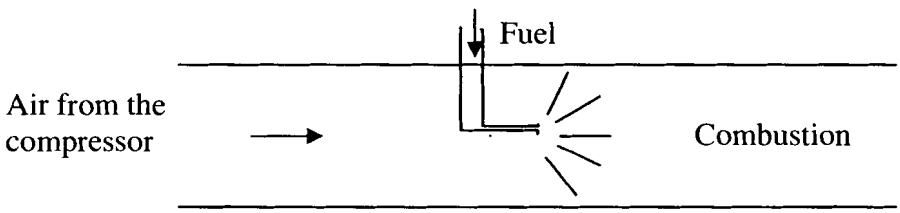

Figure 6.1: Illustration of a basic combustion chamber.

Air moving at high velocities also causes high pressure losses over the combustion chamber, as the force loss is proportional to the gas velocity squared. The configuration illustrated in Figure 6.1 can be impractical as the pressure loss over the combustor will be too high. A low air speed will limit pressure loss through the combustion chamber while maintaining a relative high mass flow.

By using a diffuser that increases the cross sectional area of the combustion chamber, the pressure loss experienced can be reduced. The air speed, however, needs to be reduced and is done by inserting a baffle plate in the air steam as illustrated in Figure 6.2. As the air moves around the baffle plate, an eddy is created where reverse flow occurs and flame stability is ensured. This is illustrated in Figure 6.3 where the air entering the combustion chamber has to move around the baffle plate and the air speed has been reduced sufficiently to allow flame propagation down the combustor.

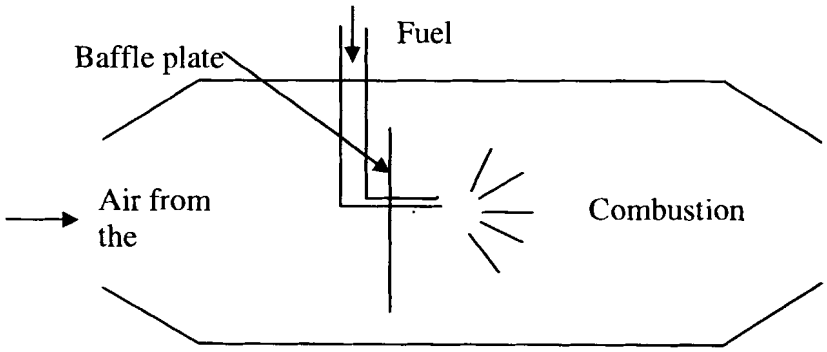

Figure 6.2: Baffled combustion chamber.

The stoichiometric air/fuel ratio for kerosene is 15:1 (later in this chapter), while the overall air/fuel ratio is in the region of 100:1, which is well outside the limits of flammability for hydrocarbon mixtures. The use of a perforated liner will solve the problem of creating a stable flame region where the stoichiometric ratio is equal to 15:1. This is illustrated in Figure 6.3, where the air flow is introduced in stages into the combustion zone.

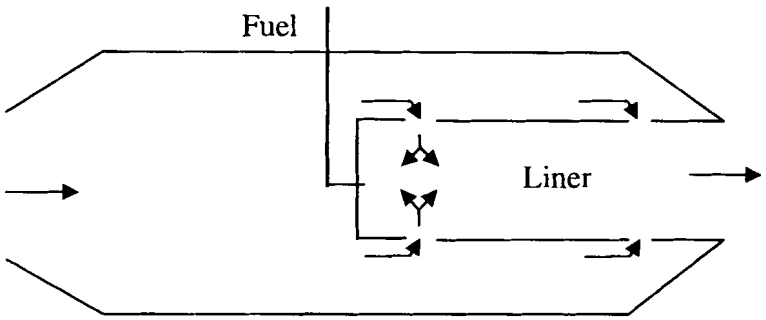

Figure 6.3: Combustor with perforated liner.

The perforated liner causes the air stream to split into two or more streams which enter the combustion chamber through different liner holes at specific points. A stable flame propagation region is thus created where fresh air can be re-circulated, mixed with the injected fuel and burn before mixing with the un-burnt gas along the perforated liner. This stable region where combustion occurs is called the primary stage and is accompanied by a number of primary holes. Surplus air that is not used during the initial combustion process will be entered into the liner downstream. These stages will be discussed later in this chapter.

Different flame propagation methods are used by different types of combustion chambers, but the most common types are: Tubular, annular and the can-annular combustor. Only the 'single can tubular combustor' version will be considered in this study.
Factors that need to be addressed during the design of a combustion chamber were summarized by Lefebre (1996) and Cohen et al.(1996):

- Combustion efficiency: high efficiency needed to burn all the fuel and liberate as much of the chemical energy stored in the fuel as possible.
- Ignition: reliable and smooth.
- Wide range of stability limits.
- Low pressure loss over the combustor.
- Temperatures of gases leaving the turbine should be within turbine blade limits.

- The temperature distribution at the end of the combustor should be known to ensure that the turbine is not damaged.
- Flame propagation and stability in different air velocities that varies form idle to full load applications. Air/fuel ratios differ at these conditions as well.

6.3 COMBUSTION CHAMBER AERODYNAMICS

As shown in Figure 6.3, the air will be introduced into the liner in stages. The first stage called the primary stage, uses 15 to 20 % of the incoming air to create the stable burning zone. The other zone, shown in Figure 6.3, is known as the dilution zone, where the leftover air is introduced into the liner. This air is used to cool down the combusted gas to temperatures that are acceptable for the turbine. The mixing of hot and cold streams is essential for reducing the occurrence of hot streaks that can damage the turbine.

Since it is possible that some of the fuel has not reacted during the short time in the primary zone, in practice, it is necessary to introduce a secondary zone where more fresh air enters the liner before the dilution zone. The secondary zone helps recover some of the losses due to chemical dissociation of the primary combustion products and is achieved by a number of inlets between the primary and dilution zones. This accounts for less than 12 % of the total incoming air.

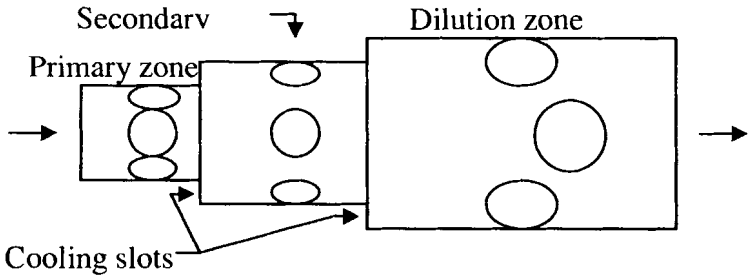

Figure 6.4: Illustration of the zonal liner air introduction method.

Flame temperature for stoichiometric mixtures is in the region of 1600°C, which is higher than the material limits of the liner. The liner therefore has to be cooled down to ensure that no wall failures occur and this is achieved by cooling slots in the liner wall. Cooling slots introduce a cooling barrier layer between the hot gas and the liner wall. This cooling air should be directed into the same general direction as the gas stream, not to penetrate the gas stream like the dilution holes. Distinction between these two introduction methods can be seen in the illustration in Figure 6.5.

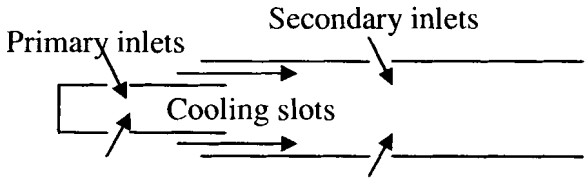

Figure 6.5: Illustration of liner inlet flow direction.

The aerodynamic process plays a vital role in the design process of gas turbine combustion chambers and demands knowledge of flow recirculation, jet penetration and mixing, and discharge coefficients for all the air inlets in the liner. Some variables need to be defined before any of the combustor parameters are discussed: The reference velocity $[U_{ref}]$, which is the mean

velocity across the plane of maximum cross-sectional area of the casing$\left[A_{ref}\right]$ in the absence of the liner and the dynamic pressure q_{ref}. They are defined as

$$U_{ref} = \frac{\dot{m}}{\rho_{in} A_{ref}} \qquad \text{Eq 6.8}$$

and

$$q_{ref} = \frac{1}{2}\rho_{in} U_{ref}^2 \qquad \text{Eq 6.9}$$

Combustion chamber aerodynamic performances are dictated by the following aspects: pressure loss parameters, relation between pressure loss and size and the gas flow through the annulus and line inlet holes and are discussed in Appendix D.

6.4 COMBUSTOR CHAMBER PERFORMANCES

Combustor chamber performance parameters include: combustion efficiency, stability limits and the ease of starting and igniting.

6.4.1 Combustion efficiency

The efficiency of a combustor is derived by analysing the combustion products chemically. By knowing the air/fuel ratio and the proportion of incomplete burnt constituents, it is possible to calculate the energy released by the fuel and compare this value to the theoretical value. Therefore, the definition of combustor efficiency by Cohen et al. (1996) and Lefebvre (1998) is:

$$\eta_{comb} = \frac{\text{theoretical } f \text{ for actual } \Delta T}{\text{actual } f \text{ for actual } \Delta T} = \frac{\text{heat released by combustor}}{\text{heat available in fuel}} \qquad \text{Eq 6.21}$$

The size of the combustion chamber is determined by the rate of heat required by the gas turbine, and is dependent on the fuel mass flow rate, air/fuel ratio and the calorific value of the fuel. Both Lefebvre (1998) and Cohen et al.(1996) discuss the combustor efficiency in detail, but for the purpose of this study, the definition given is adequate in providing the reader with some background knowledge on this field, and no further discussion will follow on this topic.

6.4.2 Stability limits

A combustor chamber has a weak and a rich limit of the air/fuel ratio beyond which the flame becomes unstable. Instability takes the form of rough running and indicates poor combustion and generates vibration that reduces the life of the chamber and turbines.
The bigger the mass flow rate into the chamber, the smaller the range between the weak and rich limit becomes. If this air mass flow is increased beyond the limit, no combustion will be possible. A typical stability loop is shown in Figure 6.6, where the limiting air/fuel ratio is plotted against air mass flow. The limit is taken as the air/fuel ratio at which the flame blows out, although instability occurs before this limit is reached. The combustion chamber should be capable of operating within the stability loop of air/fuel ratio and air mass flow, (Cohen et al. 1996)

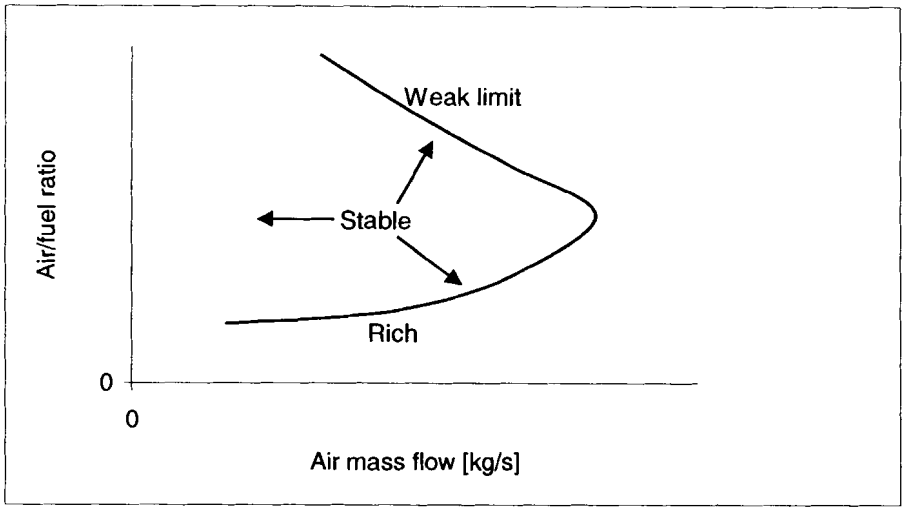

Figure 6.6: Combustion stability loop.

6.4.3 Starting and igniting

Gas turbine combustion has to be continuous and self-sustaining, but the starting and ignition systems should be closely integrated. Starting a gas turbine involves rotating the turbo machine at speeds that are able to induce self-sustainable operation of the turbine machine (also known as boot-strap). The compressor is driven to produce mass flow through the combustion chamber at an elevated pressure where fuel is mixed with this air stream. Ignition is therefore required to generate the initial flame, in order to start the combustion process.

Boot-strap occurs when the gas turbine is self sustained, thus no external work is needed to drive the engine and the only energy entering the machine is in the form of chemical energy (the calorific value) of the fuel into the combustion chamber. It is necessary to rotate the turbo-compressor unit at a minimum idling speed by means of an external system, thus creating a low gas flow through the combustor, combusting the gas, and ultimately bringing the gas turbine into a self-running condition (Pardeepkumar 2002).
By definition, boot-strap occurs when turbo machinery rotating speeds are in the region of 15 to 20% of normal operation speeds and the flame is self sustained. The ignition system can then be shut down.

The TCIR cycle will be started with the aid of an external motor/generator system, which will drive the turbo–machinery until boot-strap conditions. Thereafter, power to the motor/generator system will be shut down and the cycle will run unaided and self sustained, stabilizing itself with no external load on the shaft. Power generation will only be activated once the TCIR system is running unaided without any external load of power generation influencing the system. This will be discussed in Chapter 8.

Combustor chamber performance is mostly dependent on the liner geometry, and different parameters regarding the geometry need to be evaluated. This is done in Appendix D where the liner geometry is discussed. Liner geometry that is discussed includes the diffuser, primary and secondary zones, the dilution zone and the cooling slots.

6.5 CONCLUSION

Considering all the constraints mentioned during this chapter, a computer aided simulation program was written in EES [Engineering Equation Solver] to calculate and optimize a possible combustion chamber that will be able to supply the TCIR cycle with gas with the necessary mass flow rate, TIT and within the allowable pressure loss over the combustion chamber. This algorithm can be seen in Appendix G.

Table 6.1: Resulted boundary conditions of the combustion chamber

Combustion chamber boundary conditions		
Mass flow rate	0.68	kg/s
Inlet pressure	272	kPa
Inlet temperature	507	°C
Exit temperature	700	°C
Pressure drop	1	%

7 Micro gas turbine system layout

Most of the subsystems and components were discussed during the previous part of this study. Systems not included in the previous part like the pipe network and auxiliaries will be discussed now. With all off these subsystems in place, it is time to consider the system as a whole, to do system analysis. These simulations will be done with the simulation package Flownex® and both steady state as well as transient conditions will be evaluated.

7.1 INTRODUCTION INTO MICRO GAS TURBINE SYSTEM CHARACTERISTICS

In the previous chapters it was proven that the TCIR cycle was the best suited out of all those evaluated for this micro gas turbine application. Different key components that were considered included the turbo machinery, heat exchangers (inter-cooler and recuperator) as well as the combustion chamber that will be used in the micro gas turbine generator. Some components of the micro gas turbine system that are not yet discussed, include the pipes that link the components, the motor/generator configuration and other auxiliaries like the coolant system, lubrication system and fuel supply system. The interface between the auxiliaries and the turbine system also needs to be addressed and are done. All of the components are compared and initially by regarding the micro gas turbine system as if in steady state conditions. Calculations and assumptions were used to reach the initial boundary conditions for these steady state calculations. These boundary conditions were revised as more information surfaced, as the subsystems influence each other when operating as a system. Steady state conditions were simulated and evaluated with the aid of the Flownex® code. The performance of the micro gas turbine generator will now be evaluated under certain transient condition. Transient studies will include the system's capability to do start-up and load-following in order to verify the integrity of the designed components and subsystems.

In this chapter some of the components that were not examined in previous chapters will be discussed. A simulation consisting of all the components, with all their limitations as discussed in previous chapters, is done here to calculate the parameters for these selected components. Figure 7.1 shows the TCIR cycle as illustrated in Chapter 4, with the inclusion of the specified inter-cooler and recuperator, while the combustion chamber is still represented as a pipe with a constant exit temperature of 700 °C (due to limitations of the current simulation package). Both the heat exchangers represent the units in Chapter 5, with the exact limitations and performances, while the combustion chamber was covered in Chapter 6.
Flownex® is a general thermal-dynamic network analysis code that can deal with both steady-state and transient flows. With the network approach, a complex thermal-fluid system is represented as a network of one-dimensional elements connected at common nodes. Elements are denoted by circles while nodes are denoted by squares. Elements represent components such as pipes, compressors, turbines, heat exchangers, control valves or reactors. Complex components such as heat exchanges are not treated as lump systems but are automatically expanded into large sub networks consisting of elemental flow paths in contact with solid or porous structures. Flownex® can also deal with convection heat transfer between flow and solid structures as well as conduction heat transfer within solid material heat transfer between surfaces. Another features of the code is its ability to deal with gas mixtures and PID controllers. Input data of compressors and turbines are provided in the form of performance maps, which gives the pressure ratio as a function of corrected speed, $N/\sqrt{T_0}$, and corrected mass flow, $\dot{m}\sqrt{T_0}/p_0$, for different geometries such as blade angle. Any number of compressors can be placed on a single shaft and steady-state load balancing can be done by varying be either the shaft speed or the master turbine geometry, typically the blade angle. In the case of transient flows, Flownex® calculates the shaft speed transients by taking the inertia of all rotating parts into account. Greyvenstein & Rousseau (2003).
Flownex®'s solver is based on the implicit pressure corrections of mass and energy at all nodes and momentum (or pressure drop) in all elements in the network. The code has been extensively validated against other codes and experimental data. Van Ravenswaay (2003).

Among the components that built up the micro gas turbine system, there are some which were not discussed previously in this study. The influence of these components will be discussed briefly and some light will be shed on the controlling of these auxiliary systems. An illustration of the physical layout of the micro gas turbine system will also be represented in this chapter, where the true dimensions of all of these components were used in the configuration layout during steady state conditions.

7.2 PIPES

A pipe can be defined as the volume between any two consecutive components, with the presence of losses during the transfer of fluid (gas) between these two components through the volume (pipe). The fluid dynamic characteristics of the fluid (gas) flow through pipes needs to be evaluated to calculate losses that can be expected under these circumstances.

Note that during this study the assumptions that no heat transfer occur through any pipe wall, and that the fluid used in the system is atmospheric air (called gas for the rest of this study) is applied. Maximum allowable pressure loss over a pipe is limited to 1% of the pipe's inlet pressure for all pipes used in the micro gas turbine system. Pressure losses, due to friction between the moving gas stream and the stationary pipe wall, are a function of mass flow rate and the geometry of the pipe. Parameters needed for the evaluation of pipes are: Inlet and outlet pressure $[p_{in}, p_{out}]$, Darcy-Weisbach friction factor $[f]$, mass flow rate and geometry factor [K]. The geometry factor is influenced by obstacles in the pipes such as L-bows, T-pieces, orifices and valves.

The pressure drop over a pipe with the length L and diameter D due to a mass flow rate of $\dot{m}$ is defined as:

$$\Delta p = \left(\frac{fL}{D} + \sum K \right) \frac{|\dot{m}|\dot{m}}{2\rho A^2} \qquad \text{Eq 7.1}$$

where A is the cross-sectional area of the pipe. The Darcy-Weicbach factor f is a factor of the Moody diagram and uses the Reynolds number [Re] and the ratio of wall smoothness over pipe diameter $\left[\frac{\varepsilon}{D}\right]$ to calculate the factor.

Table 7.1: Pipe geometry

Pipe number	Pin [kPa]	ΔP [kPa]	Tin [°C]	Diameter [m]	Length [m]	$\left[\frac{\varepsilon}{D}\right]$
4	418.44	2.14	97.75	0.075	0.75	0.00003
6	416.19	2.9	423.30	0.075	0.5	0.00003
7	413.19	2.52	423.30	0.080	0.5	0.00003
9	300.0	1.76	649.12	0.080	0.2	0.00003

All the pipes, with all their parameters, are listed in Table 7.1. The results of the Flownex simulation package for the steady state conditions can be seen in Appendix E.

7.3 AUXILIARIES

In order for the TCIR system to produce electrical power reliably, it is necessary to define the auxiliary systems needed by this system. These systems include the coolant supply, lubrication, electrical power distribution and fuel supply system. All of these systems need to be reliable and fail-safe, meaning that these systems have back-up systems to ensure unconditional safe shutdown of the micro gas turbine system, even under emergency conditions.

7.3.1 Motor/generator configuration

The generator to be used in this micro gas system can be transformed to be used as an electrical motor when the need occurs, and will therefore be called the motor/generator configuration. This motor/generator configuration will be used during start-up as a motor to drive the LP compressor until boot-strap occurs. The start-up procedure will follow in Chapter 8, but will operate as follows: The motor drives the system during the start-up stage, idles during the system stabilising stage, and is driven as a generator under normal working conditions.

The motor unit will drive the LP compressor at a speed of 30 000 min^{-1} during start-up, and will rotate at a speed of 72 000 min^{-1} under full load conditions. The motor/generator is equipped with an inverter that enables the motor/generator to rotate at different speeds, but still deliver power at a constant frequency of 50 Hz. The power level differs as the generator's speed differs.

The maximum power that can be generated continuously by the motor/generator configuration is 72.5 kW of electrical power. The generator's full time maximum output will be limited to 82% of maximum output: 60 kW. When needed, one can produce more than 60 kW, but this will not be within normal operational requirements. This will be illustrated later in this chapter.

7.3.2 Coolant System requirements

The inter-cooler and its design are discussed in Chapter 5. The coolant supply may be either a closed, or an open cycle, both under the limitation of having thermal inertia to provide coolant with a constant temperature of less than 20°C at a flow rate of 1.5 kg/s and a pressure of 300 kPa. In the event of an open coolant cycle, there has to be enough coolant readily available (such as a lake or the sea), while a closed coolant cycle has to have a reservoir with cooling capabilities that are able to provide within the limitations stated earlier.
The supply needs to have a back-up system that will ensure the inter-cooler is operational even if the primary cooling system fails.

7.3.3 Lubrication system requirements

All the turbo machinery consists of rotational parts mounted on shafts in housings with minute tolerances. The lubrication in this application does not only provide lubrication for the bearings, but also cools the rotating parts. Turbo machinery operates at high temperatures and these temperatures of the fluid and turbo housings are transferred to the bearings. When bearings experience large temperature differences, their geometrical characteristics change and may lead to the seazing of these bearings to the rotating shafts. Even after operation, when the shaft of the turbo unit is stationary, the need to cool these parts still persists due to the temperature in the housing as discussed by Greyvenstein et al. (2002)
The importance of the lubrication system is of such priority that it needs at least two reliable back-up systems in order to guarantee that the system will have adequate lubrication to be able to

shut down, even if its first back-up system fails as well. The cost of replacing turbo machinery in the event of a failure of the lubrication system is higher than the extra back-up system. A discussion of a suitable lubrication system may be followed in Appendix F.

7.3.4 Fuel supply system requirements

The fuel supply system requirements include a reliable system that delivers various mass flows as required by the combustor chamber. This need to be controlled by the TIT, for the more power needed, the more heat needs to be added to the system and therefore more fuel in to the combustion process.
The fuel supply system needs to deliver vaporised fuel at a certain pressure and mass flow rate to the combustion chamber. A safety shut-down system is also needed to ensure that the fuel supply can be shut-off in an instant in the event of an emergency. Without fuel, the combustion chamber cannot operate and the TIT will drop, causing the micro gas turbine system to terminate operation simultaneously.
Although some experiments were conducted to prove the feasibility of a similar fuel system, it is not part of this study to include the detail of these experiments.

7.4 CONCLUSION FOR STEADY STATE OPERATING CONDITIONS

Using all the information on all the different components and sub systems that are assembled to operate as the micro gas turbine system, steady state simulations were done in Flownex®. The steady state conditions as well as the results of the configuration of the TCIR system are tabulated in Table 7.2 to Table 7.4:

The boundary conditions for the micro gas turbine system during the steady state conditions are

Mass flow rate (gas) 1.376 kg/s
Ambient temperature: 20°C
Ambient pressure: 100 kPa

Table 7.2: Turbine machinery results

Turbine machinery Type	LPC	LPT	HPC	HPT
Pressure ratio	2.7	2.967	1.58	1.369
Shaft speed	72000 min^{-1}		40470 min^{-1}	
NDM	23.72	13.97	9.2	10.42
Efficiency	64.14%	81.27%	76.99%	68.22%
Work	- 211 kW	280 kW	- 79 kW	79 kW
Temperature difference	153°C	182°C	57°C	51°C
Surge margin	53.91%		47,85%	

Table 7.3: Heat exchanger results

Heat exchangers		
Intercooler		
Efficiency	81.76%	
	Gas Side	Coolant side
Mass flow rate	0.68 kg/s	1.5 kg/s

Inlet pressure	178 kPa	300 kPa
Inlet temperature	96°C	20°C
Exit temperature	30°C	
Recuperator Efficiency	88.91%	
	Cold side	Hot side
Mass flow rate	0.68 kg/s	68 kg/s
Inlet pressure	273 kPa	100 kPa
Inlet temperature	77 °C	536 °C

Table 7.4: Combustion chamber results

Combustion chamber	
Mass flow	0.68 kg/s
Inlet pressure	272 kPa
Inlet temperature	507°C
Exit temperature	700°C
Pressure drop	1%

7.5 MODELLING OF THE TCIR SYSTEM WITH FLOWNEX®

The Flownex® model of the layout is shown in Figure 7.1. The initial steady state values for the simulation are as follows:

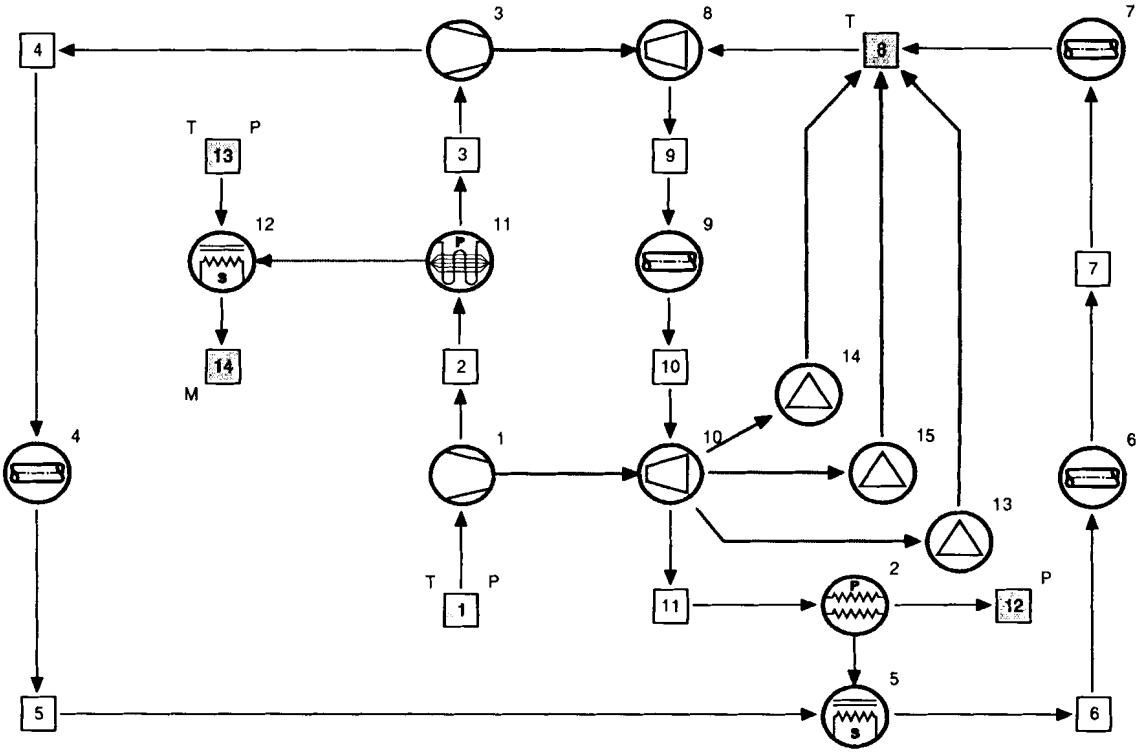

Figure 7.1: The TCIR cycle.

Note: The acronyms used in Figure 7.1 can be followed in Chapter 4.
During transient simulation PID Controllers [13, 14 and 15] were added for control purposes. These controllers control the speed of the turbine by altering the turbine inlet temperature [TIT]. This is accomplished by altering the combustor's fuel supply. (The control is similar to that of an internal combustion engine). The operation of all of the controllers is similar and will be discussed later in this chapter. The specifics of the controllers together with the boundary conditions of all the components and subsystems are available in Appendix E.

7.5.1 Start-up

It is important to simulate start-up in order to prove the operation of the micro gas turbine system. The micro gas turbine system's ability to start can be simulated in the Flownex® code and will commence in stages, each controlled by a Controller (13, 14 or 15). The first stage is controlled by Controller 13, second stage by Controller 14 and the third stage by Controller 15. The various stages of start-up are discussed in Appendix E, while the combined start-up sequence will be discussed here.

Start-up: Combined sequence
Illustrated in Figure 7.2 and Figure 7.3 is the resulting turbine speed and the controlled TIT for the start-up sequence.

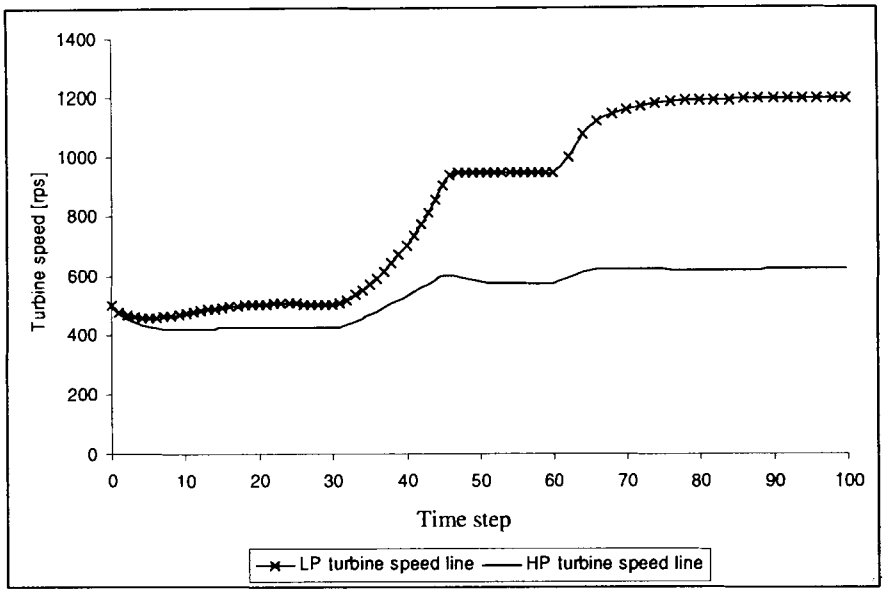

Figure 7.2: Start-up stages combined turbine speed over time

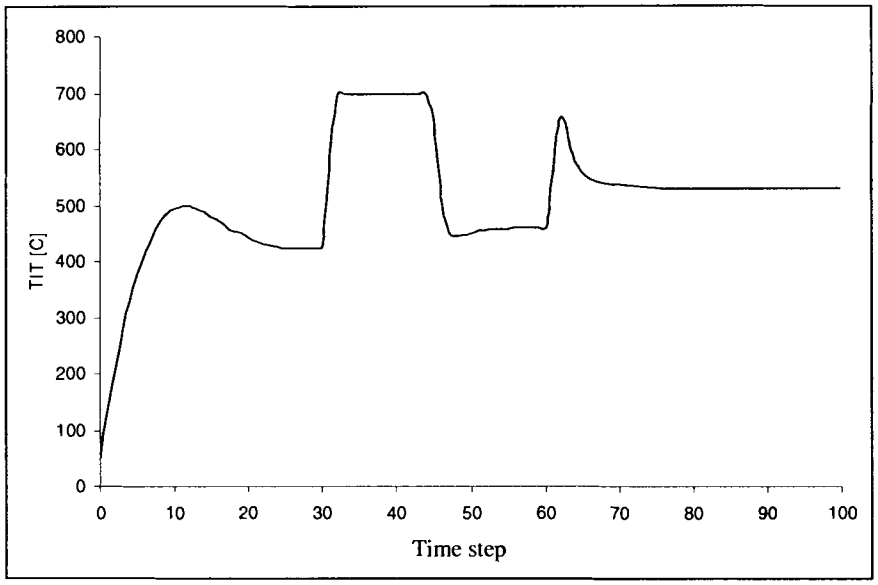

Figure 7.3: Start-up stages TIT over time

The change of temperature is rapid, while the speed changes are more sedate. These figures also prove that both the TIT and turbine speeds stabilize each time after a change to conditions were made. Later in this study, some examples will be shown where the system became unstable and that operation could not be continued. It is important that the system stays within operational stable conditions for reliable contingency of power generation. Simulation of load-following is therefore essential for the development of a micro gas turbine generator.

7.5.2 Load-following

Once stabilised operation of the micro gas turbine system with no load is established, load-following simulations can be conducted. Two different sets of load-following will be investigated:

(i) Gentle load-following and

(ii) Instantaneous (rapid) load following.

A stable running system is needed for load following, and the start-up results of the previous section will be used as starting conditions.

7.5.3 Gentle load-following

Gentle load-following will be simulated as a transient set (illustrated in Figure 7.4 to Figure 7.6):

Time step 0 to 15:	Stabilization of system. (No load)
Time step 15 to 23:	Load is applied at a gentle slope up to 40 kW.
Time step 23 to 27:	Constant load of 40 kW.
Time step 27 to 31:	Gentle load applied to 60 kW.
Time step 31 to 36:	Constant load of 60 kW
Time step 36 to 41:	Gentle load reduction to 30 kW.
Time step 41 to 50:	Constant load of 30 kW.

By evaluating the changes in turbine speed during the transient set (Figure 7.5), one can see that neither of the turbines shaft speeds is much affected by gentle changes in generator load. The TIT, however, reacts more severely to the change in load-following as can be seen in Figure 7.6. The micro gas turbine system reacts thus to gentle changes in load by altering the fuel supply to the combustor effectively in order not to affect the turbine shaft speed by much. The generator is driven by the LP turbine and therefore does not experience much change in rotation speed, which causes a more continuous power supply without sudden changes in power generated.

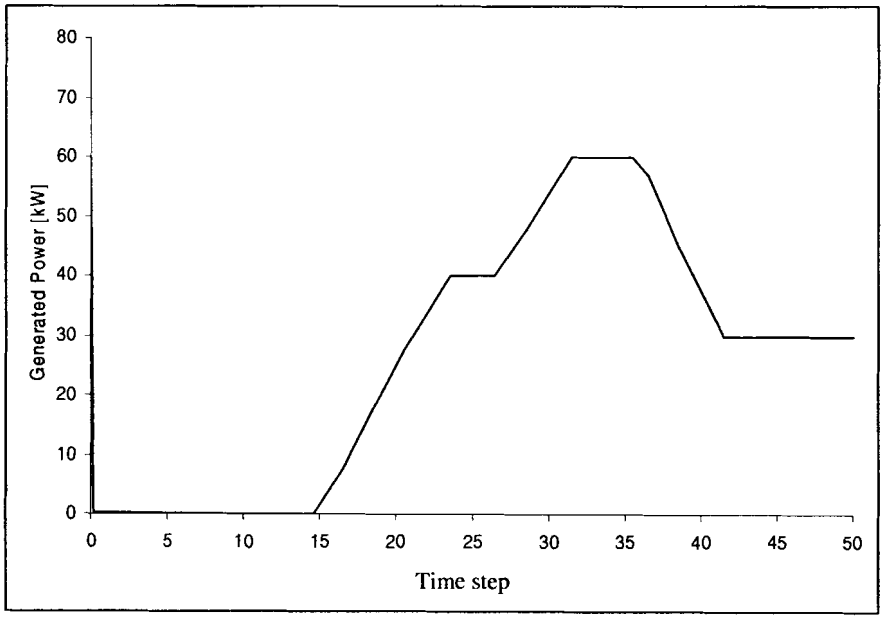

Figure 7.4: Power generated during gentle load-following

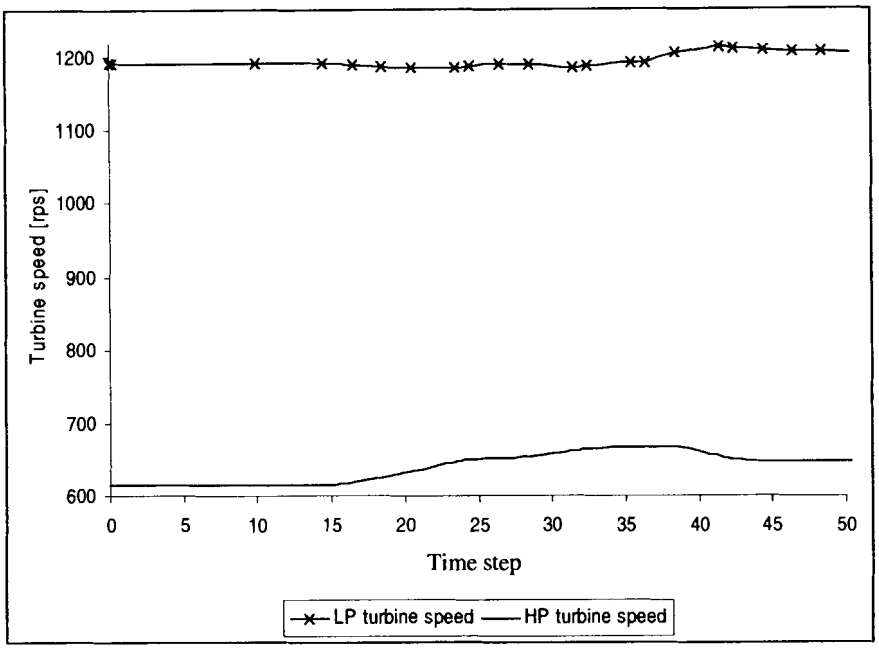

Figure 7.5: Turbine speed due to gentle load-following

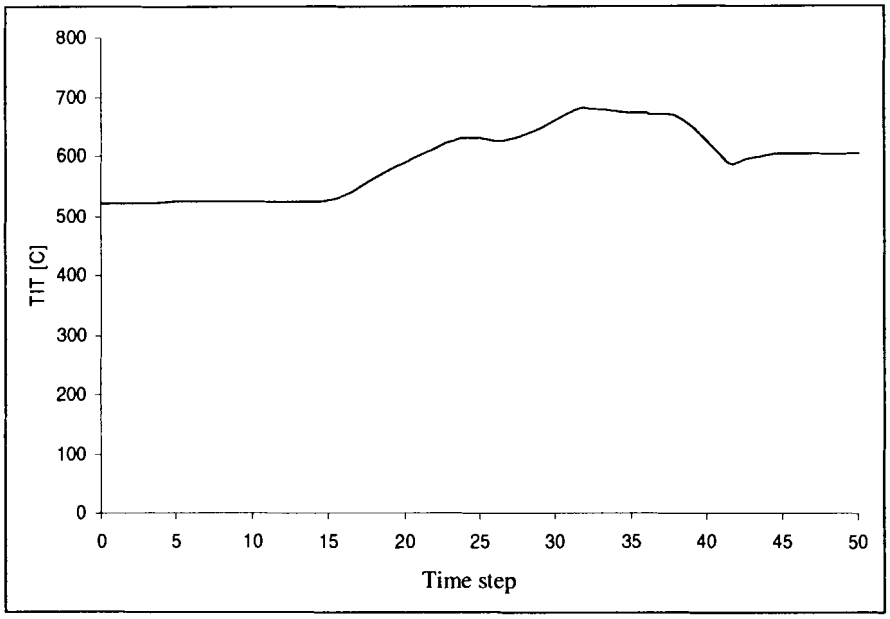

Figure 7.6: TIT control due to gentle load-following

The micro gas turbine system handles gentle changes to demand in power with ease and delivers uniform high quality electrical power. It is however necessary to simulate sudden changes in power demands in order to evaluate the system's reaction to such incidents.

7.5.4 Instantaneous load-following

Using the results of the start-up procedure as the input values, instantaneous load-following will be simulated as a transient set (illustrated in Figure 7.7 to Figure 7.9):

Time step 0 to 15:	Stabilization of system. (No load)
Time step 15 to 19:	A 30 kW load applied immediately.
Time step 19 to 23:	30 kW load is dropped instantaneously.
Time step 23 to 35:	65 kW load is instantaneously applied.
Time step 35 to end:	No load is applied by system.

In comparison to the gentle load-following simulation, turbine speeds are more affected by the aggressive change in power demand during the instantaneous load-following simulation. The controller responsible for TIT also reacted more vigorously and reached the limits more regularly in its attempt to govern the turbine speed. (The controller's limits are 400 to 700 °C.)

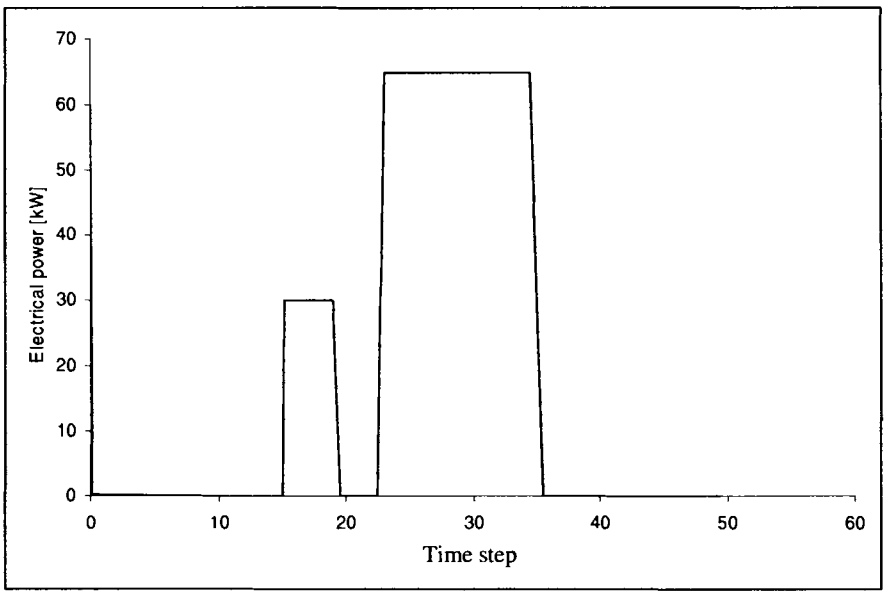

Figure 7.7: Power generated during instantaneous load-following

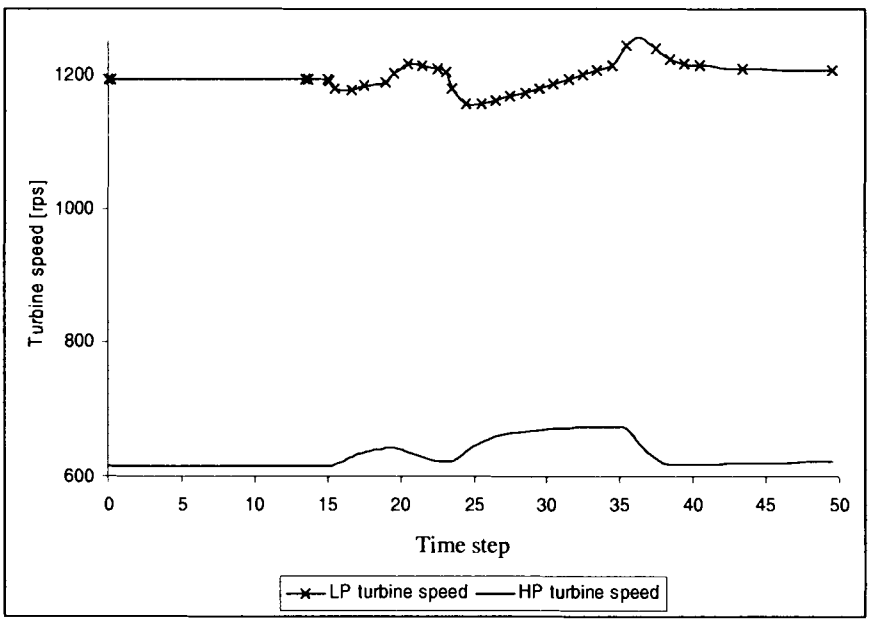

Figure 7.8: Turbine speed due to instantaneous load following

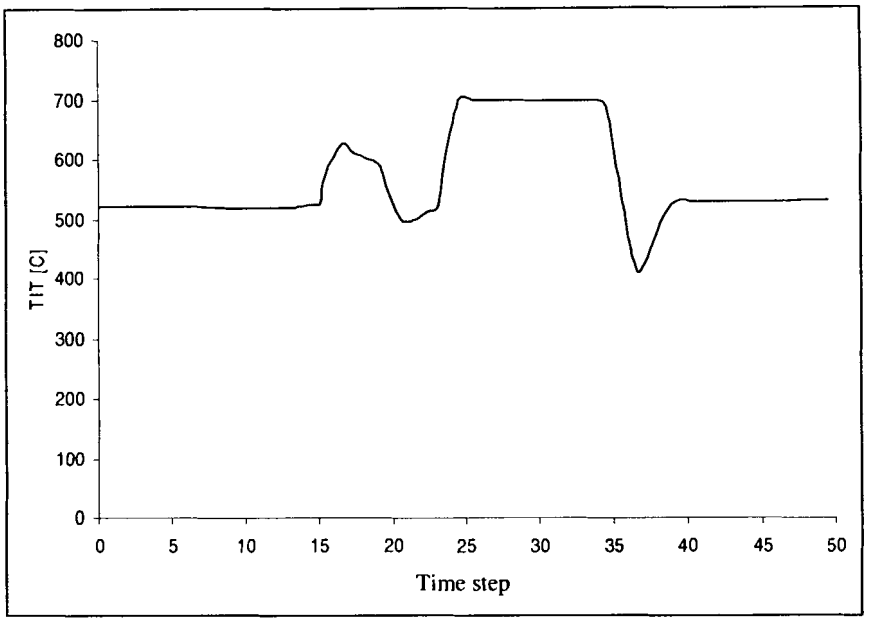

Figure 7.9: TIT control due to instantaneous load-following

The system was able to react to instantaneous load changes by altering the TIT more rapidly than during gentle load-following, while operating the system well within its stability limits, reacting to the change in a controlled manner, finding its operational conditions fast without any difficulty.

The gentle load-following introduces the least stress to the system as the change can be absorbed by the controller without much change to the turbine operating point (rotation speed). It is advisable that when electrical load is applied or removed from the generator, it is done gently. Unfortunately, this is only possible in ideal conditions. However in reality, the load demands vary and load changes can be instantaneous. Simulations show that the proposed micro gas turbine system can handle instantaneous load changes, as long as the changes are within the system's operational range.

7.5.5 Catastrophic load applications

Despite the system's ability to cope with sudden and gentle load following, there are conditions that are outside the system's capabilities. These situations occur where the system is placed under unrealistic operating conditions. Although these conditions may include a wide variety of situations, only the following situations were simulated:

Overload conditions
Compressor Surging

(i) Overload conditions occur when the load is higher than the maximum power that the micro gas turbine can provide (which is a continuous load of 72 kW). This simulation will be done with a continuous load demand of 80 kW and an illustration of the turbine reactions can be seen in the transient set (Figure 7.10 to Figure 7.12). The start-up results will be considered as the input condition for this overload conditions:

Time step 0 to 10: Stabilization of system. (No load)
Time step 10 to 16: Electrical demand is applied gently up to 60 kW.
Time step 16 to 26: Constant demand of 60 kW (stabilising the system).

Time step 26 to 30: Gentle load demand increase to 80 kW (over load demand).
Time step 30 to end: Continuous overload demand at 80 kW.

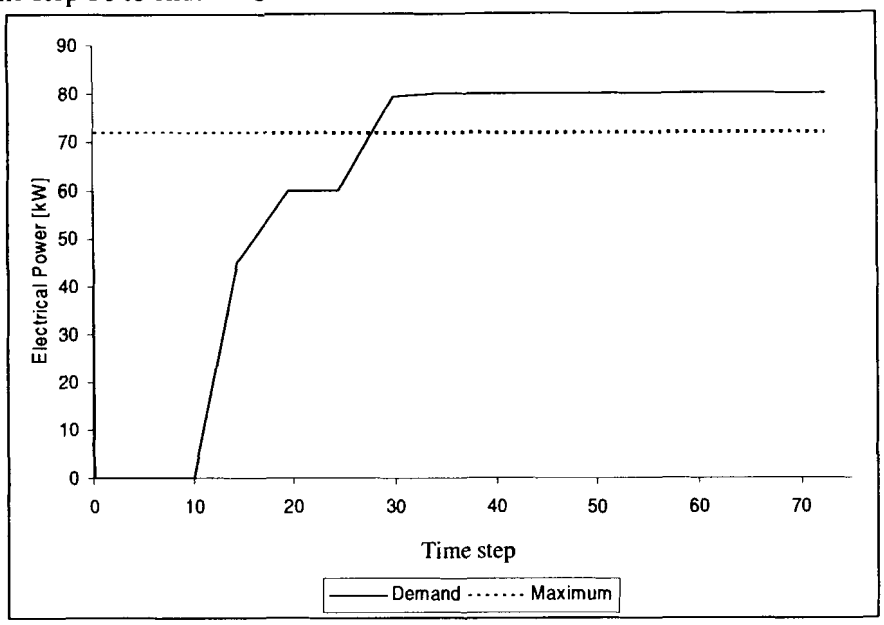

Figure 7.10: Over load condition simulation.

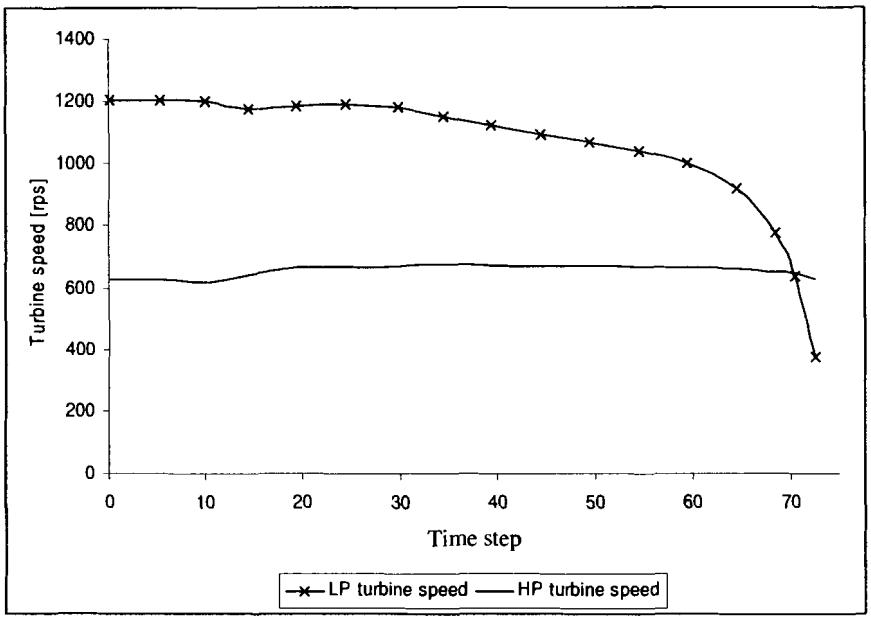

Figure 7.11: Turbine speed due to overload conditions

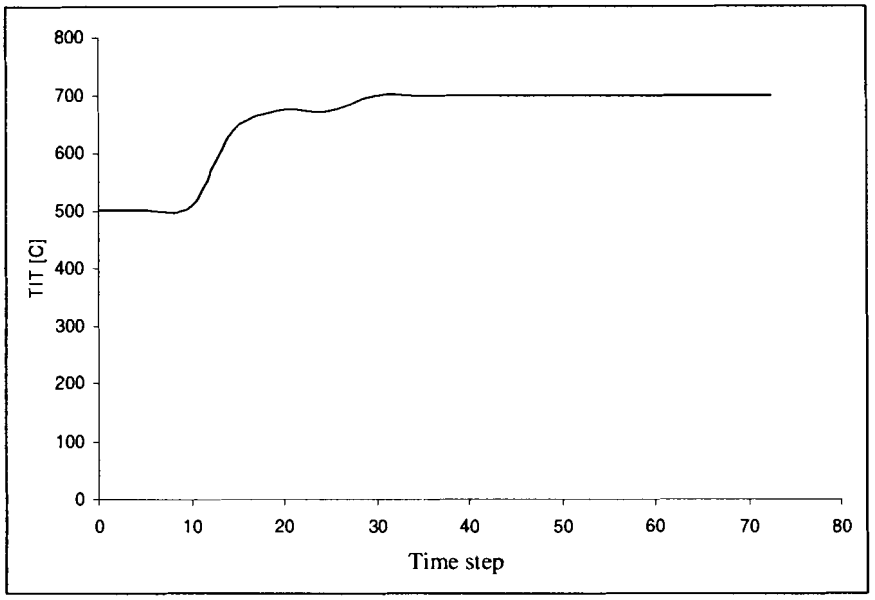

Figure 7.12: TIT due to overload conditions

The combined energy needed by the generator and LP compressor is higher than the LP turbine can provide, therefore losing speed. Reacting to the loss in speed, a higher TIT is introduced to provide more energy to the LP turbine, but the upper TIT limit of 700°C (the safe temperature the combustion chamber and turbine can handle) govern the heat energy provided to the turbine. The maximum energy that the combustion chamber can supply is less than that which is needed by the generator; therefore, the LP turbine will start losing speed as illustrated in Figure 7.11. However, the overload condition still continues, while the combustion chamber is still unable to provide sufficient energy to meet the load condition. The lack of thermal momentum will cause the LP turbine to continue decelerating until the system eventually reaches the point where it can no longer sustain itself, and all operation will cease. This emphasizes the need for an external load control system that will guard against overloading. The control system needs to govern the gas turbine system in order to produce at the system's maximum safe power level (even if this is lower that the demand). This control system will not be discussed in this study.

(ii) Surging of the LP compressor occurs when the load is suddenly dropped and the compressor connected to the LP turbine accelerates, causing oscillating flow through the compressor itself, also known as surging (the phenomena described in Chapter 4 and Appendix B of this study). Figure 7.13 illustrates the rapid change of the LP turbine's shaft speed until the simulation program can no longer predict the performance of the system anymore.

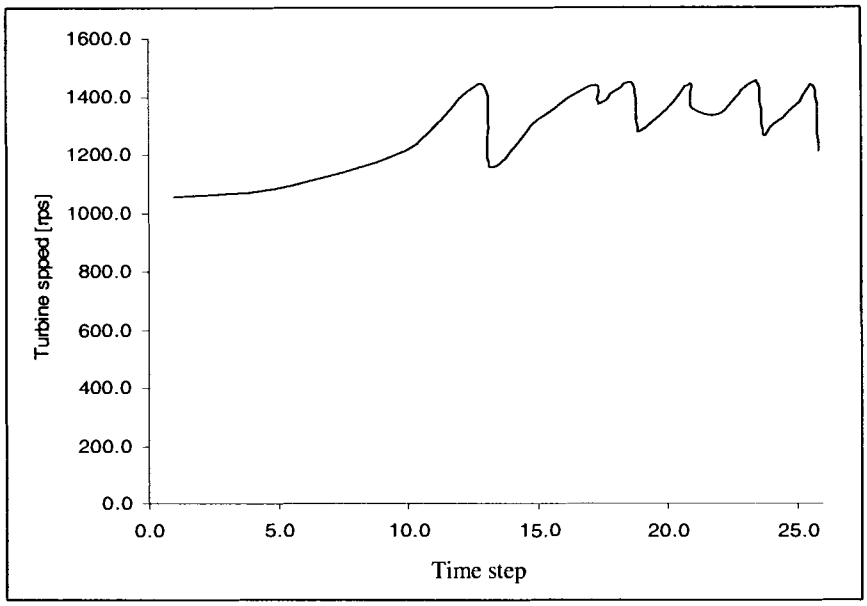

Figure 7.13: Surging of the LP Turbine

Surging causes the rapid acceleration and deceleration of the impeller in the compressor, which causes high frequency shock waves to propagate through the gas turbine system. This can lead to catastrophic failure of turbine machinery, and have to be avoided

The micro gas turbine system is thus unable to accommodate all conditions that may be presented to it, however, it is capable to deliver high quality undisturbed electrical power when the load is within the system's ability to operate in.

7.6 CONCLUSION

All the components and sub systems have been discussed together with their boundary conditions and operating conditions. All of these inputs have been captured and simulated with the software simulation package Flownex®. Both steady state as well as transient conditions were evaluated. Start-up and load-following were evaluated. The system reactions to some catastrophic situations were simulated as well in this part of the study. The micro gas turbine system conceptual design is thus proven.

8 Micro gas turbine system

8.1 THE MICRO GAS TURBINE GENERATOR SYSTEM

The aim of this study is to do a conceptual thermo-fluid design of a low cost micro-turbine power generator with commercially available turbo machinery and to simulate this system using the thermal fluid network solver Flownex®.

Operation of elementary turbo machinery was explored, evaluation of different variations of the real Brayton cycle was done and the influence of performance parameters on the systems was explained during the initial parts of this study. It was followed by a detail discussion of the turbo machinery that includes information on types of turbine machinery and the turbine components (compressor and turbine). The selection process that was followed in this study to appoint the relative machines to be used in the micro gas turbine generator was shown.

Part of this included an investigation into the custom design of turbine machinery, especially for this application. Once the selection process was concluded, it was possible to calculate the selected combination of turbo machinery's ideal operating conditions by doing system analysis. Limitations of the selected turbine machinery were used to calculate the operating conditions of the other subsystem that are part of the micro gas turbine system. The results of the system analyses set the initial boundary conditions for the rest of the subsystems like heat exchangers and the combustion chamber.

The system's combustion chamber can operate with various fuel sources with little or no changes to the fuel control system. This ability to operate on a variety of fuels, including biogas, highlights the wide spectrum of application of this micro gas turbine system. It can be used in rural environments without a constant supply of fuel.

Detail design of the heat exchanger and combustion chamber subsystems were done in the Chapter 5 of this study, followed by a steady state simulation done in the code Flownex®. This simulation proved that the configuration of the combination of turbine machinery, together with the designed heat exchangers and combustion chamber can produce an operating micro gas turbine system, which proved that this system is operational under steady state conditions. Therefore, transient simulations that prove the operation of the system at different operating conditions had to be done. Firstly, start-up was proven by controlling the system from low speeds onwards to high speeds (close to that of working conditions) without any load on the generator. Gentle load following simulation followed to prove the system's ability to generate power under normal operating conditions, followed by instantaneous load following. Here, the micro gas turbine generator system was subjected to harsher load following conditions as associated with load rejection. Thereafter, the system's performance to off-design conditions like overload and surging were investigated, but showed that it cannot be accommodated and control system therefore will have to be implemented.

8.2 PRELIMINARY PYSICAL MICRO GAS TURBINE LAYOUT

It is now possible to consider a preliminary cycle layout. An illustration of the physical layout is shown in Figure 8.1. According to this layout, the system will cover a floor area of approximately 1.5 x 2.2 m, and will be covered by housing. The height of the housing is 0.9 m, while the highest point of the system is the air intake filter and is 1.4 m high.
Note: The dimensions of this system make it an easily transportable system and even a small truck can convey the micro gas turbine to its location. The micro gas turbine system's

accessibility to remote locations around the world that can only be reached by land makes it an attractive commodity for users in remote places that do not have the transportation infrastructure to accommodate big systems. Another factor that offers interest is the flexibility of the system, i.e: Temporary sites can make use of this system wherever the location, as long as the necessary auxiliary systems is available also.

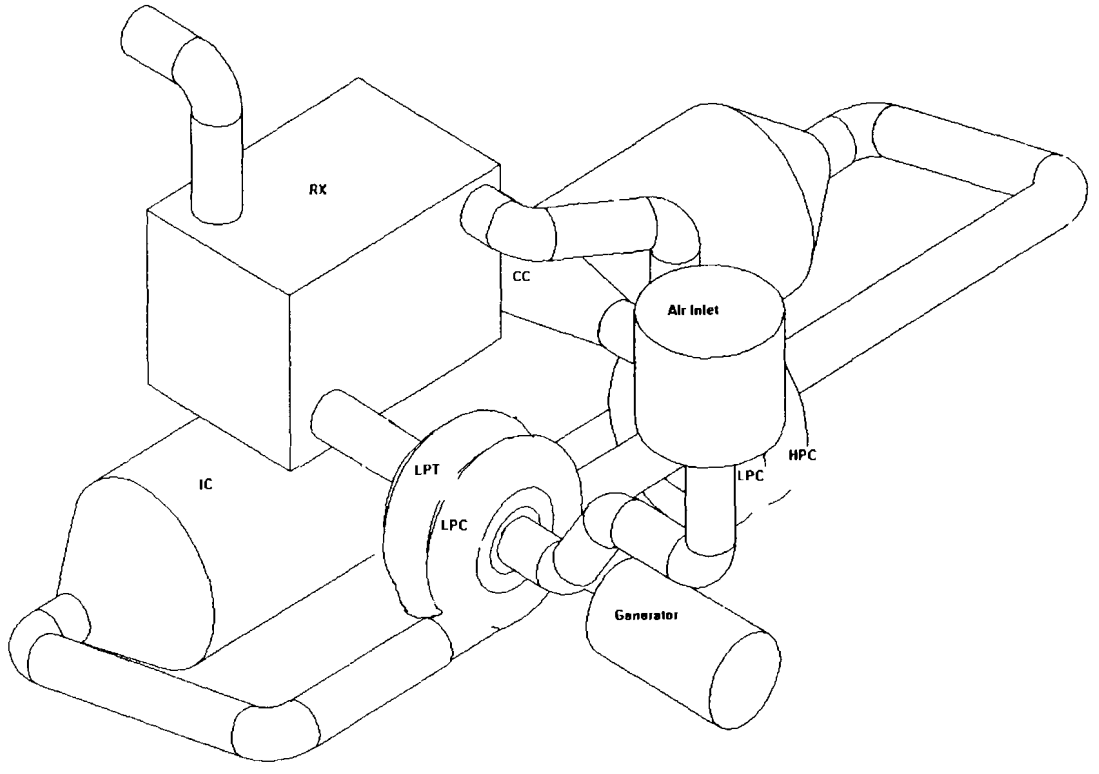

Figure 8.1: Illustration of the physical layout of the micro gas turbine system

8.3 RECOMMENDATIONS

The conceptual design and simulation of a micro gas turbine generator system was done as part of Master's study in order to prove the concept, therefore with limited funds. With the concepts proven more effort should be put in to demonstrate a functional operating unit. For this more attention should be paid to:

Turbo machinery:

Although touched during this study, more money and time has to be invested into the feasibility study of using custom designed turbo machinery. In this case, funding play an essential role, for turbine machinery is expensive, while developing turbine machinery are extremely expensive. Henceforth the need for a good simulation package like Concepts NREC – COMPAL is emphasised to limit expenses of developing machinery.

During this study, only centrifugal turbine machinery was evaluated. More research is needed to assess the feasibility to use axial turbines for gas turbine systems with higher efficiencies, but also a higher cost.

Thermal barrier technology is constantly growing allowing higher TIT's by using barrier technology on turbine blades. If this technology is acquired to allow higher TIT's significantly higher thermal efficiencies as well as specific work output can be reached even with the current conceptual micro turbine design.

Heat exchangers

More research on heat exchanger designs that have an improved efficiency. An increase in efficiency means that a smaller heat exchanger can be used and therefore lower costs to produce the heat exchanger. These include spherical heat exchangers that are incorporated around the turbo machine, allowing the gas turbine to occupy a lot less space, while producing high efficiencies.
Lower the coolant inlet temperature. This will cause the drop in temperature between the LP and HP compressors bigger, therefore enhancing the system's thermal efficiency.
Combustion chamber:
The design done for the combustion chamber in this study for this micro gas turbine generator system is a theoretical design. Therefore, more time and research are needed to be able to design a more efficient combustion chamber.
Simulation packages of combustion chambers are limited and even Flownex® was unable to simulate this rather common combustion chamber satisfactorily. Using CFD with more complex models will enable the designer to produce a combustion chamber with satisfactory performances and efficiencies. This can be done by optimisation of the combustion chamber combustion zones, dilution and wall cooling need to be researched in more depth.
The fuel supply and control system need to be designed. The combustion chamber controls the TIT, therefore, it is essential that the fuel control system is efficient to be able to react swiftly in order to supply high volumes of fuel, followed immediately by low fuel requirements moments later.
Auxiliaries
Load following control system: in order to allow for the reliable operation of the micro gas turbine system, a system is needed that is able to follow the electrical power load, while being able to protect the system against overloading and sudden load changes.
Lubrication system: As stated in this study, a reliable lubrication system is needed for both the lubrication as well as cooling of the turbo machinery's bearings. This system needs a back-up system as well.
Cooling system: A constant supply of coolant is needed; therefore the logistics of the cooling system has to be evaluated.
Generator/motor configuration: this unit serves as both the generator systems, as well as the start-up motor, that need to operate at different shaft speeds. An inverter is needed to control the motor's speed, as well as inverting the developed power to a constant frequency of 50 Hz.

8.4 CONCLUSION

The conceptual design and simulation of a micro gas turbine system that generates 72kW of electrical power continuously has been proved during in this study. Turbo machinery that has been used in this study is standard centrifugal turbo machines commonly used in big internal combustion, diesel powered machinery. As stated in the study, development of a custom turbo machine for this application to produce better thermal efficiencies is possible but costly and was not included in this study.
The heat exchangers and combustion chamber used by the micro gas turbine system have been designed and simulated.
The complete system was simulated under both steady state as well as transient conditions. The system's characteristic was proven, and the some of the transient conditions evaluated include start-up, load-following, as well as some catastrophic conditions.

9 References

AHLROTH M, DALILI F, ANHEDEN M & SVEDBERG S. System Analysis of Part Flow Humidified Closed Cycle Gas Turbines Fueled by Biomass. Literature Report, Department of Chemical Engineering and Technology/Energy Processes. Royal Institute of Technology, Stockholm, Sweden. 2000.

ANHEDEN M & AHLROTH M. System Studies on a Biomass Fired CHP Closed cycle Gas Turbine with CFB Furnace. Department of Chemical Engineering and Technology/Energy Processes. Royal Institute of Technology, Stockholm, Sweden. 2000.

ANHEDEN M, AHLROTH M, MARTIN AR & SVEDBERG G. 2000 Externally Fired Gas Turbine Cycles for small scale Biomass Cogeneration. 2000. ASME Turbo Expo 2000. Munich May 8-11, 2000-GT-0016.

ANTOINE H & PRIEELS L. 2002. The ACTE recuperator for gas turbine engines. ASME Turbo Expo 2002. Amsterdam June 3-6, GT-2002-30405.

AutoSpeed. Micro Turbine Power. [WEB:] http://www.autospeed.com/A_1245/P/article.html [Date of access: March 25, 2003]

BADRAN OO. 1999. Gas-turbine performance improvements. Applied Energy 64 (2999) 263-273.

BOYCE WP. 1982. Gas Turbine Engineering Handbook. Gulf Publishing, Houston. 603p.

Capstone. Explore Capstone Micro Turbine Technology. [WEB] http://www.capstoneturbine.com/index.cfm [Date of access: March 25, 2006]

CARMAN BG, KAPAT JS & CHOW LC. 2002 Impact of a ceramic micro channel heat exchanger on a micro turbine. ASME Turbo Expo 2002. Amsterdam June 3-6, GT-2002-30544.

CNN.com/world. 2003. London power failure engraves mayor. [WEB] http://www.cnn.com/2003/WORLD/europe/08/29/london.power/ [Date of access: October 10,2003]

COHEN h, ROGERS GFC & SARAVANAMUTTOO HIH. 1996. Gas Turbine Theory 4th ed. Prentice Hall. Harlow. England. 433p.
DER. Distributed Energy Resources. Advanced Generation: Micro Turbine Systems. [WEB] http://www.eere.energy.gov/der/pdfs/tech_briefs/microturbines.pdf [Date of access: October 12, 2003]

DOTY FD, HOSFORD G & SPITZMESSER JB. 1991. The Microtube Strip Heat Exchanger. Heat Transfer Engineering 12(1991) 31-41

Ebara. "We power your world": Elliott Energy systems. [WEB:] http://www.tapower.com [Date of access: June 05, 2002; March 25, 2006]

Find Law Corporate Council Centre. 2003. Tripp little protection against lightning strikes, power shortages and other summer power problems. [WEB] http://news.corporate.findlaw.com/prnewswire/20030523/23may2003152624.html [Date of access: 20 July 2003]

FLORES RM, McDONELL VG & SAMUELSEN GS. 2002. Impact of Ethane & propane Variation of a Model Gas turbine Combustor. ASME Turbo Expo 2002. Amsterdam June 3-6, GT-2002-30517.

Global-micro. Microturbine Cogeneration – Global Energy. [WEB:] http://www.globalmicroturbine.com [Date of access: October 12, 2003]

ISLAS J. The Gas Turbine: A New Technological Paradigm in Electricity Generation. 1999. Technological forecasting and Social change 60 (1999) 129-148.

KAYO D. 2002. Power sector reforms in Zimbabwe: will reforms increase electrification and strengthen local participation. Energy Policy 30 (2002) 959-965.

KLETT B.R. & WILSON R.J. 2001. Energize with state of the art technologies. Clearwaters. 31(2001)1-6

LAGERSTROM G & XIE M. 2002 High performance & cost effective recuperator for micro gas turbine. ASME Turbo Expo 2002. Amsterdam June 3-6, GT-2002-30402.

LEFEBRE AH. 1998. Gas Turbine Combustion. 2nd Ed. Taylor & Francis. London. 400p.

McDONALD CF, & WILSON DG. 1996. The utilization of recuperator and regenerator engine cycles for high-efficiency gas-turbines in the 21st century. Applied Thermal Engineering 16 (1996) 635-653.

McDONALD CF. 2000. Low-cost compact primary surface recuperator concept for microturbines. Applied Thermal Engineering 20 (2000) 471-497.

McDONALD CF. 2003. Recuperator considerations for future higher efficiency microturbines. Applied Thermal Engineering 23 (2003) 1463-1487.

NAN M. 2006. S. Africa plans to construct a second nuclear power plant. China view [WEB] http://news.xinhuanet.com/english/2006-03/24/content_4342429.htm [Date of access: 25 March 2006]

NAJJAR YSH. 1996. Relative effect of pressure losses and inefficiencies of turbo machines on the performance of heat-exchange gas turbine cycle. Applied Thermal Engineering 16 (1996) 769-779.

O'CONNER M. 2006. ESCOM is hiding something. Die Burger. 20/02/2006. [WEB] http://www.news24.com/News24/South_Africa/News/0,,2-7-1442_1885038,00.html [Date of access: 25 March 2006]

PILAVACHI PA. 2000. Power generation with gas turbine systems and combined heat and power. Applied Thermal Engineering 20 (2000) 1421- 1429.

PILAVACHI PA. 2002. Mini- and micro-gas turbines for combined heat and power. Applied Thermal Engineering 22 (2002) 2003-2014.

PRESTOR A. 2003. Big Dividends from a small footprint. WIP: Worldwide Independent Power. June 2003. 40p

ROUSSEAU PG. 2002 Advanced Thermal-Fluid System Course Notes. MEGI 885 Potchefstroom : PU for CHE 50 p.

STEWARD M, HAMRIN D, LIPOVICH N, DeMORE D, LARA-CURZIO E, MAZIASZ PJ & PINT BA. 2002. The ACTE recuperator for gas turbine engines. ASME Turbo Expo 2002. Amsterdam June 3-6, GT-2002-30581.

STOECKER WF. 1989. Design of Thermal Systems 3rd ed. McGraw-Hill. New York. 565p.

STONE C. 2003. Software plays major role in nuclear design. SA Mechanical Engineering. August 2003. 52p.

TERRETT J & CARTER L. 2003 Blackouts cause North America chaos. BBC News [WEB] http://news.bbc.co.uk/2/hi/americas/3152451.stm [Date of access: October 10,2003]

TREECE B, VESSA P & McKEITRNAN R. 2002. Micro turbine recuperator manufacturing and operating experience. ASME Turbo Expo 2002. Amsterdam June 3-6, GT-2002-30404.

VT Mechanical Engineering. 1997. Thermodynamics - Basic cycles and components [WEB] http://filebox.vt.edu/eng/mech/scott [Date of access: March 27,2003]

WALLöNFER W, KREMPL P.W & KRIPSEL F. 2001. Growth zones and their boundaries. Annales de Chime Science de Materiaux. 21 (2001) 75-78

WALLöNFER W, KREMPL P.W & KRIPSEL F. 2000. Anharmonic phonon coupling in piezoelectric $GaPO_4$. Proc. XVIIth International Conference on Raman Spectroscopy. J.Wiley & Sons. 526 p.

WANG FJ & CHIOU JS. 2002. Performance improvement for a simple cycle gas turbine GENSET – A retrofitting example. Applied Thermal Engineering 22 (2002) 1105-1115.

WILLCOCK RC, YOUNG JB & HORLOCK JH. 2002. Gas Properties as a Limit to Gas Turbine Performances. ASME Turbo Expo 2002. Amsterdam June 3-6, GT-2002-30517.

10 Appendix A: The Brayton cycle

The Brayton cycle is generally seen as the basis of all turbine machinery. Therefore, it is necessary to inform the reader on the Brayton cycle. The differences between the ideal and real Brayton cycle, as well as some variants of the Brayton cycle are discussed in this part of the study as a support function to Chapters 2 and 3.

10.1 INTRODUCTION INTO THE BRAYTON CYCLE AND ITS VARIATION

This appendix informs the reader on the differences between the ideal and real Brayton cycle, as well as the variant of these cycles. The impacts of the variances are shown and the detail system analysis is done on both the real as well as the ideal Brayton cycles. Different cycle configurations are evaluated in order to find the best suited configuration to be used in the micro gas turbine system.

10.2 THE IDEAL BRAYTON CYCLE

The ideal Brayton cycle is the theoretical cycle which forms the basis for the design of most modern gas turbines. An illustration of the ideal open Brayton cycle is shown in Figure 10.1.
Since shaft work is applied to the working fluid during the compression stage, both the temperature and pressure of the fluid will rise as shown in Figure 10.2 (Stage 1 – 2). Heat is added during the combustion stage (stage 2 – 3), raising the temperature of the working fluid, at constant pressure (The ideal Brayton cycle does not consider pressure losses of components). The combustion gas expands through the turbine (stage 3 – 4), transferring heat energy into shaft power, dropping the temperature and pressure of the working fluid over the turbine. These changes can be seen in an illustration of the temperature – entropy [T-s] diagram of the ideal Brayton cycle in Figure 10.2.

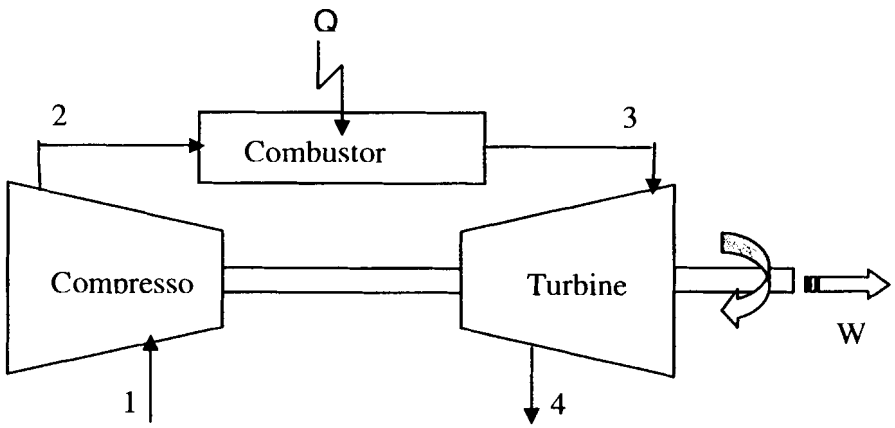

Figure 10.1: The open Brayton gas turbine cycle.

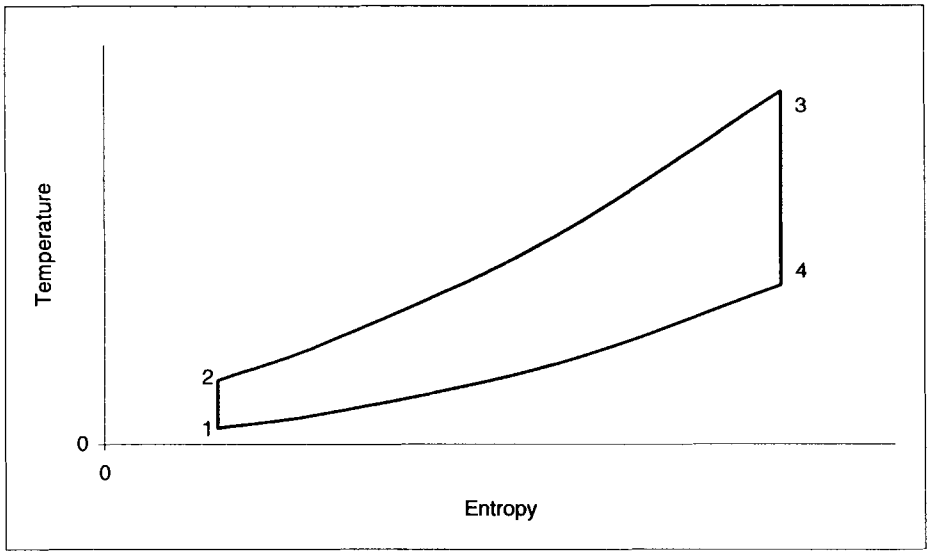

Figure 10.2: T-s diagram of the ideal Brayton cycle.

An important assumption that is made when analyzing the ideal Brayton cycle is that the working fluid is an ideal gas with constant specific heats. Using this assumption it can be shown that the thermal efficiency of the ideal Brayton cycle is given by:

$$\eta_{th} = \frac{\dot{W}_{nett}}{Q_{in}} = \frac{cp\left[(T_3 - T_4) - (T_2 - T_1)\right]}{cp(T_3 - T_2)} \qquad \text{Eq 10.1}$$

By deriving this equation as done in Appendix A, it can be proven that:

$$\eta_{th} = \left(1 - T_2/T_3\right) \qquad \text{Eq 10.2}$$

Also known is the relation between pressure and temperature:

$$\frac{T_4}{T_3} = \left(\frac{P_4}{P_3}\right)^{\frac{\gamma-1}{\gamma}} \qquad \text{Eq 10.3}$$

and

$$\frac{T_1}{T_2} = \left(\frac{P_1}{P_2}\right)^{\frac{\gamma-1}{\gamma}} \qquad \text{Eq 10.4}$$

Figure 10.3 illustrates that, in the ideal Brayton cycle, thermal efficiency η_{th} is a function of the pressure ratio [Pr] $\left[\eta_{th} = f(\mathrm{Pr})\right]$. This shows that a high pressure ratio is required to produce a system with good thermal efficiency.

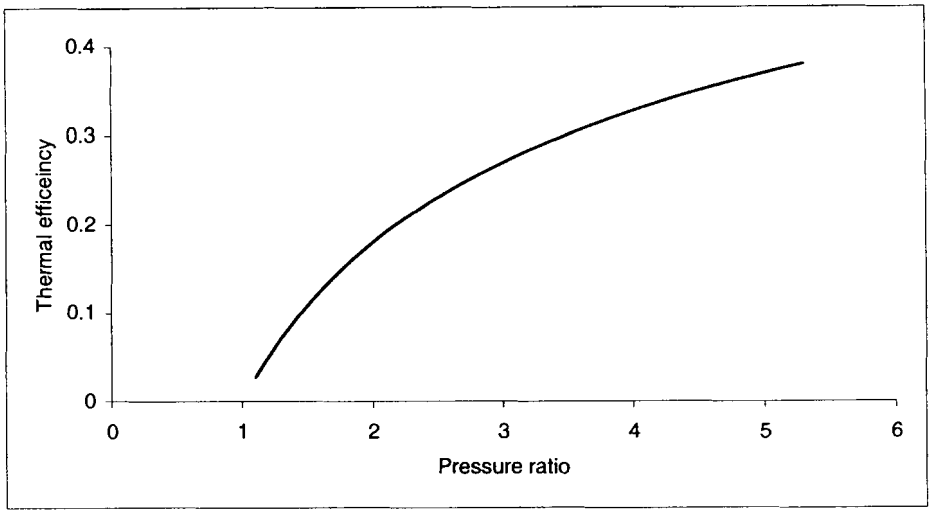

Figure 10.3: Thermal efficiency as a function of the pressure ratio for the ideal Brayton cycle.

The specific work output $\left[\dot{W}\right]$ of a cycle is a function of the turbine inlet temperature [TIT] as illustrated in Figure 10.4. The system's TIT value needs to be as high as possible to ensure a high work output value.

Both the pressure ratio and the TIT need to be optimized to produce a highly efficient system with a good work output. This is a process of finding the optimal ratio between the two parameters, and will be discussed in Chapters 3 and 4.

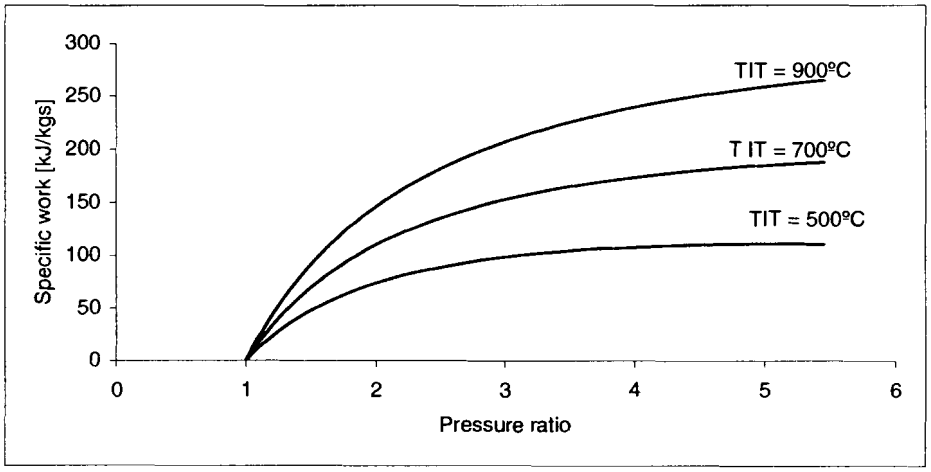

Figure 10.4: The effect of TIT on the specific work for the ideal open Brayton cycle.

The ideal Brayton cycle is only a theoretical cycle, as it is impossible to build cycle components with no inefficiencies. The real Brayton cycle will be discussed and evaluated against the ideal Brayton cycle to prove that optimisation of both the pressure ratio and the turbine inlet temperature will produce a system with the best efficiency as well as output work for that particular layout.

10.3 THE REAL BRAYTON CYCLE

The real Brayton cycle differs from the ideal cycle because of losses in turbo machinery, heat exchangers, flow passages and combustion chamber. The deviation of actual cycle from the ideal cycle is shown in Figure 10.3. It is shown that the entropy changes during the compression and expansion stages, while isobaric combustion is not achieved, as assumed in the case of the ideal Brayton cycle.

The mathematical analysis of the real Brayton cycle can be seen in Appendix G. According to this analysis not only the thermal efficiency, but the specific work output as well, are both functions of the pressure ratio and the turbine inlet temperature:

$$\left[\eta_{th} = f\left(\mathrm{Pr}, TIT\right) \text{ and } \dot{W} = f\left(\mathrm{Pr}, TIT\right)\right] \qquad \text{Eq 10.5}$$

as illustrated in Figure 10.6 and Figure 10.7.

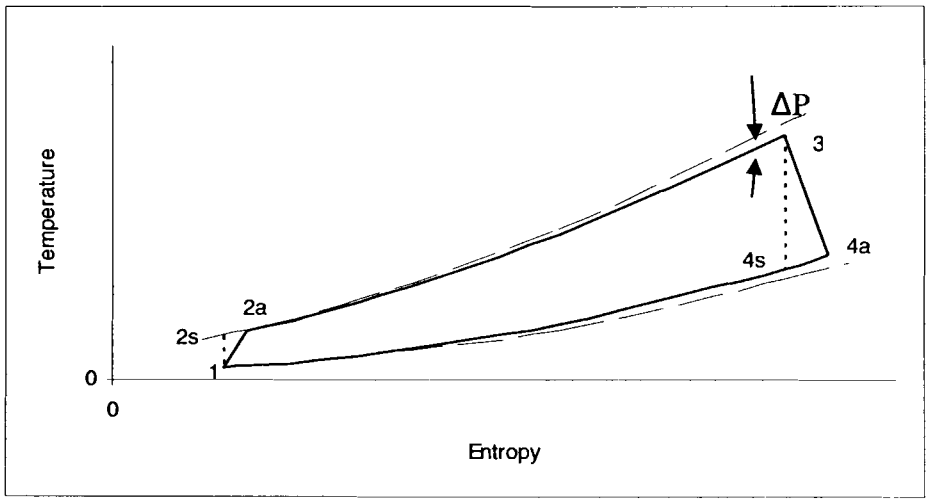

Figure 10.5: T-s diagram of the real Brayton cycle.

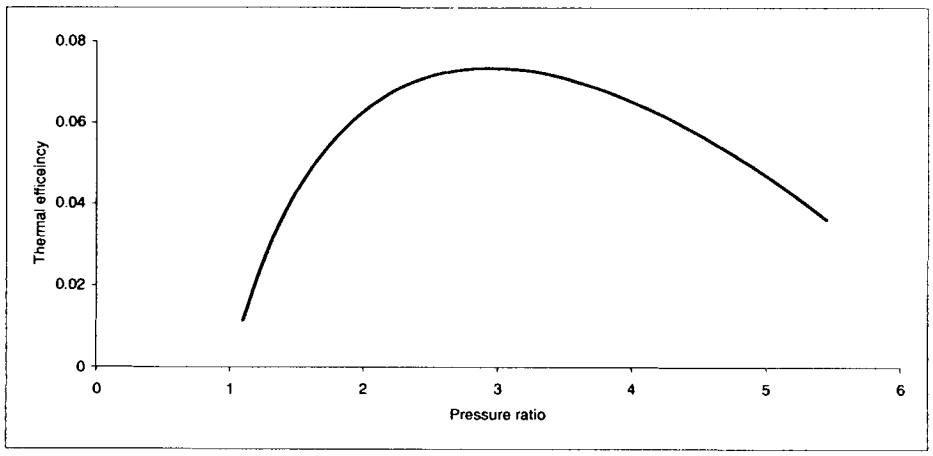

Figure 10.6: Thermal efficiency as a function of pressure ratio of the real Brayton cycle.

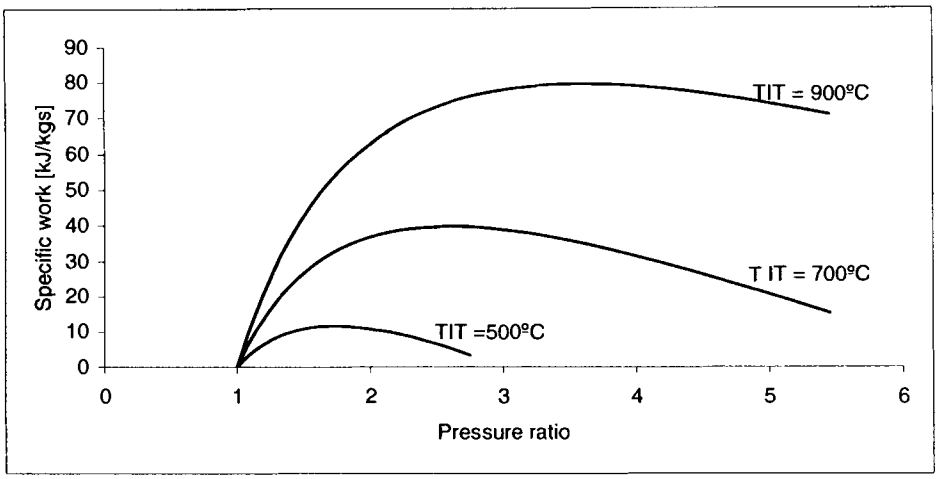

Figure 10.7: The effect of turbine inlet temperature on the specific work for the real Brayton cycle.

A comparison of the thermal efficiency and specific work output between the ideal and real Brayton cycles can be seen in Figure 10.8 and Figure 10.9 Note that the ideal Brayton cycle out-performs the real Brayton cycle in both comparisons, due to the presence of losses in the real cycle.

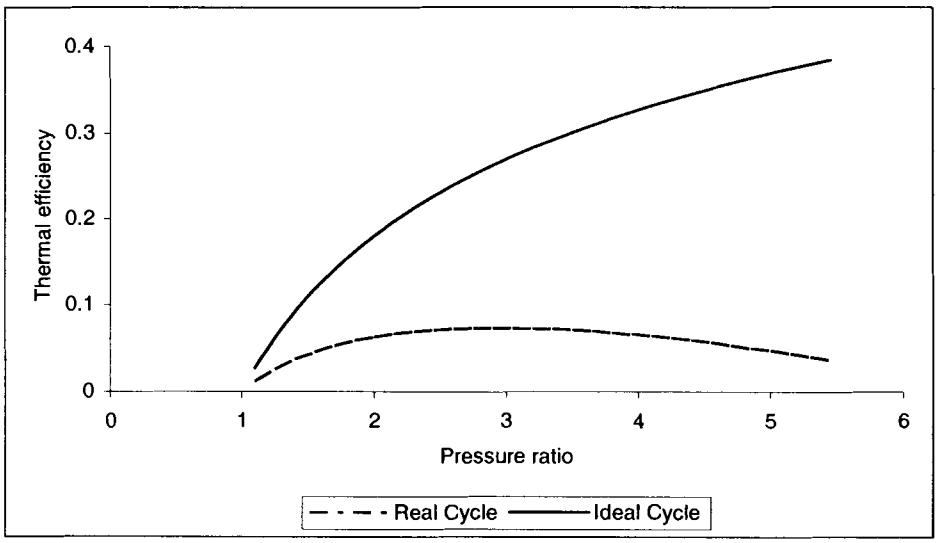

Figure 10.8: Comparison of the specific work between the ideal and real Brayton cycles.

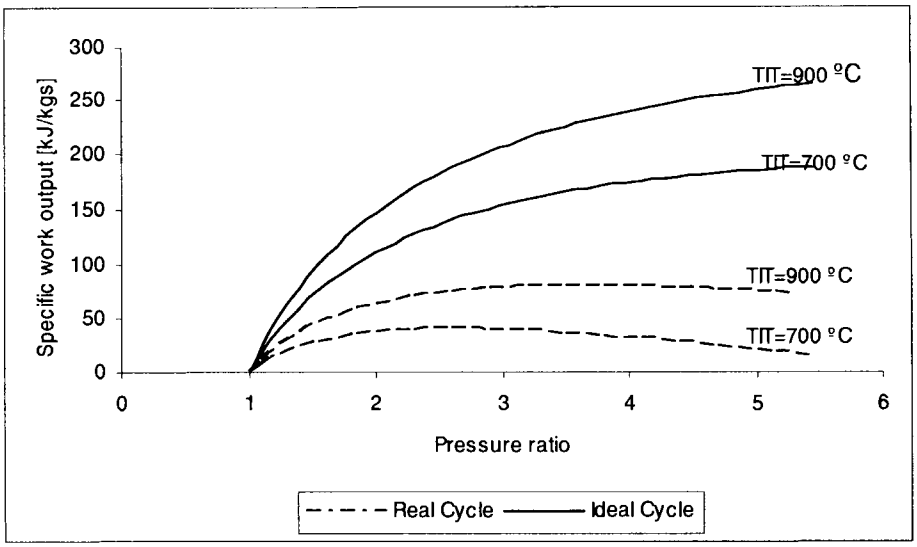

Figure 10.9: Comparison of thermal efficiency between the ideal and real Brayton cycles.

The above results were calculated with the compressor and the turbine efficiencies taken to be 0.7 and 0.76 respectively, with loss in pressure over the combustor $\left[\left(\frac{(P_{2a}-P_3)}{P_{2a}}\right)x100\right]$ equal to 1% of the combustor chamber inlet pressure $[P_{2a}]$ for the real Brayton cycle. A sensitivity analysis of the real Brayton cycle will be done in Chapter 3.

10.4 VARIATIONS ON THE BRAYTON CYCLE

By using the Brayton cycle as a basis, cycle variations can be evaluated by changing the configuration of the system. Note that all component parameters like efficiencies and pressure losses will stay constant, equal to the values stated previously. Completely different cycle characteristics are created with each of the variations and will be investigated for the best optimisation. The cycles that will be considered in this study are:

Recuperated cycle
Multi-stage compression with inter-cooling

10.4.1 The recuperated Brayton cycle

A characteristic of gas turbines is their high exhaust temperatures and by utilizing this heat, preheating the compressed air before combustion, it is possible to reduce fuel consumption and thus the energy needed by combustion. The cold inlet air never comes in direct contact with the hot exhaust gas, thus only exchanging heat in the recuperator. An illustration of the recuperated Brayton cycle can be seen in Figure 10.10, followed by the temperature – entropy [T-s] diagram in Figure 10.11. The temperature difference of the cold gas $T_2 - T_3$ is equal to the temperature difference of the hot gas $(T_5 - T_6)$ and the recuperator efficiency is defined as actual heat exchanged over the maximum heat difference of the heat exchanger:

$$\eta_{rec} = \frac{(T_3 - T_2)}{(T_5 - T_2)} \qquad \text{Eq 10.6}$$

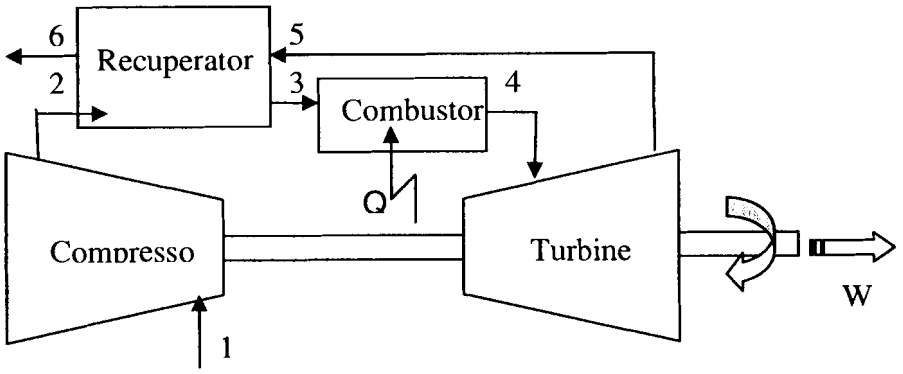

Figure 10.10: The recuperated Brayton cycle.

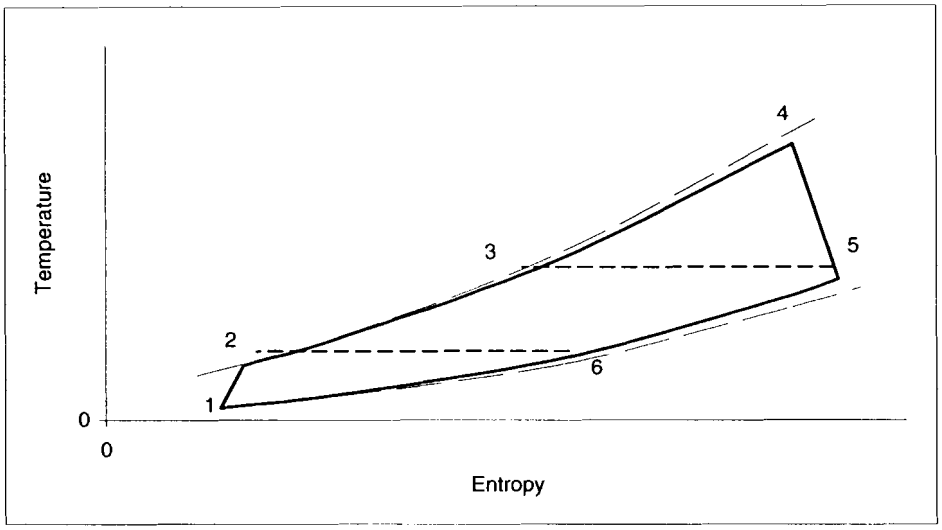

Figure 10.11: T-s diagram of the recuperated Brayton cycle.

The specified work output differs only slightly from that experienced with the real Brayton cycle, and will not be evaluated in this part of the study.

The recuperator increases the temperature of the air entering the combustion chamber, which leads to a reduction in the fuel-to-air ratio and an increase in the thermal efficiency. The thermal efficiency is thus a function of the recuperator efficiency $\left[\eta_{th} = f(\eta_{rec})\right]$. The effect of different recuperator efficiencies ranging from 80% to 95% are shown in Figure 10.12. A detailed discussion of the recuperator and its design will follow in Chapter 5.

The comparison between the recuperated Brayton cycle and the real Brayton cycle is also shown in Figure 10.12. This proves that a system's efficiency can be boosted by utilising the heat of the exhaust gas [also known as waste heat], but note that this is limited by both low and high pressure values. An optimum operation pressure ratio value needs to be found, and will be discussed during Chapter 3 and 4 of this study.

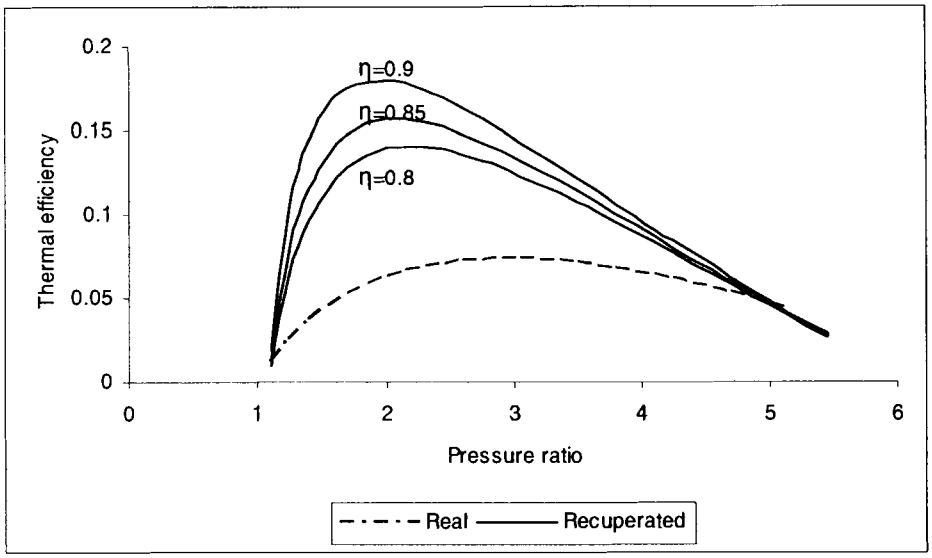

Figure 10.12: Thermal efficiency as a function of pressure ratio of the recuperated Brayton cycle.

10.4.2 The multi-stage Brayton cycle

Multi-stage systems that are common today have evolved from the recuperated Brayton cycle by adding compressor or turbine stages. Various configurations of the multi-stage system are possible. Either the compressor or the turbine can be split into multiple stages. When the turbine is split into stages, each turbine can rotate independently. Multi-shaft turbine configurations are mainly used for high torque and large load applications.

In this study emphasis will fall on multi-stage compression systems as illustrated in Figure 10.13. The following assumptions have been made:
1) Temperature at the inlet of the second stage compressor is equal to the temperature of the first compressor,
2) All the compressors have the same efficiencies and
3) The pressure ratios in both compressors are equal to $\sqrt{P_4/P_1}$.

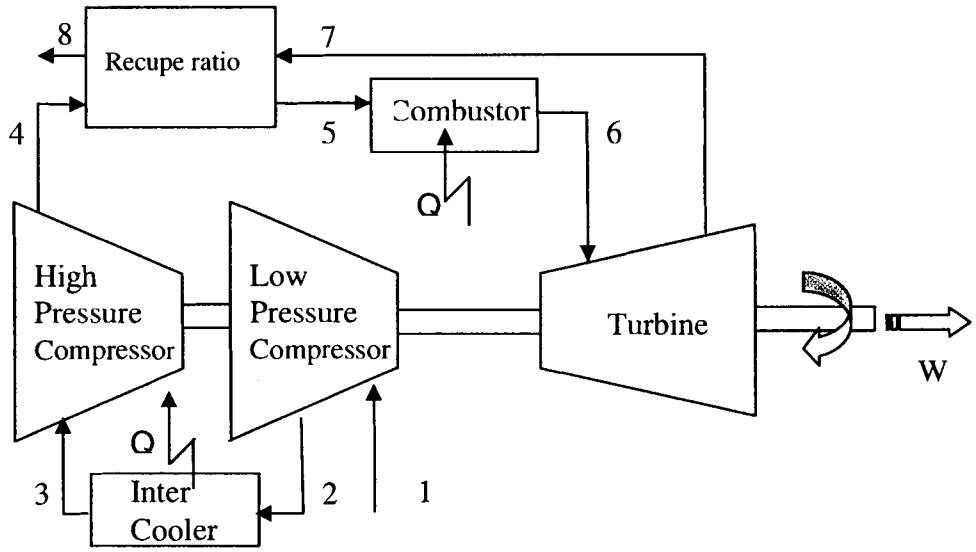

Figure 10.13: The multi-stage compression Brayton cycle.

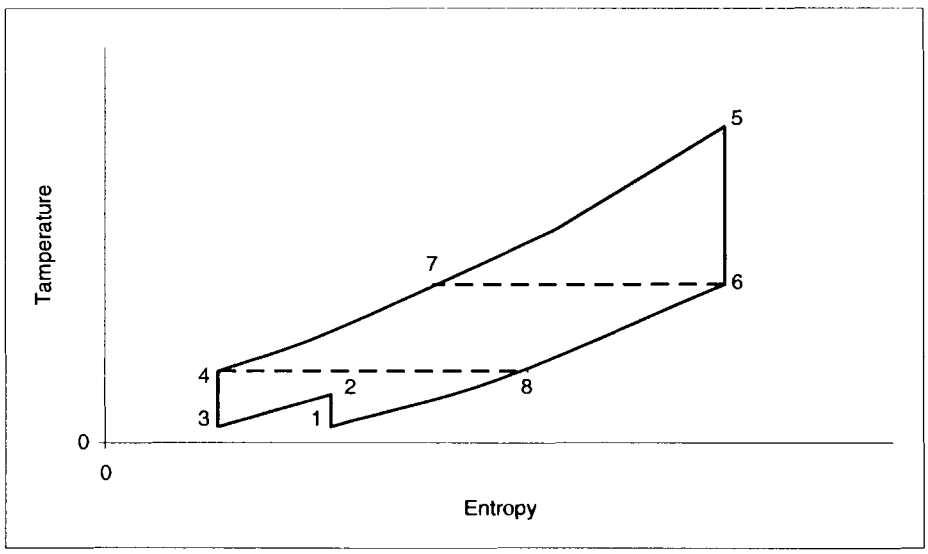

Figure 10.14: T-s diagram of a multi-stage compression Brayton cycle.

Both the thermal efficiency and the specific work output are functions of pressure ratio, recuperator efficiency and turbine inlet temperature [TIT].

$$\eta_{th} \text{ and } \dot{W} = f(\mathrm{Pr}, \eta_{rec}, TIT). \qquad \text{Eq 10.7}$$

A sensitivity analysis will be conducted where the effects and interaction of these parameters will be discussed in Chapter 3.

9.5 ANALYSIS OF THE IDEAL CYCLE

Ideal cycles considered in this study are based on the following assumptions: the pressure ratio(s) of the compressor(s) and the turbine(s) remain the same, all components operate at 100 % efficiency and no pressure losses occur due to friction or inertia.
The following ideal conceptual cycles will be investigated:

Ideal cycle without recuperation [IB]. (Standard Brayton cycle as discussed in the previous chapter.)

Ideal cycle with recuperation [IBR]. (Similar to the IB cycle, but with a recuperator added.)

Ideal two-stage compression with inter-cooling and recuperation [ITCIR]. (IBR cycle with two compressors and inter-cooling.)

The boundary conditions in Table 10.1 will hold true during the first order analysis of this ideal cycle analysis.

Table 10.1: Boundary conditions for the first order analysis (Ideal Brayton cycles).

Component	Condition
Mass flow rate	1 kg/s
Low pressure compressor inlet temperature	26°C
Maximum Turbine Inlet Temperature TIT	700°C
Pressure ratio range	1.3 - 5.56

Ideal basic cycle without recuperation [IB]
Simple inspection of the IB cycle proved that efficiency is dependent on pressure ratio (Figure 10.15). The graph shows that in order to obtain high cycle efficiency, it is necessary to operate at high pressure ratios.

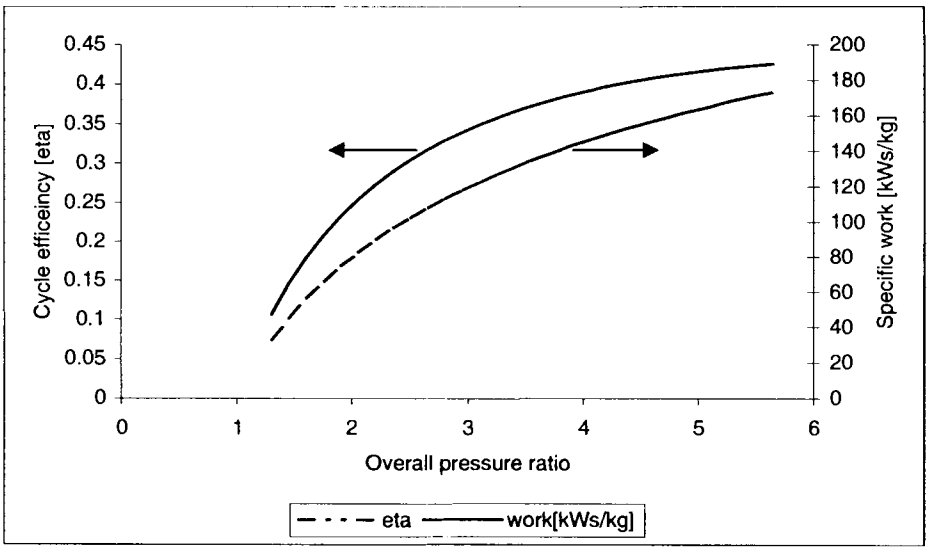

Figure 10.15: IB cycle efficiency and specific work as a function of overall pressure ratio.

10.5.1 Ideal basic cycle with recuperation [IBR]

An IBR cycle is created by adding a recuperator to the IB cycle. The benefit of having a recuperator in the cycle is discussed in Chapter 2 of this study. Having the ability to utilise the exhaust heat (waste heat) to heat the combustion inlet air minimizes the energy needed by the

combustor to reach the optimum TIT of 700°C. The cycle's thermal efficiency is hereby improved as illustrated in Figure 10.16.

The enhanced thermal efficiency of the IBR cycle ensures its specific work almost equals that of the IB cycle. Therefore the specific work of the IBR cycle is almost equal to that of the IB cycle, and has high values at increased pressure ratios. IBR cycle efficiency is significantly higher than that of the IB cycle, but reaches maximum work at a lower pressure ratio.

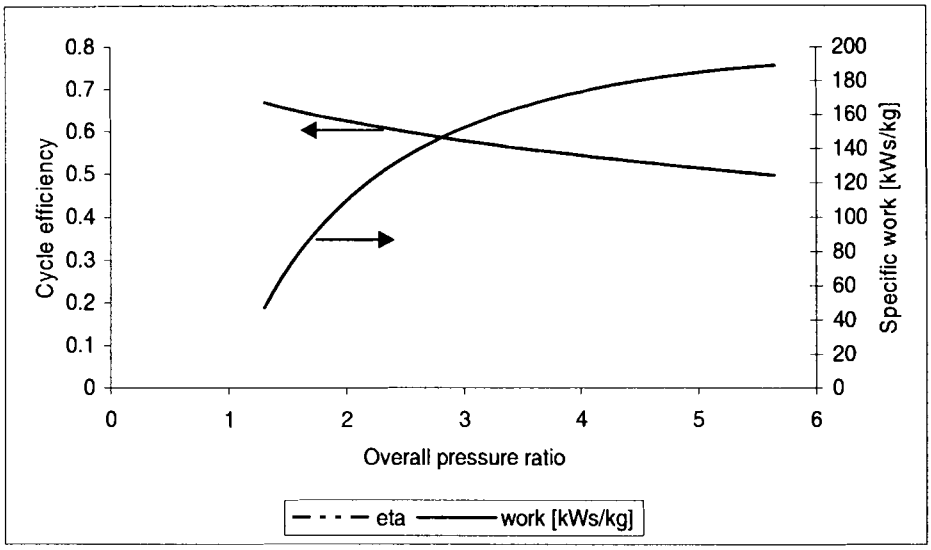

Figure 10.16: IBR cycle efficiency and specific work as a function of overall pressure ratio.

10.5.2 Ideal two-stage compression cycle with inter-cooling and recuperation [ITCIR]

An ITCIR cycle is created by adding a second compressor stage, with inter-cooling, to the TBR cycle. The addition of this inter-cooling will bring the temperature of the gas leaving the first stage compressor back to inlet temperatures. The following assumptions will hold true: Compressor inter-stage temperature is equal to that of the inlet temperature and the compressor ratio of both compressors are equal to $\sqrt{P_4/P_1}$.

The cycle efficiency of the ITCIR cycle is equal to that of the IBR cycle, but the specific work output is boosted. The trends of the efficiency and specific work are the same as the IBR cycle and can be seen in Figure 10.17.

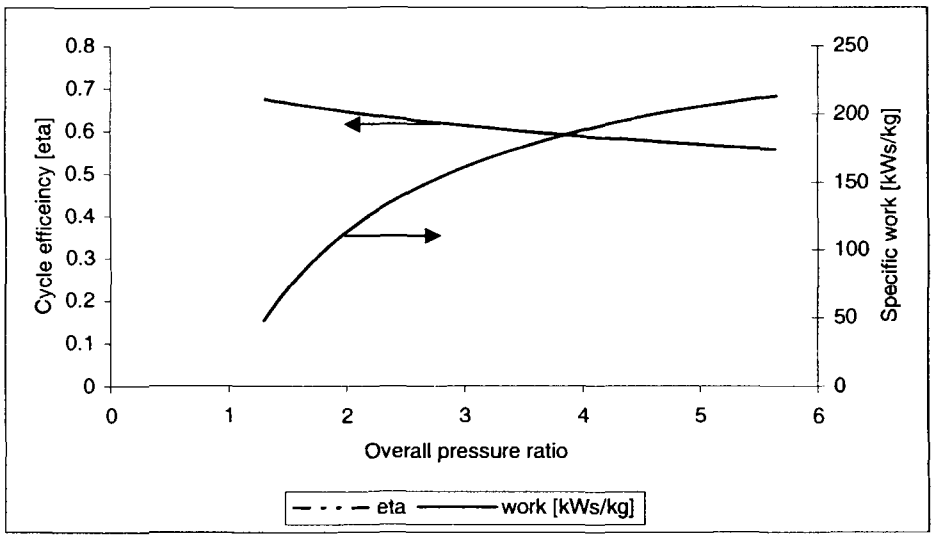

Figure 10.17: ITCIR cycle efficiency and specific work as a function of overall pressure ratio.

10.6 ANALYSIS OF THE REAL CYCLE

In Chapter 2, the difference between the ideal and real cycles is illustrated. As it is nearly impossible to build a physical cycle that represents the ideal cycle, real cycles are simulated with certain predefined losses and inefficiencies in mind. During this evaluation of real cycles the assumed boundary conditions in Table 10.2 will hold true.

Table 10.2: Boundary conditions for the first order analysis (Real Brayton cycle).

Component	Condition
Mass flow	1 kg/s
Inlet Temperature	26°C
Turbine Inlet Temperature [TIT]	700°C
Pipe pressure loss (each)	2 %
Heat exchanger pressure loss (each)	10 %
Recuperator efficiency	90 %
Mechanical Efficiency	98 %
Compressor Efficiency	76 %
Turbine Efficiency	70 %

The real cycle will be evaluated by the following conceptual cycles:
Basic cycle without recuperation [BC]. The modified "Real Brayton cycle" with some assumptions regarding losses and inefficiencies.
Basic cycle with recuperation [BCR]. BC cycle with the addition of recuperation.
Two-stage compression with inter-cooling and recuperation [TCIR]. Same cycle as ITCIR, but with assumptions regarding inefficiencies and losses [turbine and compressor efficiencies are equal].

10.6.1 Basic cycle without recuperation [BC]

The real basic cycle has an optimum pressure ratio range where both the thermal efficiency and the specific work output are close to their maximum as illustrated in Figure 10.18. An optimum value for the overall pressure ratio exists and will be evaluated during Chapter 4.

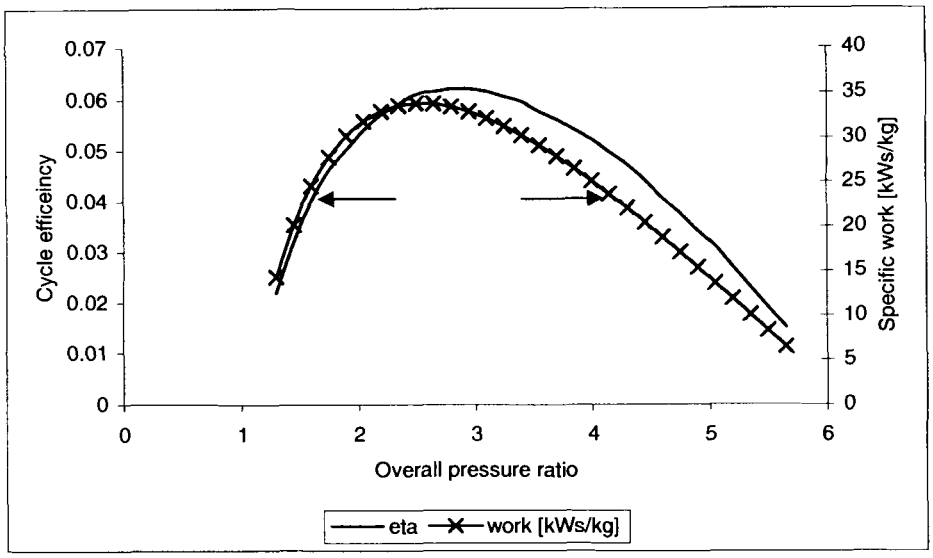

Figure 10.18: RB cycle efficiency and specific work as a function of overall pressure ratio.

10.6.2 Basic cycle with recuperation [BRC]

The specific work output of a recuperated cycle is less than that of the basic cycle, but the thermal efficiency is improved [Figure 10.19]. The value for the pressure ratio at peak thermal efficiency is smaller in the recuperated cycle than in the basic cycle, while the value is the same in both cycles when considering specific work output.

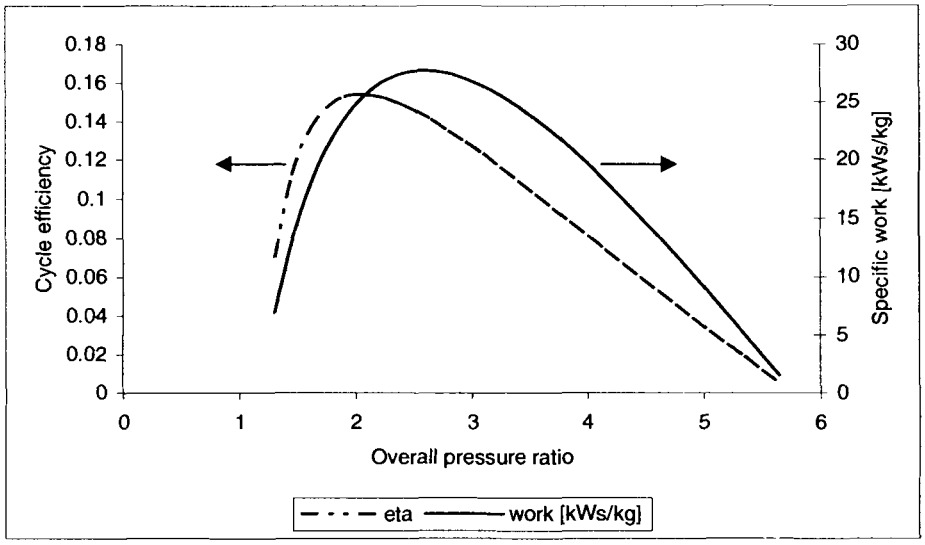

Figure 10.19: RBC cycle efficiency and specific work as a function of overall pressure ratio.

10.6.3 Two-stage compression cycle w ith inter-cooling and recuperation [TCIR]

The same assumptions used for the evaluation of the ITCIR cycle will be used with the addition of one condition: both the compressors and the turbines have equal efficiencies. Adding an inter-cooler decreases the high pressure compressor inlet temperature. This results in a reduction in the compressor power requirement, and is accomplished by cooling the inlet temperature in the second stage to the same as ambient air and maintaining the same overall pressure ratios, as illustrated in Figure 10.20.

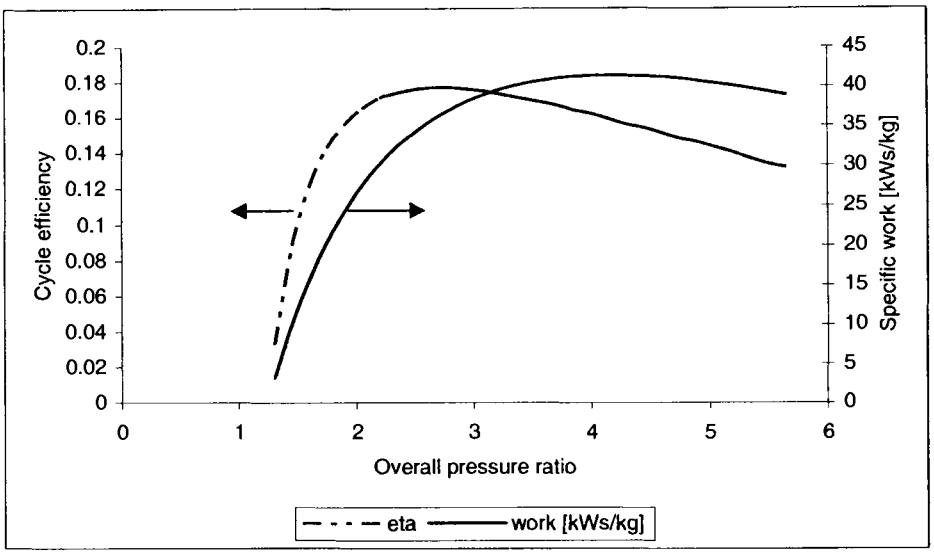

Figure 10.20: TCIR cycle efficiency and specific work as a function of overall pressure ratio.

10.7 COMPARISON OF REAL CYCLES

Due to the near impossibility of achieving cycle layouts that represent the ideal cycle, only the real cycles will be evaluated in this study. It should be noted that the ideal cycle represents the best possible optimum cycle towards research strive: to create a real cycle that represents the ideal cycle as close as possible.

Various outputs for the real cycles can be seen in Figure 10.21 and Figure 10.22, illustrating the different thermal efficiency and specific work output. These curves are drawn for a TIT of 700 °C, recuperator efficiency of 90 % and a wide overall pressure ratio range.

By investigating the cycle's efficiency as a function of overall pressure ratio [Figure 10.21], it can be seen that the TCIR cycle has the best efficiency over most of the pressure ratio range. The optimal thermal efficiency for TCIR occurs at an overall pressure ratio of approximately 2.8 and drops slightly as the pressure ratio rises, but remains better than the RBC cycle's efficiency. The TCIR cycle therefore achieves higher efficiency than the RBC cycle's maximum efficiency over the range of overall pressure ratio.

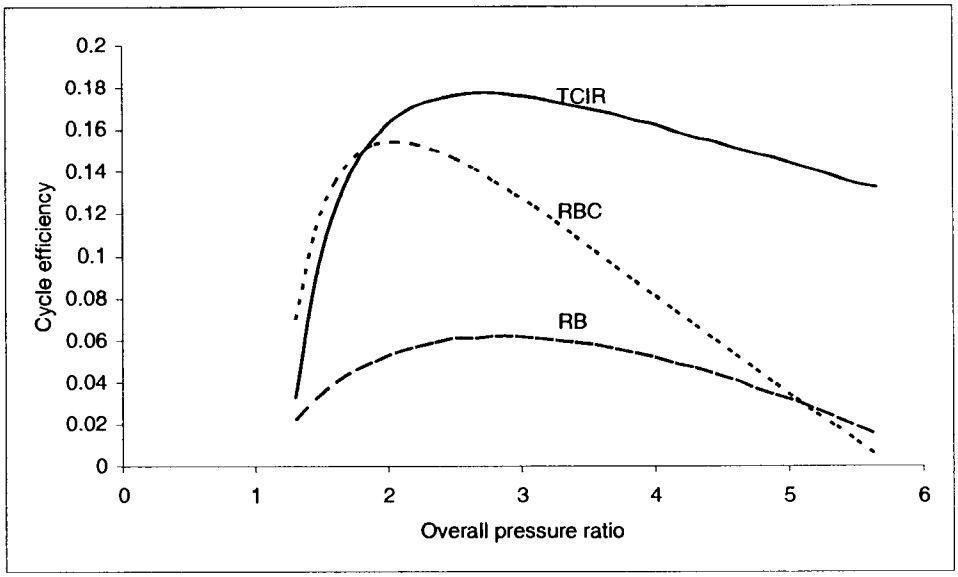

Figure 10.21: Cycle efficiency comparison at a TIT of 700 °C.

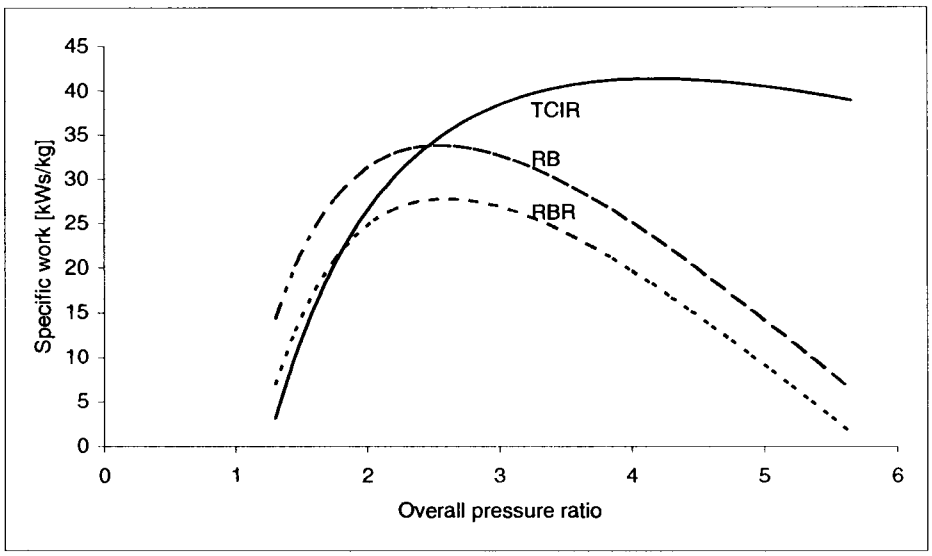

Figure 1022: Cycle specific work output comparison for a TIT of 700 °C.

Specific work output definition: Work output per mass flow unit (1 kg/s). When considering specific output work, the TCIR cycle has a maximum specific work output at pressure ratio values in the region of 3.1, but the work output's values drops slightly when the overall pressure ratio increases or decreases as seen in Figure 10.22. However, the specific work output of the TCIR cycle is still better than both the RBC and RB cycles over the overall pressure ratio range (excluding pressure ratios lower than 2.1).

Both these graphs prove that the TCIR cycle is the best cycle of those investigated, and is therefore the only cycle configuration that will be considered during investigations to follow in this study.

11 Appendix B: Turbine machinery and their performance characteristics

This chapter serves as a support for Chapter 4, where more information on turbine machinery performance characteristics can be obtained. The turbine selection process is done in detail where all the differences between Configurations (both 2nd and 3rd order) can be seen.

11.1 INTRODUCTION INTO TURBINE M ACHINERY PERFORMANCE CHARACTERISTICS

In this chapt, the differences between the types of turbine machinery will be explained. The detail selection process is i llustrated and information on surging is given.

11.2 TURBINE MACHINE TYPES

It is necessary to distinguish between the terms "aircraft gas turbine" and "industrial gas turbine" in this study. The first term is self explanatory, while the second term includes all gas turbine machines that are not included in the first term. This distinction has to be made for the following three reasons as stated by Cohen et al. (1996): Life expectancy of an industrial plant is in the order of 100 000 hours without major overhaul. Due to the hunt for light, highly efficient and compact machines, aircraft turbine machine's life expectancy is a lot less that that of an industrial engine. Secondly, size and weight limitations are less critical in industrial engines than in aircraft turbine machinery, thus heavy, bulky machinery is not a limitation when turbine machinery is considered for use in the power generation industry. Lastly, aircraft engines can make use of the kinetic energy of the gas leaving the turbine, which is wasted in industrial applications. These differences in requirements have an effect on design, despite the fact that the fundamental theory applies to both categories. Most modern aircraft gas turbine engines and large industrial machines have axial configurations while smaller industrial machines usually use centrifugal configurations, (Cohen et al. 1996). Most turbine machinery can be divided into two basic groups: radial and axial machinery.

11.2.1 Compressors

A compressor is a device that pressurizes a fluid. The compressor transfers energy by dynamic means from a rotating member to the continuously flowing fluid. The two types of compressors used in gas turbines are axial and centrifugal.

Axial flow compressors compress fluid by accelerating the fluid before diffusing it to obtain a pressure increase. The fluid is compressed by a row of rotating blades (rotor), and diffused by a row of stationary blades (stator). One rotor and stator makes one stage, although axial compressors usually consist of a number of stages. The gas passes from one stage to the next, with each stage raising the pressure slightly. By producing low pressure increases per stage, high efficiencies and pressure ratios can be obtained, but at the cost of more stages.

In centrifugal compressors the gas enters in an axial direction and leaves the compressor in a radial direction into a diffuser. This combination of a rotor and diffuser comprises a single stage. The single stage compressor can produce pressure ratios from 1.5:1 to 5:1.

The use of stages in axial compressors enables axial compressors to obtain higher pressure ratios than centrifugal (radial) compressors. Axial compressors can also reach higher efficiencies and use larger mass flow rates per given frontal area compared to centrifugal compressors. The axial flow machine dominates the field of large power, while centrifugal compressors are restricted to the lower end of the power spectrum where the mass flow rate is too small to be handled effectively by axial configurations. Axial compressors operate effectively in the pressure ratio range of 5:1 to 30:1; while centrifugal compressors are more suited in installations where pressure ratios are smaller than 5:1, (Cohen et al. 1996). Due to the simplicity of centrifugal compressors

when compared to the multi stage configurations of the axial compressors, centrifugal compressors enjoy higher stability and are more robust.

11.2.2 Turbines

As with the compressor, there are two basic types of turbine - radial flow and axial flow. Both these types of turbines are similar to the two types of compressors if considered with reverse flow. The radial turbine can handle low mass flow rates better than the axial flow machine. The axial turbine normally has the higher efficiency of the two types (Cohen et al. 1996).

11.3 SECOND ORDER ANALYSIS

AS shown in Chapter 4, different layouts (Layout A, B and C) are possible, each with its own possible configurations. All of these configurations need to be evaluated in order to establish the best possible configuration to be used in the micro gas turbine system.

Table 11.1: Second order configurations.

		LP Unit	HP Unit
Layout A	Configuration 1	Model A	Model A
	Configuration 2	Model A	Model B
Layout B	Configuration 3	Model B	Model B
	Configuration 4	Model B	Model C
	Configuration 5	Model B	Model D
Layout C	Configuration 6	Model C	Model C

11.3.1 Configuration 1

This option is only available for overall pressure ratios less than or equal to 3, due to the operation point of the high pressure unit in Figure 11.1. Since both the low pressure and high pressure unit is the same turbine machine model, only one compressor map is needed to show the operating points for this configuration.

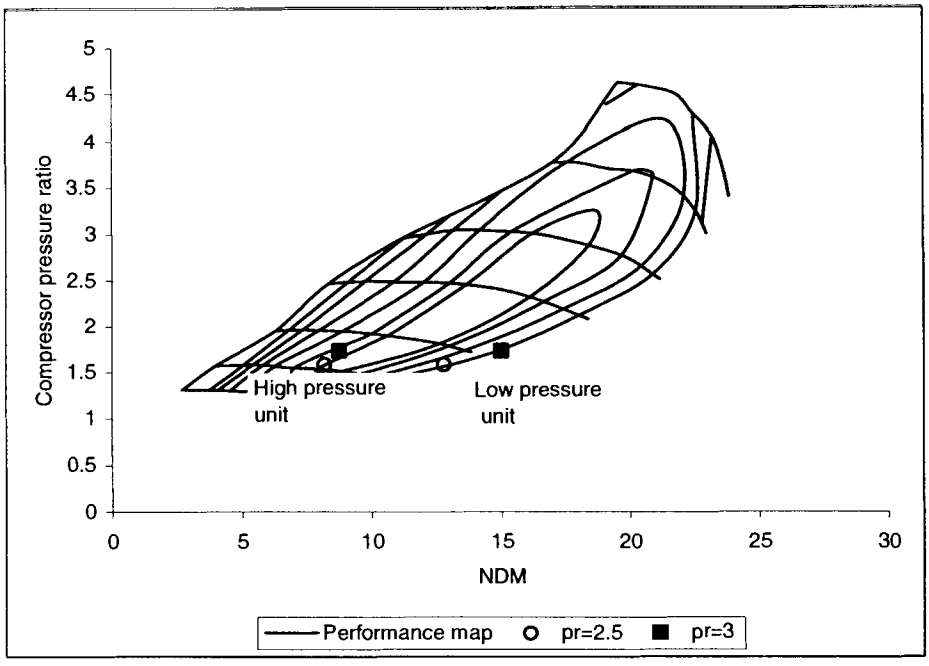

Figure 11.1: Compressor performance of Configuration 1.

The high pressure compressor unit's operating points lay close to the high efficiency region with a good surge margin. The low- pressure compressor, however, lies in a less efficient region towards the lower right.

11.3.2 Configuration 2

Since two different models will be used for the low- and high-pressure turbine machines, the operating points for the units are shown on two separate performance maps. Configuration 2 is applicable in situations where the overall pressure ratio is expected to be equal or higher than 3. Inspection of Figure 11.2 shows the operational points of the low pressure unit to be on the lower right region of the map, in the less efficient region. The low-pressure compressor's operating points, however, lie in the optimum operational region with good surge margins.

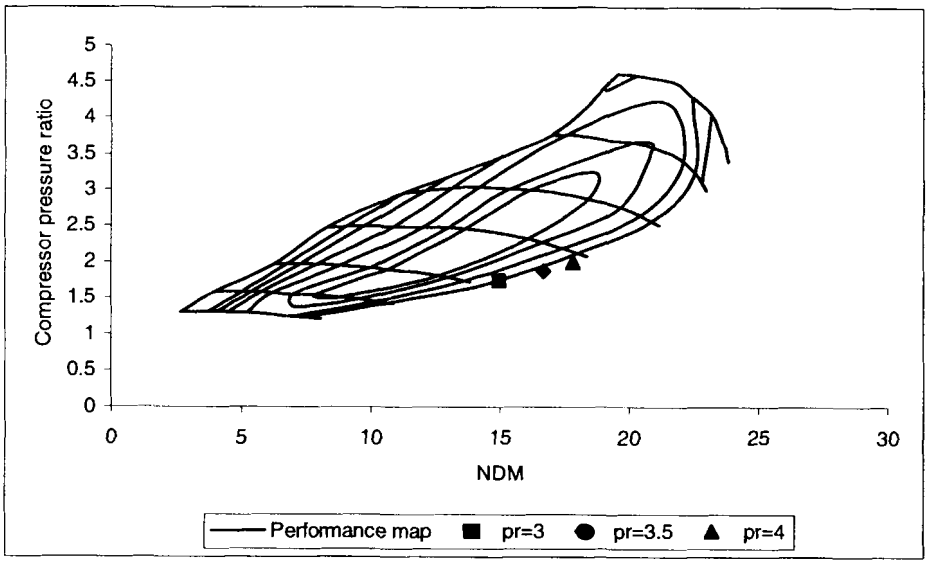

Figure 11.2: Low pressure compressor performance for Configuration 2.

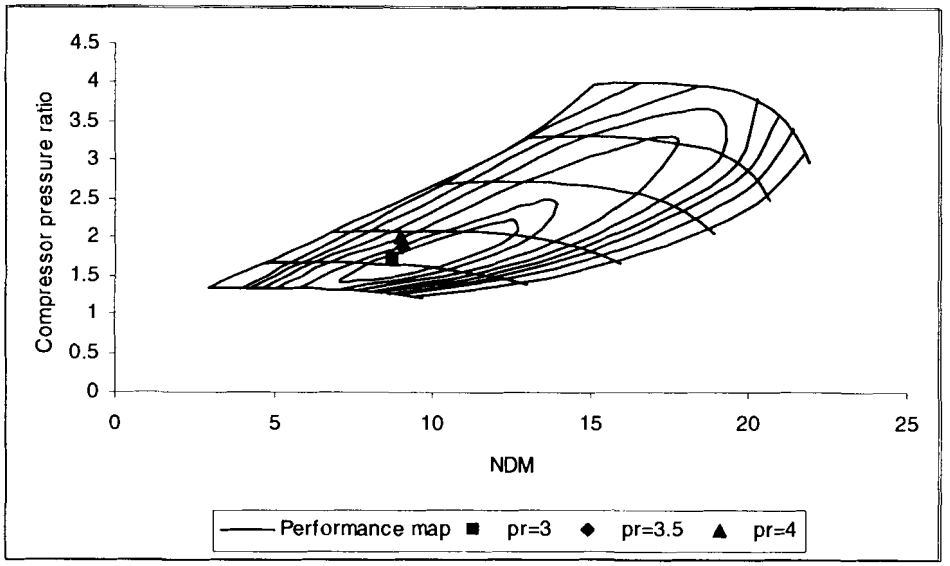

Figure 11.3: High pressure compressor performance for Configuration 2.

11.3.3 Configuration 3

Both the low and high pressure compressors are of the same turbine machine model and will be plotted on one compressor performance map (Figure 11.4). This configuration is suitable for the use of overall pressure ratios less than 3.5, according to Figure 4.7.

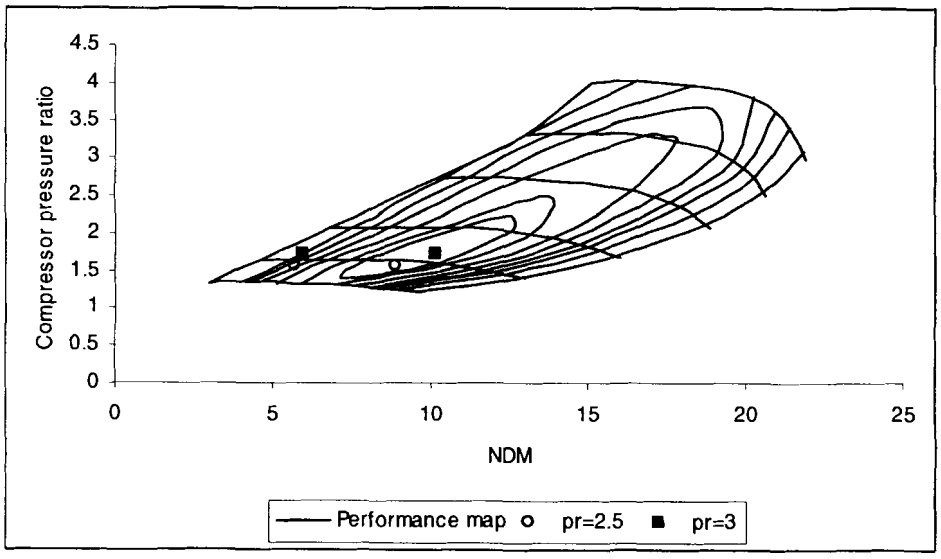

Figure 11.4: Compressor performance of Configuration 3.

Inspection of the compressor performances shows a lower surge margin for the high pressure compressor, while the points of the low pressure compressor lie in the optimum efficient region with good surge margins.

11.3.4 Configuration 4

The overall pressure ratios that are applicable to this layout are: 3, 3.5 and 4, and will be shown on two compressor maps for the different models to be used.

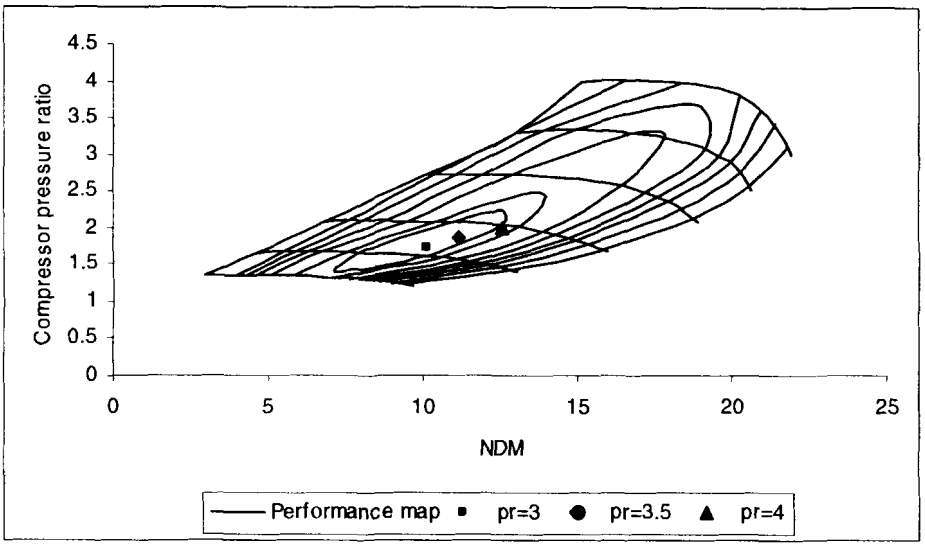

Figure 11.5: Low-pressure compressor performance for Configuration 4.

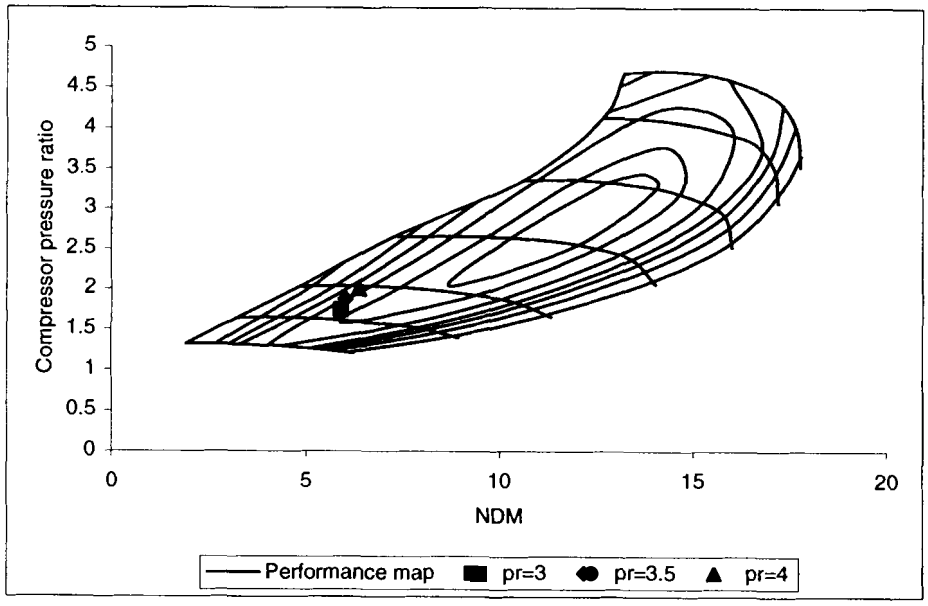

Figure 11.6: High-pressure compressor performance for Configuration 4.

Inspection of Configuration 4 shows good efficiencies and surge margins for both compressors. The high pressure compressor characteristics (Figure 11.6) showing that this machine is more suitable for use in applications with higher pressure ratios.

11.3.5 Configuration 5

The overall pressure ratios are limited to 3.5 and 4 for this configuration.

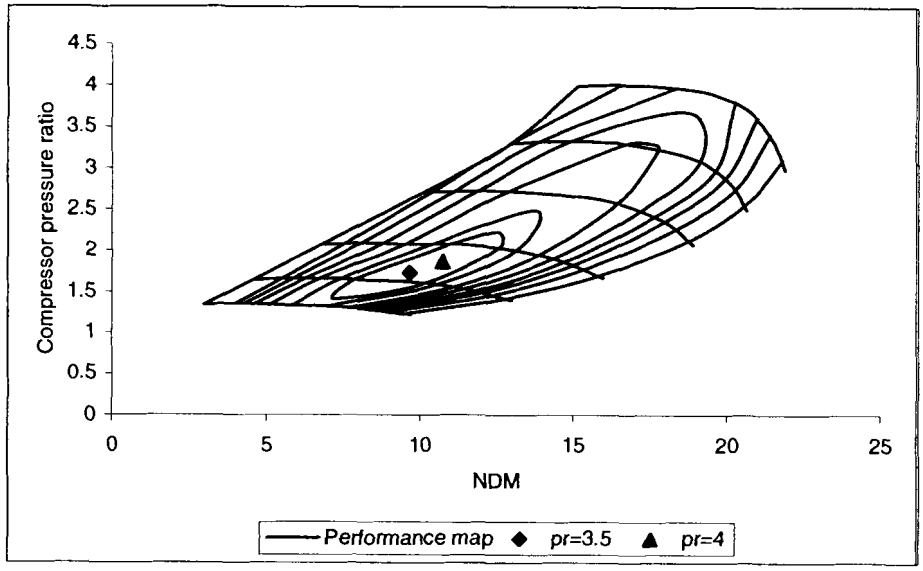

Figure 11.7: Low-pressure compressor performance for Configuration 5.

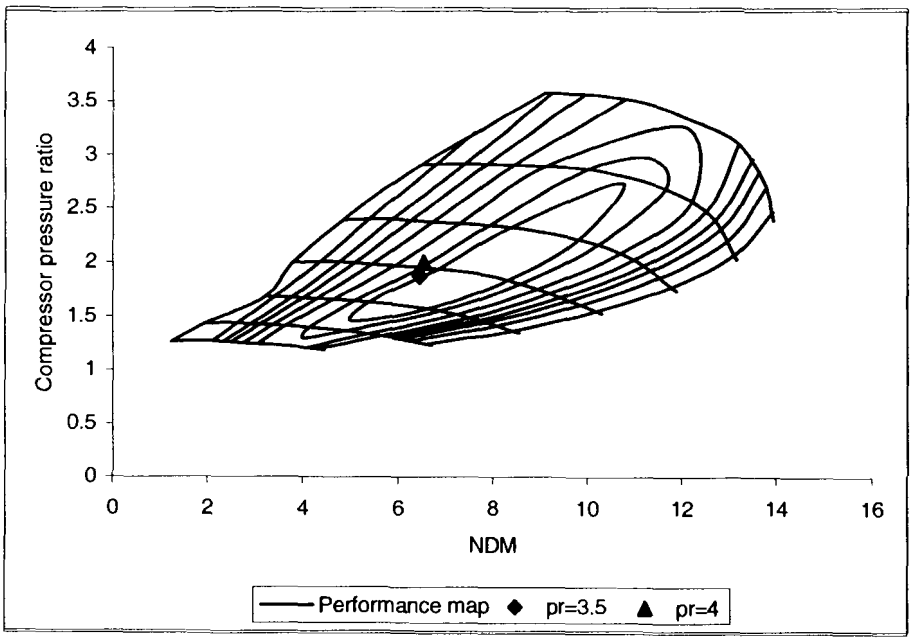

Figure 11.8: High-pressure c ompressor performance for Configuration 5.

Both the low-pressure and high-pressure compressor points lay in the optimum region of each unit, and this will ensure a wide range with good overall efficiency.

11.3.6 Configuration 6

This option will result in a small work output, but will be investigated as well.

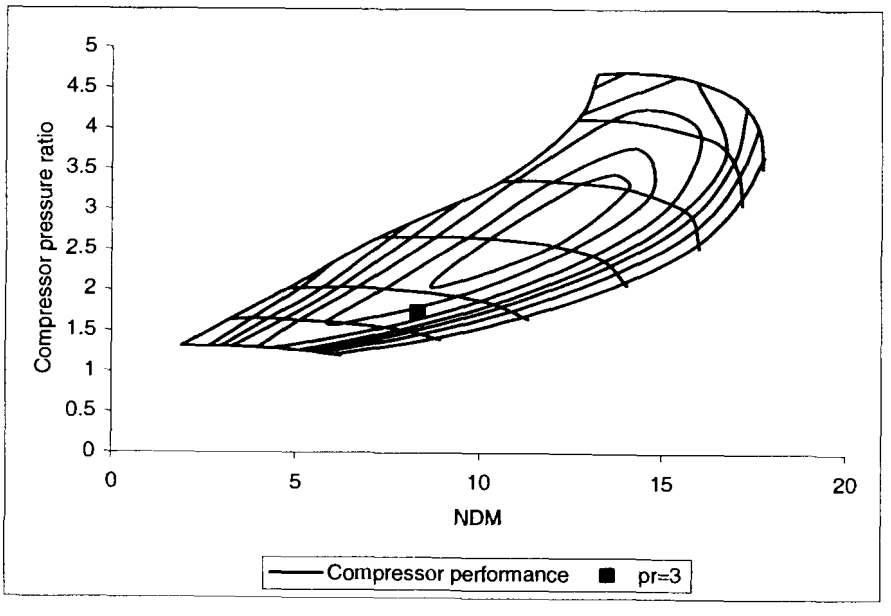

Figure 11.9: High-pressure compressor performance for Configuration 6.

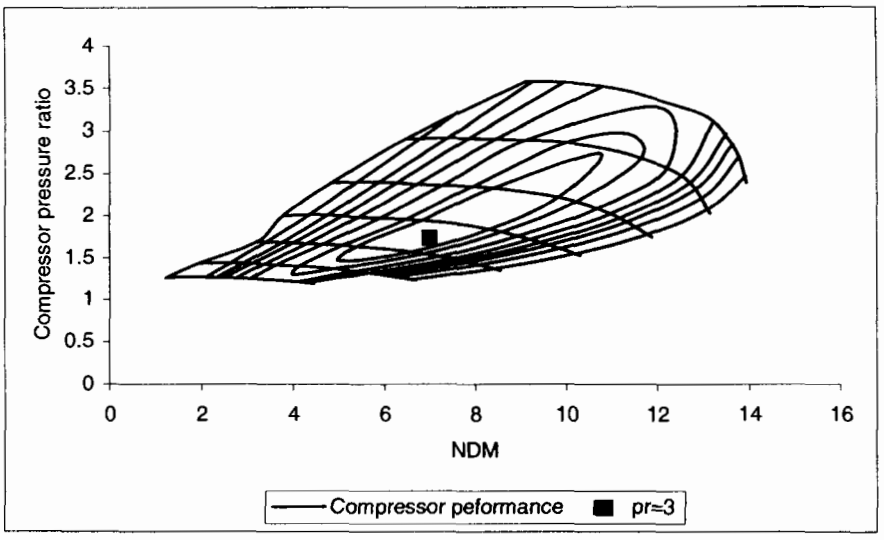

Figure 11.10: High-pressure compressor performance for Configuration 6.

Both compressors show good surge margins, while the high-pressure compressor has good efficiency and the low-pressure unit is not as efficient.

11.4 THIRD ORDER ANALYSIS

Evaluation of the different configurations in the second order evaluation eliminated all but two configurations for possible turbine machine configurations for the micro gas turbine system. These two Configurations, 1 and 3 have to be evaluated under transient conditions where the LPT's shaft speed is simulated over a range from 400 to 1200 rps.

11.4.1 Third order analysis of Configuration 1

As predicted during second order analysis, the LPC operating points over the speed range lie to the lower right of the compressor performance map. The HPC operating points, however, lie close to the high efficiency area. The average LPC efficiency in Figure 10.11 is 68.9%, while the average HPC efficiency equals 76.9%.

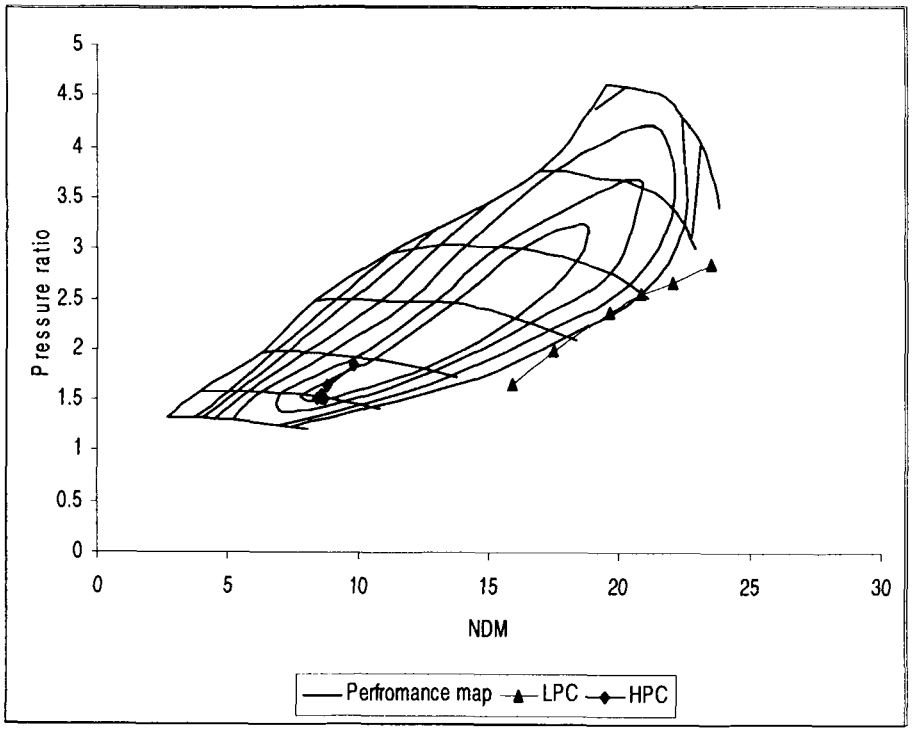

Figure 10.11: The effects of speed variation on the LPC and HPC operating points for Configuration 1.

Figure 11.11 prove that the compressor efficiency do not differ much over the LPC shaft speed range for Configuration 1. Surge margins for both compressors are very high.

11.4.2 Third order analysis of Configuration 2

The performance of the LPC follows the trend stated in section 11.3 with the operating points to the lower right of the compressor performance map as seen in Figure 11.12. The average LPC efficiency for configuration 2 is 68.2%

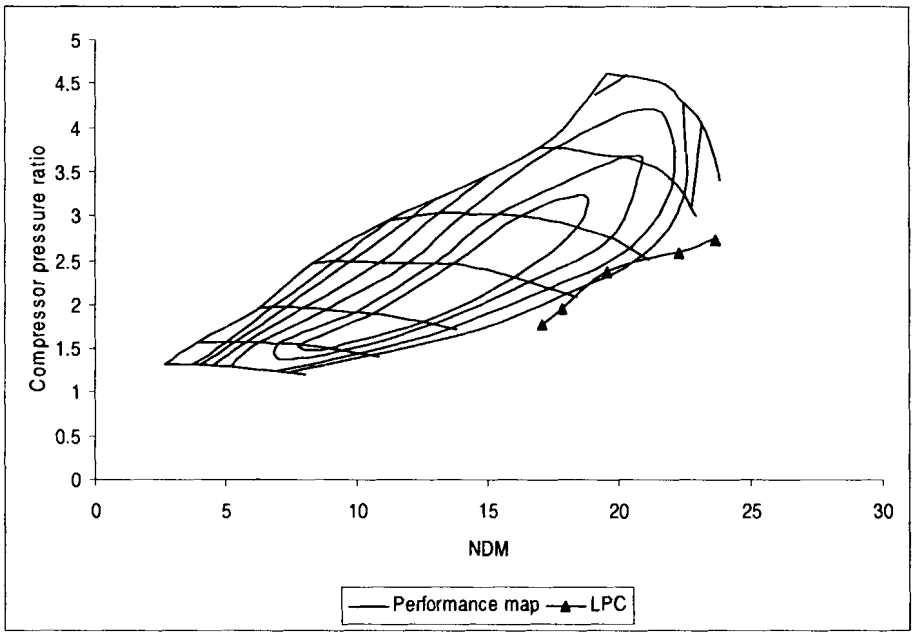

Figure 1112: The effects of speed variation on the LPC operating points for Configuration 2.

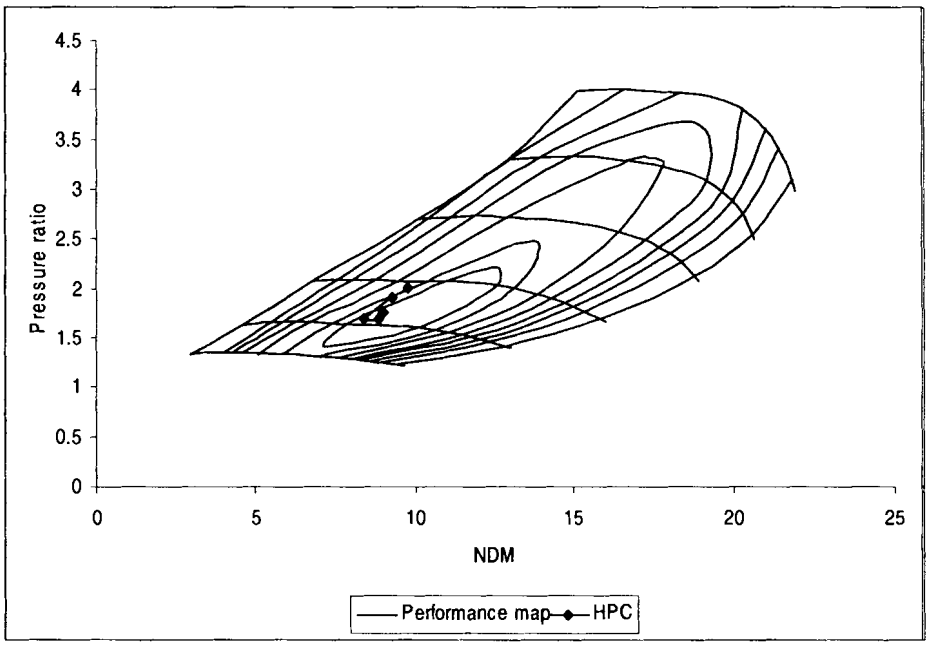

Figure 11.13: The effects of speed variation on the HPC operating points for Configuration 2.

The HPC operating points are on target for the best efficient region of the compressor performance map, shown in Figure 11.13, with an average HPC efficiency of 76.9%. Both compressors enjoy high surge margins as well.
Configuration 2 compressors provide steady efficiency over the LPC shaft speed range of 800 – 1200 rps. Sudden speed changes will not influence either compressor's efficiency much.

11.4.3 Third order analysis of Configuration 3

The change of the operating points of both the low and high pressure compressor due to the variation of speed of the low pressure compressor is shown in Figure 11.14.

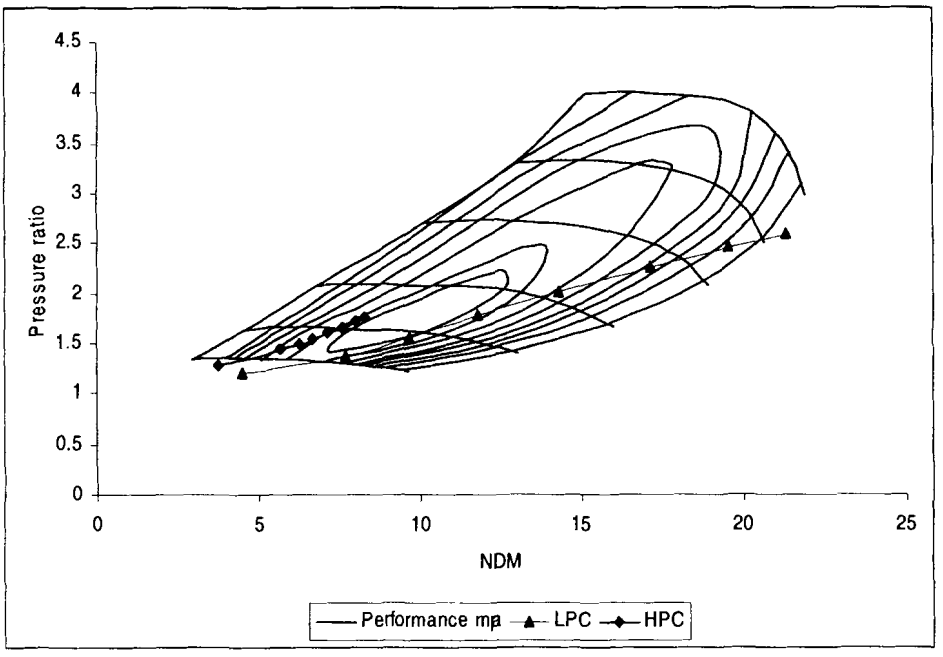

Figure 11.14: The effects of speed variation on the LPC and HPC operating points for Configuration 3.

The low-pressure unit's operating points vary with the change of speed (and mass flow rate), touching the optimum regions, while maintaining a good surge margin. A sudden change in compressor shaft speed will affect the LPC's efficiency.
The HPC is shown to have a smaller surge margin, but operates closer to the high efficiency region than the LPC.
The LPC compressor enjoys an average compressor efficiency of 70.8%, while the HPC's average value equals 75.2%.

11.4.4 Third order analysis of Configuration 4

Operation points of the LPC in Configuration 4 drift through the compressor's performance map over the whole range of efficiencies, providing an average efficiency of 73.9%. Swift compressor efficiency changes can be expected during compressor shaft speed changes.

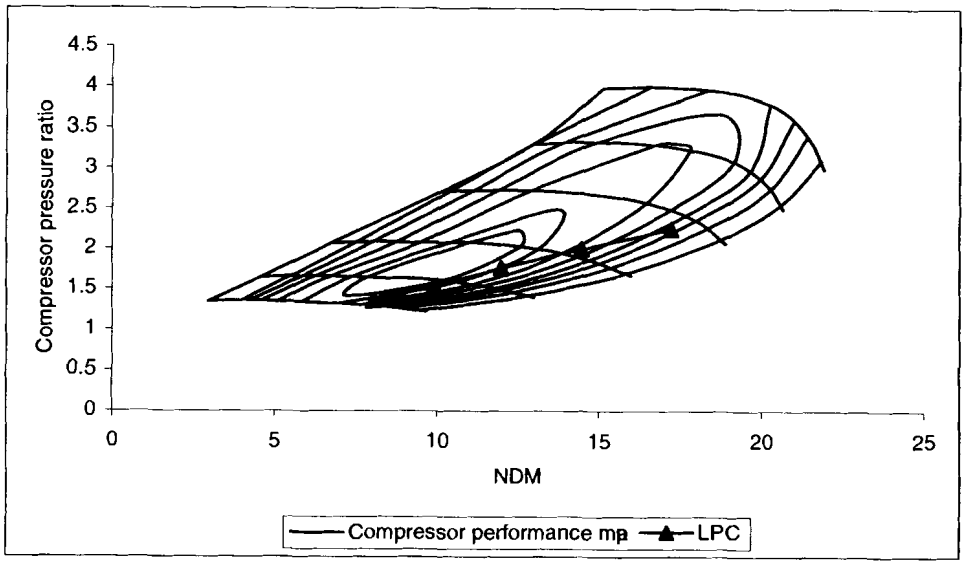

Figure 11.15: The effects of speed variation on the LPC operating points for Configuration 4.

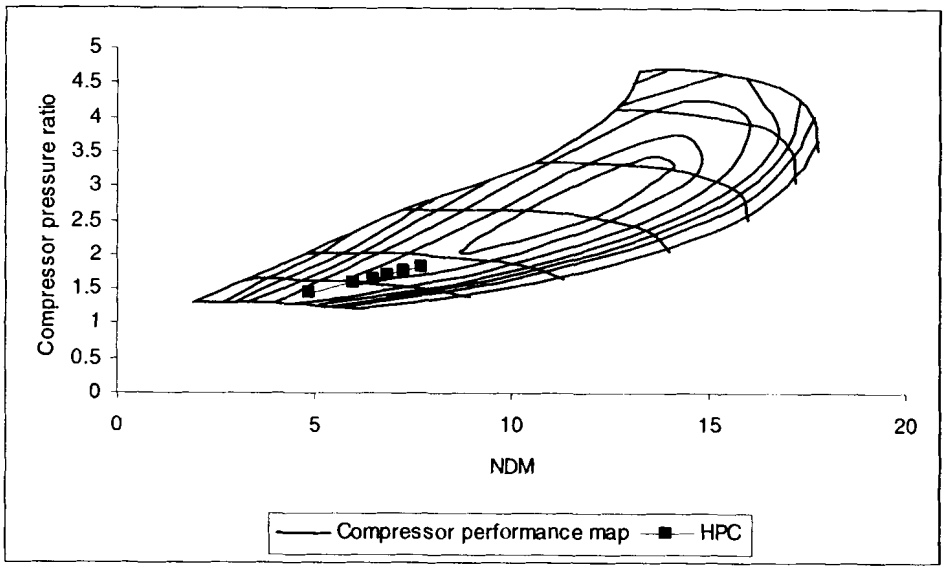

Figure 11.16: The effects of speed variation on the HPC operating points for Configuration 5.

The HPC operating points run in the centre of the compressor's performance map, but do not reach the high efficient region. An average compressor efficiency of 73.7% over the LPC shaft speed of 400 – 900 rps is calculated, while good surge margins are experienced by both compressors in this configuration.

11.4.5 Third order analysis of Configuration 5

The operating points, due to a change in the low pressure unit's rotational speed (400 – 900 rps), are plotted in Figure 11.17 and Figure 11.18.

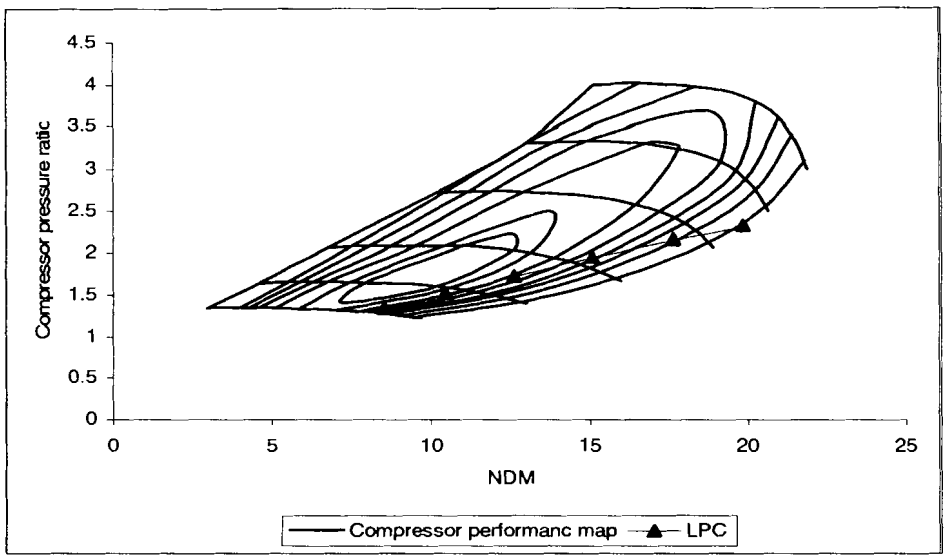

Figure 11.17: The effects of speed variation on the LPC operating points for Configuration 5.

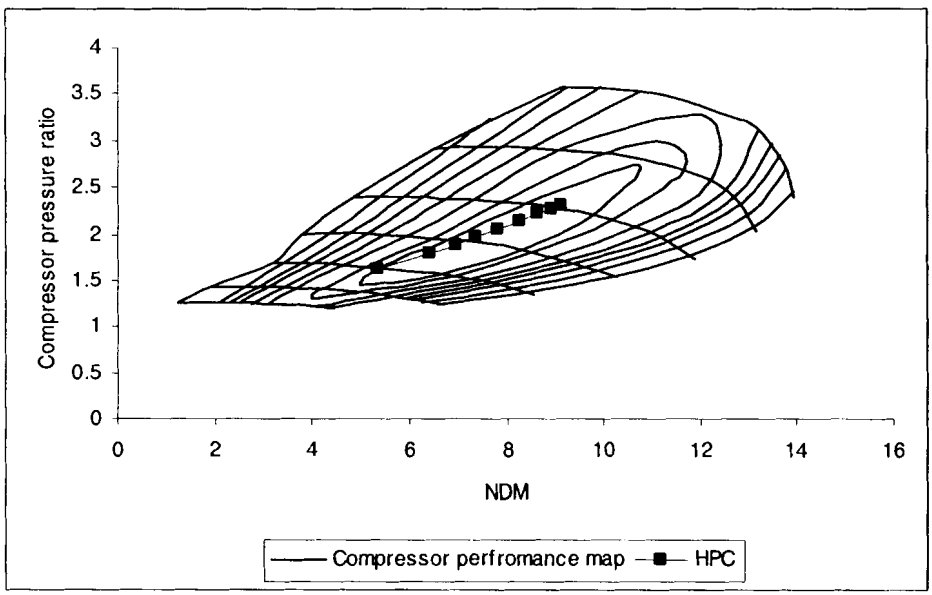

Figure 11.18: The effects of speed variation on the HPC operating points for Configuration 5.

Again, the operating points of the LPC drift across the compressor's performance map, not touching the high efficiency island, but managing an average efficiency of 71.4%. The HPC operating points, however, run through the centre of the high efficiency island, resulting in an average value of 76.9%.

Both compressors have good surge margins, but tend to introduce a rapid change in compressor efficiency under LPC shaft speed changes.

11.5 SURING OF COMPRESSORS

When dealing with compressors, it is necessary to evaluate the reaction of compressors at operation conditions that differ from the optimum design operational region of the compressor. One of these 'off-design' regions are surging:

It is necessary to consider what might be expected when a valve is placed in the delivery line of the compressor running at constant speed and is opened slowly. The variation in pressure is shown in Figure 11.19. With the valve shut, the mass flow rate is zero, while the pressure ratio will be greater than zero [A] (due to the pressure head produced by the action of the impeller on the air trapped between the vanes). While the valve is opened and flow begins, the pressure ratio over the compressor will increase to point [B] where the compressor's efficiency and pressure ratios reach their maximum values. Any further increase in the mass flow rate (due to the opening of the valve to full open state at point [C]) will result in a loss in pressure ratio. The curve in Figure 10.19 drops from B to C due to the drop in efficiency, (Cohen et al. 1996).

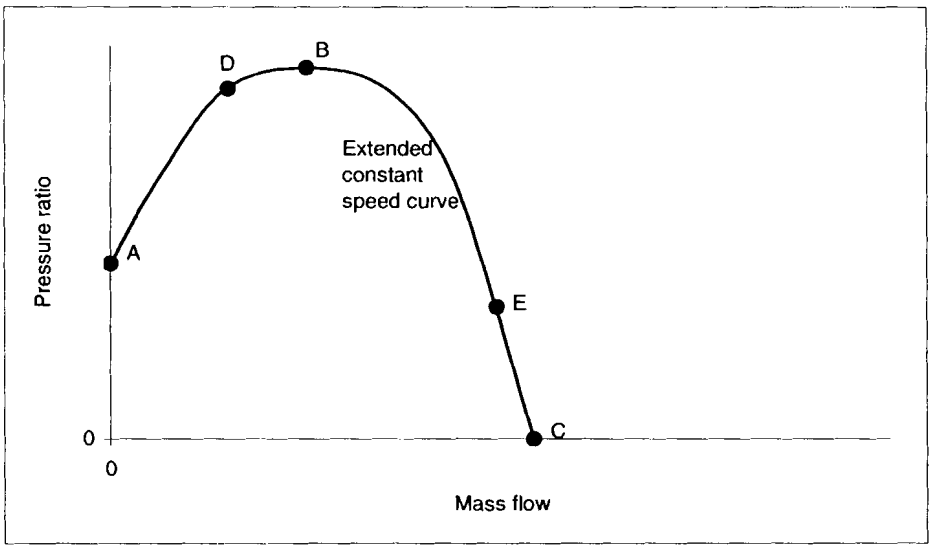

Figure 11.19: Theoretical compressor characteristics.

In practice, point A could be reached, but the curve B to A does not exist due to a phenomenon called "surging". Surging is associated with a sudden drop in delivery pressure, and violent aerodynamic pulsation that is transmitted through the machine. Surging occurs when a machine can not withstand the static pressure behind the compressor, (Botha 2002) and could lead to catastrophic failures.

Surging can be described as follows: If the compressor is operating on the positive slope of AB at point D, a decrease in mass flow will be accompanied with loss of delivery pressure. If the downstream pressure does not fall fast enough, the air tends to reverse its direction, flowing back towards the inlet of the compressor instead of toward the outlet. When this occurs, the pressure ratio drops rapidly. Meanwhile, the pressure downstream

of the compressor has also fallen, and the compressor will be able to build pressure again. This process repeats itself at high frequency.

Surging may not appear immediately after the operating point moves to the left of B, as the pressure downstream of the compressor may fall at a higher rate than the delivery pressure, but conditions between points A and B are inherently unstable. The compressor will be stable only while the operating point falls on a negative slope, as a loss in the mass flow rate is accompanied by a gain in delivery pressure ratio which increases the mass flow returning to the original position, i.e. assuring stall operation.

In gas turbines, the actual point where surging occurs depends on the "swallowing capacity" of the component downstream of the compressor and the way the swallowing capacity varies over the range of operational conditions, (Cohen et al. 1996).

There has to be sufficient area to allow shifting of the operating point during normal operation, while preventing the operating point from crossing the surge line. This shifting of the operating point can occur due to sudden acceleration of the gas turbine, changes in mass flow and start-up and shut-down requirements. By definition, the surge margin is calculated using the following equation:

$$\text{Surge Margin} = \frac{\text{MF}_\text{W} - MF_S}{MF_\text{W}} \text{x100} \qquad \text{Eq11.1}$$

with MF_S the non-dimensional mass flow on the surge line
MF_W the non-dimensional mass flow on the working line, (Botha 2002).

There is a limitation to the operating range between B and C (Figure 11.19) due to the definition of mass flow: $\dot{m} = \rho A v$. As the mass flow increases $\left[\dot{m} \uparrow\right]$ and the pressure ratio decreases, the gas's density is reduced $\left[\rho \downarrow\right]$, thus the radial component of velocity must increase $\left[v \uparrow\right]$.

At some point [E], the point is reached where no further increase in mass flow can be obtained and choking has occurred. This point represents the maximum delivery obtainable at the particular rotating speed for which the curve is drawn. Other curves may be obtained for different speeds. Illustration of the actual variation of pressure ratio over the complete range of flow and rotational speed is shown in Figure 11.19. The left-hand extremities of the constant speed lines may be joined up to from the surge line, as seen in Figure 11.19, while the right-hand extremities represents the point where chocking occurs, (Cohen et al. 1996) also seen in Figure 11.20.

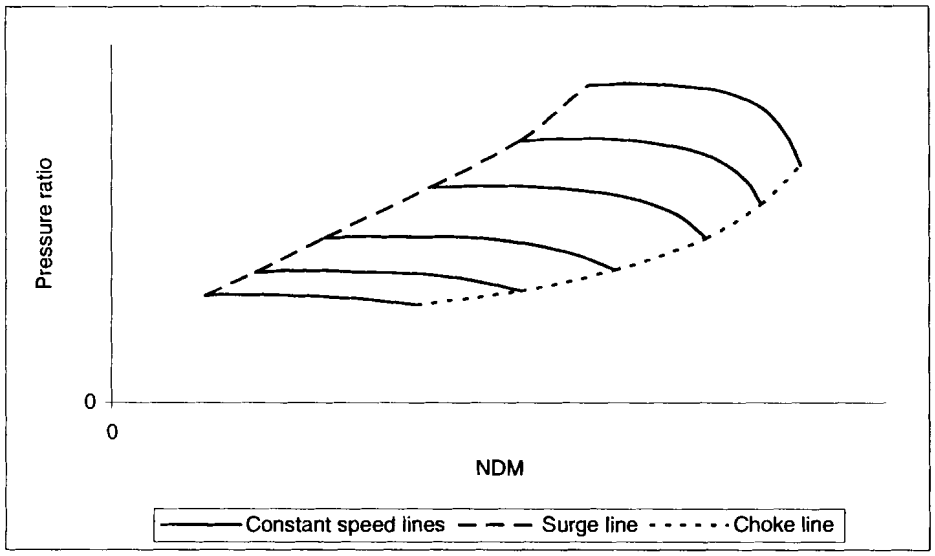

Figure 11.20: Typical compressor map

12 Appendi x C: Heat exchanger performance characteristics

Heat exchangers are complicated components and all the various parameters that influence the design need to be addressed. Appendix C shows the design process of both the inter-cooler and the recuperator, supporting Chapter 5 by providing information on the design process.

12.1 INTER-COOLER CHARACTER ISTICS

As stated in Chapter 5, the inter-cooler's performance is regulated by geometrical dimensions and the inter-relationship between these dimensions. Inter-cooler characteristic parameters will be evaluated over a range of the geometric dimensions: shell diameter$[D_{shell}]$, tube inside diameter$\left[D_{i[tube]}\right]$ tube outside diameter$\left[D_{o[tube]}\right]$, the number of tubes[n] and the length [L] of the inter-cooler.

12.1.1 Inter-cooler efficiency

The effect of the geometric parameters on the inter-cooler efficiency can now be investigated.

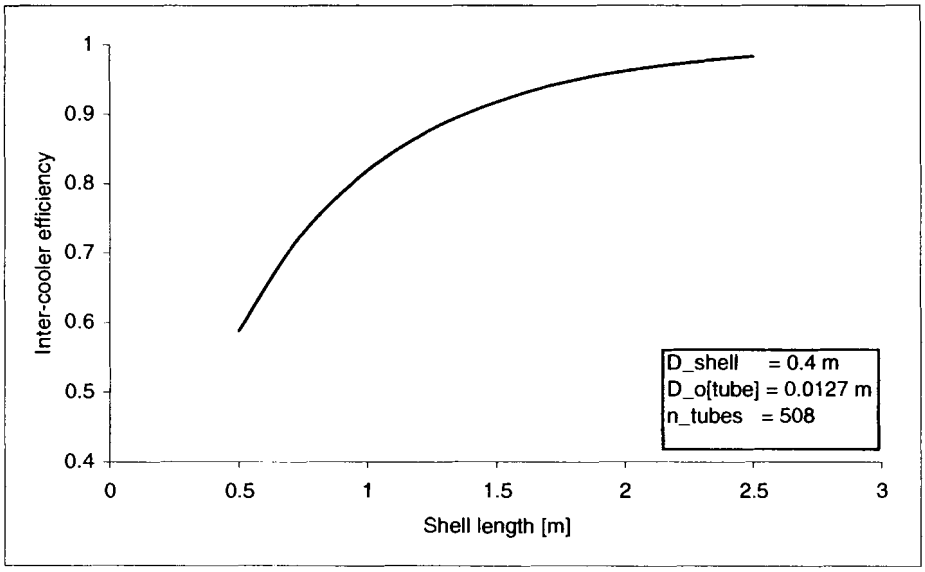

Figure 12.1: Inter-cooler efficiency as a function of shell length.

Figure 12.1 shows that the inter-cooler efficiency increases with an increase in shell length, but the curve flattens at high length values. This indicates that there is an optimal shell length; thereafter increasing the shell length no longer improves the inter-cooler efficiency. Enhancing the efficiency more than 90% by lengthening the heat exchanger is not feasible as a huge extension in length will only result in a small rise in efficiency. For this reason, a lower limit for the length of the inter-cooler is set to the minimum limit of 0.9444 m.

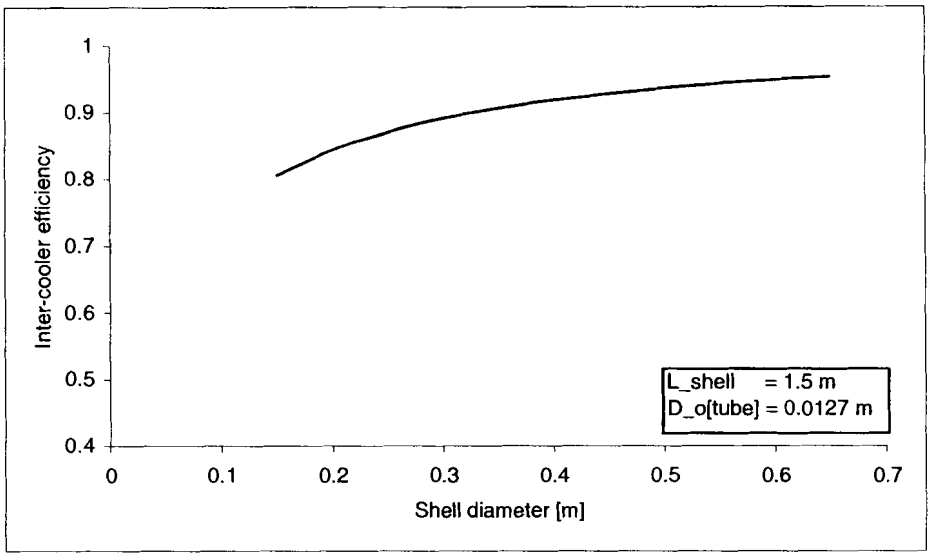

Figure 12.2: Inter-cooler efficiency as a function of shell diameter.

The inter-cooler's efficiency is also influenced by the shell diameter as seen in Figure 12.2, showing that an increase in shell diameter will result in a small increase in efficiency, as the cross-sectional heat transfer and the number of tubes increase. This implies that an increase in the shell diameter greater than 0.5389 m will not result in an increase of inter-cooler efficiency.

Figure 12.3 illustrates that an increase in the tube outer diameter leads to a decrease in efficiency. By increasing the tube outer diameter, the number of tubes decreases and the total heat transfer area decreases. The maximum tube diameter is limited to 0.015 m, as the efficiency tends to drop below the accepted level of 90% for larger diameters.

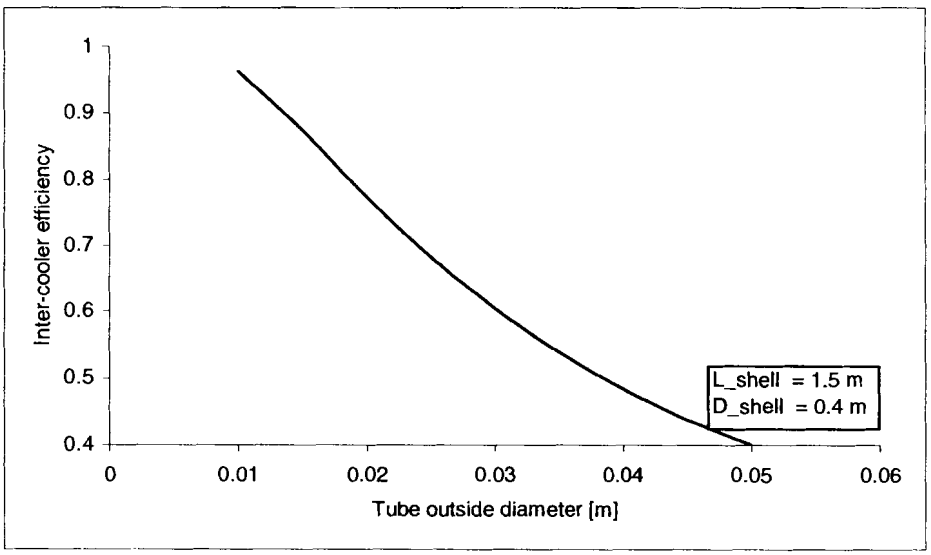

Figure 12.3: Inter-cooler efficiency as a function of tube outside diameter.

Inter-cooler efficiency is affected by all the geometric factors, but is most sensitive to tube diameter, followed by the intercooler length, while a change in the shell diameter does not affect the efficiency as much.

12.1.2 Inter-cooler pressure losses

The work needed to overcome fluid friction in the heat exchanger can be represented by the pressure loss over the heat exchanger. In the TCIR cycle only the gas side's pressure losses are calculated, but the coolant side is important for the auxiliary design.
Pressure drop of the fluid through the inter-cooler is limited to 1% of the inlet pressure.

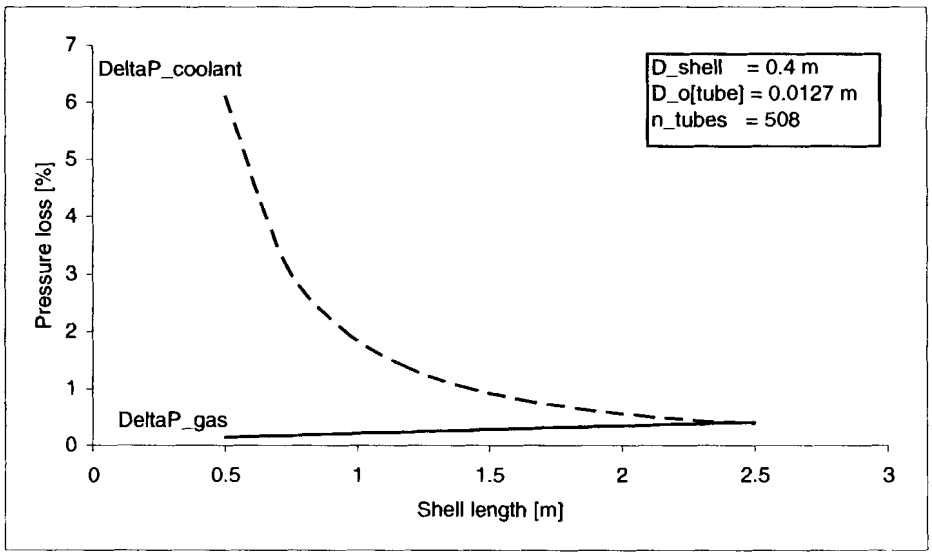

Figure 12.4: Inter-cooler pressure-loss as a function of shell length.

In this configuration the length of the shell has little effect on the pressure loss of the gas side, but has a significant influence on the coolant side of heat exchanger. In order to minimize the pressure loss in the coolant side it is essential that the minimum length of the inter-cooler is limited to 1.389 m. By inspection of Figure 12.5 it is possible to limit the minimum shell diameter to 0.344m, due to the pressure loss considerations of both the hot and the cold stream.

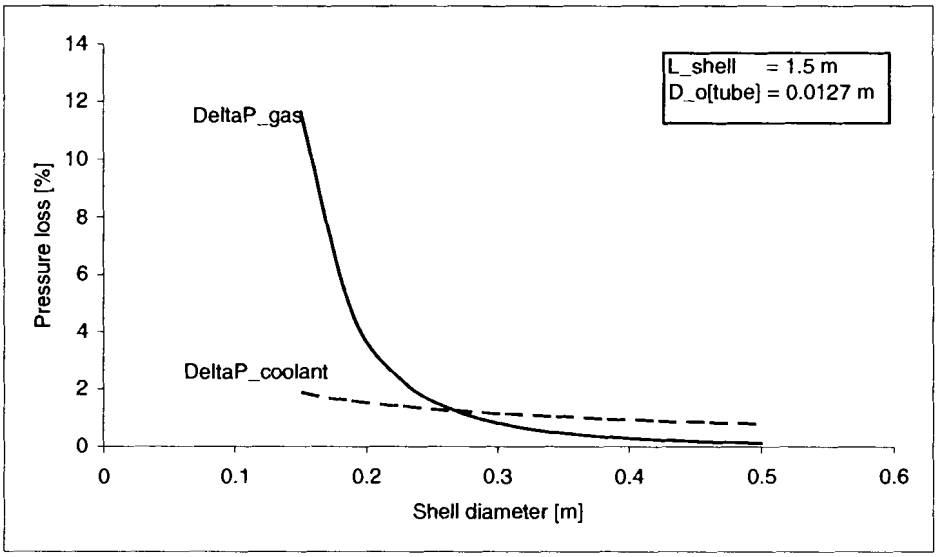

Figure 12.5: Inter-cooler pressure-loss as a function of shell diameter.

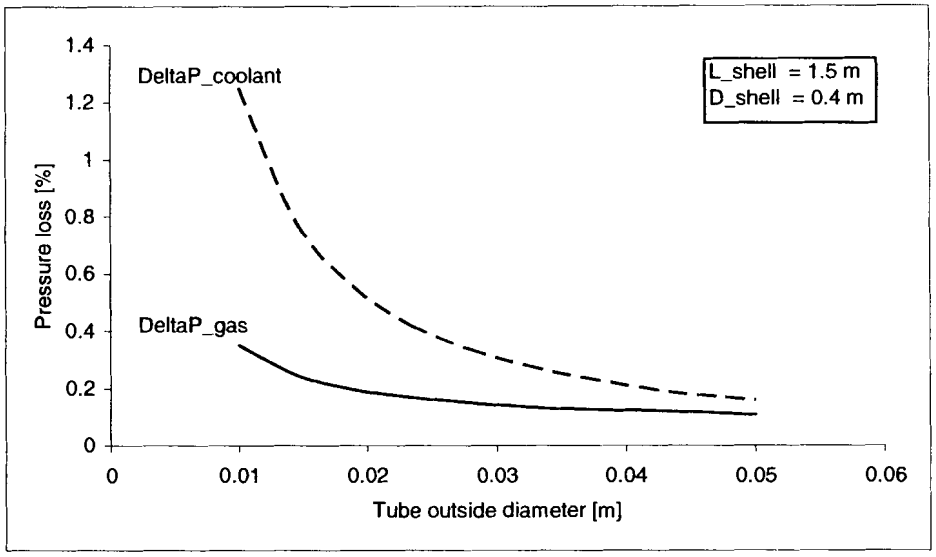

Figure 12.6: Inter-cooler pressure-loss as a function of tube outside diameter.

The maximum allowable pressure loss across the cooler is limited to 1% of the inlet pressure of the fluid. Figure 12.6 shows that a lower limit is needed when considering the dimensions of the tubes in order to limit the pressure loss experienced by the coolant. The minimum tube diameter that will result in a maximum pressure loss of 1% is equal to 0.011 m.

A limitation set previously, [$D_{o[shell]} \leq 0.03m$] (the effect the tube diameter has on the cooler's efficiency) still holds true for pressure losses and is the upper limit and is not affected by the pressure loss limitation of 1%.

12.1.3 Inter-cooler limits an results

The geometrical parameters were evaluated against the effects on efficiency and pressure loss and resulted in the following limitations:

$1.5 \leq L \leq 1.9$

$D_{shell} \geq 0.3444$

$0.011 \leq D_{o[tube]} \leq 0.03$

A relationship between $D_{o[tube]}$ and D_{shell} exists. The relationship between these two parameters is calculated from the cross sectional area of the inter-cooler.

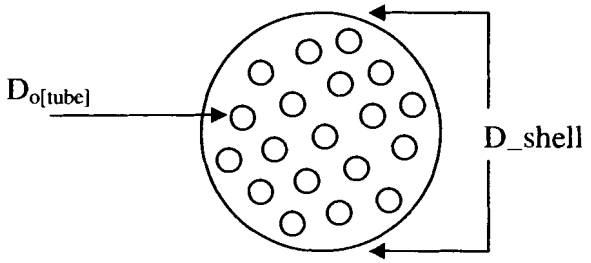

Figure 12.7: Illustration of the cross sectional area of the inter-cooler.

The total area of the tubes must be smaller than the shell area (in order for the tubes to fit inside the shell):

$A_{shell} \geq n \cdot A_{o[tubes]}$ Eq 5.12

thus:

$$\pi/4\left(D^2_{shell}\right) \geq n \cdot \left(D^2_{o[tubes]}\right)\pi/4 \quad \text{Eq 12.1}$$

By introducing a constant $k \leq 1$:

$$D_{shell} = \sqrt{kn} \cdot D_{o[tubes]} \quad \text{Eq 12.2}$$

An illustration of this relation can be seen in Figure 12.8.

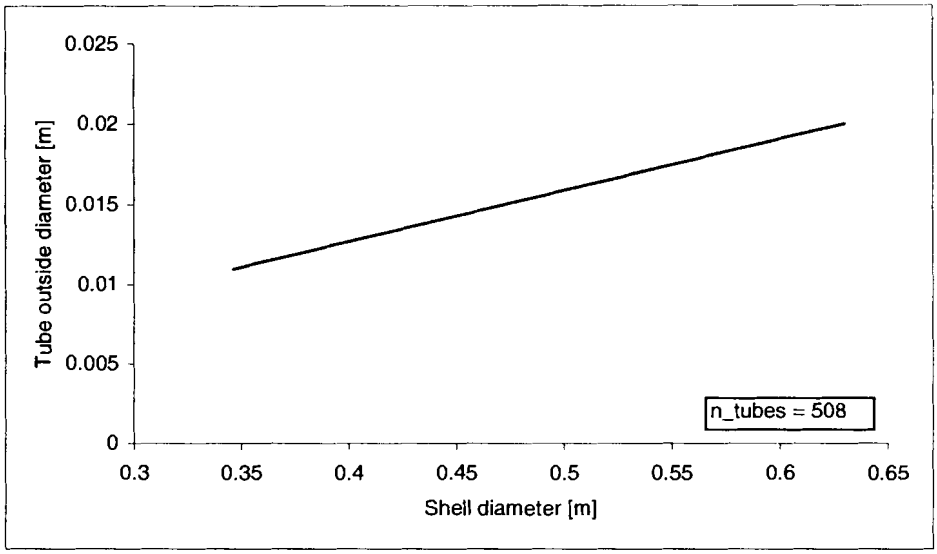

Figure 12.8: Illustration of the relation between D_{shell}, $D_{o[tube]}$.

All of these limitations have been considered and calculated in a simulation written to simulate and heat exchanger with this inter-cooler's characteristics. The results are as follows:

Geometric dimensions:

Inter-cooler length [L]:	1.5	m
Inter-cooler shell diameter $[D_{shell}]$:	0.4	m
Inter-cooler tube diameter $[D_{o[tube]}]$:	12,7	mm
Number of tunes [n]:	508	

Inter-cooler characteristics:

Efficiency $[\eta_{ic}]$:	82	%
Real heat transfer [Q]:	43	kW
Maximum heat transfer [Q_{max}]:	47	kW

Inter-cooler boundary conditions for the gas side:

Inlet pressure:	180	kPa
Inlet temperature:	97	°C
Exit pressure:	179.85	kPa
Exit pressure:	28	°C
Pressure loss:	0.15	%

Inter-cooler boundary conditions on the coolant side:

Inlet pressure:	300	kPa
Inlet temperature:	20	°C

Exit pressure:	295.66	kPa
Exit temperature:	27	°C
Pressure loss:	1.44	%

Figure 12.9 shows the axial temperature distribution through the inter-cooler with the given geometric limitations. Note that the gas enters at increment 0, and exits at increment 10, while the coolant (water) enters at 10 and exits at increment 1, thus cross-flow heat exchanger.

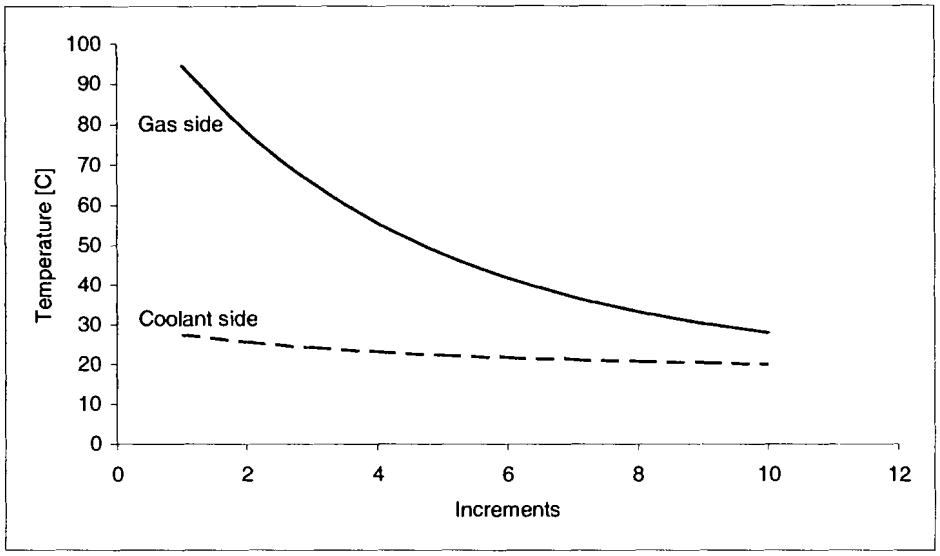

Figure 12.9: The axial temperature distribution of the inter-cooler.

12.2 RECUPERATOR CHARACTERISTICS

The micro-channel recuperator that will be used for the micro gas turbine system is also dependable on the geometric dimensions of the total heat transfer area of the recuperator. Geometrical parameters that influence characteristic parameters are: channel width [b] (width = height), number of channels [m], and length [L] of the channels. The characteristic parameters that will be evaluated are: Efficiency, pressure loss, Effect of the Reynolds number and the volume of the recuperator.

12.2.1 Recuperator efficiency

The effect of recuperator efficiency on cycle performance is proven in Chapter 3 and effort has to be made to ensure that the efficiency is higher than 90%.

Investigation of Figure 12.10 and Figure 12.11 shows that in order to expect efficiency higher than 90%, a minimum length of 0.4556 m is required, while the channel dimension has no effect on the recuperator efficiency. High efficiency values are associated with a high number of channels. The lower limit of 27 778 channels will ensure efficiencies higher than 90%. The following limitations are set: $L \geq 0.4556$ m and $m \geq 27778$ channels due to efficiency considerations.

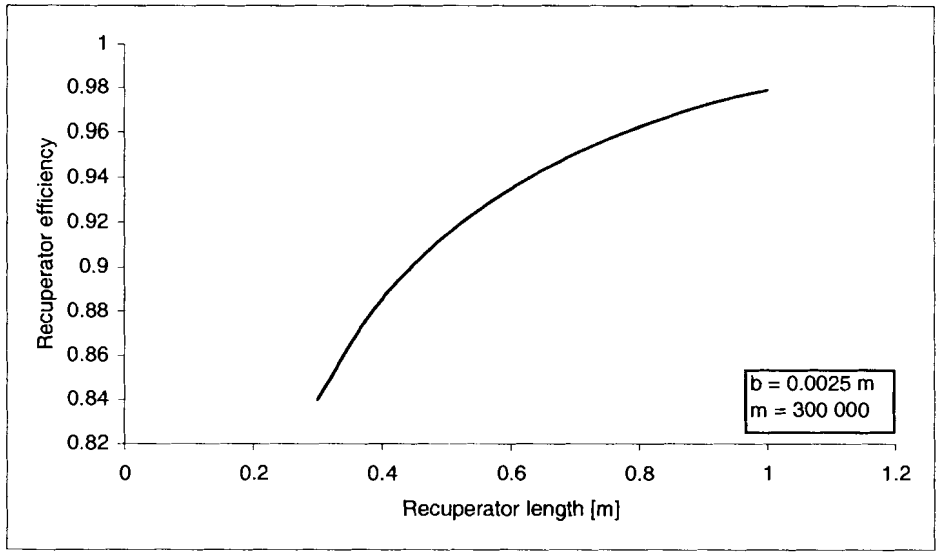

Figure 12.10: Recuperator efficiency as a function of length.

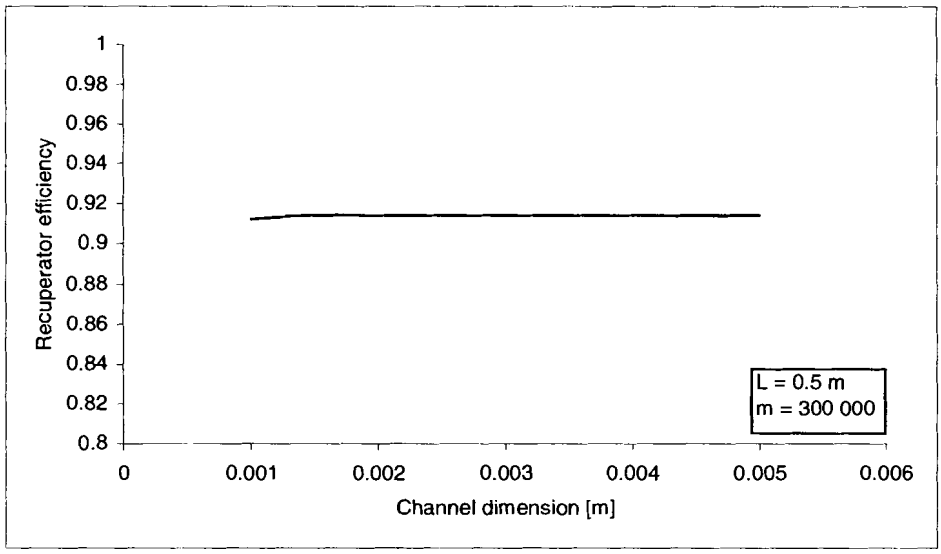

Figure 12.11: Recuperator efficiency as a function of channel dimension.

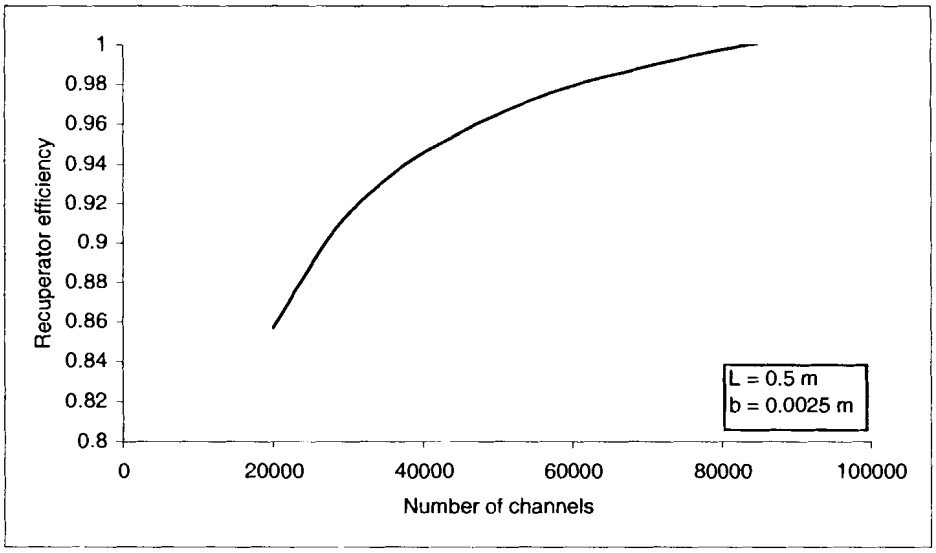

Figure 12.12: Recuperator efficiency as a function of number of channels.

12.2.2 Recuperator pressure loss

Both the hot side and the cold side of the gas stream experience pressure loss through the recuperator. The relatively small channel dimensions, that are associated with recuperators, affect the pressure losses. As was the case with the inter-cooler, a maximum pressure loss of 1% per air stream is allowed through the recuperator.

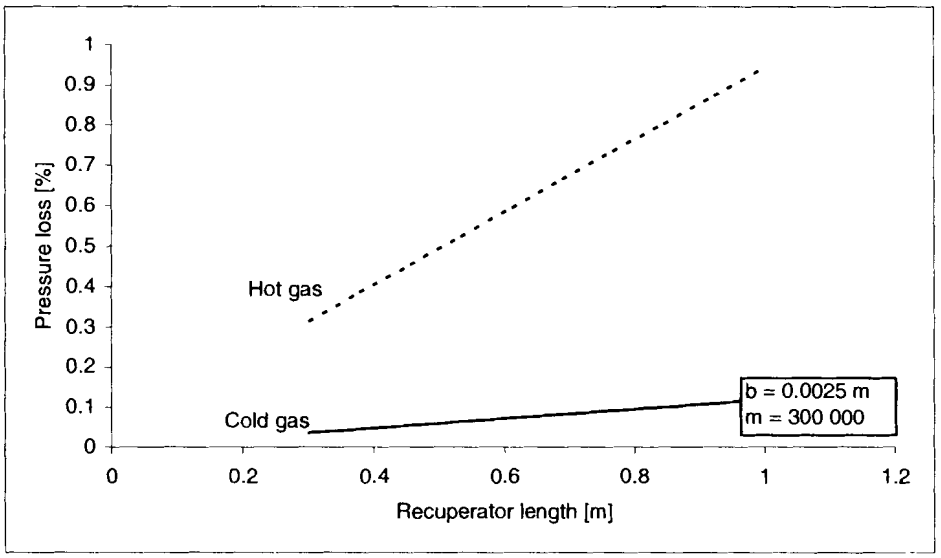

Figure 12.13: Recuperator pressure losses as a function of recuperator length.

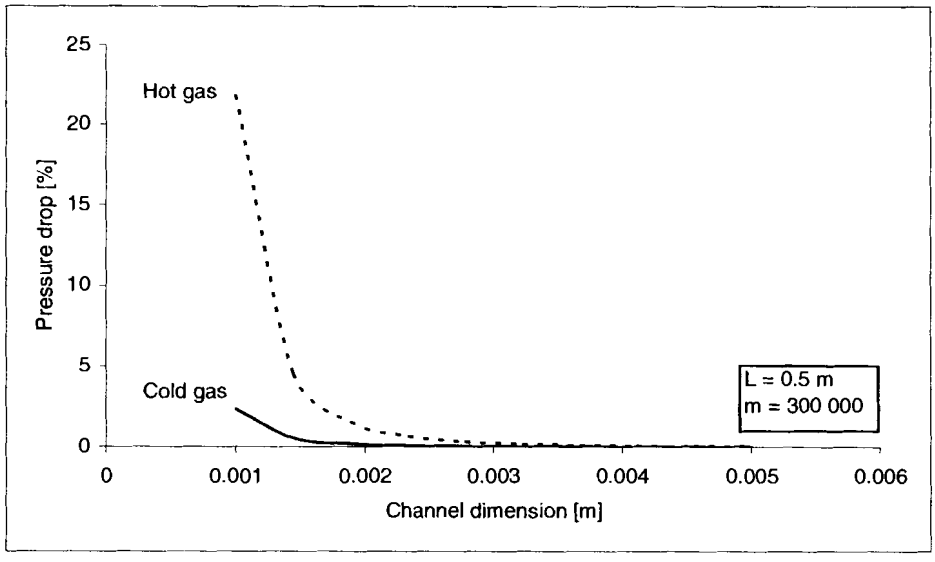

Figure 12.14: Recuperator pressure loss as a function of channel dimension.

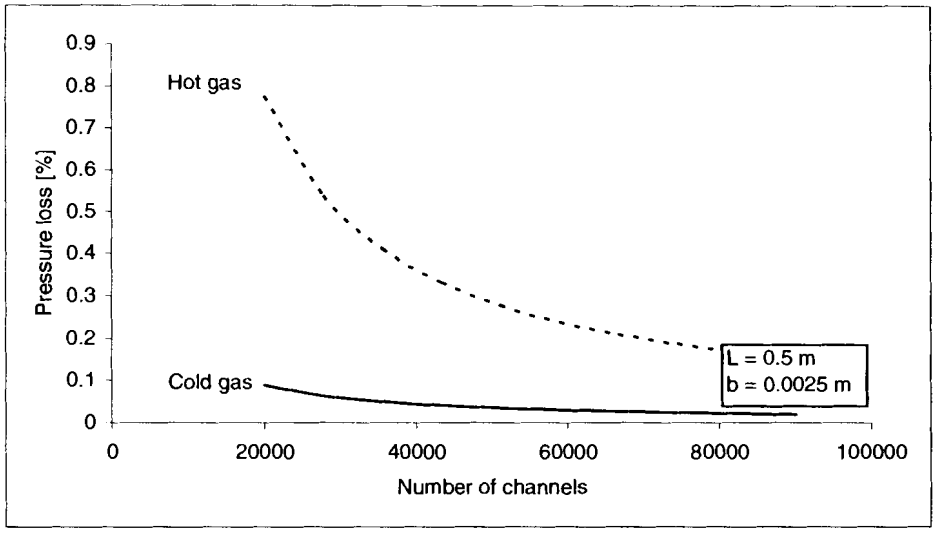

Figure 12.15: Recuperator pressure loss as a function of the number of channels.

Limitations due to the pressure boundaries are: $b \geq 0.002$ m and $m \geq 20000$ channels.

It can be seen that the hot gas (leaving the turbine) experiences a higher pressure loss over the recuperator than the cold gas. This is due to the difference in density which is driven by the temperature difference of the gas streams.

12.2.3 Recuperator Reynolds number

Doty et al. (1991) argued that laminar flow heat exchanger designs have the advantage of reducing thermodynamic and hydrodynamic irreversibilities, and hence increase efficiency. The recuperator used for the TCIR cycle should have laminar fluid flow therefore the Reynolds number must be smaller than 2300 ($\mathrm{Re} \leq 2300$).

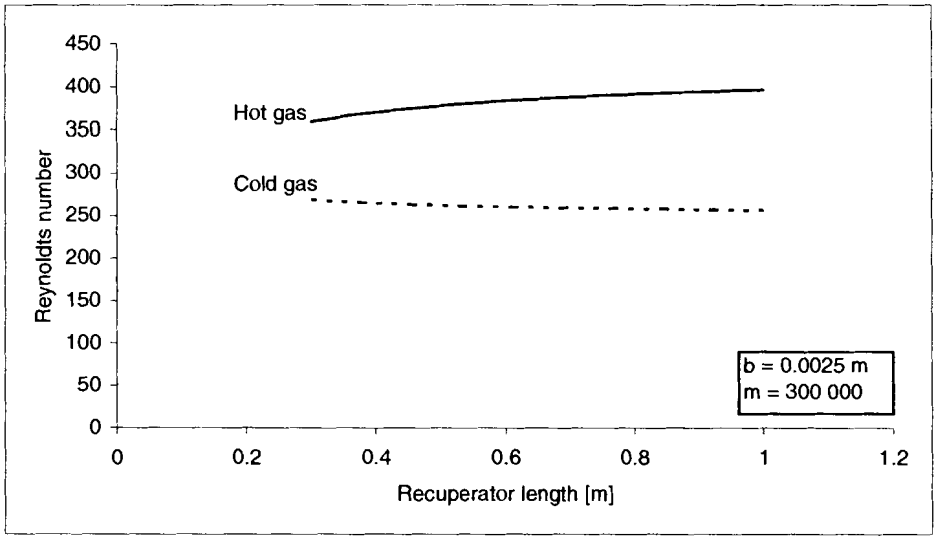

Figure 12.16: Reynolds number as a function of recuperator length.

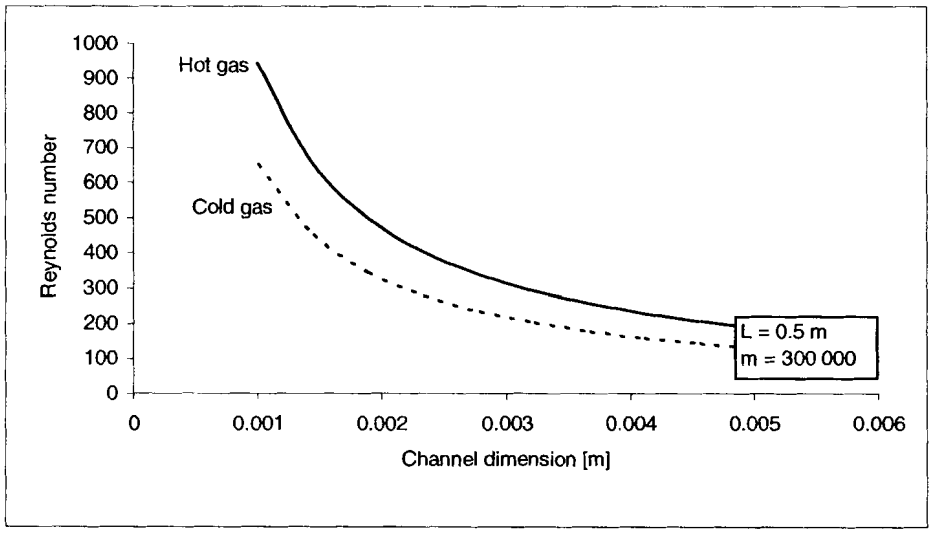

Figure 12.17: Reynolds number as a function of recuperator channel dimension.

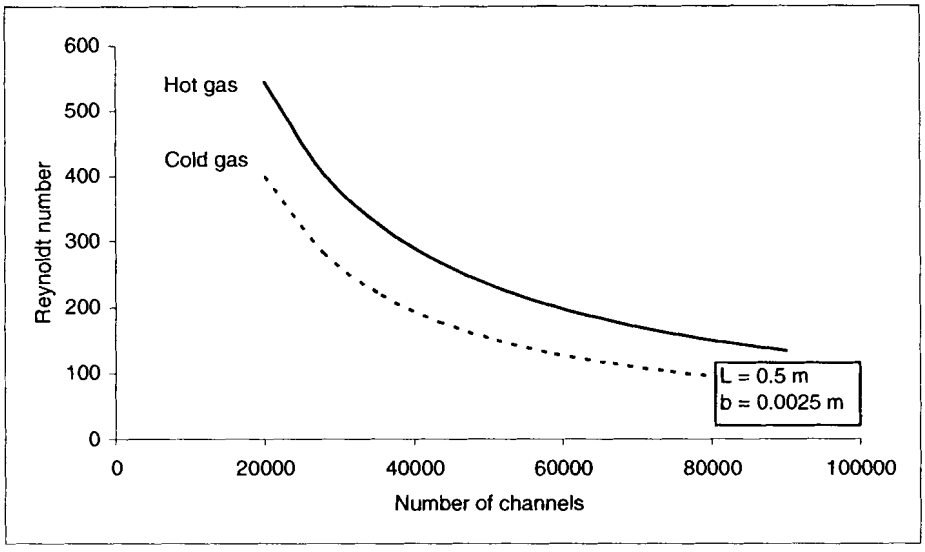

Figure 12.18: Reynolds number as a function of the number of the recuperator channels.

The Reynolds number does not affect the boundary conditions chosen initially. The calculated Reynolds number values are less than the limits for turbulent flow over the whole range of simulated boundary conditions. Thus, no turbulent flow will occur through the recuperator.

12.2.4 Recuperator volume

The volume of the heat exchangers and the recuperator in particular, represents the majority of the material used for manufacturing and thus the cost of recuperators. An investigation into limiting the volume of the recuperator needs to be done.

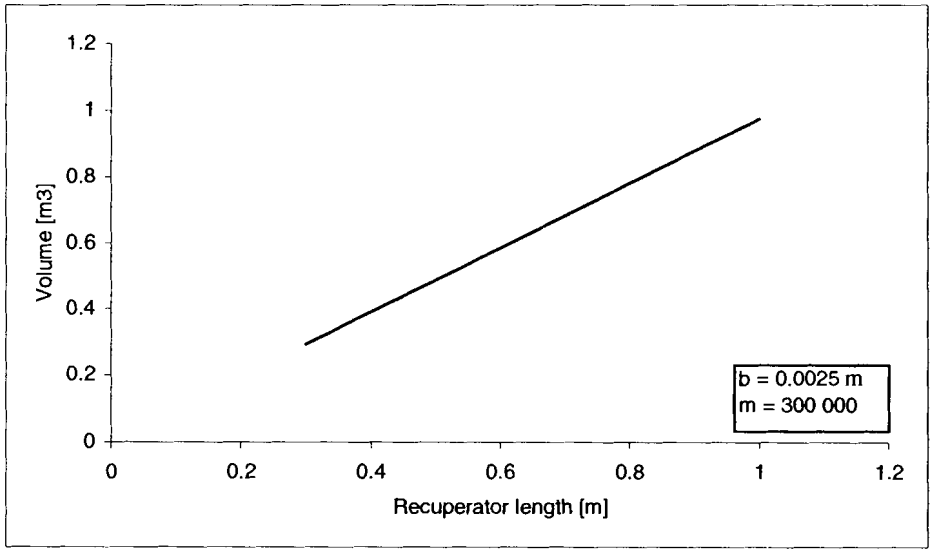

Figure 12.19: Recuperator volume as a function of length.

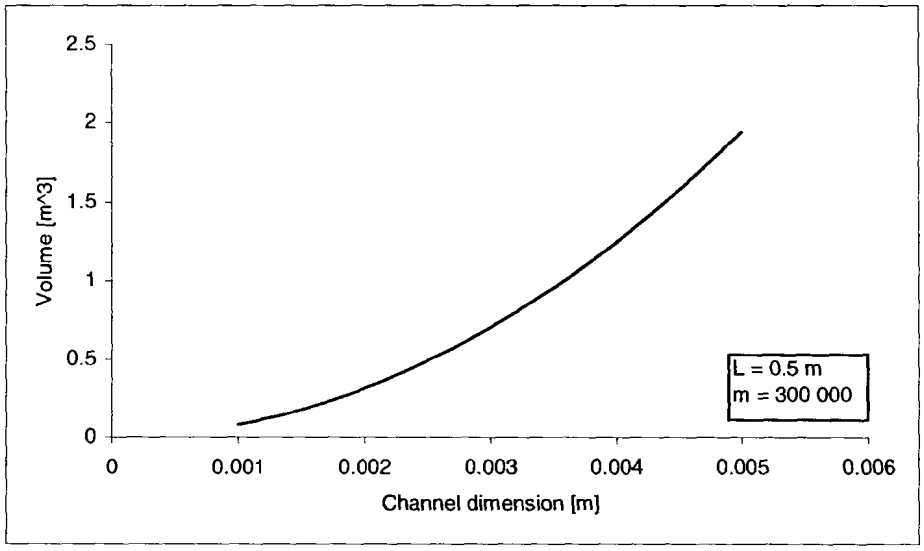

Figure 12.20: Recuperator volume as a function of channel dimensions.

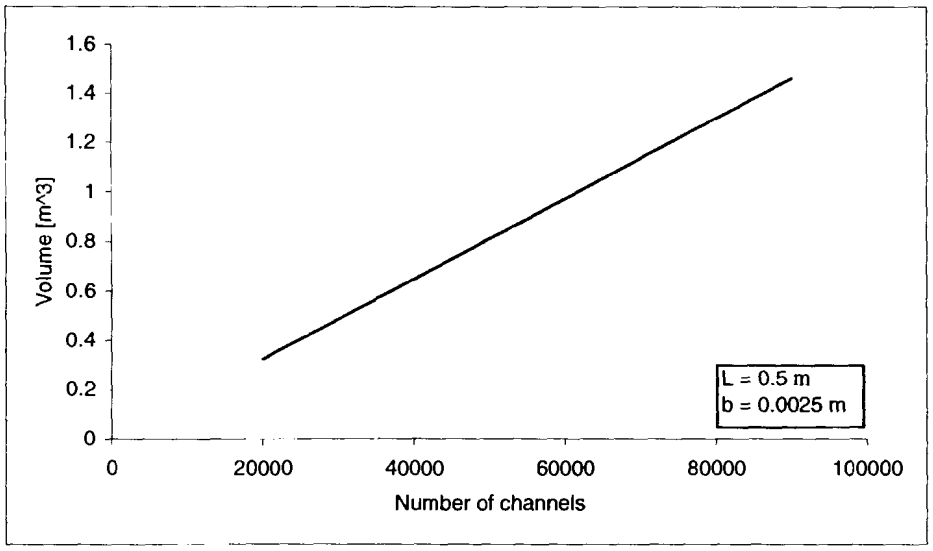

Figure 12.21: Recuperator volume as a function of number of channels.

To achieve efficiencies higher than 90%, the recuperator's volume has to be more than 0.4442 m^3 but the maximum volume still has to be limited. An upper boundary of 0.8 m^3 is selected to set a cost limit that will ensure that the recuperator will have both high efficiency and good economic feasibility.

$L \leq 0.8444$ m, $lb \leq 0.0032$ m and $m \leq 51111$ channels .

12.2.5 Recuperator limits and results

Inspection of the geometrical parameters resulted in the following boundaries.

$0.4556 \leq L \leq 0.8444$

$0.002 \leq b \leq 0.0032$

$27778 \leq m \leq 51111$

Optimizing, designing and simulation of the TCIR cycle recuperator was done and is available in appendix E. These analyses resulted in the following:

Geometric dimensions:

Recuperator length [L]: 0.5 m
Recuperator height [H]: 0.9874 m
Recuperator width [W]: 0.984 m
Channel dimension [b]: 0.0025 m (height = wdth)
Number of channels [m]:60 000

Recuperator characteristics:

Efficiency:	91.4	%
Real heat transfer [Q]:	279.9	kW
Max heat transfer [Q_{max}]:	306.1	kW

The input and outputs for the recuperator are:

Cold gas side (high pressure side):

Inlet pressure:	274	kPa
Inlet temperature:	84.46	°C
Exit pressure:	273.876kPa	
Exit temperature:	508.734°C	
Pressure loss:	0.045	%

Hot gas side (low pressure side):

Inlet pressure:	100.379kPa	
Inlet temperature:	536.395°C	
Exit pressure:	100	kPa
Exit temperature:	114.545°C	
Pressure loss:	0.38	%

Axial temperature distribution through the Recuperator with the given geometric limitations is illustrated in Figure 12.22. Note that the hot gas enters at increment 1, while the cold gas enters at 11 and exits at increment 1, thus cross-flow heat exchanger.

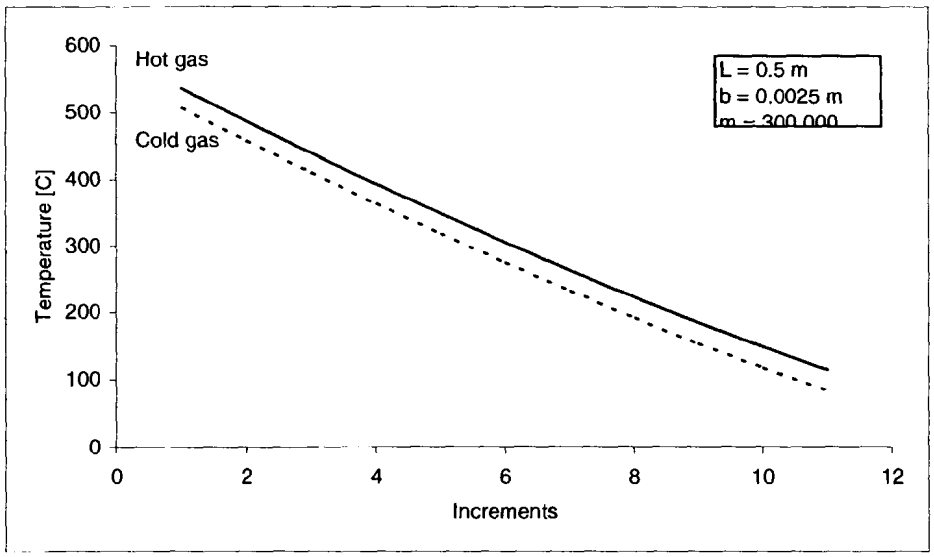

Figure 12.22: Axial temperature distribution through the recuperator.

The hot gas enters the recuperator and cools down towards the exit, while the cold gas heats up from entering the recuperator until exiting at a high temperature. Note that the exit temperature of the hot gas still exceeds 100°C, thus still possessing energy that can be utilized.

13 Appendix D: Combustion chamber performance characteristics

Appendix D serves as a support chapter for Chapter 6 where the combustion chamber for the micro gas turbine system is discussed. Literature on improvements that may be applied to the combustor chamber are discussed here as well. The technical aspects of the combustion chamber design are discussed here. These include the chemical reaction of the fuel (kerosene) during combustion, the combustion aerodynamic parameters and liner geometry.

13.1 LITERATURE ON POSSIBL E IMPROVEMENTS ON COMBUSTORS

In order to keep the turbine inlet temperatures at a suitable high level, gas turbine combustion is a steady process in which a hydrocarbon fuel is burnt in a large amount of air. In the past, emission gases were not seen as a problem with the only factor worth considering being the elimination of smoke.

Historically, the function of engine control systems was to provide the correct amount of fuel for all operating conditions and emission control was the function of the combustor design. With modern engines, the control system plays a major role in adjusting fuel/air ratios to minimize emissions over the complete operating range. This may involve supplying fuel to different areas in the combustor at different operation conditions, and has only become possible with the advent of sophisticated digital fuel control systems. Gas turbines usually provide power at an even level, thus running at the same speed most of the time. The load may however be lowered for short periods of time.
The emission of pollutants into the atmosphere may be tackled either during the combustion process or post combustion by exhaust cleanup, as used in coal burning plants. There are three major new methods of minimizing emissions:
Water or steam injection into the combustor,
Selective catalytic reduction and
Dry low NO_x. (Cohen et al.1996).
A short discussion is therefore given on each.

13.1.1 Water and steam injection

By injecting water into the combustor, the flame temperature decreases, this means that the emission pollutants also decrease. The amount of water to be injected is substantial, but de-materialized water must be used to prevent corrosive deposits in the turbine. There is a small increase in power due to the higher mass flow through the turbine, but is offset by a decrease in thermal efficiency. Increasing the water/fuel ratio, while decreasing NO_x emissions, will increase the forming of both CO and UBC emissions (Cohen et al.1996).
Wang & Choiu (2002) found that the generation efficiency of a simple cycle gas turbine generation set can be increased by using steam –injection gas turbine (STIG) technology. The power output of a STIG cycle is less sensitive to changes in ambient temperature than a simple cycle. Higher thermal efficiencies are possible with water injection instead of steam injection as proved by *Cardu & Baica*, (2002). They did a study where they compared water injected combustion chambers with steam injection combustors.

13.1.2 Catalytic combustion

Catalytic reduction is a system of exhaust clean-up, where a catalyst is used together with injection of controlled amounts of ammonia (NH_3), resulting in the conversion of NO_x to N_2 and H_2O. The catalytic reaction only occurs in a limited temperature range of (285-450°C), and is i nstalled in the waste heat recovery system. A lot of new factors occur with the use of catalytic systems, like the control of the NH_3, additional cost and the handling and storage of the NH_3 (Cohen et al.1996).
Carroni et al. (2002) listed a few salient operational considerations concerning the application of an catalytic combustor to gas turbines:

Fuel/air mixtures with high flame temperatures, while the surface temperature of the combustor is lower resulting in poor thermal stability, while mechanical integrity must be maintained.
Catalytic inlet temperatures are low, thus igniting temperatures are critical. Pressures inside the flame tube result in the risk of homogeneous ignition.
Catalysts are not well suited for high mass flow rates and volumetric heat releases, which are characteristics of gas turbines.
A catalyst system and combustor has been designed for a gas turbine that operates at temperatures below the required combustion discharge temperature and completes the combustion downstream of the catalyst (Della Betta & Rosrtup-Nielson 1999). While *Sadamori et al.*(1995) developed a combustion system composed of high-temperature ceramic catalysts made of fine manganese-substituted hexaalumunate particles and noble metal-carrying cordierite honeycomb resulting in ultra low NO_x emissions and a feasible long term catalyst durability.

13.1.3 Dry low NOx

A decrease in the NOx emissions is possible by either lean or rich burning in the primary zone to activate the necessary reduction in flame temperature. Rich burning results in smoke forming in the primary zone, while lean burning leads to problems of maintaining stable combustion. An important concept of dry NOx reduction is fuel staging, where the total fuel flow is divided into two parts which are supplied separately to distinct combustion zones as proved by Davis & Washam, (1989). The fuel enters the flame tube through the primary burners during start-up and idling phases, while the fuel inlet shifts gradually to the secondary burners as speed and load is applied.

13.2 CHEMICAL REACTION DURING COMBUSTION

Combustion of liquid fuel involves the vaporizing of the fuel, breaking down the heavy hydrocarbons into lighter fractions, mixing of these hydrocarbons with oxygen, and finally the chemical reaction where the fuel and air combusts. The combustion process consists of the oxidation of constituents in the fuel that are capable of being oxidized and can be represented by a chemical equation (Sonntag et al. 1998).
First consider the reaction of carbon with oxygen:

$$C + O_2 \rightarrow CO_2 \qquad \text{Eq 13.1}$$

This states that 1 mol of carbon reacts with 1 mol of oxygen to form 1 mol of carbon dioxide. Subsequently: 12 kg of carbon reacts with 32 kg of oxygen to produce 44 kg of carbon dioxide

When a hydrocarbon fuel is burnt, both the carbon and the hydrogen are oxidized. Consider the combustion of kerosene:

$$C_{12}H_{24} + 18O_2 \rightarrow 12CO_2 + 12H_2O \qquad \text{Eq 13.2}$$

Here the products of combustion include both carbon dioxide and water. Note that many intermediate products are formed during combustion, but only the initial and final products are considered in this investigation.

Oxygen used in combustion is supplied as air of which the composition on a molecular basis is approximately 21% oxygen and 79% nitrogen. This assumption leads to the conclusion that, for every oxygen mol used, $^{79}/_{21} = 3.76$ mols of nitrogen are involved. Therefore, if the oxygen for the combustion of kerosene is supplied as air, the reaction must be written as:

$$C_{12}H_{24} + 18O_2 + 18(3.76)N_2 \rightarrow 12CO_2 + 12H_2O + 67.68N_2 \qquad \text{Eq 13.3}$$

Therefore, the minimum amount of air that is needed to supply sufficient oxygen for complete combustion of all elements in the fuel that may oxidize is called the theoretical air. When complete combustion is achieved with theoretical air, the products contain no oxygen. However, the theoretical amount [AF_s] of air needed is equal to 35.7 mol for every mol of fuel, and can be defined as:

$$AF_s = {}^{m_{air_s}}\!/_{m_{fuel}} \qquad \text{Eq 13.4}$$

A subscript 's' is used to indicate the ratio for 100% theoretical air, and is also called the stoichiometric mixture.

In practice, however, complete combustion is not likely to be achieved unless the amount of air supplied is somewhat greater than the theoretical amount (Sonntag et al.1998). A ratio called the equivalence ratio [ϕ] is the actual fuel-air ratio divided by the theoretical fuel-air ratio as:

$$\phi = {}^{AF_s}\!/_{AF} \qquad \text{Eq 13.5}$$

When the term "theoretical air of 150%" is used, it means that 50% excess air is used and the mixture is weak. For weak mixtures ($\phi < 1$), the equation may be written as:

$$\phi C_{12}H_{24} + 18O_2 + 18(3.76)N_2 \rightarrow 12(\phi CO_2 + H_2O) + \phi C_{12}H_{24} + 18(1-\phi)O_2 + 67.68N_2 \qquad \text{Eq 13.6}$$

and for rich mixtures:

$$\phi C_{12}H_{24} + 18O_2 + 18(3.76)N_2 \rightarrow 18(1-\phi)O_2 + \phi C_{12}H_{24} + 12\phi(CO_2 \text{or } CO_2) + 12\phi(H_2 \text{ or } H_2O) + 67.68N_2$$

Eg 13.7

Rich mixtures occur when $\phi > 1$. Note: the combustion efficiency has an impact on these equations (Lefebvre 1998), but is not taken into account in this equation.

13.3 COMBUSTION CHAMBER AERODYNAMICS

As shown in Figure 13.3, the air will be introduced into the liner in stages. The first stage called the primary stage, uses 15 to 20% of the incoming air to create the stable burning zone. The o ther zone, shown in Figure 13.3, is known as the dilution zone, where the leftover air is introduced into the liner. This air is used to cool down the combusted gas to temperatures that are acceptable for the turbine. The mixing of hot and cold streams is essential for reducing the occurrence of hot streaks that can damage the turbine.

Since it is possible that some of the fuel has not reacted during the short time in the primary zone, in practice, it is necessary to introduce a secondary zone where more fresh air enters the liner before the dilution zone. The secondary zone helps recover some of the losses due to chemical dissociation of the primary combustion products and is achieved by a number of inlets between the primary and dilution zones. This accounts for less than 12% of the total incoming air.

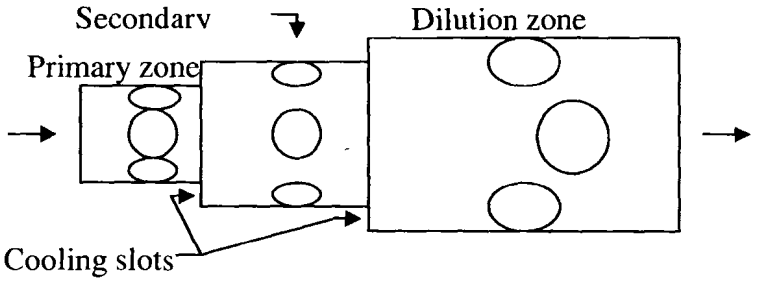

Figure 13.1: Illustration of the zonal liner air introduction method.

Flame temperature for stoichiometric mixtures is in the region of 1600 °C, which is higher than the material limits of the liner. The liner therefore has to be cooled down to ensure that no wall failures occur and is done by cooling slots in the liner wall. Cooling slots introduce a cooling barrier layer between the hot gas and the liner wall. This cooling air should be directed into the same general direction as the gas stream, not to penetrate the gas stream like the dilution holes. Distinction between these two introduction methods can be seen in the illustration in Figure 13.2.

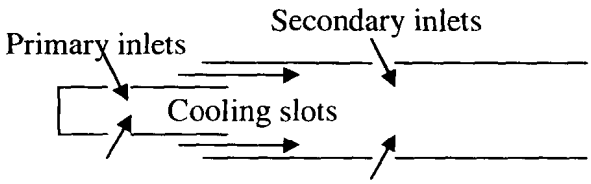

Figure 13.2: Illustration of liner inlet flow direction.

The aerodynamic process plays a vital role in the design process of gas turbine combustion chambers and demands knowledge of flow recirculation, jet penetration and mixing, and discharge coefficients for all the air inlets in the liner. Some variables need to be defined before any of the combustor parameters are discussed: The reference velocity $\left[U_{ref}\right]$, which is the mean velocity across the plane of maximum cross-sectional area of the casing $\left[A_{ref}\right]$ in the absence of the liner and the dynamic pressure q_{ref}. They are defined as

$$U_{ref} = \frac{\dot{m}}{\rho_{in} A_{ref}} \qquad \text{Eq 13.8}$$

and

$$q_{ref} = \frac{1}{2}\rho_{in} U_{ref}^2 \qquad \text{Eq 13.9}$$

13.3.1 Pressure loss parameters

Both *Lefebvre* (1998) and *Cohen et al.*(1996) noted two dimensionless pressure-loss parameters i.e.: (1) The total pressure loss to inlet pressure ratio (also known as the *overall pressure loss*) $(\Delta p_{in-out})/p_{in}$ and (2) the total pressure loss to dynamic pressure ratio (also known as the pressure loss factor[PLF]) $(\Delta p_{in-out})/q_{ref}$.

The two parameters are related:

$$\frac{(\Delta p_{in-out})}{p_{in}} = \frac{(\Delta p_{in-out})}{q_{ref}} \cdot \frac{R}{2}\left(\frac{\dot{m}\sqrt{T_{in}}}{A_{ref}\, p_{in}}\right)^2 \qquad \text{Eq 13.10}$$

Lefebvre (1998) tabulated typical pressure losses in combustion chambers. These values are, however, for cold losses only.

Table 13.1: Pressure-losses in combustors.

Combustor type	$\frac{(\Delta p_{in-out})}{p_{in}}$	$\frac{(\Delta p_{in-out})}{q_{ref}}$	$\left(\frac{\dot{m}\sqrt{T_{in}}}{A_{ref}\, p_{in}}\right)^2$
Tubular	0.07	37	0.0036
Tubo-annular	0.06	28	0.0039
Annular	0.06	20	0.0046

Losses due to combustion are normally not included in the overall pressure loss and values are in the range of 4 to 8 % depending on operational conditions. Flow resistance introduced into the air stream between the recuperator outlet and the turbine inlet is represented by the PLF and is a fixed property of the combustor chamber and corresponds to the sum of the pressure drop in the diffuser and the drop across the combustor liner:

$$\frac{(\Delta p_{in-out})}{q_{ref}} = \frac{\Delta p_{diff}}{q_{ref}} + \frac{\Delta p_{liner}}{q_{ref}} \qquad \text{Eq 13.11}$$

The pressure loss over the diffuser will be discussed later in this chapter under the liner geometry section. Pressure drop over the liner has to be sufficiently high as it promotes high injection air velocities, steep penetration angles, high turbulence levels that encourage good mixing, which can result in a shorter liner. An optimum pressure loss over the liner has to be established as a high pressure loss over the combustor reduces some work done by the compressor, and is thus a disadvantage to the system output.

The PLF over the liner is determined by the total effective hole area [$A_{h[eff]}$] in the liner.

$$PLF = \frac{\Delta p_{in-out}}{q_{ref}} = \frac{U_j^2}{2} = \frac{R}{2}\left(\frac{\dot{m}\sqrt{T_{in}}}{A_{h[eff]}\, p_{in}}\right)^2 \qquad \text{Eq 13.12}$$

Lefebvre (1998) derived that the effective inlet hole area in the liner is determined by the casing reference area and the available pressure drop over it:

$$A_{h[eff]} = \frac{A_{ref}}{\sqrt{\left[\left(\frac{\Delta p_{in-out}}{p_{in}}\right) - \left(\frac{\Delta p_{in-out}}{q_{ref}}\right)\right]}} \qquad \text{Eq 13.13}$$

The effective flow area of the liner [$A_{h[eff]}$] can also be calculated

$$A_{h[eff]} = \sum_{i=1}^{i=n} Cd_{[i]} A_{h[i]} \qquad \text{Eq 13.14}$$

with $Cd_{[i]}A_{h[i]}$ the effective of i^{th} inlet hole, and n the total number of holes.

13.3.2 Relation between size and pressure loss

By inspection it seems that only the maximum casing area $\left[A_{ref}\right]$ is variable since all the other values are fixed by the combustor design. This casing area needs to be optimized in order to achieve the best fuel consumption, while keeping the overall pressure loss at a minimum. One percent increase in pressure loss results into either half a percentage point reduction in thrust, or a quarter percentage point increase in fuel consumption. For use in the TCIR cycle, a large diameter and low-pressure-loss is required and this will result into low fuel consumption. The overall pressure loss dictates the casing size, and A_{ref} is obtained from

$$A_{ref} = \sqrt{\left[\frac{R}{2}\cdot\left(\frac{\dot{m}\sqrt{T_{in}}}{p_{in}}\right)^2 \frac{\Delta p_{in-out}}{q_{ref}}\left(\frac{\Delta p_{in-out}}{p_{in}}\right)^{-1}\right]} \qquad \text{Eq 13.15}$$

Optimization of A_{ref} can be done by providing as large as possible liner cross sectional area. This will result in lower velocities and longer combustion times, which are beneficial to ignition and combustion efficiency. However, the only possibility of obtaining a larger liner diameter is to enlarge the annulus area. This will raise the annulus velocity and lower the annulus static pressure, thus reducing the pressure drop over the liner holes. A high static pressure drop over the longer holes is needed to ensure adequate penetration and sufficient turbulence intensity to promote rapid mixing with the combustion products. *Lefebvre* (1998) suggested that the optimal value for the ratio of liner cross-sectional area to casing cross-sectional area [k] can be derived from:

$$k = 1 - \left[\frac{(1-\dot{m})^2 - \lambda}{\frac{\Delta p_{in-out}}{q_{ref}} - \lambda r^2}\right] \qquad \text{Eq 13.16}$$

with λ the diffuser pressure loss and r the ratio of casing area to combustor inlet area and results in

$$A_{liner} = k * A_{ref} \qquad \text{Eq 13.17}$$

The value of k may be assumed as 0.7.

13.3.3 Flow in the annulus and line inlet holes

Flow conditions in the annulus have an effect on the airflow pattern within the liner and the level and distribution of liner temperatures. Gas velocity in the annulus is governed by the combustion reference velocity as well as the ratio of liner area to casing area. Therefore, a change in the velocity profile further along the liner occurs due to air that is drawn through the liner holes and cooling ducts from the annulus. Gas flow through the liner inlet holes depends on factors shush as the size and pressure drop over the inlet hole, and on duct geometry and flow conditions in the vicinity of the inlet hole:

$$U_{ref} = \frac{\dot{m}}{\rho_{in} A_{ref}} = \sqrt{\frac{2q_{ref}}{\rho_{in}}} \qquad \text{Eq 13.18}$$

Lefebvre (1998) expressed the equation for flow through a hole as

$$\dot{m}_h = CdA_{h.geom}\sqrt{\left[2\rho_{in}\left(P_i - p_j\right)\right]} \qquad \text{Eq 13.19}$$

with P_1 the total pressure upstream of the inlet hole, p_j the static pressure downstream of the inlet hole.

The discharge coefficient [Cd] of a hole is the relation between the smallest area of the flow and the actual area of the flow. The discharge coefficient is used to describe the inlet hole's characteristics and the flow through the hole. Only plain, circular liner inlet holes will be utilized in this study, and for non-swirling flow, the coefficient of discharge for plain circular holes is defined by *Lefebvre* (1996) as

$$Cd = \frac{K-1}{0.8\left[4K^2 - K(2-\alpha)^2\right]} \qquad \text{Eq 13.20}$$

with α the relation of mass flow through the hole $[\dot{m}_h]$ to the annulus mass flow rate $[\dot{m}_{an}]$ ratio and K the ratio of the jet dynamic pressure to the annulus dynamic pressure upstream of the holes. K should vary between 2 and 6.

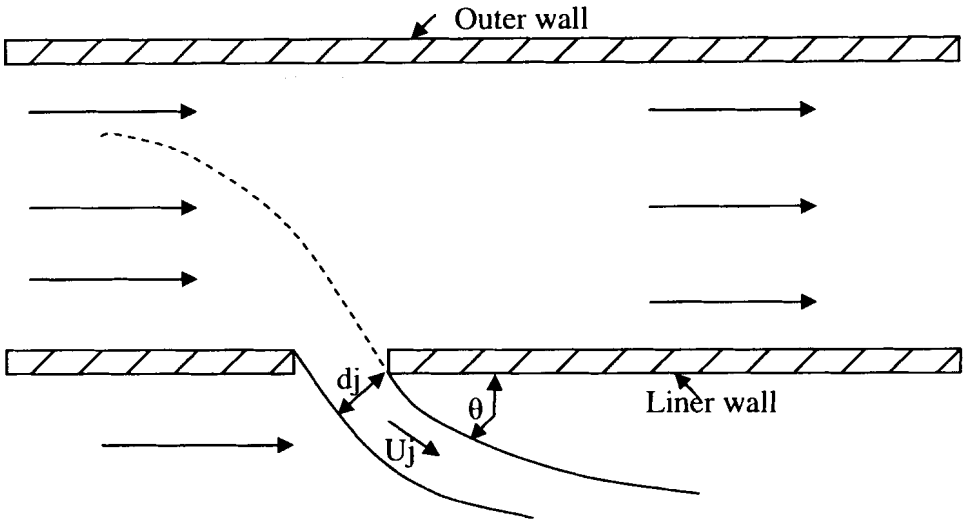

Figure 13.3: Illustration of flow through liner wall.

Other factors that influence the combustor chamber's aerodynamics that will not be discussed in this study include jet trajectories and duct geometry.

13.4 LINER GEOMETRY

The typical combustion chamber consists of the following components: Diffuser, annulus and the combustor liner, which consists of the primary, secondary and dilution zones. These zones were mentioned previously (illustrated in Figure 12.4) and will be discussed in more detail in this section of the study.

13.4.1 Diffuser

The reduction of combustion pressure losses and the decrease in air velocity entering the combustor is achieved by the diffuser. It is defined as a diverging flow passage in which the air flow is decelerated by converting kinetic energy into an increase in the static pressure of the air by alternating the geometric dimensions of the passage. An optimum diffuser is one that achieves

the required velocity reduction in the shortest distance, with minimum loss in total pressure and uniform, stable flow conditions at the exit.

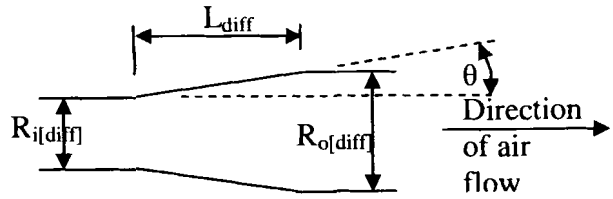

Figure 13.4: Diffuser geometries.

The design parameters of a diffuser are the air ratio [AR], wall length$\left[L_{diff}\right]$, the inlet radius$\left[R_{i[diff]}\right]$ the divergence angle$\left[\theta\right]$. Their relationship is defined by:

$$AR = 1 + 2\left(\frac{L_{diff}}{R_{diff}}\sin\theta\right) + \left(\frac{L_{diff}}{R_{diff}}\sin\theta\right)^2 \qquad \text{Eq 13.22}$$

The pressure loss over the diffuser$\left[\lambda\right]$ needs to be at a minimum, since any pressure loss incurred in the diffuser makes no contribution to combustion. Typical pressure loss values for diffusers with high length/ depth ratios are in the range of 0.15 to 0.45.

13.4.2 Primary zone [Pz]

The function of the primary zone is to anchor the flame and provide sufficient time, temperature and turbulence to achieve near complete combustion of the incoming air/fuel mixture as illustrated in Figure 12.4 and Figure 12.5. About 15 to 20 % of the combustion inlet air is fed through the liner around the jet and the primary inlet holes. The inlet hole position of the primary zone is in the range of 0.5 to 0.6 times the downstream liner diameter. Recirculation is created by the positions of the primary inlet holes in the liner, and the inlet hole diameter in relation to the liner diameter: $0.17 \cdot d_{h[pz]} = d_{liner}$ if six or eight inlet holes are used around the liner.

Around 50 % of the injected air is re-circulated in the primary zone and an illustration of re-circulation can be seen in Figure 12.5. The equivalence ratio$\left[\phi\right]$ should never be lower than 1.5 to minimize smoke and emission gas.

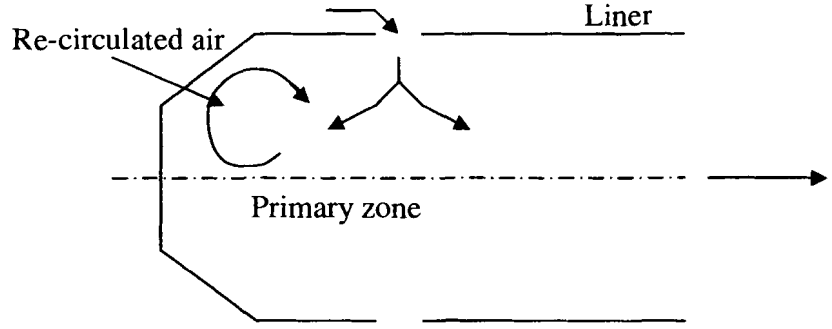

Figure 13.5: Illustration of air flow in primary zone.

13.4.3 Secondary zone [Sz]

In order to achieve an effective burning process in the combustor, the gas leaving the primary zone should be given more air and time to combust, while more oxygen is needed to complete the intermediate chemical processes. The equivalence ratio $[\phi]$ in the secondary zone is in the order of 0.8, and only 10 % of the total inlet mass flow enters the liner through the secondary zone. Secondary zone length is set as 1.5 times the liner diameter (Lefebvre 1998).

13.4.4 Dilution zone [Dz]

The role of the dilution zone is to admit the air remaining after combustion for wall cooling requirements, to produce an exit gas stream with a temperature distribution that is acceptable for the turbine. The ideal temperature distribution pattern is one that gives minimum temperature at the turbine blade root, where stresses are the highest, and also on the blade tip, to protect seal materials. Lefebvre (1998) defined the pattern factor as follows:

$$\text{Pattern factor} = \frac{T_{max} - T_{out}}{T_{out} - T_{in}} \qquad \text{Eq 13.23}$$

Dilution air is introduced by one or more rows of inlet holes in the liner wall. The inlet hole geometry and the dilution length is related to the liner width. Note: The liner length to diameter ratio $\left[L_{liner} / d_{liner} \right]$ of the dilution zone lies in the range of 1.5 to 1.8.

The number of inlet holes in the dilution zone has to be optimized. If the total dilution-hole area is spread over a large number of small inlet holes, penetration will be inadequate, and a hot core will persist through the dilution zone. The use of a small number of large inlet holes will result in a cold core, due to over penetration, and unsatisfactory mixing. *Lefebvre* (1998) provide two methods for determining the number and geometry of dilution holes; 1) The Cranfield method and 2) The NASA method, and compare them as well. In this study the Cranfield method will be used to design the dilution zone of the combustor to be used in the TCIR cycle.

13.4.5 Liner cooling slots

Removing heat from the liner wall by injecting a cold air stream in between the hot gas and the liner wall is known as film cooling. This is done by a number of cooling slots through which air is injected axially along the inner liner wall in order to protect the liner wall from the hot gas. The film is gradually destroyed by the turbulent nature of the combustion gas, so more slots occur at regular intervals down the liner length.

The use of cooling slots has the advantage of enhancing the stiffness of the liner considerably, without adding much weight, and is mechanically robust. The limitation with cooling slots is that it is impossible to have a uniform wall temperature down the length of the liner. *Lefebvre* (1998) evaluated the following cooling mechanisms: Wiggle strip, stacked ring, splash-cooling ring, machined ring, rolled ring and the Z-ring. The author also discussed some advanced cooling methods that include: Angled fusion cooling, tiles, thermal barrier coatings and some materials to be used for liner construction. These wall-cooling methods will not be discussed in this study.

14 Appendix E System layout boundary conditions

This appendix serves as a support for Chapter 7 where the micro gas turbine system is simulated under both steady state, as well as transient conditions. The logic of start-up are explained in this Appendix as well

14.1 INTRODUCTION INTO THE SYSTEM LAYOUT APPENDIX

All the components and subsystems have been decided on and are fixed in the previous part of this study. Here all the components and their specific stating boundary conditions are specified for all of these components. The specific sequence of start-up are also illustrated in this part of the study.

14.2 GAS TURBINE SYSTEM COMPONENT BOUNDARY CONDITIONS

Turbo machinery (Chapter 4):
Low pressure turbine:

Type:	Model A [TV95]
Initial speed:	500 rps
Master turbine:	none

Low pressure compressor:

Type:	Model A [TV92]
Initial speed:	500 rps
Master turbine:	LPT

High pressure turbine:

Type:	Model A [TV95]
Initial speed:	500 rps
Master turbine:	none

High pressure compressor:

Type:	Model A [TV92]
Initial speed:	500 rps
Master turbine:	HPT

Heat exchangers (Chapter 5):

Inter cooler:

Type:	Shell and tube
Number of tubes:	508
Length:	1.5 m
Tube diameter:	0.012.7 m
Shell diameter:	0.4 m

Recuperator:

Type:	Micro channel complex
Number of tubes:	60 000
Recuperator Length:	0.5 m
Recuperator Width:	0.984 m
Recuperator Height:	0.984 m
Tube Width:	0.0025 m
Tube Height:	0.0025 m

Combustion Chamber (Chapter 6):

Type:	External In-line baffled stage burner
Number of stages:	3
Primary zone:	15 – 20%
Secondary zone:	10%

Dilution zone: 70 – 75%
Fuel: Kerosene
Primary losses: Darcy-Weisbach
Fixed heat transfer: None
Fixed exit temperature: 700°C

Pipes (Chapter 7):
Primary losses: Darcy-Weisbach
Fixed heat transfer: None
Fixed exit temperature: None
Dimensions: Table 14.1

Table 14.1: Geometry of pipes in the Flownex® simulation.

Pipe number	Diameter [m]	Length [m]	$\left[\frac{\varepsilon}{D}\right]$
4	0.075	0.75	0.00003
6	0.075	0.5	0.00003
9	0.080	0.2	0.00003

Controllers:

PID controller [13]
Sensed entity: LPT Rotation speed [rps]
Controlled entity: Combustion chamber exit temperature [°C]
Set point: 700 rps
Dead band: 1 rps
Upper limit: 700°C
Lower limit 50°C

PID controller [14]
Sensed entity: LPT Rotation speed [rps]
Controlled entity: Combustion chamber exit temperature [°C]
Set point: 950 rps
Dead band: 1 rps
Upper limit: 700°C
Lower limit 100°C

PID controller [15]
Sensed entity: LPT Rotation speed [rps]
Controlled entity: Combustion chamber exit temperature [°C]
Set point: 1200 rps
Dead band: 10 rps
Upper limit: 700°C
Lower limit 400°C

14.3 MICRO GAS TURBINE SYSTEM START-UP SEQUENCES

14.3.1 Start-up: First stage

The first stage (PID Controller 13) will simulate cold starting where all the temperatures in the different components are still equal to atmospheric conditions. The generator/motor configuration drives the LP turbine at a starting speed of 500 rps and the TIT of 50°C. Controller 13 will control the LP turbine speed at 500 rps. The motor will drive the turbine for a short time only, thereafter, the motor will be switched off, causing the LP turbine to loose speed. In an attempt to generate more power, Controller 13 will add more heat, causing the LP turbine to speed up, providing the power needed by the turbine machine. This is accomplished by increasing the fuel to the combustion chamber, hereby adding the chemical energy to be converted into heat. The TIT will rise until the turbine's speed is equal to the controller's set point once more. The controller controls the turbine speed by adjusting the TIT. (This is done by adding heat to speed up the turbine, or by reducing TIT to allow the gas to cool in order to reduce turbine speed.) The first stage control is done by Controller 13, and the reactions to the adjustments can be seen in Figure 14.1 and Figure 14.2.
The HP turbine also reacts to the change in temperatures, but only the LP turbine need to be controlled for the generator is driven by the latter. The HP turbine's speed can also be seen in Figure 14.1 for the first stage of start-up.

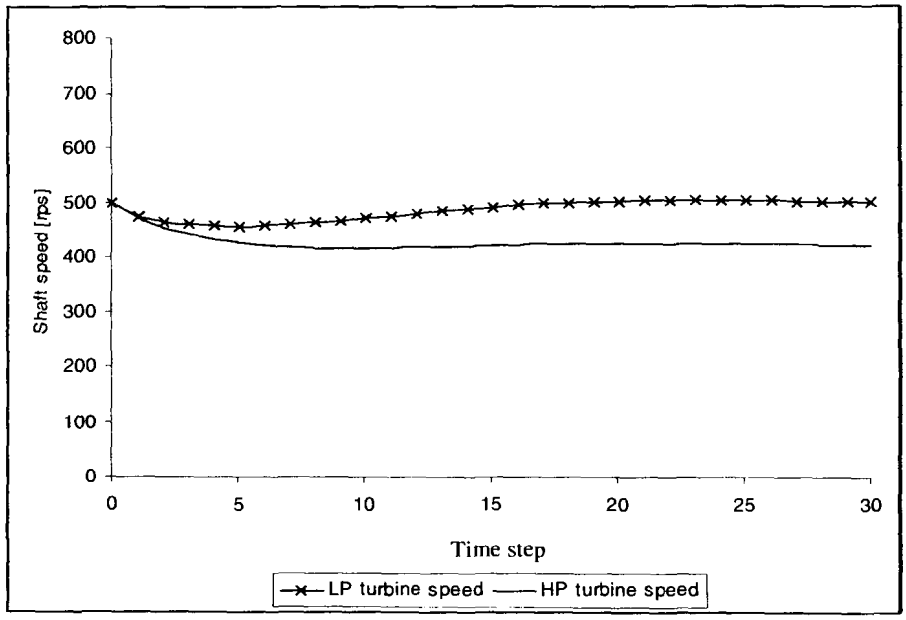

Figure 14.1: Turbine speed for the 1st stage of start-up

Note: Initially, both turbines will loose speed until the combustion chamber produces enough heat to maintain the power needed by the system during the first stage of start-up.

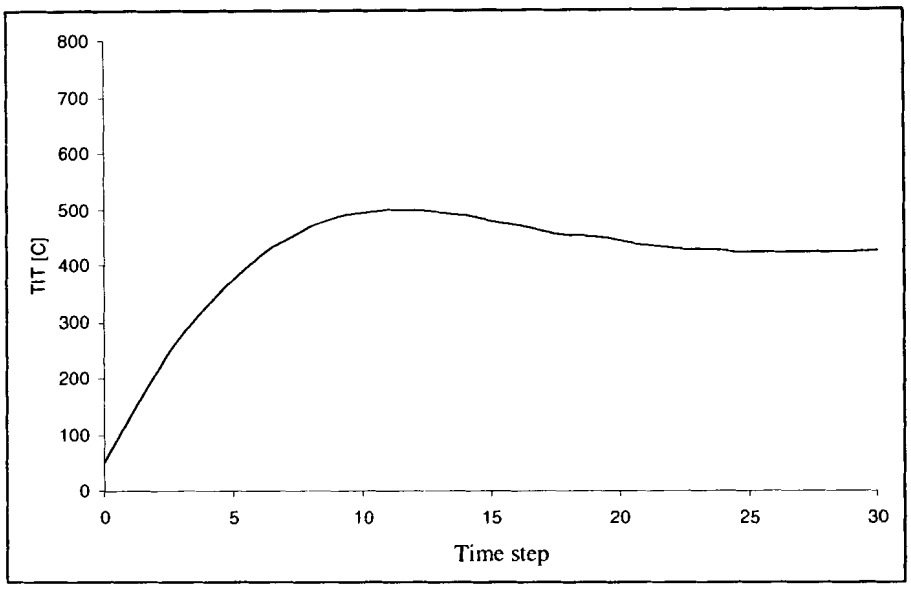

Figure 14.2: TIT for the 1st stage of start-up

Illustrated in Figure 14.2, one can see Controller 3 will manipulate the TIT in order to maintain a constant LP turbine shaft speed.

14.3.2 Start-up: Second stage

The LP turbine needs to accelerate to a higher speed close to operating conditions. This process is controlled by Controller 14, replacing Controller 13. The resulting values of Controller 13 (TIT of 424°C and LP turbine speed of 500 rps) are used as the input values for Controller 14. The second stage control is identical to the first stage, but the turbine speed limit is set at a different level.

The LP turbine speed is accelerated (Figure 14.3) by increasing the fuel mass flow to the combustion chamber (Figure 14.4).

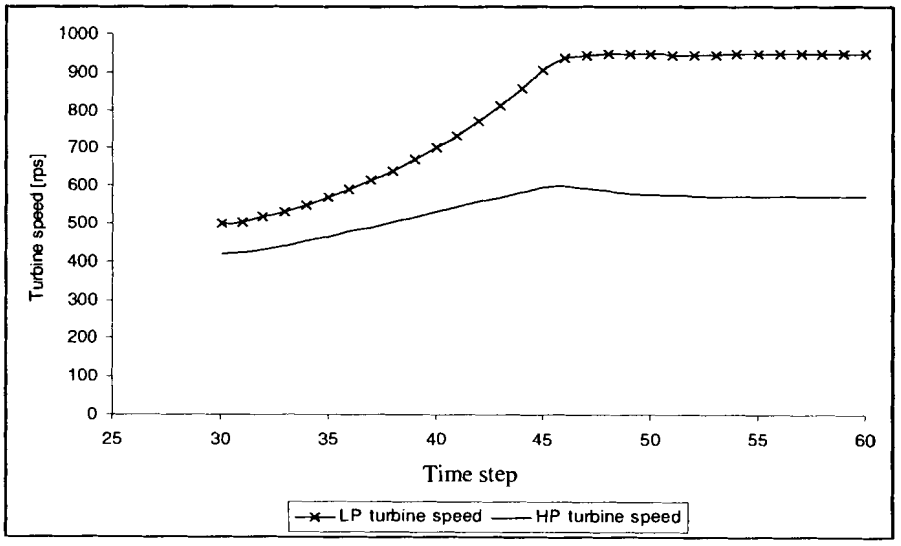

Figure 14.3: Turbine speed for the second stage of start-up

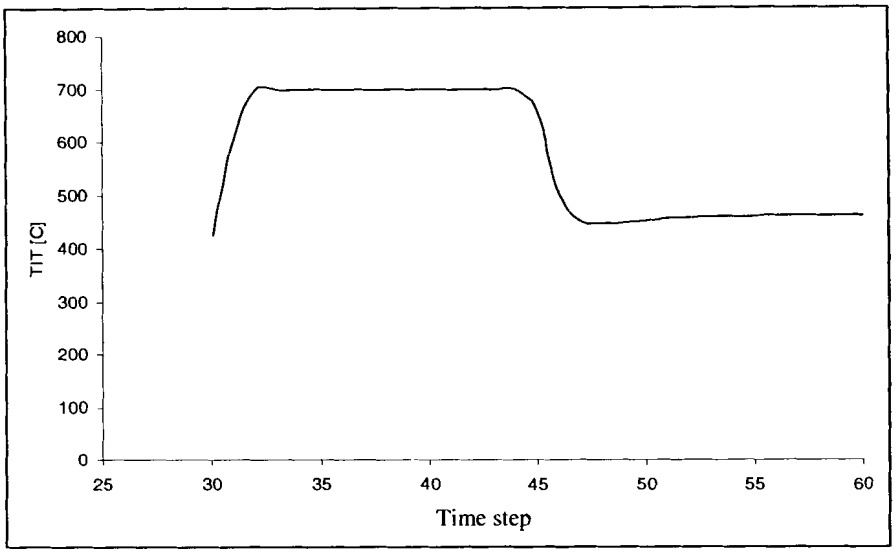

Figure 14.4: TIT for the second stage of start-up

Note: The TIT temperature initially increased from the first stage conditions to the maximum allowable temperature of 700°C to accelerate the turbine. Controller 14 enforced a constant TIT of 700°C until the LP speed reached the target speed of 950 rps. Only then the TIT are allowed to drop to a lower condition that allows the LP turbine to rotate steady at 950 rps. The system is allowed to stabilise at these conditions for a few time steps before the third stage of the start-up process is activated.

14.3.3 Start-up: Third stage

This stage will prepare the micro gas turbine for load following, by controlling the micro gas turbine system to operate close to the expected operating conditions. Therefore, once the load is applied, the micro gas turbine system is already on a running start, but it will be discussed in more detail later in this study.
Controller 15 concludes the start-up procedure by taking over from controller 14 controlling the LP turbine speed at 1200 rps. The third start-up stage's turbine speed and TIT can be seen in Figure 14.5 and Figure 14.6 respectively.

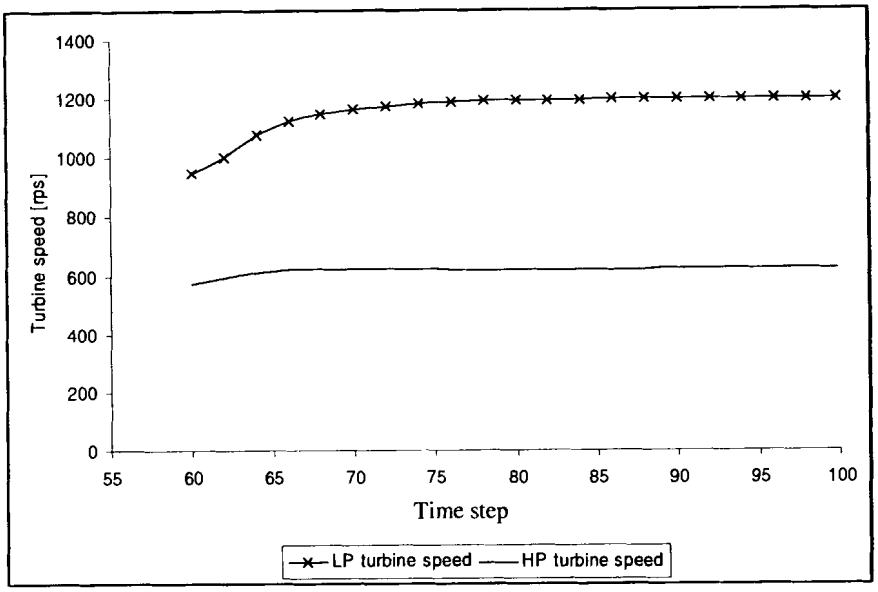

Figure 14.5: Turbine speed for the third stage of start-up

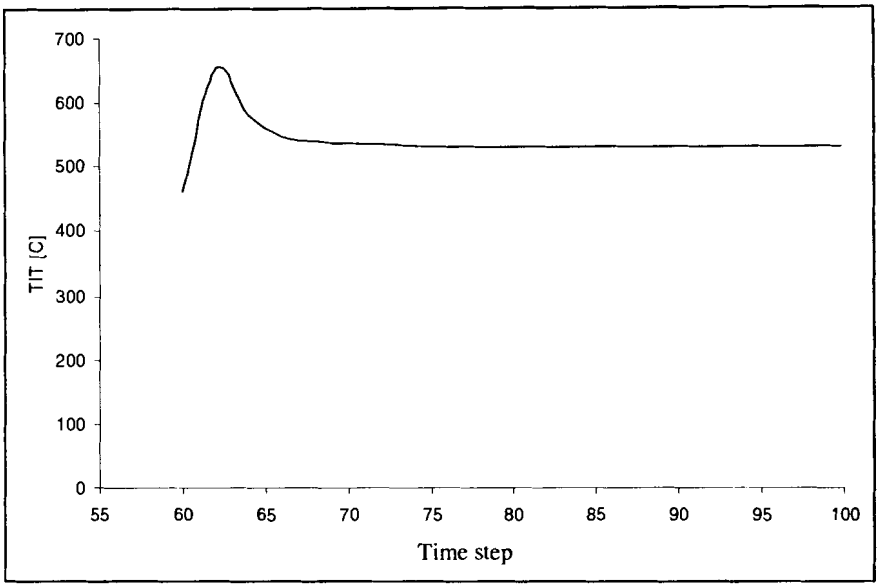

Figure 14.6: TIT for the third stage of start-up

Note: The TIT as well as both the turbine speed values is stable towards the end of this start-up simulation. The TIT value is well within the bounds of the controller (400 – 700 °C), and well clear of the upper limit of 700°C.

The controller increases the TIT initially in order to accelerate the LP turbine, but decreases the TIT as soon as the turbine's speed approaches the target range. This allows the system to operate more smoothly, limiting shocks that accompany sudden changes.

15 Appendix F Lubrication system

The turbine machinery have rotating parts, therefore the need for some kind of lubrication. For this study, standard liquid lubrication will be used on the micro gas turbine machines. This appendix serves as a support chapter for Chapter 7 where the auxiliaries are discussed.

15.1 INTRODUCTION INTO LUBR ICATION OF TURBINE MACHINES

The small tolerances of the turbochargers, as well as the high operating speed, contribute to the need for a reliable and a non-contaminated lubrication system. Therefore a reliable lubrication system is required to supply sufficient oil to the bearings. The lubrication system should provide the necessary lubrication as well as cooling the bearings. A further requirement is a reliable filtration system, which is able to keep the cleanliness of the oil at an optimum level.
Since the turbo chargers are ordinary off-the-self units they are not equipped with special air- or magnetic-bearings. These units have bearings that need to be lubricated. The lubrication has two main functions: to lubricate the bearing to avoid friction and damage to the bearings, and to keep the temperature low. Lubrication oil is used to cool the bearings since a lot of heat is being transferred from the shaft of the turbo to the bearings. It is very important that the lubrication system has to be able to transverse the heat away from the units' bearings even when the units are not moving. The heat capacity of the lubrication system has to be bigger than the heat transferred to the shaft from the turbine and thus the combustion chamber.

15.2 LUBRICATION OF THE TURBO UNIT

Figure 15.1 shows the flow of lubrication oil through the turbo charger. Note that the lubrication oil in the feed side of the turbocharger experiences a higher oil pressure than the drain side. There are small orifices in the turbine hosing that allow only a certain mass flow through the turbo charge. The lubrication pressure is a function of the drain pressure, and not depended on the inlet pressure. Figure 15.3 also shows that the return side of the shaft is a sump, under atmospheric pressure only, and that the back pressure to the pumps is done through the small channels itself and not the return lines to the reservoir. For this reason no backpressure may occur in the return lines.
The two seals in Figure 15.2 and Figure 15.3 show all the internal oil channels in the housing of the turbocharger.
Another factor to consider is the fact that a certain amount of lubrication oil is going to leak through the seals on the shaft. This is dynamic seals, and most of the leakage occurs when the lubrication system is running and the shaft stationary. The leakage could be minimized by synchronizing the shaft movement with the lubrication system.

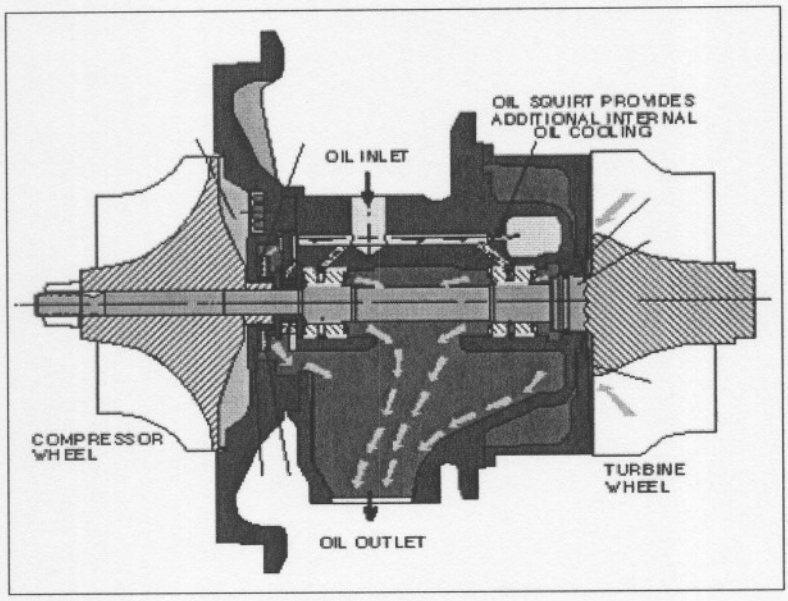

Figure 15.1: Lubrication of a typical turbo unit

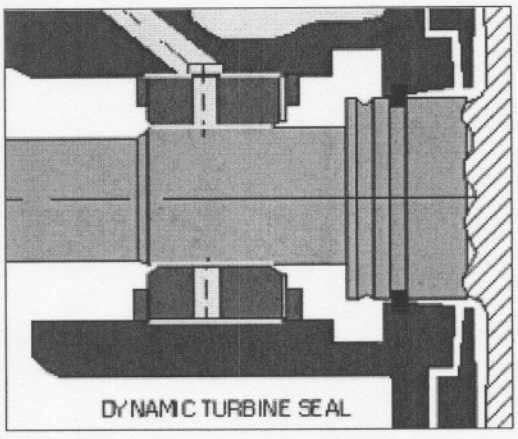

Figure 15.2: Lubrication of the turbine-side bearings

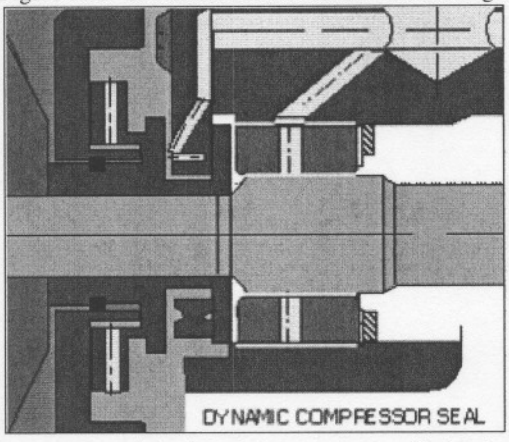

Figure 15.3: Lubrication of the compressor-side bearings

15.2.1 Requirements of the lubrication system

Priority number one: reliability. As a system that can supply lubrication at any time, and during any event. This includes secondary auxiliary failures like a power cut or instrumentation fault. This indicates that a dedicated back-up system has to be in place.
The lubrication system needs a filtration system to ensure that no foreign objects could enter and damage the shaft or bearing bed. This system has to have a clogging indicator to warn the operator that the filter should be replaced.
The system needs to be controlled to ensure that a pre-set pressure will always be maintained independent of the oil flow rate.
A heater should be included to heat the lubrication oil to the working temperature before the oil enters the turbo charger, thus preventing thermal shock on the bearings and shaft. It will also need a lubrication oil cooler, because once the system is running; the temperature of the oil will rise because of the elevated temperature of the turbo.
A reservoir to supply the pumps and to contain the drained oil will be needed.
A simplified system with only one of the three feed lines is shown in Figure 15.4.

1) Reservoir
2) Variable speed motor and pump
3) Filter
4) Flow indicator
5) Pressure indicator
6) Proximity switch valve
7) Turbo charger
8) Solenoid valve
9) Back-up accumulator
10) Pressure regulator
11) Low level switch
12) Heater
13) Temperature transmitter
14) Sight glass
15) Filler cat and breather
16) Cooler
17) Mechanical valve
18) Constant speed motor and pump

15.2.2 Reservoir

A reservoir in which the oil could be stored from which the feed lines suck. The pumps may never suck air, thus there has to be a surplus oil, not only to keep all the lines filled, but also for the heat transfer of the oil. It takes time for the oil to change its state and with that its temperature. All so in the event of a failure, there is a surplus of oil. When oil is returned into the reservoir from the drain it may include air and these bubbles need time to reach the surface. If oil with bubbles is sucked into the pumps, it will result in capitation. It is a process where the air bubbles are flung to the pump casing, under high speed and pressure, and hit the wall with little explosions. These explosions will damage the pump wall and gears and will result in pump failure.
The reservoir will also house the heater. It will be discussed later in this section, and can be seen in Figure 15.4.

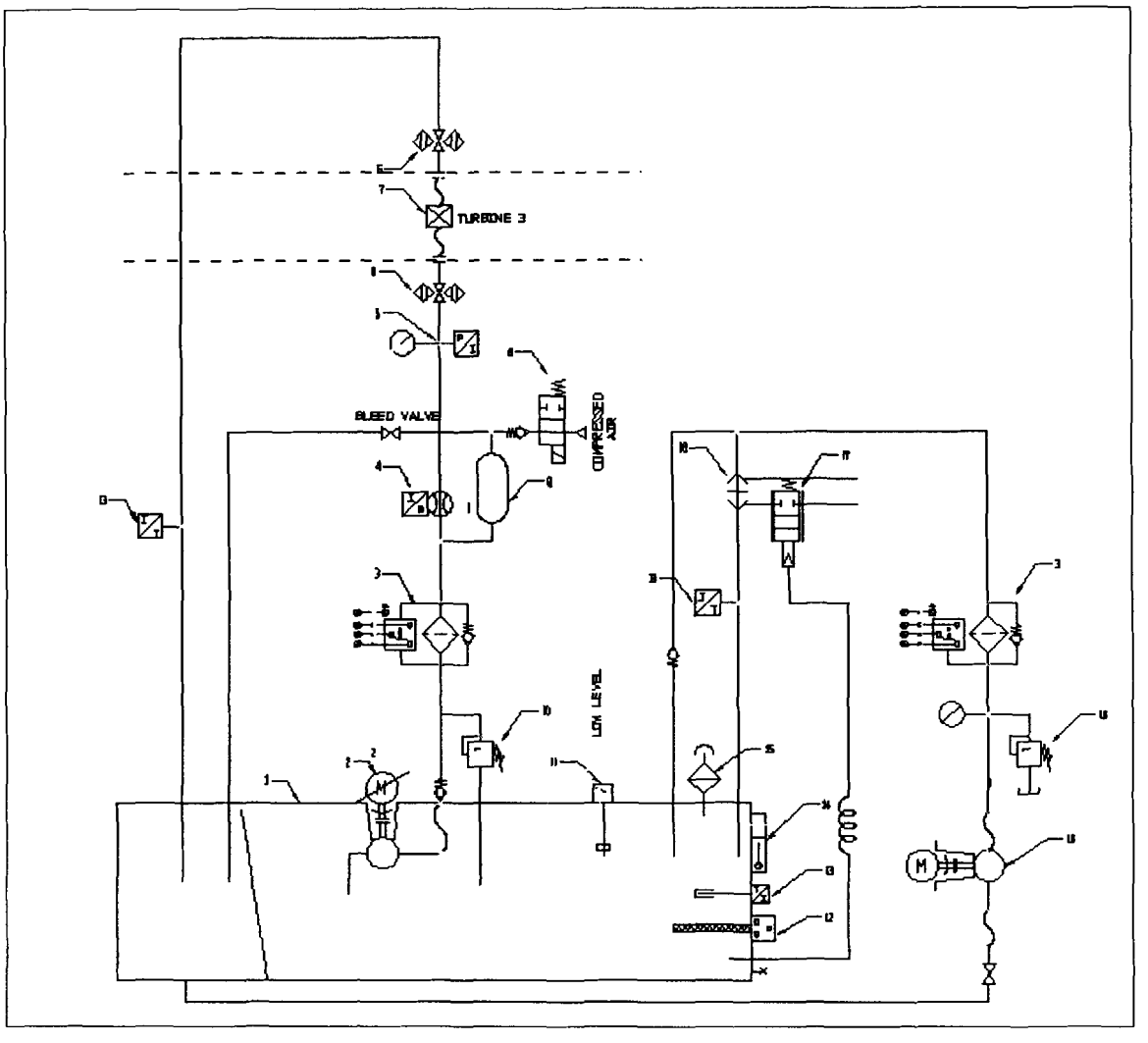

Figure 15.4: Simplified lubrication system

The reservoir will comply with the following:
Pumps, coolers, or filters will not be mounted on top of the reservoir.
The top of the reservoir will be sloped at least 1:100. [If flat top].
All oil return flow streams shall be located as far as possible from the pump suction connections as possible.
All atmospheric return lines will be located above the oil level.
Pump suction connections shall be located near the high end of the sloped reservoir bottom.
To ensure complete drainage, the bottom of each reservoir will slope continuously, at least 1:50, to a low point.
The drain will be mounted at the lowest point of the reservoir.
The reservoir will have the capacity to settle moister and foreign matter adequately and to provide allowance for rundown from the entire system.
The oil level glass will be located as far away as possible from the oil return lines and be visible from the perimeter of the unit.
Joints, pads, and connections will be both internally and externally welded to eliminate cavities, potential sources of corrosion and contamination.

The reservoir's wall-to-top junctions may be welded from the outside if a full-penetration weld is used.
All welds will be continuous.
Internal joints will be made smooth by grinding or other suitable means as necessary to eliminate pockets and provide an unbroken finish.

15.2.3 Feed lines

Since each of the turbo units need oil at a pre-set pressure that is independent of the flow rate of the oil through the unit, each of the units will have its own feed line. This feed line includes a pump coupled onto a variable speed motor (2), a pressure regulating valve (10) and a filter (3). All three feed lines are identical, except for the flow rates though the turbo chargers. The pumps are submerged under the oil low level in the reservoir (1). The secondary filter follows the pump before it leads to the turbo unit (7) and back through the drain into the far side of the reservoir. A pressure indicator (5) is mounted on the feed line and enables the control system to read the pressure in the line, compare it to the pre-set pressure and send a pulse to the variable speed motor to correct if necessary.
By varying the speed of the pump, while the orifices stay constant, one could vary the pressure in front of the orifice. The turbo charger's orifice stays constant and will allow a certain oil flow rate through it under a certain pressure. Thus, the oil flow rate is a function of the pressure and orifice opening. If a turbo charger needs a bigger flow rate, the control will allow the motor to speed up until the pump is able to provide a constant pressure. This pressure will vary until all the air is out of the system.
Note that in front and just following the turbo charger (7), one would find two proximity valves (6). These valves enable you to isolate the turbo in an event like maintenance, but also protect the system. It sends a signal to the control, so the system could not be stated before both these valves are open.

15.2.4 Filtration and cooling

As previously mentioned each feed line will have its own filter (3), but this is used as secondary filtration units. The primary filtration system is in the cooling line (18). This line is not linked to a turbo charger, but merely circulates the oil back into the reservoir (1). It is used both as a filtration system as well as a circulating system to condition the lubrication oil to the optimum temperature. Situated in this line is the cooler (16). When the oil temperature rises, the cooler will be activated and the oil will be cooled. The cooler is passive until the temperature reaches a pre-set value. Then a valve (17) will open, allowing cooling water to enter the cooler, and the cooler becomes active. The cooler also has a clogging warning device. Important is that the oil pressure in the cooler will always be higher than the water pressure. This way, in the event of a failure, the oil will leak into the water and not water into the oil. Water can damage the turbo units if it gets pumped into the feed lines. The secondary system is driven by a constant speed motor and the pressure and flow rate of this line can not be controlled.

15.2.5 Heater

Under operation, the shaft will heat up with the turbine wheel, while the oil from the reservoir will be at ambient temperature. If this cold oil is pumped onto a hot shaft thermal shock will occur and will lead to failure of the unit. The thermal shock can be avoided by heating (12) the oil to near working conditions. A heater will be mounted inside the reservoir (1), and will be controlled by the temperature transmitter (13) measuring the reservoir temperature. While the

temperature of the oil is be neath working conditions the heater will be activated and once that temperature is reached the heater will shut down.
A thermostatically controlled, removable electric immersion-heating element will be provided for heating the charge capacity of oil prior to start-up in cold weather. The device will have sufficient capacity to heat the oil in the reservoir from ambient temperature to start-up temperatures. Heater elements in contact with oil will be sheeted in austenitic stainless steel, copper or copper-bearing materials will not contact the oil.

15.2.6 Back-up

The moment in which the gas turbine generator experiences some failure and seizes working the shafts will still be rotating and need lubrication and cooling. There has to be some system that will ensure that there will still be oil pressure and flow over the bearing in such an event.
Two back-up systems are considered. The first back-up system is an uninterrupted power supply (UPS) that stores power while the generator is providing power. The UPS charges a battery while the generator is operational, and will be able to drive the feed pumps. The second back-up system (9) will be using instrumentation air to produce pressure in the feed lines, if the UPS fails, or if it is not able to drive the pumps in the event of a failure. The control of this consists of a normally open, "energized to close solenoid valve (8)" that receives an impulse from the electrical feed line (and UPS). The moment this impulse fails the valve opens and allows the pressurized air into the oil feed lines. The air pressure will force the oil in the accumulator into the feed lines.

By using the equation: $P = \frac{F}{A}$, where P the pressure is, F the force on the Area (A). Since the instrumentation air's pressure is maintained at a constant pre-set value, we can deduct that with a smaller area, a larger force could be obtained. For this reason, the back-up accumulators will be of cylinder type, small diameter, but with a big height. This way, you can get a stable force, with a long working time once the solenoid valve is opened. To ensure that the accumulator is full of lubrication oil, and not air, there is a bleed valve on the return line. To bleed the system, the proximity valve before the turbo unit must be closed, while the bleed valve is opened. Start the motor under bleed mode and let it run until clear lubrication oil without air bubbles pass through the bleed valve. Open the proximity valve before closing the bleed valve. The control should be in running mode again.

15.3 LUBRICATION SYSTEM'S INSTRUMENTATION

As seen in Figure 15.4 which is only a simplified system, there are a lot of signals that can be used as warning, controlling and operating signals. All off these have to be processed and computed to enable the operator to handle the system. For every feed line (there are three) the following instrumentation is needed:
Line pressure transmitter (visual and electronic)

* Flow rate line indicator
* Temperature transmitter
* Filter clogging sensor
* Speed of the motor
* Condition of the proximity valve
* Power to the solenoid valve (back-up)

The reservoir needs the following instrumentation.

* Temperature transmitter
* Low level switch
* Sight glass
* Heater control

While the secondary lines needs the following;

* Return temperature indicator
* Cooler clogging sensor
* Filter clogging sensor
* Mechanical valve
* Pressure transmitter

15.4 LUBRICATION SYSTEM CONTROL

As previously mentioned, a lot of signals from the lubrication system have to be interpreted and controlled to ensure the reliability of this system. Some of the warning signals should shut down the system immediately, while others should be noted to be corrected on a later stage. All of these signals have to integrate into the main control, but it will be discussed in a later section. The lubrication control and the effect it have on the complete system will be discussed here:

15.4.1 Warning signals

The warning signal will be addressed in two stages. Stage one: the system is in pre-start mode. Stage two: the system is in running mode.

- Reservoir low level indicator. This switch will be activated when 25% of the total working oil level is reached. Stage 1: Add lubrication oil immediately. Stage 2: Allow safe shut down and fill reservoir.
- Return oil temperature is too high. Stage 1: Do not start (should be impossible, thus investigate, instrumentation failure). Stage 2: Allow save shut down, and investigate (check cooler).
- Proximity valves in the wrong position. Stage 1: Open valves to the turbo unit. Stage 2: Immediate shut down and open valves right away!
- Feed line pressure to high/low. Stage 1: Stop start procedure and investigate (line blocked). Stage 2: Shut down immediately, investigate and repair failure
- Flow rate to high/low. Stage 1: Stop start procedure, and investigate (line blocked). Stage 2: Shut down immediately, investigate and repair failure
- Filter clogged. Stage 1: Replace filter before restart. Stage 2: Save shut down and replace filter before restart is attempted.
- Back-up solenoid valve's power source fail. Stage 1: This should be repaired immediately. Stage 2: Save shutdown and repair. Important to note is that since the valve was open, compressed air has entered the lubrication system. Air is compressible, thus will the pressure control react to the air and the pressure will be uncontrollable. The pressure will be lower, for the pumps won't be able to pressurize the system, while the control will run the variable speed motors at full speed. It is important to bleed the back-up accumulator system before start up is attempted when ever the solenoid valve was opened.
- Cooler clogged. Stage 1: Investigate the cooler and the primary filter. Do not start before the failure is repaired. Check the primary filter and its clogging device. Stage 2: Save shut down and investigates.

All of the sensors have an allocated number which the operator can follow to check each instrument's condition at any time. This also give the maintenance crew an indication as to where a failure or fault has occurred (by saving the instruments that tripped the alarm's number).

15.4.2 Control signals

The most important requirement of the lubrication system is for lubrication oil under pressure. For this a control system was designed with pressure control in mind. In principle, the system varies the speed of the motors driving the pumps, resulting in variable flow rates through constant sized orifices. By setting a wave band in which the pressure may fluctuate, and reacting on input from the sensors to change the speed of the motor to compensate pressure.
For instance, pressure is set on 4 bar. Start up. Sensing that line pressure is zero, the speed of the motors accelerates, pressure is picking up until the line pressure reaches the set pressure. The motors will be running at a constant speed. If the line pressure falls due to a valve opening or a leak, the motor will speed up until the pressure is equal to the pre-set pressure. If the valve closes, the motors will slow down until the line pressure is again equal to the pre-set pressure. The set pressure can be changed by the operator during operating and the motors will follow the set point. A simulation is shown in Figure 14.5 where the pressure following can be seen.

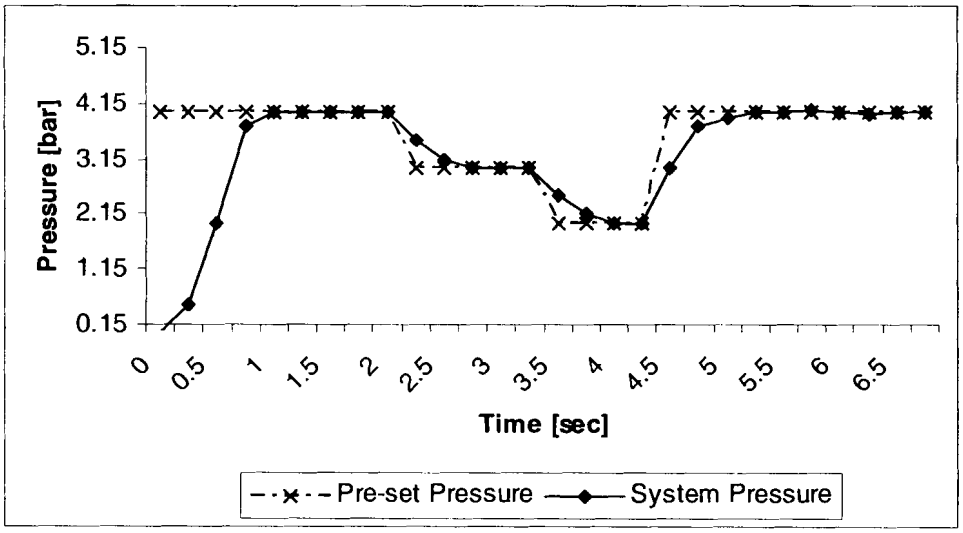

Figure 15.5: Simulation of the pressure following for the lubrication system

While the operator can set the operating pressure, there is also a high and low pressure region in which the set pressure should stay. If the operator sets a pressure that is lower than the minimum pressure, the pressure will not drop below the minimum pressure. The same will happen if the set pressure is higher than maximum value. See the simulation in Figure 14.6 to see the effect where the control overrides the operator.

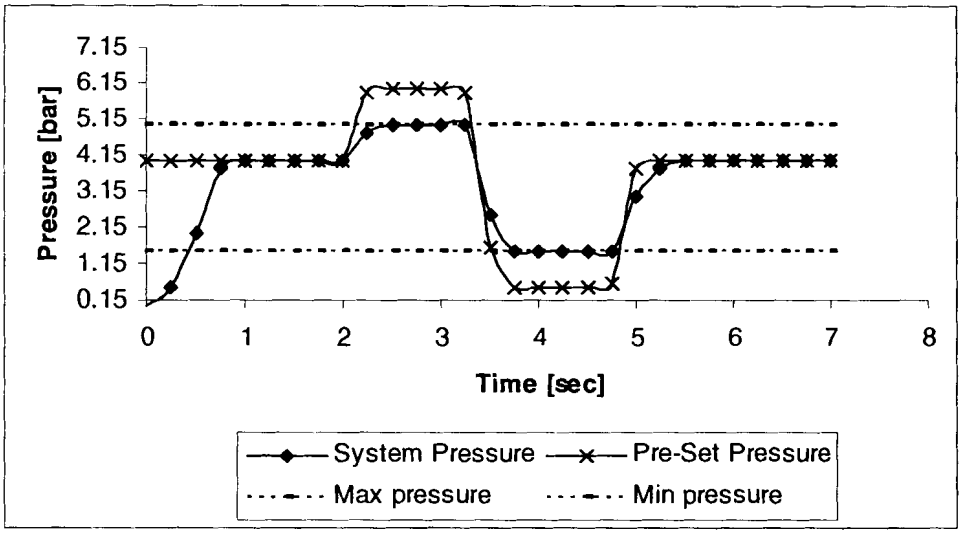

Figure 15.6: Simulation of the upper and lower level of lubrication oil pressure

15.4.3 Control modes of operation

Start mode

Before start up there are some crucial inputs from the lube system that need to be checked. The level of the reservoir (11), the condition of the proximity valves (6) and the back-up solenoid valve (8) status. During this mode the operator has to make a visual check of the lubrication system to look for any obvious failures like oil spills, leaks, ext. If any warning signal is received the system will go into the fault mode and start up will be terminated. This will continue until the operator resets the fault mode to standby mode. If start up is initiated while a fault is still persist, the system will again go to fault mode. Start up will only go into running mode if no more faults are detected.

Running mode

Start mode completed its checks, thus no warnings have been sound, the system will initiate running mode. The control will sense that the oil pressure in the feed lines is lower than the set pressure (line pressure should be equal to zero). The motors will start and the control process will continue like previously explained. During the running mode all sensors will be monitored and if any fault is detected, warning shall be sound and save shut down mode will commence.

This is also the time where the operator should check whether the accumulators are charged (full of oil), by opening the bleed valve fractionally and checking that the oil is bubble free.

Bleed mode

If the operator suspects that the accumulators have air in them, he should initiate the bleed mode. Most of the times this mode will be ignored only activated when the solenoid valve was opened or if the operator expects that air has entered the system. Once the system is in the bleed mode, it will allow the operator to switch the proximity valve (6) (in front of the turbo unit) to close position, while the bleed valve is open. If the operator closes the other proximity valve (following the turbo charger), the system will go into the fault mode. Note that while you are in the bleed mode, the control still receives signal from the system, and in case of any fault (like low oil level) the system will trip back to fault mode.

Save shut down mode

With all the systems running, that is all the auxiliaries and main components, shut down are not as simple as cutting the fuel feed. The turbo chargers are running at high speed, and the combustion chamber is at an elevated temperature. The fuel has to be cut gradually, to make sure that the temperature gradient is not to steep while the combustion chamber cools down. The turbine shaft and bearings are also cooling down. But the shafts are still running and need constant lubrication. Even after the shafts have stopped rotating, the shaft bed and bearings have to be cooled by the lubrication oil. Thus, in any event where a fault is detected while the system is running, a shut down mode has to be initiated, to ensure fast, but save shut down of all sub-systems. The save shut down mode of the lubrication system will be discussed here, while all the sub-system's shut down procedures will be discussed in there own allocated sections in this study.

In the event of a fault occurring in the lubrication system while in running mode, save shut down mode will be initiated. This means that the system will shut down, but the lubrication system will be running as no fault has occurred until five minutes after the last shaft has stopped turning. Then the motors will stop and the lubrication system will go into fault mode. Since every instrument has a number, the fault as well as the number of the instrument who tripped the system will be saved to assist with the repair and also the maintenance of the system.

Fault mode

When ever the system comes into the fault mode, the operator has to reset the control before start up can commence once again. If the fault persists the system will go into fault mode again and this will be repeated until no warning or faults occur. (Only then will start up be possible and go into running mode). It is not dependent on which mode the system was before it went into the fault mode. The system will always start with the start up mode after it has been reset by the operator. As previously mentioned, the fault and the part responsible for the alarm and trip will be saved and the operator will be able to see where the problem occurred.

The software is designed in such a way that it is impossible to override the warning s ignals or the trips.

16 Appendix G Definitions and Mathematical equations

16.1 COMPONENTS

Micro gas turbine machine systems are built up by the following basic components: Compressor, Turbine, Combustion chamber / Heater and various heat exchangers. Some of them are discussed here.

16.1.1 Compressor

Definition of a compressor: A device used to pressurize a fluid. The purpose of a compressor is to raise the pressure of the fluid by converging shaft power to a rise in enthalpy of the fluid. The inlet pressure and temperature of the ideal cycle is equal to ambient conditions, for it is not a closed system. The compressor converts shaft power (attached to a blade assembly) to rise in enthalpy of the gas. The rotating blades push on the gas and increase the pressure, thereby increasing the enthalpy. (VT Mechanical Engineering, 1997)

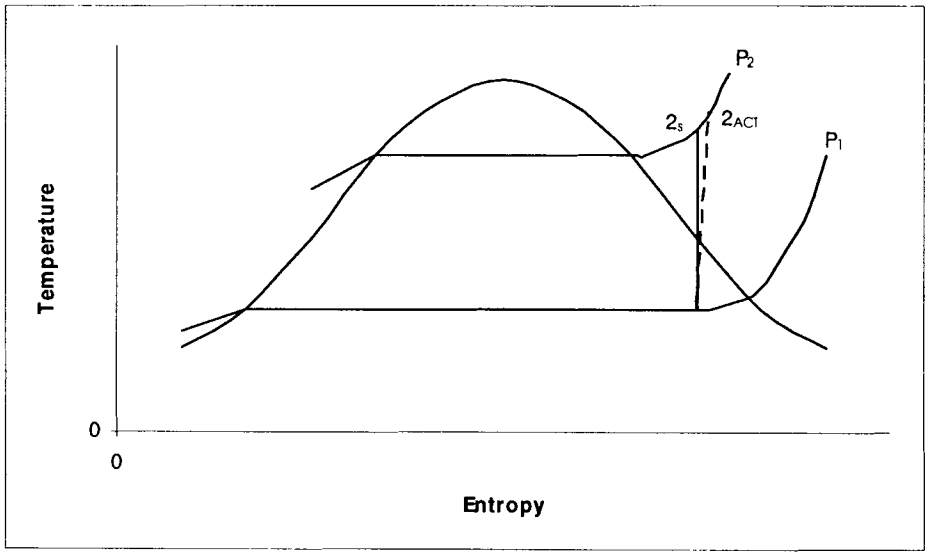

Figure 16.1: T-s diagram for a compressor

Isentropic efficiency $[\eta_c]$ is defined as: $\eta_c = \frac{\text{ideal input work}}{\text{Actual input work}} = \frac{(h_{2_s} - h_1)}{(h_{2_{ACT}} - h_1)}$, with h_1 =enthalpy at state 1, h_2 = actual enthalpy at state 2 and h_{2_s} = isentropic enthalpy at state 2.

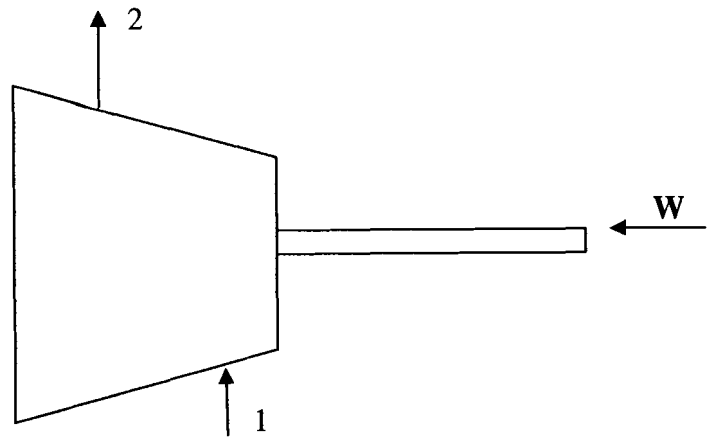

Figure 16.2: Illustration of a compressor

In the simulation, the following held true:

$$T_{in} = T_1, \qquad P_{in} = P_1$$

$$T_{out} = T_2, \qquad P_{out} = P_2$$

$$T_2 - T_1 = {}^{T_1}\!/_{\eta_c}\left[\left({}^{P_2}\!/_{P_1}\right)^{(\gamma-1)/\gamma} - 1\right]$$

The specific work needed by the compressor $\left[\dot{W}\right]_c$ is defined as: $\dot{W}_c = cp\left(T_2 - T_1\right)$

16.1.2 Turbine

Definition of a turbine: A turbine is a device which converts the enthalpy and kinetic energy of a moving fluid into some form of mechanical work. A basic turbine consists of a rotor that is composed of fins connected to a shaft. When a fluid flows trough the fins, the angle of the fins causes the rotor to spin, which causes the shaft to rotate. The torque in the shaft is able to do some mechanical work, such as rotate a compressor or turn a generator which produces electrical current. (VT Mechanical Engineering, 1997)

Isentropic efficiency of a turbine $[\eta_t]$ is the comparison between the actual power output with the isentropic case. Typical efficiencies range from 65 – 90 %.

$$\eta_t = \frac{\dot{W}_{T_{ACT}}}{\dot{W}_{T_s}} \frac{\left(h_1 - h_{2_{ACT}}\right)}{\left(h_1 - h_{2_s}\right)}$$

Where $\dot{W}_{T_s}$ = isentropic power output, $\dot{W}_{T_{ACT}}$ = actual power output, h_1 =enthalpy at state 1, $h_{2_{ACT}}$ = actual enthalpy at state 2 and h_{2_s} = isentropic enthalpy at state 2.

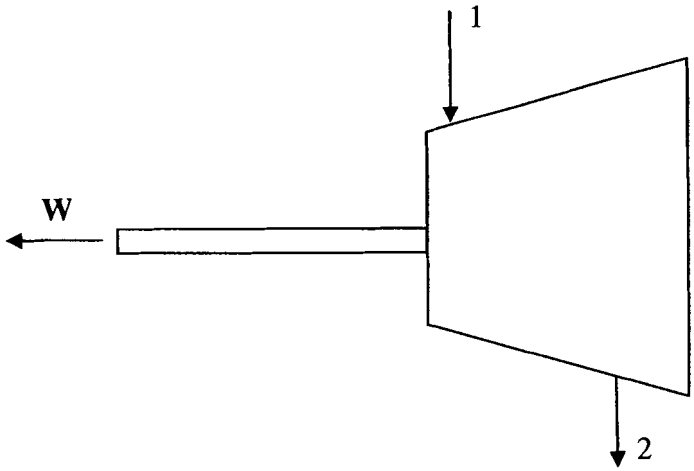

Figure 16.3: Illustration of a Turbine

$$T_{in} = T_1, \qquad P_{in} = P_1$$

$$T_{out} = T_2, \qquad P_{out} = P_2$$

$$T_1 - T_2 = \eta_t T_1 \left[1 - \left(\frac{1}{P_1 / P_2} \right)^{(\gamma-1)/\gamma} \right]$$

The specific work done by the Turbine $\left[\dot{W}\right]_t$ is defined as: $\dot{W}_t = cp(T_1 - T_2)$

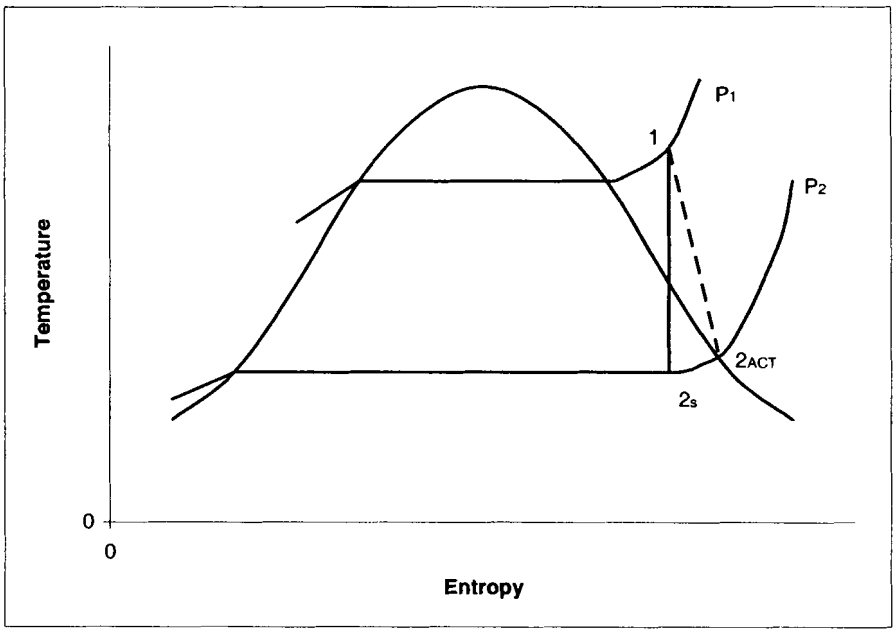

Figure 16.4: T-s diagram for a turbine

16.1.3 Combustion chamber

A combustion chamber converts the chemical energy stored in the fuel to an increase enthalpy in the gas passing through the combustor. The combustion releases large amounts of energy to be absorbed by the gas. This increases the temperature and enthalpy of the gas. (VT Mechanical Engineering, 1997)

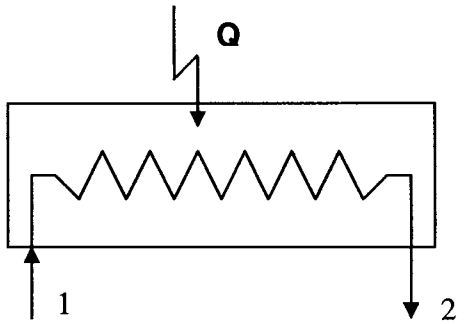

Figure 16.5: Illustration of combustion chamber

The specific heat induced by the combustor $\left[\dot{Q}_{heat}\right]$ is defined as: $\dot{Q}_{heat} = (h_2 - h_1)$, with h_1 =enthalpy at state 1 and h_2 = actual enthalpy at state 2. Note that h_2 is greater than h_1. This makes the energy positive, indicating that the fuel enters the system from the fuel and exits with the gas.

$T_{in} = T_1, \qquad P_{in} = P_1$

$T_{out} = T_2, \qquad P_{out} = P_2$

In the simulation, specific heat is calculated with: $\dot{Q}_{heat} = cp(T_2 - T_1)$, and a pressure drop Δp_{cc} occur over the combustion chamber: $\Delta P_{cc} = \frac{(P_1 - P_2)}{P_1}$.

The combustion chamber's efficiency is the ratio of the heat added to the gas stream $\left[\dot{Q}_{heat}\right]$ and the heat provided by the fuel $\left[\dot{Q}_{fuel}\right]$: $\eta_{cc} = \frac{\dot{Q}_{heat}}{\dot{Q}_{fuel}}$

A detail discussion on the design of a combustion chamber is available in chapter 6 of this study.

16.1.4 Inter-cooler

The intercooler is a heat exchanger where energy is exchanged between two fluids that are not in contact with each other. The got gas heats the coolant, resulting in the cooling of the hot gas.

For the gas side, the following apply: $T_{in} = T_1, \qquad P_{in} = P_1$

$T_{out} = T_2, \qquad P_{out} = P_2$

And for the coolant side: $T_{Coolant_{in}} = T_{C1}, P_{Coolant_{in}} = P_{C1}$

$T_{Coolant_{out}} = T_{C2}, P_{Coolant_{out}} = P_{C2}$

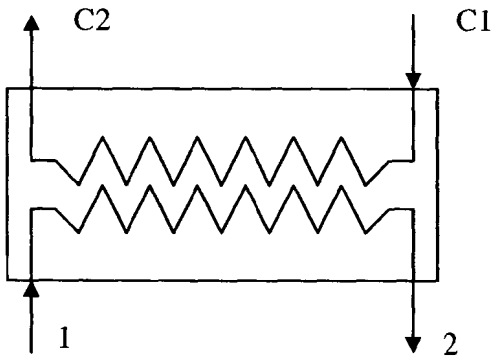

Figure 16.6: Illustration of an intercooler

The heat rejected by the gas $\left[\dot{Q}_{gas}\right]$ is defined as: $\dot{Q}_{gas} = cp_{gas}\left(T_1 - T_2\right)$

A pressure drop $\left[\Delta P_{ic}\right]$ occurs in both the gas and the coolant side of the cooler, but only the gas side has an effect on the system. $\Delta P_{ic} = \dfrac{\left(P_1 - P_2\right)}{P_1}$

A detail discussion of the design of an intercooler is available in chapter 5 in this study.

16.1.5 Recuperator

A recuperator is a heat exchanger where cold gas is heated by hot gas. A typical application is to preheat the gas before entering the combustion chamber with the exhaust gas. No contact between the fluids occurs, but energy is exchanged. The recuperator differs from the cooler for it has a double pressure loss effect on the system. Differentiation between the two streams will be done by calling the exhaust gas stream as the hot side, and the gas entering the combustor will be known as the cold stream.

For the cold side, the following apply: $T_{Cold_{in}} = T_{1_{Cold}}$, $P_{Cold_{in}} = P_{1_{Cold}}$

$$T_{Cold_{out}} = T_{2_{Cold}}, \quad P_{Cold_{out}} = P_{2_{Cold}}$$

And for the coolant side:

$$T_{Hot_{in}} = T_{1_{Hot}}, \quad P_{Hot_{in}} = P_{C_{Hot}}$$

$$T_{Hot_{out}} = T_{2_{Hot}}, \quad P_{Hot_{out}} = P_{C_{Hot}}$$

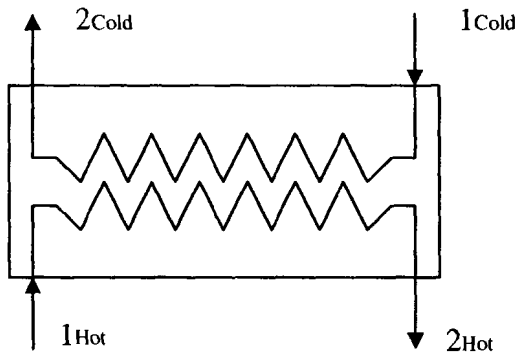

Figure 16.7: Illustration of a recuperator

The recuperator efficiency $[\eta_{rec}]$ is defined as follows: $\eta_{rec} = \frac{(T_{1_{Hot}} - T_{2_{Cold}})}{(T_{1_{Hot}} - T_{2_{Cold}})}$, the pressure drop in the hot stream: $\Delta P_{Hot} = \frac{(P_{1_{Hot}} - P_{2_{Hot}})}{P_{1_{Hot}}}$, and the cold stream; $\Delta P_{Cold} = \frac{(P_{1_{Cold}} - P_{2_{Cold}})}{P_{1_{Cold}}}$.

A detail discussion of the design of a recuperator is available in chapter 5 in this study.

16.1.6 Pipes and diffusers

In this study, an assumption is made that no heat transfer will occur through the wall of any pipe or diffuser. Pressure drop occur and is simulated as follows: $\Delta P_{Pipe} = \frac{(P_1 - P_2)}{P_1}$

16.2 COMPLEX MULTI-SHAFT CYCLE

Starting at (1), air at ambient pressure and temperature is compressed by the low-pressure compressor (LPC) to an intermediate pressure (2) after which it is cooled in an intercooler to state (3) where the temperature is again equal to ambient temperature, but at a higher pressure. The high-pressure compressor (HPC) then compresses the air to state (4). In the recuperator (5-6) heat is exchanged with exhaust gas (11-12). The air is preheated in the recuperator before entering the combustor chamber, which heats the air to state (8). After the combustor the hot high-pressure air is expanded in the high-pressure turbine (HPT) to state (9) after which it is further expanded in the low-pressure turbine (LPT) to state (11). The high-pressure turbine drives the high-pressure compressor while the low-pressure turbine is driving the low-pressure compressor. From (11) to (12) the still hot air is cooled in the recuperator after which it is released into the atmosphere. The heat rejected from (11) to (12) is equal to the heat transferred to the air from (5) to (6).

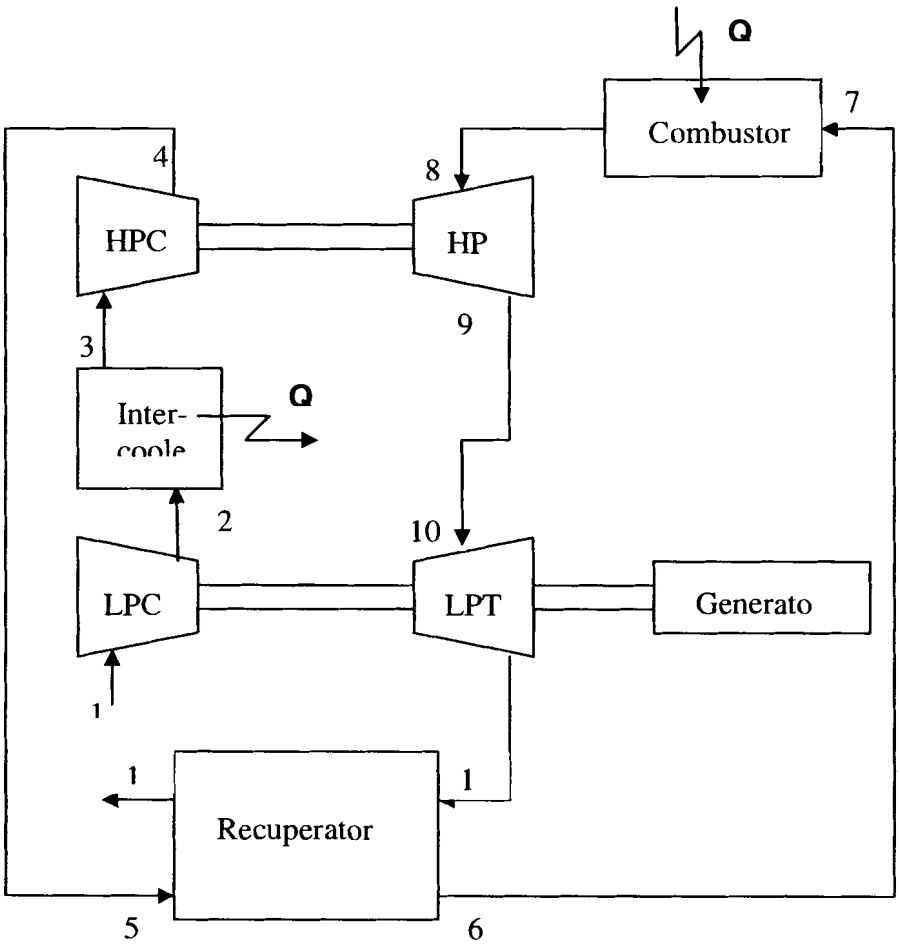

Figure 16.8: Illustration of a complex multi-shaft turbine system

16.2.1 The formulas for the cycle that needs to be solved simultaneously.

Gas properties:

$$R = 287$$
$$\gamma = 1.4$$
$$cp_{gas} = \gamma R / (\gamma - 1)$$

Efficiencies:

$$\eta_c = 0.76$$
$$\eta_t = 0.7$$
$$\eta_{rec} = 0.9$$
$$\eta_m = 0.98$$

Ambient conditions:

$$T_{ambient} = 26°C$$
$$P_{ambient} = 100kPa$$
$$\dot{m} = 1kg/\sec$$
$$pr = 2$$
$$T_{hot} = 700°C$$

Pressure losses:

$$\Delta P_{pipe} = 0.002$$

$$\Delta P_{component} = 0.01$$

Cycle equations:

Intel conditions:

$$T_1 = T_{ambient}$$

$$P_1 = P_{ambient}$$

$$P_2 = pr \cdot P_1$$

Low pressure compressor:

$$T_2 - T_1 = {T_1}/{\eta_c}\left[\left({P_2}/{P_1}\right)^{(\gamma-1)/\gamma} - 1\right]$$

$$\dot{W}_{c_{LPC}} = \dot{m} \cdot cp\,(T_2 - T_1)$$

$$P_3 = P_2 - \Delta P_{component}$$

Inter-cooler:

$$T_3 = T_{ambient}$$

$$\dot{Q}_{ic} = \dot{m} \cdot cp\,(T_2 - T_3)$$

$$P_4 = pr \cdot P_3$$

High pressure compressor:

$$T_4 - T_3 = {T_3}/{\eta_c}\left[\left({P_4}/{P_3}\right)^{(\gamma-1)/\gamma} - 1\right]$$

$$\dot{W}_{c_{HPC}} = \dot{m} \cdot cp\,(T_4 - T_3)$$

$$P_5 = P_4 - \Delta P_{pipe}$$

Pipe $_{4,5}$:

$$T_5 = T_4$$

$$P_6 = P_5 - \Delta P_{component}$$

Recuperator:

$$(T_5 - T_6) = (T_{11} - T_{12})$$

$$\eta_{rec} = \frac{(T_{11} - T_{12})}{T_{11} - T_5}$$

$$P_7 = P_6 - \Delta P_{pipe}$$

Pipe $_{6,7}$:

$$T_7 = T_6$$

$$P_8 = P_7 - \Delta P_{component}$$

Combustion chamber:

$$T_8 = T_{hot}$$

$$\dot{Q}_{heat} = \dot{m} \cdot cp\,(T_8 - T_7)$$

High pressure turbine:

$$T_8 - T_9 = \eta_t T_8\left[1 - \left(\frac{1}{{P_8}/{P_9}}\right)^{(\gamma-1)/\gamma}\right]$$

$$\dot{W}_{t_{HPC}} = \dot{m} \cdot cp\,(T_9 - T_8)$$

Pipe $_{9,10}$:

$$P_{10} = P_9 - \Delta P_{pipe}$$
$$T_{10} = T_9$$

Low pressure turbine:

$$T_{10} - T_{11} = \eta_t T_{10}\left[1 - \left(\frac{1}{P_{10}/P_{911}}\right)^{(\gamma-1)/\gamma}\right]$$

$$\dot{W}_{t_{LPC}} = \dot{m} \cdot cp\left(T_{11} - T_{10}\right)$$

Total Compressor work: $\dot{W}_c = \dot{W}_{c_{LPC}} + \dot{W}_{c_{HPC}}$

Total Turbine work: $\dot{W}_t = \dot{W}_{t_{LPC}} + \dot{W}_{t_{HPC}}$

Work output: $\dot{W}_G + \dot{W}_t + \eta_m \cdot \dot{W}_c = 0$

System efficiency: $\eta = \frac{\dot{Q}_{heat}}{\dot{W}_G}$

16.2.2 Results for these equations

For the conditions stipulated here, the results will have one value for thermal efficiency and specific work, but by doing a series of calculations, one can determine the reaction the system have due to the change. For instance: by adjusting the pressure ratio value, the system will react and a pattern can be recognized. By using this pattern the performance prediction can be done.

16.3 EXTRA LITERATURE REGARDING GAS TURBINES AND THEIR COMPONENTS

At present gas turbines represent a revolutionary technology in the electrical industry, as they enable cuts in production costs and improvement in the technological characteristics, [Islas 1999].
Literature on the components and systems is widely available, and will be discussed with the component itself.

16.3.1 Gas properties

The easiest way to increase the cycle's specific work output is to increase the TIT. Recent studies have shown that an unforeseen limitation was met concerning the effect on cycle performance of real gas properties at high temperatures [Wilcock et al.2002]. The higher the TIT became, the more important the effect of real gas properties became. By increasing the TIT at a constant pressure ratio, an optimum TIT for maximum cycle efficiency is reached below the stiometric air/fuel ratio limit.

16.3.2 Fuel and emissions

One advantage of a micro gas turbine is its fuel flexibility. Gaseous fuels that are traditionally used include natural gas, process gas, coal gas and vaporised fuel oil gas.

Process gas is a broad term used to describe gas formed by some industrial process and is compared to natural gas. Natural gas is used as the basis for comparing gas turbine performances, as it is a clean fuel, which promotes longer machine life. Vaporized fuel oil gas (diesel, petroleum and kerosene) provides high performance with a minimum reduction of machine life, thus it behaves like a gas [Boyce 1982]. This led to the growing interest regarding the role that gaseous fuel composition plays in the performance of natural gas-fired turbine systems [Flores et al.2002].

Dependence on fossil fuels will be around 90% in 2020 unless measures are taken to introduce renewable energies into the systems. Oil, coal and natural gas will have the largest share of energy supply, whilst nuclear fuels will remain stable. It is forecasted that natural gas will experience the best growth in use for power generation, the European Union's electrical generation from natural gas has tripled over the last years [Pilavanchi 2002].

A trend in fuels receiving a lot of attention is the use of biological fuel also known as biomass. Biomass is gaining popularity as the fuel of choice in the European Union and the United States. With proper harvesting practices, biomass is a sustainable energy resource that is commonly available. The major advantage of biomass fuel, in contrast with fossil fuels is zero net release of CO_2 from combustion. Emission of CO_2 into the atmosphere is reabsorbed by growing biomass. SO_2 emissions from biomass combustion are low and NO_x levels can be minimized [Anheden et al. 2000].

Biomass is not suitable for use in turbines in their natural form and either have to be refined or the turbine combustion system has to undergo modifications. Gasification is the most common way to refine biomass fuels. The biogas is fed into the combustion chamber as fuel and combust with the oxygen in the working fluid that is fresh air [Ahlroth et al. 2000]. The results of a thermodynamic study done in Sweden by *Anheden & Ahlroth* [2000] indicated that the electrical and total efficiencies are just above the efficiencies of conventional steam cycle power plants of comparable size.

16.3.3 Pressure losses and inefficiencies

The gas turbine engine is known to be more sensitive to losses and inefficiencies of components than any other engine. *Najjiar* [1990] investigated the performance of gas turbines. Performance parameters that include thermal efficiency, work and air mass flow are evaluated over a wide range of operating conditions, namely compressor pressure ratio and efficiency as well as turbine efficiency. The effect of pressure drop and inefficiencies of turbo machines on the performance of the gas turbine cycle is plotted previously in Chapter 2. These curves show the variation of the performance parameters with the operating variables.